Investigating the CaMKKβ signalling pathway and its role in the regulation of blood pressure

Jiexin Zhao

A thesis submitted to Imperial College London

for the degree of Doctor of Philosophy

February 2014

Cellular Stress Group

Medical Research Council Clinical Sciences Centre

Imperial College London

Declaration of Originality

I declare that the work presented in this thesis is my own and has not been submitted in any form for another degree or diploma at any university or other institute of tertiary education. Information derived from the published or unpublished work of others has been acknowledged in the text and a list of references is given.

Signed:……Jiexin Zhao…….. Date:…..…15/02/2014…….

Copyright Declaration

Acknowledgments

I would like to thank my supervisors Prof Dave Carling and Dr Angela Woods for all their patience, guidance, encouragement and support throughout my time in the Cell Stress lab.

I am very grateful to Dr James Leiper for all the discussions and timely advice; and also to Dr Zhen Wang for the many days spent helping me with surgical procedures. Many thanks to Phil Muckett for his invaluable help with animal work and for the many suggestions throughout my PhD. I would also like to thank Anna Slaviero for her help with the animal imaging studies.

A very big thankyou to all members of the Cell Stress lab, past and present, for their advice, support and encouragement. Many thanks to Dr Fiona Leiper for guiding me through my initial trials with western blotting; to Dr Alicia Garcia for her help with the Seahorse assays; to Dr Alex Sardini for helping me with cell imaging; also to Dr Nav Naveenam and Dr David Carmena for their kind provision of reagents.

I would like to acknowledge Medical Research Council UK, Imperial College London and the NIHR Biomedical Research Centre at Imperial College NHS Trust for funding my studies.

Finally, I would like to thank my family for all their advice and support; and Peter, who has supported me through the ups and downs over the last three years with patience and encouragement.

Abstract

Calcium/Calmodulin dependent protein kinase kinase beta (CaMKKβ) is a serine/threonine kinase involved in the Calcium/Calmodulin dependent protein kinase (CaMK) cascade. In 2005, CaMKKβ was shown to phosphorylate and activate AMP-activated protein kinase (AMPK), a master regulator of metabolism. Activation of AMPK has previously been reported to inhibit vascular smooth muscle myosin light chain (MLC) phosphorylation. The phosphorylation state of MLC in smooth muscle is known to directly control the contractility of blood vessels and the maintenance of blood pressure.

This thesis describes the characterisation of the global CaMKKβ knockout (CaMKK KO) mice, as well as the investigation of CaMKKβ signalling pathways involved in blood pressure regulation using CaMKK KO mice in a model of lipopolysaccharide induced septic shock. Septic shock is a syndrome defined by persistently reduced blood pressure despite fluid resuscitation leading to multiple organ failure resulting from overwhelming infection. Using implantable telemetry probes, aortic blood pressure was recorded in age matched male wild-type (WT) and CaMKK KO mice under both basal conditions and during lipopolysaccharide induced septic shock. In mice with global deletion of CaMKKβ, basal blood pressure was found to be increased compared to their WT littermates. In addition, when treated with intraperitoneally injected bacterial lipopolysaccharide, the lack of CaMKKβ appears to confer protection against hypotension, with significantly higher blood pressure seen in CaMKK KO mice, as well as improved mobility and general physiological state, compared to WT mice. To investigate the mechanism for the increased blood pressure in CaMKK KO mice, aorta lysate MLC kinase activity and MLC phosphorylation were measured and found to be increased in lipopolysaccharide treated CaMKK KO mice compared to WT mice. In contrast to a recent independent study, no indication of altered inflammatory response was found in CaMKK KO mice compared to WT littermates following intraperitoneal lipopolysaccharide injection. *Ex vivo* lipopolysaccharide treatment induced similar levels of nitric oxide production and phagocytosis in primary peritoneal macrophages isolated from WT and CaMKK KO mice.

In summary, CaMKKβ appears to be involved in the regulation of blood pressure. Loss of CaMKKβ in mice protects against septic shock through increased phosphorylation of MLC and the maintenance of blood pressure. Currently, septic shock is associated with a high mortality rate despite the available pharmacological treatments; inhibition of CaMKKβ could provide an alternative strategy to assist with the maintenance of blood pressure during sepsis.

List of Abbreviations

ACC	Acetyl CoA carboxylase
ADP	Adenosine diphosphate
AgRP	Agouti-related protein
AICAR	5-Aminoimidazole-4-carboxamide ribonucleoside
Akt	Protein kinase B
ALT	Alanine transaminase
AMP	Adenosine monophosphate
AMPK	AMP activated protein kinase
ATF1	Activating transcription factor
ATP	Adenosine triphosphate
BP	Blood pressure
BSA	Bovine serum albumin
Ca/CaM	Ca^{2+} bound calmodulin
CaMK I	Ca^{2+}/Calmodulin dependent protein kinase I
CaMK II	Ca^{2+}/calmodulin dependent kinase II
CaMK IV	Ca^{2+}/Calmodulin dependent protein kinase IV
CaMKK	Ca^{2+}/Calmodulin-dependent protein kinase kinase
CaMKKα	Ca^{2+}/Calmodulin dependent protein kinase kinase α
CaMKKβ	Ca^{2+}/Calmodulin dependent protein kinase kinase β
CBS	Cystathionine β-synthase
CDK5	Cyclin-dependent kinase 5
CFTR	Cystic fibrosis transmembrane conductance regulator
cGMP	Cyclic guanosine monophosphate
CPT1	Carnitine palmitoyltransferase 1
CREB	cAMP response-element binding protein
DBP	Diastolic blood pressure
DMEM	Dulbecco's Modified Eagle's Medium
DMSO	Dimethyl sulfoxide
DP	Double positive
DTT	Dithiothreitol
EDTA	Ethylenediaminetetraacetic acid
EDV	End diastolic volume
EGTA	Ethylene glycol tetraacetic acid
ERK	Extracellular signal-regulated kinase
eNOS	Endothelial NOS
FACS	Fluorescence-activated cell sorting
FCCP	p-trifluoromethoxy carbonyl cyanide phenylhydrazone
GAPDH	Glyceraldehyde 3-phosphate dehydrogenase
GLUT4	Glucose transporter type 4
GM-CSF	Granulocyte macrophage colony stimulating factor
GSK3	Glycogen synthase kinase 3
HBSS	Hanks' balanced salt solution
HDAC	Histone deacetylase
HDL	High density lipoprotein
HEPES	4-(2-hydroxyethyl)-1-piperazineethanesulfonic acid

HEK	Human embryonic kidney
HMG-CoA	Hydroxyl-3-methylglutaryl-coA
HSL	Hormone sensitive lipase
HSP	Heat shock protein
HUVEC	Human umbilical vein endothelial cell
IL1β	Interleukin 1β
IL4	Interleukin 4
IL6	Interleukin 6
IL8	Interleukin 8
IL10	Interleukin 10
iNOS	Inducible NOS
IFN	Interferons
INF	Interferon regulatory factors
LDL	Low density lipoprotein
LKB1	Liver kinase B1
LPS	Lipopolysaccharide
MAP	Mean arterial pressure
MAPK	Mitogen-activated protein kinase
MEF	Myocyte enhancer factor
MIF	Macrophage inhibitory factor
MLC	Myosin light chain
MLCK	Myosin light chain kinase
MLCP	Myosin light chain phosphatase
MRI	Magnetic resonance imaging
MTT	3-(4,5-Dimethylthiazol-2-yl)-2,5-diphenyltetrazolium bromide
MyD88	Myeloid differentiation factor
MYPT1	Regulatory subunit of MLCP
NaPP	Sodium pyrophosphate
NFκB	Nuclear factor κ B
NKCC2	Na^+-K^+-$2Cl^-$ co-transporter 2
NO	Nitric oxide
NOS	Nitric oxide synthase
nNOS	Neuronal NOS
NPY	Neuropeptide Y
NRF	Nuclear respiratory factors
OCR	Oxygen consumption rate
OD	Optical density
PBS	Phosphate buffered saline
PEPCK	Phosphoenolpyruvate carboxykinase
PGC1α	Peroxisome proliferator activated receptor γ coactivator 1α
PI3K	Phosphoinositol-3-kinase
PKA	Protein kinase A
PKC	Protein kinase C
PMSF	Phenylmethylsulfonyl fluoride
PVDF	Polyvinylidene difluoride
qRT-PCR	Quantitative reverse transcription polymerase chain reaction
ROCK	Rho-associated kinase
SBP	Systolic blood pressure
SDS	Sodium lauryl sulfate

SEM	Standard error mean
SF1	Steroidogenic factor 1
SNP	Single nucleotide polymorphisms
SNP	Sodium nitroprusside
SP	Single positive
TCR	T cell antigen receptor
TEMED	N,N,N’,N’-tetramethylethylenedamine
TMPD	N,N,N',N- tetramethyl-1,4-phenylenediamine
TNFα	Tumour necrosis factor α
TLR	Toll-like receptor
TLR4	Toll-like receptor 4-CD14 complex
Tris	Tris(hydroxymethyl)aminomethane
VEGF	Vascular endothelial growth factor

Contents

Declaration of Originality 1

Copyright Declaration 2

Acknowledgements 3

Abstract 4

List of Abbreviations 6

Contents 9

List of Figures 17

List of Tables 19

Chapter 1. Introduction 20

1.1 Ca^{2+}/Calmodulin dependent protein kinase kinase β 21

1.1.1 CaMKKβ and the CaMK cascade 22

1.1.2 Tissue specific activation of the CaMK cascade 23

1.1.3 CaMKKβ and AMPK phosphorylation 25

1.1.4 Structure and function of AMPK complexes 26

1.1.5 Tissue specific roles for AMPK and CaMKKβ 28

1.1.5.1 Brain 28

1.1.5.2 Liver 29

1.1.5.3 Adipose tissue 30

1.1.5.4 Skeletal muscle 31

1.1.5.5 Heart 32

1.1.5.6 Blood cells 33

1.1.5.7 Bone 33

1.1.5.8 Kidneys 34

1.1.6 Pharmacological activators and inhibitors 34

1.2 The Regulation of Blood Pressure 35

1.2.1 Blood pressure regulation 36

1.2.2 The regulation of vascular resistance 38

1.2.2.1 Establishment of vessel tone 38

1.2.2.2 AMPK and MLC phosphorylation 39

1.2.2.3 Nitric oxide and vasodilation 39

1.2.2.4 AMPK and eNOS 40

1.2.3 Pathophysiology of Septic Shock 40

1.2.3.1 Pathogenic microbes 41

1.2.3.2 Lipopolysaccharide (LPS) 41

1.2.3.3 Inflammatory signal transduction network 42

1.2.3.4 Cytokine release 43

1.2.3.5 TLR4 activation in endothelial cells 45

1.2.3.6 Neutrophils and macrophages 45

1.2.3.7 The progression to septic shock 45

1.3 Project aims 47

Chapter 2. Materials and Methods 48

2.1 Materials 48

2.1.1 General reagents 48

2.1.2 Antibodies 49

2.1.3 Protein 50

2.1.4 Mice 51

2.2 Methods 52

2.2.1 Genotyping 52

2.2.2 Body composition and serum measurements 53

2.2.3 Tissue lysate preparation 53

2.2.4 Immunoprecipitation 54

2.2.5 AMPK activity assay 54

2.2.6 LKB1 and CaMKKβ activity assays 54

2.2.7 Primary hepatocyte isolation and culture 55

2.2.8 Glucose output measurement 56

2.2.9 Mitochondrial function 56

2.2.10 Bone measurements 56

2.2.11 Faxitron analysis of bone mineral density 57

2.2.12 Bone RNA extraction and reverse transcription 57

2.2.13 Quantitative real-time PCR 58

2.2.14 Erythrocyte fragility test 59

2.2.15 Lipopolysaccharide (LPS) induction of sepsis 59

2.2.16 Serum cytokine measurements 59

2.2.17 Nitric oxide measurement 60

2.2.18 cGMP measurement 60

2.2.19 White cell count by flow cytometry 61

2.2.20 Splenocyte, thymocyte and lymph node cell isolation.....61

2.2.21 Peritoneal macrophage isolation and culture.....61

2.2.22 Macrophage activation.....62

2.2.23 Macrophage phagocytosis assay 63

2.2.24 Macrophage migration assay.....63

2.2.25 3-(4,5-Dimethylthiazol-2-yl)-2,5-diphenyltetrazolium bromide (MTT) assay....

.....63

2.2.26 Human umbilical vein endothelial cell (HUVEC) culture 64

2.2.27 HUVEC permeability assay 64

2.2.28 Haematocrit measurement 65

2.2.29 LPS sepsis study with STO-609 pretreatment.....65

2.2.30 Telemetry transmitter implantation.....66

2.2.31 Telemetry recording.....66

2.2.32 Aorta lysate preparation.....67

2.2.33 Polyacrylamide gel electrophoresis 67

2.2.34 Western blotting.....67

2.2.35 MLCK activity assay 68

2.2.36 Aorta immunohistochemistry 68

2.2.37 Urinary epinephrine and electrolyte measurements 69

2.2.38 High salt study 69

2.2.39 Wire myography.....70

2.2.40 Cardiac ultrasound.....70

2.2.41 Statistical analysis 71

Chapter 3. Global phenotyping 72

3.1 Global Phenotyping Results 72

3.1.1 Confirmation of Genotype 72

3.1.2 Body weight and composition 74

3.1.3 Serum metabolites 76

3.1.4 Primary hepatocyte function 77

3.1.4.1 Hepatic glucose production 77

3.1.4.2 Hepatic AMPK activity and mitochondrial respiration 79

3.1.5 Kinase activity in tissue lysates 82

3.1.5.1 Tissue specific CaMKKβ activity 82

3.1.5.2 Tissue specific AMPKα1 and AMPKα2 activity 83

3.1.5.3 Tissue specific LKB1 activity 85

3.1.6 CaMKK β KO mice have normal bone length and bone density 86

3.1.7 Increased osmotic fragility seen in CaMKKβ KO erythrocytes 88

3.1.8 Loss of CaMKKβ confers protection against LPS induced sepsis 90

3.2 Discussion 92

3.2.1 Summary of principal chapter findings 92

3.2.2 No overt metabolic phenotype in global CaMKKβ KO mice under basal conditions 93

3.2.3 CaMKKβ KO mice have normal long bone length and bone mineral density 95

3.2.4 CaMKKβ KO erythrocytes have increased osmotic fragility 96

3.2.5 Loss of CaMKKβ activity confers protection against LPS induced sepsis 97

3.2.6 Comparing LPS and the Caecal ligation puncture model of sepsis 99

Chapter 4. The function of CaMKKβ in inflammation 100

4.1 Investigating the function of CaMKKβ in inflammation 100

4.1.1 Measurement of serum cytokine production following LPS treatment 100

4.1.2 Serum NO production following LPS treatment 102

4.1.3 Leukocyte count following 6 hour LPS treatment.....104

4.1.3.1 Leukocyte populations in blood and the lymphoid organs 104

4.1.4 CaMKKβ function in macrophage migration 107

4.1.4.1 AMPK activity in LPS treated macrophages 107

4.1.4.2 LPS induced macrophage activation 107

4.1.4.3 CaMKKβ regulates VEGF dependent macrophage migration 108

4.1.5 Loss of CaMKKβ activity does not affect endothelial permeability.....111

4.1.5.1 CaMKKβ inhibition does not affect endothelial permeability under basal conditions 111

4.1.5.2 Loss of CaMKKβ does not affect haematocrit increase during LPS sepsis 111

4.1.6 Loss of either AMPKα1 or AMPKα2 does not confer protection against LPS induced sepsis.....114

4.2 Discussion 116

4.2.1 Summary of principal chapter findings.....116

4.2.2 LPS inhibits AMPK activity independently of CaMKKβ 117

4.2.3 CaMKKβ regulates LPS induced NFκB activation but does not affect PI3K signalling 118

4.2.4 CaMKKβ regulates VEGF induced macrophage migration.....119

4.2.5 CaMKKβ is not involved in macrophage phagocytosis 121

Chapter 5. The regulation of blood pressure by CaMKKβ 123

5.1. Investigating the regulation of blood pressure by CaMKKβ 123

5.1.1 CaMKKβ KO mice have higher baseline systolic and diastolic blood pressure compared to WT mice 123

5.1.2 CaMKKβ KO mice are resistant to LPS induced hypotension 125

5.1.3 Investigating CaMKKβ and downstream affects in vasculature 127

5.1.4 Loss of CaMKKβ increases myosin light chain phosphorylation in aorta lysates 128

5.1.5 Loss of CaMKKβ increases myosin light chain kinase activity in aorta lysates 129

5.1.6 Loss of CaMKKβ has no effect on nitric oxide activity in aorta lysates 130

5.1.7 AMPK activity in aorta lysates 131

5.1.8 CaMKKβ KO mice have normal aorta histology 132

5.1.9 CaMKKβ KO mice have normal kidney function 135

5.1.10 Aged CaMKKβ KO mice have reduced cardiac function 137

5.2 Discussion 139

5.2.1 Summary of principal chapter findings 139

5.2.2 LPS reduces aorta MLC phosphorylation 140

5.2.3 CaMKKβ regulates aorta MLCK activation of MLC during LPS sepsis 141

5.2.4 CaMKKβ regulates vessel contraction through activation of MLC 143

5.2.5 Loss of CaMKKβ does not significantly alter aorta structure 143

5.2.6 Loss of CaMKKβ does not affect kidney function 144

5.2.7 Loss of CaMKKβ affects long term cardiac function 145

5.2.8 The benefits and limitations of mouse models 146

Chapter 6. Summary and future directions 147

6.1 Conclusions 147

6.2 Future directions 149

References 151

List of Figures

Figure 1.1 Diagram of the downstream targets of CaMKK. 26

Figure 1.2 The regulation of blood pressure by central and renal mediated pathways.....

.....37

Figure 2.1 Optimization of primary macrophage activation with overnight IFNγ priming and LPS treatment 62

Figure 3.1 Confirmation of CaMKKβ exon deletion and loss of CaMKKβ activity in tissue.....73

Figure 3.2 Body weight and fat composition of CaMKKβ KO mice.....75

Figure 3.3 Serum metabolite measurements from WT, CaMKKβ KO, and CaMKKα KO mice.....76

Figure 3.4 Glucose output by WT and CaMKKβ KO cultured primary hepatocytes. 78

Figure 3.5 AMPK activity in cultured primary hepatocytes from WT and CaMKKβ KO mice following AMPK activation treatment. 80

Figure 3.6 Hepatocyte mitochondrial function. 81

Figure 3.7 CaMKKβ activity from WT tissue lysates.....82

Figure 3.8 Comparing AMPK activity in a panel of tissues from WT and CaMKKβ KO mice.....84

Figure 3.9 LKB1 activity from tissue lysates.....85

Figure 3.10 Bone mineralization measurements. 87

Figure 3.11 Investigating osmotic fragility in erythrocytes from CaMKKβ KO mice. 89

Figure 3.12 The effect of CaMKKβ deletion on LPS induced sepsis. 91

Figure 3.13 Diagram of murine CaMKKβ illustrating the main functional domains.....94

Figure 4.1 Serum cytokine concentrations 12 hour post LPS injection. 101

Figure 4.2 Serum NO and cGMP concentration following LPS treatment. 103

Figure 4.3 Macrophage and neutrophil count in blood. 105

Figure 4.4 Leukocyte count in blood and lymphoid organs. 106

Figure 4.5 Macrophage function. 109

Figure 4.6 Human umbilical vein endothelial cell monolayer permeability and *in vivo* LPS induced haematocrit change 113

Figure 4.7 LPS sepsis study in global AMPKα1 KO mice. 115

Figure 4.8 LPS sepsis study in global AMPKα2 KO mice. 115

Figure 5.1 Baseline telemetry results. 124

Figure 5.2 LPS telemetry results 126

Figure 5.3 CaMKKβ expression and activity in the aorta 127

Figure 5.4 MLC phosphorylation in aorta lysates. 128

Figure 5.5 Aorta MLCK activity. 129

Figure 5.6 cGMP concentration and PKG expression in the aorta. 130

Figure 5.7 AMPK activity in the aorta 131

Figure 5.8 Aorta histology. 133

Figure 5.9 Aorta histology measurements. 134

Figure 5.10 Comparing kidney function in WT and CaMKKβ KO mice. 136

Figure 5.11 Comparing cardiac function in 6 to 12 month old WT and CaMKKβ KO mice 138

Figure 5.12 Proposed mechanism of MLC regulation by CaMKKβ through MLCK to control blood pressure during LPS sepsis. 142

List of Tables

Table 1.1 Substrates of CaMK I identified *in vitro* and/or *in situ*. 24

Table 1.2 Cytokine and non-cytokine mediators of sepsis and septic shock. 44

Table 2.1 List of primers used in PCR and real-time PCR reactions. 52

Appendix 1. Substrates of AMPK containing the α1 or α2 subunit. 194

Chapter 1. Introduction

Protein phosphorylation is one of the critical mechanisms within biological organisms. Proteins are phosphorylated by kinases and dephosphorylated by phosphatases. The phosphorylation of a protein can either activate or inactivate the protein.

The discovery of protein phosphorylation begins in the early 1940s. The conversion between an active and inactive form of glycogen phosphorylase was shown in a series of publications on glycogen metabolism (Cori and Green, 1943). Following on from this, research by Fischer and Krebs in 1955 presented evidence for the regulation of glycogen phosphorylase by reversible phosphorylation, and the identification of the first protein kinase as the cause of the conversion between the active and inactive forms of glycogen phosphorylase (Fischer and Krebs, 1955; Krebs and Fischer, 1955). Since then, protein phosphorylation has been the focus of a large body of research. In 2002, Manning et al. identified 518 putative human kinase genes which have been collectively described as the human kinome (Manning *et al.* 2002).

A considerable amount of literature has been published on the phosphorylation of proteins and protein phosphorylation has been shown to play a significant role in the regulation of a wide range of cellular processes. For example, the mitogen-activated protein kinase (MAPK) cascade is initially activated by Mitogen-activated protein kinase kinase kinase; the cascade has been shown to function in cell proliferation, cell differentiation, and cell death (Junttila *et al.* 2008; Raman *et al.* 2007; Turjanski *et al*. 2007). In humans, the dysregulation of one of the subgroups of MAPK, p38 MAPK, has been shown to be associated with advanced stage and reduced mortality in several cancers including prostate cancer (Khandrika et al. 2009), liver cell cancer (Iyoda *et al*. 2003), and non small cell lung cancer (Greenberg *et al.* 2002).

Protein phosphorylation has been shown to be involved in biological functions ranging from energy homeostasis (Carling *et al*. 1997; Kahn *et al*. 2005), leukocyte cytokine production (Van der Bruggen *et al*. 1999; Rosengart *et al*. 2002), to smooth muscle contraction in blood pressure regulation (Adelstein and Conti 1975; Somlyo and Somlyo 1994).

The contractility of smooth muscle myosin light chain (MLC) is important for establishing vessel tone and therefore the maintenance of systemic blood pressure (Haslett *et al*. 2002). In 1975, Adelstein and Conti discovered that smooth muscle myosin light chain contractility was regulated by a calcium dependent reversible protein phosphorylation mechanism (Adelstein and Conti 1975).

In the area of metabolism, AMP-activated protein kinase (AMPK), has been shown to be a regulator of cellular and whole body energy homeostasis in response to stress conditions (Carling *et al*. 1997; Kahn *et al*. 2005). In 2005, In addition to activation by liver kinase B1 (LKB1) (Hong *et al*. 2003), AMPK was found to be activated by the protein kinase Ca^{2+}/Calmodulin dependent protein kinase kinase β (CaMKKβ) (Woods *et al.* 2005; Hawley *et al*. 2005).

With the exception of long term memory formation (Peters *et al.* 2003), very little is known regarding the physiological functions of CaMKKβ in other biological systems. In this study, the function of CaMKKβ is investigated using a mouse knockout model, under basal conditions as well as under the stress condition of hypotension resulting from sepsis.

1.1 Ca^{2+}/Calmodulin dependent protein kinase kinase β

There are two isoforms of Ca^{2+}/Calmodulin dependent protein kinase kinase: Ca^{2+}/Calmodulin dependent protein kinase kinase α (CaMKKα) and Ca^{2+}/Calmodulin dependent protein kinase kinase β (CaMKKβ), encoded by different genes. Human CaMKKβ shares 65% protein sequence homology with CaMKKα; with the greatest heterogeneity seen at the two termini outside the central kinase domain (Anderson *et al*. 1998). Although CaMKKβ and CaMKKα have common downstream targets, both of the CaMKKs can phosphorylate Ca^{2+}/Calmodulin dependent protein kinase I (CaMK I) and Ca^{2+}/Calmodulin dependent protein kinase IV (CaMK IV); the evidence suggests only CaMKKβ is capable of phosphorylating AMP-activated protein kinase (AMPK), a master regulator of metabolism (Woods *et al*. 2005).

CaMKKβ is a serine/threonine kinase also known as CaMKK2. CaMKKβ show greater than 90% amino acid conservation between mice, rats and men, with heterogeneity present in the

3' non-coding termini (Vinet *et al*. 2003). The human *CaMKKβ* locus maps to chromosome 12q24.2, and consists of 18 exons and 17 introns. Multiple transcripts have been found including two main transcripts generated through the usage of polyadenylation sites located in the last two exons, as well as additional transcripts from alternative splicing of the internal exons (Hsu *et al*. 2001).

1.1.1 CaMKKβ and the CaMK cascade

CaMKKβ and CaMKKα can both activate CaMK I and/or CaMK IV as part of the CaMK cascade. In cells, an influx of Ca^{2+} leads to a greater amount of Ca^{2+} bound calmodulin (Ca/CaM), allowing binding of Ca/CaM to all the members of the CaMK cascade including the CaMKKs, CaMK I and CaMK IV. Following binding of Ca/CaM, CaMK I and CaMK IV adopt conformation changes which allow access for the activated CaMKKs to phosphorylate their activating residues at Thr177 and Thr200 respectively and enhance their activity by 10-20 fold (Nairn and Picciotto 1994; Soderling 1996; Wayman *et al*. 1997).

CaMKKα and CaMKKβ are themselves activated by the binding of Ca/CaM through conformation change; however there are important differences in the regulation of their activation. CaMKKα is known to be inhibited by PKA phosphorylation, both directly through phosphorylation at Thr108 and Ser458, and also through the recruitment of 14-3-3 following phosphorylation of Ser74 (Davare *et al*. 2004). Whereas CaMKKα is entirely dependent on the binding of Ca/CaM for its activation; studies using CaMKKβ purified from both bacterial and mammalian sources show varying amounts of Ca/CaM independent activity (Anderson *et al*. 1996; Tokumitsu *et al*. 2001; Woods *et al*. 2005).

Two studies published in 2011 investigated the autonomous activity seen in recombinant CaMKKβ expressed in bacteria. Tokumitsu *et al* identified Thr482 in the regulatory domain as an autophosphorylation site in bacterially expressed CaMKKβ; mutation of the residue to alanine led to the loss of 65% of total activity (Tokumitsu *et al*. 2011). A separate study identified the sequential phosphorylation of three inhibitory sites, first Ser137, followed by Ser133 and Ser129, to regulate the autonomous activity of CaMKKβ from mammalian sources (Green *et al*. 2011). Mutating all three residues to alanine more than doubled the autonomous activity of mammalian CaMKKβ, from 20% to 50% maximum activity compared to bacterially expressed CaMKKβ which was shown to have 70% maximum activity

(measured in the presnce of calcium and calmodulin). The same study also showed cyclin-dependent kinase 5 (CDK5) and glycogen synthase kinase 3 (GSK3) to be the upstream kinases in human embryonic kidney (HEK293) cells; however in neurones from CDK5 conditional knockout mice, the authors reported reduced CaMKKβ protein expression but no result was shown for CaMKKβ phosphorylation or activity (Green *et al*. 2011).

1.1.2 Tissue specific activation of the CaMK cascade

The CaMK cascade is known to regulate cAMP response-element binding protein (CREB) dependent transcriptional activity *in vivo*, which is important for hippocampal long term memory formation (Lonze and Ginty. 2002). CaMKKα and CaMKKβ are both highly expressed in the brain (Anderson *et al*. 1996), and have been shown to be important in the formation of memory and neuronal plasticity (Wayman *et al*. 2008). In addition, studies show the CaMK cascade is essential for axon and dendrite elongation in cortical neurons (Ageta-Ishihara *et al*. 2009; Davare *et al*. 2009), as well as synaptogenesis in hippocampal neurons (Saneyoshi *et al*. 2008).

Global CaMKKβ KO mice generated by Peters *et al* were found to have male specific impaired spatial memory formation secondary to reduced spatial-training induced CREB activation, as well as impaired long term memory for the social transmission of food preferences secondary to the lack of late long term potentiation at the hippocampal area CA1 synapses (Peters *et al*. 2003; Mizuno *et al*. 2007). No difference was found in other types of hippocampus dependent long term memory, including contextual fear memory and passive avoidance, compared to wild-type mice suggesting that the formation of these long term memory types do not require the activation of CREB by CaMKKβ. In contrast, CaMKKα KO mice have impaired contextual fear memory, also male specific, with no difference found in spatial memory or social transmission of food preferences (Mizuno *et al*. 2006). The cause of the different long term memory impairments seen between the CaMKKα and CaMKKβ KO mice is currently unclear.

CaMKKs have also been shown to function in non-neuronal systems through the CaMK cascade. In the immune and inflammatory system, CaMKK function has been shown to be required for the development of T lymphocytes, through the phosphorylation of CaMK IV following T lymphocyte receptor binding leading to nuclear translocation of CaMK IV,

transcription of interleukin 2, CD25 upregulation and thymocyte development (Racioppi and Means. 2008). CaMK IV has also been shown to be important in the maintenance of bone turnover, Oury *et al* showed both CaMKKβ and CaMK IV deletion in Steroidogenic Factor 1 (SF1) expressing hypothalamic neurones are associated with increased osteoblast proliferation and reduced bone mass (Oury *et al*. 2010).

CaMK I can be found in most tissues where it is predominantly cytosolic (Piccioto *et al*. 1995). In addition to axonal growth, CaMK I has also been found to phosphorylate substrates involved in transcription initiation and cytoskeleton regulation (See table 1.1). The physiological consequence of regulation by CaMK I is currently unclear as is the role of phosphorylation on the function of several of its identified substrates.

Protein	Phosphorylation Site	Regulatory Consequence of Phosphorylation	Predicted or Demonstrated Physiological Effect
βPix	Ser516	increased Rac GEF activity	enhance actin polymerization, spinogenesis
MARKS2/Par-1b	Thr294 Ser92	increased kinase activity	increased axonal outgrowth
nNOS (neuronal nitric oxide synthase)	Ser741	inhibition of nNOS activity	unknown
Numb/Numbl	Ser264/Ser 304 Numb/Numbl	recuitment of 14-3-3 and decreased binding to AP-2	endocytosis?
MRLC (Myosin II Regulatory Light Chain)	Ser19	increased Mg-ATPase activity of Myosin II	Actin dynamics
CREB (cAMP response element-binding protein)	Ser133	transcriptional activation	transcriptional activation
ATF1 (activating transcription factor)	Ser63	transcriptional activation	transcriptional activation
CFTR (cystic fibrosis transmembrane conductance regulator)	unknown	unknown	unknown
Translational initiation factor 4GII	Ser1156	unknown	unknown
HDAC-5 (histone deacetylase)	Ser259, Ser498	recuitment of 14-3-3 resulting in disruption of MEF2-HDAC complex and nuclear export of HDAC5	blocks MyoD-dependent conversion of fibroblast to muscle
HSP-25 (25 kDa heat shock protein)	Ser15 + Ser85(minor site)	unknown	unknown
p300 (transcriptional co-activator)	Ser89	suppress histone acetyltransferase activity	repress transcription

Table 1.1 Substrates of CaMK I identified *in vitro* and/or *in situ*. (Wayman *et al*. 2008).

1.1.3 CaMKKβ and AMPK phosphorylation

CaMKKβ was shown to be an upstream activator of AMP-activated protein kinase (AMPK) by several groups (Hawley *et al*. 2005; Hurley *et al*. 2005; Woods *et al*. 2005) (See Figure 1.1). CaMKKβ phosphorylates AMPK at Thr172, the same site phosphorylated by the previously identified upstream kinase of AMPK, liver kinase B1 (LKB1) (Hong *et al*. 2003). Hurley et al show reduced AMPK activity in Hela cells transfected with CaMKKα small interfering RNA suggesting CaMKKα may also activate AMPK (Hurley *et al*. 2005); however, this is not consistent with work previously published from other groups,where CaMKKα does not significantly activate AMPK either *in vitro* or in mammalian cells (e.g. Hawley *et al.* 2005; Woods *et al.* 2005; Stahmann *et al.* 2006).

AMPK is a serine/threonine protein kinase conserved throughout eukaryotes. It is a regulator of energy balance and monitors cellular energy status in response to various stresses. Once activated by low energy status it, switches on adenosine triphosphate (ATP) producing catabolic pathways such as fatty acid oxidation and glycolysis, and switches off ATP consuming anabolic pathways such as lipogenesis. It does this both by immediate effects through targeted phosphorylation of substrates such as acetyl CoA carboxylase (ACC) (Kahn *et al*. 2005), and by long-term effects on transcription and gene expression (Carling *et al*. 1997). AMPK also controls whole body energy homeostasis by integrating, at the hypothalamic level, nutrient and hormonal signals that regulate food intake and energy expenditure (Schneeberger and Claret. 2012). AMPK is a well studied cellular energy sensor with many known substrates (see Appendix 1).

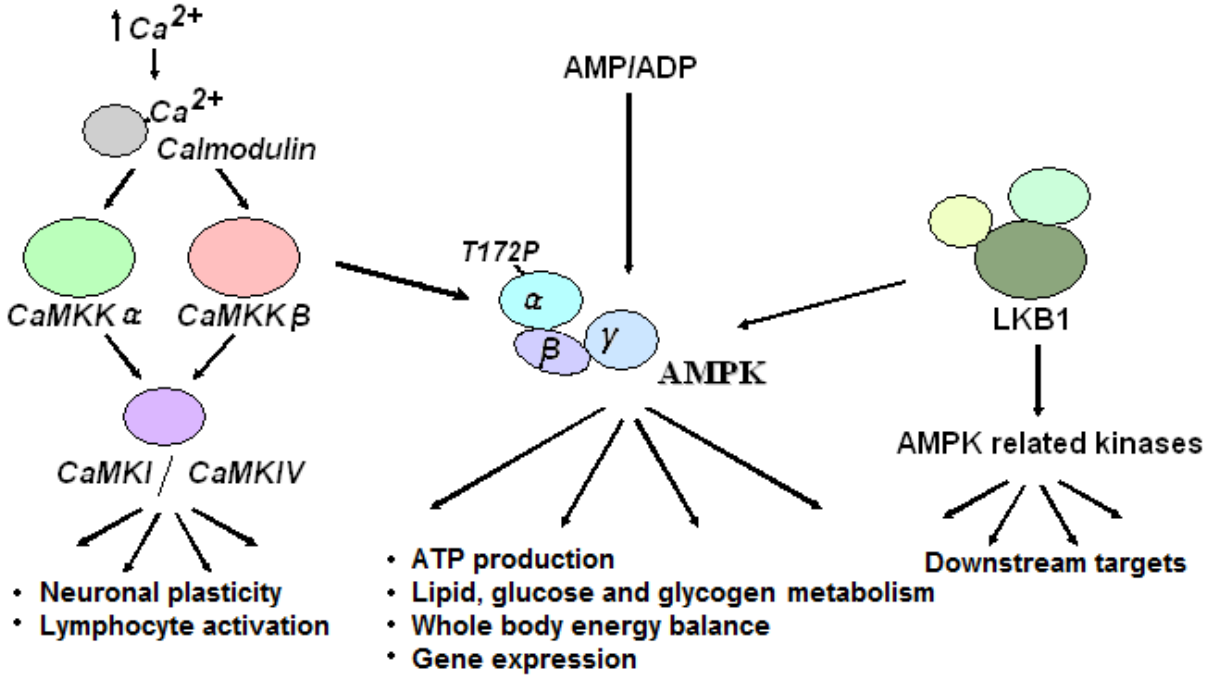

Figure 1.1 Diagram of the downstream targets of CaMKK. The influx of Ca^{2+} into cells leads to the activation of the CaMK cascade through binding of Ca/CaM to all the members of the CaMK cascade including the CaMKKs, CaMK I and CaMK IV. Both CaMKKα and CaMKKβ can phosphorylate CaMK I and CaMK IV. In addition, CaMKKβ can activate AMP kinase (AMPK) through phosphorylation of Thr172 on the α subunit of AMPK, the same site phosphorylated by the known kinase of AMPK, liver kinase B1 (LKB1). AMPK is a monitor of cellular energy status. Once activated, AMPK functions to restore energy balance at the cellular level and controls whole body energy homeostasis.

1.1.4 Structure and function of AMPK complexes

AMPK is a heterotrimeric complex consisting of a catalytic α subunit and two regulatory subunits, β and γ. The α subunit contains the activation loop where phosphorylation of the residue Thr172 by LKB1 or CaMKKβ leads to activation of AMPK through a conformational change (Carling *et al*. 2012). The γ subunit contains tandem repeats known as cystathionine β-synthase (CBS) motifs which can bind AMP, ADP or ATP in a mutually exclusive manner (Xiao *et al*. 2011). The binding of AMP to the γ subunit can allosterically activate AMPK

(Carling *et al*. 1989). It was originally proposed that AMP binding promoted the phosphorylation of AMPK by the upstream kinases LKB1 and CaMKKβ; however recent studies show that the binding of ADP, rather than AMP, to the γ subunit retains AMPK activity by protecting against the dephosphorylation of Thr172 (Xiao *et al*. 2011).

In mammals, different genes encode isoforms for each of the subunits (α1 and α2; β1 and β2; γ1,γ2 and γ3), giving rise to twelve possible heterotrimeric combinations (Carling *et al*. 2012). Differences in the tissue distribution of catalytic and regulatory isoforms expression patterns have been reported. In comparison to equivalent expression of AMPKα1 and α2 containing complexes in the liver; erythrocytes, endothelial cells and bone cells mainly express AMPK complexes containing α1 subunits, whereas skeletal and cardiac muscles mainly express AMPK complexes containing α2 subunits (Kahn *et al*. 2005; Viollet *et al*. 2009; Jeyabalan *et al*. 2012). In addition to tissue distribution, the distribution of AMPK complexes also varies at the intracellular level. AMPK complexes with α1 subunits are predominantly localized in the cytoplasm, but have also been noted at the plasma membrane in airway epithelial cells and carotid body cells (Viollet *et al*. 2009). In comparison, AMPK complexes with α2 subunits can be found in the nucleus as well as the cytoplasm (Jager *et al*. 2007). These differences between the tissue expression and intracellular localisation of AMPKα1 and α2 subunit complexes hint at differential regulation of the α subunits, potentially through the upstream kinases.

Knockout mouse model studies also suggest possible specificity in the upstream kinases for the catalytic isoforms. Lack of AMPKα2 activity was seen in mice with skeletal muscle specific deletion of LKB1, associated with impaired 5-aminoimidazole-4-carboxamide ribonucleoside (AICAR) and contraction stimulated muscle glucose uptake (Sakamoto *et al*. 2005). In cardiomyocyte specific LKB1 KO mice, ischaemia in the heart led to the loss of AMPKα2 activity whereas AMPKα1 activity was minimally affected, indicating a different kinase, potentially CaMKKβ, may be the upstream kinase for complexes containing AMPKα1 subunits (Sakamoto *et al*. 2006). The functional significance of the different AMPK isoform combinations and their upstream kinase specificity is currently unclear and remains an interesting area of study.

1.1.5 Tissue specific roles for AMPK and CaMKKβ

Many studies have been carried out to elucidate the function of AMPK in different tissues but the role of the upstream kinase is often unclear. Summaries of AMPK function have been categorised into the main organs where they occur, and are presented below with an emphasis on pathways that could potentially be activated by CaMKKβ. It is important to note that many of the AMPK functions occur in most tissues and the interaction between different tissues is essential in the control and regulation of metabolism.

1.1.5.1 Brain

CaMKKβ is highly expressed in many regions of the brain. The involvement of CaMKKβ in the formation of long term memory through the CaMK cascade has already been discussed (See section 1.1.2). CaMKKβ also appears to play a role in the hypothalamic control for whole body energy balance through the activation of AMPK; however, the details of the mechanism are currently under debate.

In the hypothalamus, AMPK is known to regulate feeding behaviour in response to multiple hormonal and nutritional signals. It is activated by fasting, hypoglycaemia and ghrelin, and inhibited by hyperglycaemia, insulin and leptin (Schneeberger and Claret 2012). Ghrelin is a hormone secreted by the stomach prior to meals and during periods of fasting or starvation. The central effects of ghrelin on increased food intake and body weight have been shown to be mediated by AMPK activation in neuropeptide Y (NPY)/agouti-related protein (AgRP) neurons in the arcuate nucleus of the hypothalamus. Under fasting conditions, ghrelin was shown to increase presynaptic AMPK activity through intracellular Ca^{2+} release and subsequent CamKKβ activation, leading to further Ca^{2+} release and setting up a positive feedback loop which activates the AgRP neurons (Yang *et al* 2011).
However, conflicting data have been published in KO mouse models regarding the role of CaMKKβ in grehlin induced feeding. In 2008, Anderson *et al* showed reduced food intake in the global CaMKKβ KO mice on a high fat diet associated with reduced AMPK activation and up regulation of NPY and AgRP gene expression in the hypothalamus. Recently, Claret *et al* showed no difference between weight gain, food intake, glucose tolerance and insulin resistance in a separate cohort of high fat diet fed global CaMKKβ KO mice compared to WT

controls (Claret *et al*. 2011). The reason for the discrepancy between the results is currently unknown.

1.1.5.2 Liver

Hepatic metabolism plays an important role in the control of whole body energy status. Evidence from mouse models confirms the importance of AMPK in the regulation of glucose production and fatty acid synthesis. LKB1 has been shown to be involved in hepatic glucose production (Shaw *et al*. 2005).

The involvement of hepatic AMPK in whole body glucose homeostasis was suggested by liver specific AMPKα2 KO mice, with hyperglycaemia and glucose intolerance through increased hepatic glucose production (Andreelli *et al*. 2006). Pharmacological activation of AMPK by AICAR in normal as well as insulin resistant obese rats was found to inhibit hepatic glucose production (Bergeron *et al*. 2001). It has also been shown that in liver specific LKB1 KO mice, increased hepatic glucose production was associated with negligible AMPK activity; in addition, the hypoglycaemic effect of metformin was also found to be absent (Shaw *et al*. 2005). However, recent studies have questioned the involvement of AMPK in AICAR and metformin induced inhibition of hepatic glucose production. Metformin and AICAR were still able to lower glucose production in AMPKα1α 2 null hepatocytes (Foretz *et al* 2010, Guigas *et al*. 2006); suggesting the hypoglycaemic effect seen following metformin and AICAR treatment does not occur through hepatic AMPK activation. AICAR was found to inhibit the expression of gluconeogenic genes including glucose-6-phosphatase and phosphoenolpyruvate carboxykinase (PEPCK) independently of AMPK activity (Foretz *et al*. 2010). The mechanism underlying the hypoglycaemic effect of hepatic AMPK remains unclear.

AMPK has been shown to control the balance between hepatic fatty acid synthesis and mitochondrial β-oxidation, the breakdown of fatty acids to acetyl-CoA. Acetyl-CoA carboxylase (ACC) is an important rate controlling enzyme for the synthesis of malonyl-CoA from acetyl-CoA. AMPK can phosphorylate both isoforms of ACC, at Ser79 on ACC1 and Ser221 on ACC2 respectively, and inhibit their function (Carling *et al*. 1989). Malonyl-CoA is both a precursor for the biosynthesis of fatty acids, and also an inhibitor of mitochondrial β-oxidation through the inhibition of fatty acid transport into the mitochondria by carnitine

palmitoyltransferase 1 (CPT1). Activation of AMPK leads to reduced triglyceride synthesis concurrent with an increase in β-oxidation, as seen following the pharmacological activation of rat hepatocytes by AICAR treatment (Muoio *et al*. 1999). Further support comes from mouse models where liver specific overexpression of a constitutively active version of the catalytic domain of AMPKα2 decreases plasma triglyceride levels and increases plasma ketone bodies, a surrogate marker for hepatic β-oxidation (Foretz *et al*. 2005); and conversely, deletion of AMPKα2 in the liver leads to increased plasma triglyceride levels and reduced plasma ketone body levels (Viollet *et al*. 2009).

AMPK also regulates cholesterol synthesis through the phosphorylation, at Ser871, and inhibition of hydroxyl-3-methylglutaryl-CoA (HMG-CoA) reductase (Carling *et al*. 1987). Inhibition of HMG-CoA reductase prevents the conversion of HMG-CoA to mevalonate, and is the rate limiting step targeted by statins, frequently used cholesterol reducing drugs. In both total and liver specific AMPKα2 KO mice, both total plasma cholesterol and high density lipoprotein (HDL) concentrations were found to be similar to WT mice (Viollet *et al*. 2009), suggesting that HMG-CoA is likely a target for AMPK complexes containing the α1 subunit.

AMPK has also been reported to regulate mitochondrial function through the regulation of transcription factors and co-activators including peroxisome proliferator activated receptor γ coactivator 1α (PGC1α) and nuclear respiratory factors (NRF) (Guigas *et al*. 2007; Jäger *et al.* 2007). Liver specific double KO of AMPKα1 and α2 was shown to have reduced mitochondrial respiration as well as mitochondrial biogenesis as measured by reduced transcript and proteins expression of PGC1α and cytochrome c (Guigas *et al*. 2007). It is likely that the control of mitochondrial function will not be limited only to hepatocytes, providing another layer of regulation by AMPK in the maintenance of cellular energy homeostasis.

1.1.5.3 Adipose tissue

Adipocytes provide energy storage for periods of increased energy expenditure or reduced food availability. In addition to the inhibition of fatty acid synthesis by AMPK phosphorylation of ACC, AICAR activation of AMPK has also been shown to inhibit lipolysis where triglycerides are hydrolyzed into fatty acids and glycerol (Sullivan *et al*. 1994, Daval *et al*. 2005). The mechanism of inhibition is not entirely clear. AMPK has been shown to

phosphorylate Ser565 on hormone sensitive lipase (HSL) which then abolishes the activating phosphorylation by protein kinase A on the adjacent S563, leading to a reduction in HSL activity and lipolysis (Garton *et al*. 1989). An alternative mechanism has also been shown in adipocytes, where AMPK activation by AICAR leads to a reduction in isoproterenol induced HSL translocation to the lipid droplet; reversible by viral overexpression of the dominant negative form of AMPK (Daval *et al*. 2005).

Consistent with this, adipocytes from mice with AMPKα1 global deletion show reduced size and increased lipolysis (Daval *et al*. 2005). Interestingly, although adipocytes contain predominantly AMPKα1 complexes, mice with AMPKα2 global deletion on a high fat diet show increased lipid accumulation in their pre-existing adipocytes compared to WT mice (Villena *et al*. 2004); indicating different downstream targets between AMPKα 1 and AMPKα2 complexes in the regulation of adipocyte metabolism.

To complicate matters, a recent study showed increased adiposity and adipocyte size in global CaMKKβ KO mice on a standard diet, opposite to the AMPKα 1 KO phenotype (Fumin *et al*. 2011). They show increased adipogenic gene expression and enhanced differentiation in CaMKKβ KO adipocytes which can be reversed by AICAR activation of AMPK, suggesting CaMKKβ enhances lipolysis through AMPK dependent expression of adipocyte differentiation genes.

1.1.5.4 Skeletal muscle

In skeletal muscle, the activation of AMPK by acute exercise is dependent on the intensity of the exercise in both rodents and humans (Treebak *et al*. 2008). AMPK activation during exercise appears to be confined locally as AMPK activation in human skeletal muscle during one-legged exercise occurs only in the exercising muscle (Kristensen *et al*. 2007). Exercise at 60-70% of maximum oxygen consumption is required for AMPK activation, and the regulation of AMPK in skeletal muscle have been shown to occur mainly through AMPKα2 complexes (Birk *et al*. 2006; Jorgensen *et al*; 2005, Klein *et al*; 2007). As the regulation of glucose uptake during muscle contraction has been shown to be regulated by LKB1 through AMPKα2 complexes (Sakamoto *et al*. 2005), the contribution of CaMKKβ in muscle metabolism during contraction is likely limited.

AMPK can regulate glucose uptake in skeletal muscle both under resting conditions and following contraction stimulation (Lee *et al*. 2002). AICAR or hypoxia stimulated glucose uptake is abolished in muscles from AMPKα2 global KO mice, where the AICAR induced phosphorylation of Akt substrates of 160kDa (AS160), an important protein in the regulation of insulin dependent glucose transporter type 4 (GLUT4) transport and glucose uptake, is lost (Treebak *et al*. 2006, Kramer *et al*. 2006). Contraction induced phosphorylation of AS160 has also been shown to occur mainly through AMPKα2 complexes, specifically α2β2γ1 (Treebak *et al*. 2008). In addition, lack of AMPKα2 phosphorylation is seen in muscle LKB1 KO mice in association with impaired AICAR and contraction stimulated glucose uptake (Sakamoto *et al*. 2005).

Muscle fatty acid metabolism is also partially regulated by AMPK activity. AMPK activation in muscle by AICAR or contraction leads to increasing rates of fatty acid β-oxidation through phosphorylation and inhibition of ACC (Mirrell *et al*. 1997; Barnes *et al*. 2004). However, the increase in β-oxidation resulting from muscle contraction have been shown to be AMPK independent at low exercise intensity (Raney and Turcotte 2006), indicating alternative pathways are also present.

In addition to glucose and fatty acid, glycogen provides another major source of energy in skeletal muscle during muscle contraction. In skeletal muscle, AMPKα2 but not AMPKα1, has been shown to phosphorylate and inhibit glycogen synthase (Jorgensen *et al*. 2004), the rate limiting enzyme in glycogen synthesis. However increased muscle glycogen content and exercise capacity was found in AMPKγ3 over expression mutants where AMPK activity is increased in skeletal muscle (Barnes *et al*. 2005).

1.1.5.5 Heart

The activation of CaMKI by CaMKKβ has been reported in hog heart lysates (Uemura *et al*. 1998) but its physiological function is unknown. AMPKα2, the predominant subunit expressed in the murine heart, and is known to play a major role in cardiac metabolism including glucose uptake, fatty acid oxidation, and ischaemia induced glycolysis (Russell *et al*. 2004; Zarrinpashneh *et al*. 2006). AMPKα2 activation in cardiac muscle is known to be regulated by LKB1 (Sakamoto *et al*. 2006); the physiological function of the small proportion of AMPKα 1 subunit and the involvement of CaMKKβ is unclear.

1.1.5.6 Blood cells

Erythrocytes, macrophages, neutrophils and lymphocytes all predominantly express the AMPKα1 subunit (Tamas *et al*. 2006; Foretz *et al*. 2010; Bae *et al*. 2011), suggesting AMPK subunit specificity in the haematopoietic lineage. The activation of AMPK by CaMKKβ has been shown in T lymphocytes following T cell antigen receptor (TCR) binding and is suggested to provide ATP for the cell proliferation and differentiation that follows TCR activation (Tamas *et al*. 2006). In erythrocytes, AMPK is essential for the maintenance of cell membrane flexibility, as Global AMPKα1 KO mice have anaemia and splenomegaly due to lysis of rigid erythrocytes sequestered in the spleen (Foretz *et al*. 2010). AMPK is also important for phagocytosis by macrophages and neutrophils. Activation of AMPK by AICAR and metformin was shown to increase phagocytosis by both macrophages and neutrophils through increased microtubule formation and actin polymerization (Bae *et al*. 2011).

Several studies have been carried out investigating the involvement of CaMKKβ and CaMK IV in T lymphocytes. CaMKKβ was shown to activate CaMK IV following TCR binding in cultured human lymphocytes (Park and Soderling. 1995), and the activation of CaMK IV has been shown to be required for CREB phosphorylation and transcription activation following TCR binding (Westphal *et al*. 1998). CaMK IV has also been found to be involved in the thymocyte transition from double positive (DP) ($CD4^+CD8^+$) to single positive (SP) ($CD4^+$ or $CD8^+$) during lymphocyte development through an unknown mechanism, with CaMK IV KO mice showing a decrease in the percentage of SP cells accompanied by a corresponding increase in the percentage of DP cells (Raman *et al*. 2001). It is currently unclear whether CaMKKα and/or CaMKKβ is the responsible kinase for the activation of CaMK IV during lymphocyte development.

1.1.5.7 Bone

Recent studies suggest the involvement of CaMKKβ in the regulation of bone turnover. CaMK I was shown to be involved in the proliferation of osteoblasts *in vitro*, with deletion by siRNA in osteoblasts leading to reduced osteoblast proliferation (Pedersen *et al*. 2008). More recently, Oury *et al* showed both CaMKK β and CaMK IV deletion in Steroidogenic Factor 1 (SF1) expressing hypothalamic neurones are associated with increased osteoblast proliferation and reduced bone mass (Oury et a. 2010), the opposite phenotype to that seen

in CaMK1 osteoblast deletion. In addition, global AMPKα1 KO mice have been shown to have reduced trabecular bone mass and density, with the AMPKα1 subunit being the predominant subunit expressed in both osteoblasts and osteoclasts (Jeyabalanet *et al*. 2012). If CaMKKβ is the upstream kinase for AMPKα 1 subunit, deletion of CaMKKβ should result in a similar phenotype to that seen in the AMPKα1 KO mice.

1.1.5.8 Kidneys

Sodium transport is known to be the major energy requiring process in the kidney (Kiil *et al*. 1961). Indications that AMPK is involved in regulation of sodium transport by the kidneys came from the finding that kidney AMPK activity was increased in rodents fed either a high salt or a low salt diet for two weeks, with reduced AMPKα1 expression seen following the low salt diet only (Fraser *et al*. 2005). Since then, AMPK has been found to phosphorylate the kidney specific Na^+-K^+-$2Cl^-$ co-transporter 2 (NKCC2) on Ser126 and shown to reduce the activity of NKCC2 in *Xenopus laevis* oocytes under basal conditions (Fraser *et al*. 2007). NKCC2 activity results in salt reabsorption, transporting Na^+, K^+, and Cl^-, across the luminal membrane in the ascending limb of the loop of Henle and the macula densa (Yang *et al*. 1996). Currently, there is no data on the physiological function of NKCC2 activation by AMPK in the kidneys.

1.1.6 Pharmacological activators and inhibitors

As CaMKKβ is activated by an increase in the concentration of Ca^{2+}, any pharmacological agent that causes an increase in intracellular Ca^{2+}, whether through activation of ion channels or release from intracellular stores, can potentially result in activation of CaMKKβ. Cytoplasmic Ca^{2+} is normally maintained in the range of 10-100 nM, compared to millimolar levels in the extracellular space, with Ca^{2+} being actively pumped from the cytosol into the extracellular space, the endoplasmic reticulum, and the mitochondria (Clapham *et al*. 2007). Ionomycin is an ionophore produced by the bacterium *Streptomyces conglobatus* that acts as a mobile ion carrier transporting Ca^{2+} across and into the cytoplasm down the concentration gradient (Liu *et al*. 1978) and has been shown to activate CaMKKβ leading to the activation of AMPK in Hela cells (Woods *et al*. 2005).

STO-609 was originally thought to be a specific inhibitor of both CaMKKα and CaMKKβ, with IC_{50} values of 120 ng/ml and 40 ng/ml, respectively (Tokumitsu *et al*. 2002). It is not a Calmodulin antagonist such as trifluoperazine, instead it targets the catalytic domains of the CaMKKs. At a concentration of 10μg/ml, STO-609 show 50% inhibition of CaMK II, 46% inhibition of myosin light chain kinase (MLCK), and less than 25% inhibition of CaMK I and CaMK IV (Tokumitsu *et al*. 2002). Used at high concentrations, STO-609 is also known to directly inhibit AMPK activity (Bain *et al*. 2007).

1.2 The Regulation of Blood Pressure

Although a few recent studies have suggested the involvement of AMPK in vasodilation through nitric oxide production (Chen *et al*. 1999; Morrow *et al*. 2003) and its involvement in the establishment of blood vessel tone (Horman *et al*. 2008), the role of CaMKKβ in blood pressure regulation and sepsis had not been previously investigated. In this study, the function of CaMKKβ in blood pressure regulation is investigated both under basal conditions and during hypotension induced in a mouse sepsis model.

Blood pressure (BP) describes the pressure exerted by the circulating blood on the blood vessel walls, and will be used to refer to arterial blood pressure unless further specified. It oscillates between a high systolic pressure (SBP) during cardiac contraction to a low diastolic pressure (DBP) during cardiac relaxation (Haslett *et al*. 2002). Blood pressure is tightly regulated within a range optimised for tissue perfusion and oxygenation. Low blood pressure predisposes to faints and falls, and persistently low blood pressure refractory to treatment as seen during sepsis is associated with a high risk of 45-50% mortality (Sakr *et al*. 2006; Esteban *et al*. 2007). On the other hand, high blood pressure is the major risk factor for the development of cardiovascular disease (Haslett *et al*. 2002).

In keeping with the importance of blood pressure maintenance, a complex regulatory network involving many systems exists to maintain blood pressure within the optimal range (See Figure 1.2). Blood pressure is regulated by altering a number of contributing factors: systemic vascular resistance, cardiac output and blood volume. Blood pressure can be raised by increasing any one or a combination of these three interconnected factors. Intrinsic

to the blood vessels, systemic vascular resistance is controlled by the constriction and dilation of the vessels through the phosphorylation state of vascular smooth muscle myosin light chain (MLC) in the vessel walls (See section 1.2.3.1). Cardiac output is controlled by both heart rate and the end diastolic volume (EDV) which is the blood volume filling the ventricle prior to being pumped out of the heart during systole. Blood volume itself, is controlled mainly by kidneys through the renin-angiotensin-aldosterone system, and also by vasopressin released from the hypothalamus in response to increased plasma osmolarity (Haslett *et al*. 2002). An increase in blood volume not only has direct effects on the blood pressure, it also increases cardiac output following Starling's Law. According to Starling's Law, cardiac output is directly proportional to EDV up to certain physiological limits; whereas the ratio between cardiac output and EDV is determined by cardiac contractility and vascular resistance (Haslett *et al*. 2002).

1.2.1 Blood pressure regulation

Regulatory systems important for the maintenance of blood pressure include the autonomic nervous system as well as the renin-angiotensin-aldosterone system (Haslett *et al*. 2002).
The autonomic nervous system continuously monitors arterial blood pressure through the baroreceptors situated in the aortic arch and the carotid sinuses of internal carotid arteries. These baroreceptors are sensory nerve endings that respond to stretching of the blood vessel wall; triggered action potentials are conducted to the brain stem with connections to the solitary nucleus in the medulla oblongata (Spyer. 1982; Haslett *et al*. 2002) A decrease in blood pressure causes rapid activation of the sympathetic nervous system resulting in the release of epinephrine and norepinephrine (also known as adrenaline and noradrenaline respectively) from the adrenal medulla. The release of epinephrine and norepinephrine returns blood pressure to within normal ranges through activation of adrenergic receptors, present in cardiomyocytes to increase heart rate and muscle contractility, as well as in smooth muscle cells in the vessel walls leading to constriction of the blood vessels and increased peripheral vascular resistance.

Produced in the kidneys, the importance of renin and angiotensin in the regulation of blood pressure has been known for many years (Haslett *et al*. 2002). During low blood pressure, renin is released from the juxtaglomerular cells in the kidney macular densa in response to reduced perfusion of the juxtaglomerular apparatus and/or reduced filtrate NaCl

concentration. Renin cleaves the inactive angiotensinogen released from the liver to angiotensin I, which is then converted to angiotensin II by angiotensin-converting enzyme present mainly in lung capillaries.

Angiotensin II acts to increase blood pressure through several pathways:
1 In the adrenal cortex, it stimulates the release of aldosterone which causes increased blood volume by increasing reabsorption of sodium and water in both the distal convoluted tubules and the collecting ducts in the kidneys.
2 In the posterior pituitary gland, it increases the release of vasopressin which not only further increases water absorption in the kidneys but also acts on the central nervous system to increase thirst and therefore water intake.
3 Angiotensin II also acts on smooth muscle cells in the blood vessel wall to cause vasoconstriction and directly increase blood pressure.

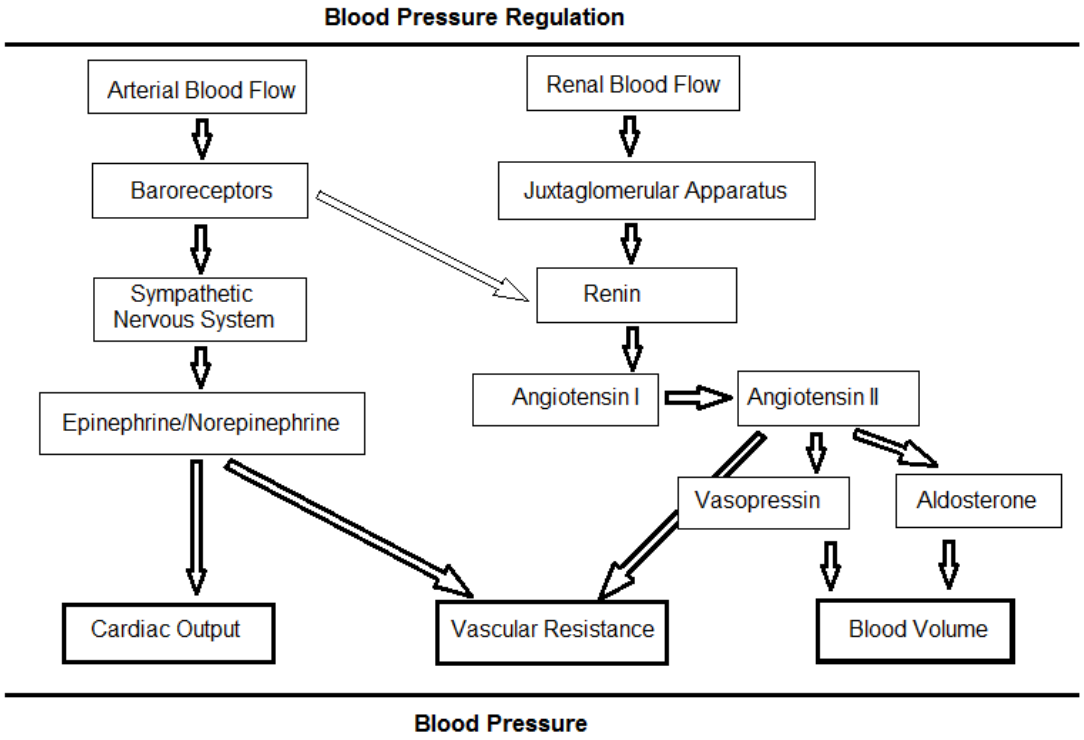

Figure 1.2 The regulation of blood pressure by central and renal mediate pathways.
The sympathetic nervous system and the mainly renal mediated renin-angiotensin aldosterone system function together to maintain blood pressure through the regulation of vascular resistance, cardiac output and fluid volume.

1.2.2 The regulation of vascular resistance

1.2.2.1 Establishment of vessel tone

Intrinsic to the blood vessels, the contractile state of vascular smooth muscle determines the vessel lumen size and therefore has a significant effect on blood pressure. The main regulatory mechanism of smooth muscle contraction is the phosphorylation state of the 20kDa MLC (Somlyo and Somlyo 1994). MLC is phosphorylated by the Ca^{2+}/calmodulin activated smooth muscle myosin light chain kinase (MLCK) on Ser19 and dephosphorylated by myosin light chain phosphatase (MLCP) (Adelstein and Conti 1975). MLC phosphorylation triggers the formation of myosin cross bridges on the actin filaments, and is sufficient for the initiation of muscle contraction (Rembold *et al*. 1992). Therefore, raised cytosolic Ca^{2+} concentration leads to smooth muscle contraction through activation of MLCK and consequently phosphorylation of MLC.

The activation of MLC by Ca^{2+}/calmodulin has been shown to be regulated by phosphorylation of MLCK, with several kinases suggested to phosphorylate MLCK at Ser1760, including protein kinase A (PKA), protein kinase C and Ca^{2+}/calmodulin dependent kinase II (CAMKII), resulting in reduced affinity of MLCK for Ca^{2+}/calmodulin (Hashimoto and Soderling. 1990; Klemke *et al*. 1997). Two transcripts of MLCK exist. The shorter form (150 kDa) present in smooth muscle and the longer form (210 kDa) present in non-muscle cells including endothelial cells (Kamm and Stull. 2001). The longer form of MLCK is involved in endothelial cell gap formation, vascular permeability, cell motility and morphology (Kamm and Stull. 2001).

MLC phosphorylation during vascular contraction has also been shown to be induced independently of changes in cytosolic Ca^{2+} concentration (Somlyo and Somlyo. 2004). Agonists such as norepinephrine, vasopressin, angiotensin etc, bind to G-protein coupled receptors and produce smooth muscle contraction by increasing both the cytosolic Ca^{2+} concentration and the Ca^{2+} sensitivity of the contractile apparatus. The increased sensitivity of vascular smooth muscle toward Ca^{2+} has been attributed to inhibition of MLCP activity leading to increased MLC phosphorylation and tension at a constant Ca^{2+} concentration. Several studies suggest sensitization to Ca^{2+} occurs through activation of Rho-associated kinase (ROCK) through the small GTPase RhoA, which in turn, phosphorylates the regulatory

subunit of MLCP (MYPT1) at Thr696 and Thr853, resulting in inhibition of MLCP activity and increased MLC phoshorylation (Uehata *et al*.1997; Feng *et al*. 1999).

1.2.2.2 AMPK and MLC phosphorylation

Recent studies suggest AMPK may be involved in the regulation of vascular tone. The pharmacological activation of AMPK by AICAR induces endothelium independent relaxation of murine aortic rings, which is abolished in aortic rings from global AMPKα1 KO but not AMPKα2 KO mice (Goirand *et al*. 2007). *In vitro*, AMPK α1β1γ1 complex was shown to phosphorylate MLCK at the same site as PKA, protein kinase C (PKC) and CaMK II (Ser1760), leading to reduced affinity of MLCK for Ca^{2+}/calmodulin binding (Horman *et al*. 2008). The treatment of aortic smooth muscle cells with 10μM STO-609 accelerated Vasopressin induced MLC phosphorylation (Horman *et al*. 2008), suggesting CaMKKβ may also act upstream of MLC in smooth muscle.

The AMPK subunit distribution in vascular smooth muscle appears to differ depending on the origin of the vessel. In murine pulmonary arterial smooth muscle, both AMPKα1 and AMPKα2 subunits have been found, with higher expression of AMPKα1 subunits and the majority of AMPK activity from complexes containing AMPKα1 subunits (Evans *et al*. 2005). AMPKα1 subunit complexes have been suggested to account for 90% of total AMPK activity in aortic smooth muscle cell lysates (Horman *et al*. 2008).

1.2.2.3 Nitric oxide and vasodilation

Nitric oxide (NO) is endogenously produced from L-arginine by nitric oxide synthase (NOS) (Bredt and Snyder. 1990). Three forms of NOS exist; endothelial NOS (eNOS), neuronal NOS (nNOS), and inducible NOS (iNOS).NO has been known as a vasodilator for many years (Furchgott *et al*. 1980) and more recent studies have shown that the vasodilation is achieved through MLCP activation and MLC dephosphorylation (Nakamura *et al*. 2007) Smooth muscle is not known to produce NO; NO produced by the eNOS present in the endothelial layer of blood vessels diffuses into smooth muscle leading to activation of soluble guanylate cyclase resulting in increased cyclic-guanosine monophosphate (cGMP) production (Hofmann *et al*. 2000). The mechanism of vasodilation caused by cGMP is not entirely clear. Increased concentration of cGMP has been shown to correlate with increased

T696 MLCP phosphorylation and induce Ca^{2+} concentration independent MLC dephosphorylation (Nakamura *et al*. 2007), suggesting the RhoA/ROCK pathway may be activated. The expression of iNOS is induced during sepsis and is important for the inflammatory response; this will be described in more detail in section 1.2.4.7.

1.2.2.4 AMPK and eNOS

In vascular endothelial cells, where AMPKα1 is the predominant subunit expressed (Davis *et al*. 2006), there appear to be two separate sets of signals for the activation of AMPK which determines whether AMPK goes on to phosphorylate eNOS. *In vitro*, AMPK has been demonstrated to phosphorylate both cardiac and endothelial eNOS at Ser1177, leading to activation of eNOS and increased NO production (Chen *et al*. 1999). AMPK activation by AICAR in human aortic endothelial cells has also been shown to increase eNOS phosphorylation and NO synthesis (Morrow *et al*. 2003). However, recent studies show activation of AMPK may also occur independently from the phosphorylation and activation of eNOS. Bradykinin, thrombin and vascular endothelial growth factor (VEGF) have all been shown to activate AMPK in endothelial cells through calcium dependent CaMKKβ pathways (Stahmann *et al*. 2006; Mount *et al*. 2008; Stahmann *et al*. 2010). In all three cases, activation of the CaMKKβ/AMPK pathway led to downstream ACC phosphorylation; in contrast, eNOS phosphorylation and NO production was shown to occur independently of AMPK activation by CaMKKβ. In addition, AMPKα1 was shown to be essential in VEGF induced matrigel plug angiogenesis assays in WT and global AMPKα1 KO mice (Stahmann *et al*. 2010).

1.2.3 Pathophysiology of Septic Shock

Blood pressure is normally tightly regulated within a range optimised for tissue perfusion and oxygenation. Low blood pressure predisposes to faints and falls, and persistently low blood pressure refractory to treatment as seen during sepsis is associated with a high risk of 45-50% mortality (Sakr *et al*. 2006; Esteban *et al*. 2007). Sepsis is defined as the systemic inflammatory response by the body to the presence of infection, and severe sepsis describes sepsis associated with organ dysfunction or tissue hypoperfusion (Bone 1992). Septic shock is defined as sepsis with refractory hypotension despite adequate fluid resuscitation (Bone 1992). Complex events that occur in septic shock can be broadly divided into

microorganism-related components as well as host-related components including inflammatory dysfunction and cardiocirculatory dysfunction.

1.2.3.1 Pathogenic microbes

Severe sepsis and septic shock are initiated by the invasion of normally sterile tissue by pathogenic microbes including bacteria, viruses, or fungi. The interactions between the host immune system and the pathogen involved may result in either a contained infectious process with minimal tissue injury or severe sepsis and septic shock. Bacterial virulence factors can confer advantages to pathogens via one of several mechanisms including modulation of host defence mechanisms, promoting attachment to host cell surfaces, invasion of host tissue, and evasion of host immune systems. One of the virulence factors able to modulate host inflammatory responses is lipopolysaccharide (Nduka and Parrilo 2009).

1.2.3.2 Lipopolysaccharide (LPS)

Lipopolysaccharide (Also known as endotoxin) is a component of the outer cell membranes of Gram-negative bacteria such as *Escherichia coli* (E coli), *Salmonella, Shigella, Pseudomonas, Neisseria, Haemophilus influenza, Bordetella pertussis and Vibrio cholera.* Although it is known that small amounts of LPS may be released in a soluble form by young cultures grown in the laboratory (Zhang *et al*. 1998); LPS is more commonly associated with the cell membrane and released into the host tissue upon destruction of the pathogen. LPS release can result from autolysis, external lysis mediated by complement and lysozyme, and phagocytic digestion of bacterial cells (Nduka and Parrillo. 2009).

LPS are complex amphiphilic molecules with a molecular weight of around 10kDa.Chemical composition can vary greatly both between and among bacterial species. However all LPS consists of three regions: a hydrophilic membrane anchoring lipid; a region attached to a core polysaccharide region similar within a specie; and an O-antigen region consisting of repeating oligosaccharide subunits with varying length and variation in saccharide composition (Rietschel *et al*. 2009). The virulence of E coli O111:B4, including its capacity to resist phagocytosis, has been shown to be dependent on the saccharide composition of its cell membrane LPS (Medearis Jr *et al*. 1968); with similar results seen from multiple batches of

LPS isolated from log-phase cultures, and reduced virulence seen in strains with altered saccharide composition.

LPS elicits a variety of inflammatory responses in the host. It is recognised by toll-like receptor 4-CD14 complex (TLR4) which is one of the pattern recognition receptors expressed by immune cells to identify the presence of invading pathogens (Takeuchi *et al*. 1999). These receptors initiate the innate immune response and regulate the adaptive immune responses to infection or tissue injury. Upregulation of toll-like receptor (TLR) expression is seen following the activation of the immune response by the presence of LPS (Mollen *et al* 2006; Uematsu and Akira. 2007). Positive feedback loops may be set up where TLR4 interaction with LPS leads to enhanced TLR reactivity, resulting in excessive inflammatory response and mortality (Paterson *et al* 2003). In contrast, single nucleotide polymorphisms (SNPs) identified in TLR4 have been linked to LPS hyporesponsiveness, predisposing carriers of these SNPs to high rates of Gram-negative septic shock following inadequate inflammatory responses (Gibot *et al* 2002).

1.2.3.3 Inflammatory signal transduction network

The mechanism of LPS induced signalling events mediated by TLR4 has been extensively studied over recent years. Much work has been carried out to elucidate the role of specific molecules comprising the signalling pathways and to identify the negative regulators of the LPS signalling. A summary of the more important pathways are described below, and the links within provide further information on the mechanisms of TLR4 activation by LPS.

The binding of LPS to TLR4 on the outer membrane of immune cells recruits myeloid differentiation factor (MyD88), activating intracellular signalling pathways leading to the activation of transcription activators such as interferon regulatory factors (IRF), phosphoinositol-3-kinase (PI3K) and its downstream kinase Akt, as well as cytosolic nuclear factor κ B (NFκB). Activated NFκB moves into the nucleus and: binds to transcription sites; induces the expression of a range of inflammatory proteins and mediators including: acute phase proteins, iNOS, coagulation factors, proinflammatory cytokines, and adhesion molecules; initiates the enzymatic activation of cellular proteases (Cinel *et al*. 2009 Review). PI3K acts at several positions downstream of TLR4, and can function either as a positive or negative regulator depending on the cell type and/or the regulatory signal (Cinel *et al*. 2009).

The downstream targets of PI3K/Akt signalling include activation of mitogen-activated protein kinase/extracellular signal-regulated kinase (MAPK/ERK) pathway important for tumour necrosis factor α (TNFα) production; as well as regulation of neutrophil functioning through p38 signalling including cytokine production, chemotaxis, adhesion, and apoptosis (Peck-Palmer *et al*. 2008). IRF has been shown to regulate the expression of not only interferon β, but also iNOS and chemokines, following TLR4 binding (Negishi *et al*. 2006). There is significant crosstalk between these signalling pathways with IRF1 known to interact with NFκB and PI3K signalling also known to activate NFκB.

The recruitment of MyD88 is essential for the expression of inflammatory cytokines including interleukin 1β (IL1β), interleukin 6 (IL6) and TNFα; these cytokines are not produced in mice lacking MyD88 in response to LPS; instead, IRF3 was found to be activated following LPS binding to TLR4 resulting in the NKκB dependent expression of interferon stimulated regulatory elements such as IP10 (Kawai *et al*. 2001).

1.2.3.4 Cytokine release

The progression of sepsis is driven by the synthesis and release of many inflammatory mediators and cytokines following TLR4 activation (See Table 1.1). This sets up a systemic environment that promotes destruction of pathogens by a variety of means including: resetting the thermoregulator in the hypothalamus to a higher temperature; blood vessel dilation to improve tissue oxygenation; the recruitment and activation of increasing numbers of immune cells; and increased vascular permeability to increase tissue infiltration by the phagocytic cells.

Cytokine cascade describes the sequential release pattern of mediators with the initial release of pro-inflammatory cytokines IL1β and TNFα, leading to the concomitant release of a range of cytokines including IL6, interleukin 8 (IL8), macrophage inhibitory factor (MIF), as well as NO produced by iNOS (Nduka and Parrillo. 2009). Interleukin 10 (IL10) is a regulatory anti-inflammatory cytokines released by monocytes and T-cells following the initiation of the cytokine cascade leading to inhibition of pro-inflammatory cytokine synthesis (Banchereau *et al*. 2012). Cytokines are normally present in the circulation at very low concentrations and can increase by >1000 fold following TLR4 activation (Damas *et al*. 1997). Very high but transient cytokine concentrations of IL6 and IL8 were associated with

the development of septic shock rather than severe sepsis, suggesting both the concentration and the time course of the cytokine production is important for sepsis severity (Blackwell and Christman. 1996; Damas *et al* 1997).

Class	Mediator	Source	Role in sepsis
Pro-inflammatory cytokines	Interleukin 1β	Monocytes Macrophages Lymphocytes Endothelial cells	Altered thermoregulation. Hypotension. T lymphocyte and macrophage activation.
	Tumor necrosis factor α	Activated macrophages	Altered thermoregulation. Hypotension. Neutrophil and endothelial cell activation.
	Interleukin 6	T lymphocytes B lymphocytes Endothelial cells	Induction of lymphocyte proliferation.
	Interleukin 8	Activated macrophages and monocytes	Chemotactic for neutrophils and T lymphocytes.
	Interleukin 18	Activated macrophages	Increased secretion of interferon γ. Initiates cell mediated immune response with interleukin 12.
	Interferon γ	Natural killer cells	Macrophage priming. Defense against viral and intracellular bacterial pathogens.
	Macrophage inhibitory factor	Activated macrophages	Increased tumor necrosis factor expression. Increased TLR4 expression.
Anti-inflammatory cytokines	Interleukin 10	Epithelial cells Monocytes Lymphocytes	Downregulation of macrophage function. Decreased tumor necrosis factor α
	Interleukin 4	unknown	Induces differentiation of naive helper T lymphocytes to Th2 cells.
	Interleukin 1Ra	Monocytes	Inhibits interleukin 1 activity.
Endothelial factors	Induced Nitric oxide	Activated macrophages Endothelial cells	Vasodilation. Myocardial depression. Increases vascular permeability. Inhibition of platelet function.
Others	Platelet activating factor	Macrophages Neutrophils Endothelial cells	Activation of endothelial cells. Histamine release from platelets.
	Complement proteins C3a-C5a		Increased capillary permeability. Histamine release.

Table 1.2 Cytokine and non-cytokine mediators of sepsis and septic shock (adapted from Nduka and Parrilo. 2009).

1.2.3.5 TLR4 activation in endothelial cells

The endothelium also plays a major role in the pathogenesis of sepsis and septic shock. Endothelial cells line the inner wall of blood vessels and functions to regulate angiogenesis, vascular permeability, vessel contractility, as well as providing an anticoagulant surface. Vascular dysfunction occurs both as a result of the direct effects of LPS and also in response to the released inflammatory mediators including TNFα, IL1β, and interferons (IFN) from macrophages and immune cells (Salgado *et al*. 1994).

1.2.3.6 Neutrophils and macrophages

Myeloid cells including neutrophils and macrophages contain vesicles of proteolytic enzymes and are capable of phagocytosing and degrading internalized pathogens. Neutrophils are proapoptotic and in addition to their antimicrobial function, they are associated with the potential for host tissue damage when they are activated during sepsis (Brown *et al*. 2006). Host tissue damage in severe sepsis can occur through a variety of mechanisms including premature neutrophil activation, extracellular release of cytotoxic molecules during microbial killing, removal of infected or damaged host cells, and failure to terminate the acute inflammatory response.

Phagocytosis of the apoptotic neutrophils by macrophages inhibits the release of proinflammatory cytokines and promotes the secretion of anti-inflammatory cytokines (Fadok *et al*. 1998). The capacity of activated macrophages to clear expanded apoptotic populations of neutrophils has been shown to contribute to immune suppression during sepsis (Swan *et al*. 2007).

1.2.3.7 The progression to septic shock

The development of septic shock involves both cardiac and vascular dysfunction. Many mechanisms have been proposed to explain the myocardial depression present in sepsis, including coronary ischaemia, interstitial myocarditis, and pathways initiated by several of the inflammatory mediators (Fernandes *et al*. 2008); however the importance of any of these mechanisms is currently unclear. Better understood is the importance of NO in the development of hypotension seen in septic shock (Petros *et al*. 1991; Cauwels. 2007). The

cytokines TNFα and IL1β induce the expression of iNOS, leading to the release of NO by neutrophils, macrophages and endothelial cells (Nduka and Parrillo. 2009). In addition to causing vasodilation through the dephosphorylation of MLC (See section 1.2.3.3), NO has also been shown to impair cardiomyocyte contractile function (Baumgarten *et al*. 2006), suggesting it may be the main mediator for both the cardiac and vascular aspects of septic shock.

1.3 Project aims

CaMKKβ is known to phosphorylate and activate CaMKI, CaMKIV as well as the master regulator of metabolism, AMPK. Recent research in AMPKα subunit KO mice suggests the involvement of AMPK and potentially CaMKKβ in the regulation of systemic blood pressure. With the exception of long term memory formation, very little is known regarding the physiological functions of CaMKKβ in other biological systems.

This project aims to further current understanding of CaMKKβ function using the global CaMKKβ KO mice;

1. To clarify the involvement of CaMKKβ in the downstream metabolic effects following AMPK activation. To assess the effect of global loss of CaMKKβ on systemic AMPK activation.

2. To investigate the function of CaMKKβ in the immune system using a mouse model of LPS sepsis.

3. To determine the involvement of CaMKKβ in blood pressure regulation duing LPS sepsis and establish the mechanism through which CaMKKβ regulates blood pressure.

Chapter 2. Materials and Methods

2.1 Materials

2.1.1 General reagents

Adenosine monophosphate (AMP), Adenosine diphosphate (ADP), Adenosine triphosphate (ATP), 4-(2-hydroxyethyl)-1-piperazineethanesulfonic acid (HEPES), Tris(hydroxymethyl)aminomethane (Tris), ethylene glycol tetraacetic acid (EGTA), ammonium persulphate, magnesium chloride ($MgCl_2$), sodium fluoride (NaF), sodium pyrophosphate (NaPP), dithiothreitol (DTT), N,N,N',N'-tetramethylethylenedamine (TEMED), protein A/G-sepharose, sorbitol, β-mercaptoethanol, water soluble dexamethasone, 3,3',5-Triiodo-L-tyronine sodium salt (T_3), bovine serum albumin (BSA), agarose, ionomycin, *Taq* DNA polymerase, NP-40, Dimethyl sulfoxide (DMSO), Triton X-100, Ponceau S solution, and 1-1,dimethyl biguanide hydrochloride (metformin) were obtained from Sigma (Poole, UK). Glucose oxidase kit was from Thermo Fisher Scientific (Leicestershire, UK). 10x Tris/glycine/SDS buffer, Protogel bisacrylamide and Ecoscint scintillant were purchased from National Diagnostics (Yorkshire, UK). Polyvinylidene difluoride (PVDF) membrane was from Perkin Elmer (Beaconsfield, UK). AICA-Riboside was purchased from Calbiochem (Nottingham, UK). Primers were generated by Sigma-Genosys (Havrehill, UK). NaOH, sodium lauryl sulfate (SDS), NaCl, Tween 20, glycerol, ethylenediaminetetraacetic acid (EDTA), ethanol, methanol, KCl, KH_2PO_4, $NaHCO_3$, choloroform and glucose were from VWR (West Sussex, UK). RNeasy columns, quantitect primers and quantitative reverse transcription PCR (qRT-PCR) kit were from Qiagen (Crawley, UK). 3MM chromatography paper and P81 phosphocellulose paper were obtained from Whatman (Maidstone, UK). DMEM, M199, Penicillin/Streptomycin, insulin, sodium pyruvate were from Gibco, Invitrogen (Paisley, UK). PageRuler Plus Prestained protein marker was from Fermentas (York, UK).

2.1.2 Antibodies

All antibodies were used at 1:1000 dilution for western blot.

Anti-pThr172 AMPKα raised in rabbit was from Cell Signalling (2535).

Anti-β actin raised in rabbit was from Sigma (A5060).

Anti-GAPDH raised in rabbit was from Abcam (ab9485).

Anti-iNOS raised in rabbit was from Santa Cruz (NOS2 N-20, sc-651).

Anti-total MLC raised in rabbit was from Cell Signalling (MLC2, 36725).

Anti-pSer19 MLC raised in rabbit was from Cell Signalling (pMLC2, 36755).

Anti-total MLCK raised in mouse was from Sigma (Clone K36, M7905).

Anti-pSer1760 MLCK raised in rabbit was from Invitrogen (441085G).

Anti-PKG raised in rabbit was from GeneTex (PRKG1, GTX111610).

Antibodies against CaMKKβ and LKB1 were generated in house. Anti-CaMKKβ raised in rabbit was used at 1:66 dilution for immunoprecipitation. Anti-LKB1 raised in rabbit was used at 1:100 dilution for immunoprecipitation.

Antibodies targeting the AMPKβ subunit, α1 subunit and α2 subunit were generated in house. Anti-AMPKβ raised in rabbit was used at 1:400 dilution for immunoprecipitation. Anti-AMPKα1 and AMPKα2 were separately raised in sheep were used at 1:100 dilution for immunoprecipitation.

Antibodies against total NKCC2 and pSer126 NKCC2 were kind gifts from Prof Dario Alessi, Dundee.

APC efluor 780 conjugated anti-mouse CD3e was from eBioscience (clone 17A2, 47-0032-80), used at 1:66 dilution to identify all mature T lymphocytes through flow cytometry.

PerCP conjugated anti-mouse CD4 was from Biolegend (clone GK1.5, 100431), used at 1:200 dilution to identify CD4 positive T lymphocytes through flow cytometry.

PE conjugated anti-mouse CD8a was from eBioscience (clone 53-6.7, 12-0081-81), used at 1000 dilution to identify CD8 positive T lymphocytes through flow cytometry.

PerCP-Cy5.5 conjugated anti-mouse CD45R (B220) was from eBioscience (clone RA3-6B2, 45-0452-80), used at 1:100 dilution to identify B lymphocytes through flow cytometry.

FITC conjugated anti-mouse CD25 was from Biolegend (clone 3c7, 101907), used at 1:100 dilution to identify CD25 positive thymocytes through flow cytometry.

APC conjugated anti-mouse CD44 (Pgp-1, Ly-24) was from Pharmigen (559250), used at 1:200 dilution to identify CD44 positive thymocytes through flow cytometry.

PE conjugated anti-mouse F4/80 was from eBioscience (clone BM8, 12-4801-80), used at 1:2000 dilution to identify mature macrophages through flow cytometry.

FITC conjugated anti-mouse Ly-6G (Gr-1) was from Pharmigen (553126), used at 1:200 dilution to identify neutrophils through flow cytometry.

2.1.3 Protein

Recombinant AMPK complex (α1β1γ1) was expressed in *Eschericha coli* and purified by Dr Faith Mayer and Dr Angela Woods as described in Sanders *et al*. 2007.

2.1.4 Mice

CaMKKβ KO mice with global deletion of exon 5 generated as described in Peters *et al*. 2003. CaMKKα KO mice with global deletion of exons 2 to 5 generated as described in Blaeser *et al*. 2006. AMPKα1 and AMPKα2 global KO mice were generated as described in Jorgensen *et al.* 2004 and Viollet *et al.* 2003 respectively. All mice were maintained on a 12 hour light/dark cycle with free access to water and standard mouse chow and housed in specific-pathogen free barrier facilities, unless otherwise stated. All *in vivo* studies were performed in accordance to the Animal Scientific Procedures Act (1986) with approval from Home Office, UK. Male mice were used unless otherwise stated. All mice used were 8-10 weeks old unless otherwise stated.

2.2 Methods

2.2.1 Genotyping

DNA from ear snip or tail tip biopsies was extracted by heating to 100ºC with 100mM NaOH for 15 min, followed by addition of 1M Tris pH 8 to adjust the pH to 8. DNA was amplified by polymerase chain reactions (PCR) using Reddymix (2x Reddymix mastermix containing Taq DNA polymerase, Thermo Scientific) and the appropriate primers (Table 2.1) in the presence of 5% DMSO.

Following amplification, DNA was analysed by agarose gel electrophoresis at 120V for 30 min on 3% (w/v) agarose gel, and bands visualised by ultra-violet light exposure (Gene Genius, Syngene).

Genotyping primers	CaMKKβ WT	5’ CAGCACTCAGCTCCAATCAA 3’ 5’ GCCACCTATTGCCTTGTTTG 3’
	CaMKKβ KO	5’ CAGCACTCAGCTCCAATCAA 3’ 5’ TAAGCACAAGCACTCATTCC 3’
	CaMKKα WT	5’ GAATGTGGCTGTGTCTTGAG 3’ 5’ GACACAGAGCAGGAACTGTA 3’
	CaMKKα KO	5’ GTGGAGGTATTGAGGCAGTC 3’ 5’ GACACAGAGCAGGAACTGTA 3’
Real-Time PCR primers	LKB1 short and long form	5’ TGGACTCCGAGACCTTATGC 3’ 5’ CATTGTACAGCACGTCCACA 3’
	CaMKKβ	5’ CCCCACAGTCCTCTCCCCGG 3’ 5’ CGACGTGGGAAGCCAGCCTG 3’
	GAPDH	5’ AGGTCGGTGTGAACGGATTTG 3’ 5’ TGTAGACCATGTAGTTGAGGTCA 3’

Table 2.1 List of primers used in PCR and real-time PCR reactions.

2.2.2 Body composition and serum measurements

For serum metabolite measurements, tail vein blood was collected in heparinized microvettes (Sarstedt) and centrifuged at 3000g for 30 min at 4°C. Serum was stored at -80°C until all samples had been collected. Serum levels of total cholesterol, low density lipoprotein (LDL), high density lipoprotein (HDL), free fatty acids, triglycerides, and alanine transaminase (ALT) were determined by the Mouse Biochemistry Laboratories, Cambridge, UK. To measure fasting glucose, mice were fasted overnight before tail vein blood collection and measurement of blood glucose using a Glucometer Elite (Bayer Corporation).

Body composition measurement of anaesthetized mice was kindly carried out by Mr Phill Muckett by quantitative magnetic resonance imaging using EchoMRI (Houston Medical Systems).

2.2.3 Tissue lysate preparation

Tissue was snap frozen in liquid nitrogen immediately following extraction. Adipose tissue was collected from peritesticular and perirenal areas. Lung and muscle were ground in liquid nitrogen with pestle and mortar. All tissues were homogenised (IKA T10 basic ULTRA-TURRAX using dispersing tool S10N-5G) for 1 min on ice, in HBA (50mM Tris-HCl pH 7.4, 50mM NaF, 5mM NaPP, 1mM EDTA, 0.25M sucrose with 1% (v/v) triton-100, 1mM DTT, 0.1mM phenylmethylsulfonyl fluoride (PMSF), 1mM benzamidine, 4µg/ml Trypsin inhibitor). Supernatant was collected following centrifugation at 13000g at 4°C for 15-20 min. Protein concentrations were measured by Bradford protein assay (Bio-Rad) (Bradford, 1976).

2.2.4 Immunoprecipitation

Tissue lysate was incubated with antibody and protein A/G slurry (Sigma) in HBA for 2 h at 4°C. Immune complexes were washed once in HBA, followed by a second wash in HGE (HBA without NaF and NaPP).

2.2.5 AMPK activity assay

Immunoprecipitation was carried out from 50µg tissue or cell lysate incubated with antibody against AMPKβ (Woods *et al.* 1996). To measure non-specific antibody binding, immunoprecipitation was also carried out with no antibody. Immune complexes were added to 30µl SAMS assay mix (333µM AMP and 333µM SAMS peptide [HMRSAMSGLHLVKRR] (In house synthesis, MRC Peptide Synthesis Unit) in HGE), 10µl HGE and 10µl γ-^{32}P-ATP/$MgCl_2$ (1mM γ-^{32}P -ATP (Perkin Elmer), 25mM $MgCl_2$, 1mM ATP), before incubating for 20min at 37°C. Immune complexes were then centrifuged at 13000g and 20µl supernatant spotted onto P81 paper (Whatman). P81 paper was washed in 1% (v/v) orthophosphoric acid, blotted dry, then counted for 30 seconds in Tri-Carb Liquid Scintillation Counter (Perkin Elmer).

2.2.6 LKB1 and CaMKKβ activity assays

50µg tissue lysate was incubated with rabbit antiserum against LKB1 (Denison *et al.* 2009) or rabbit antiserum against CaMKKβ (Stahmann *et al.* 2006) for 2 h at 4°C. The resulting immune complexes were incubated with 800ng bacterially expressed AMPK α1β1γ1 complex (Neumann *et al.* 2003) and 10mM HGE, 100µM ATP, 5mM $MgCl_2$, 2mM DTT, with or without 2mM $CaCl_2$, 2µM Bovine Brain Calmodulin (Calbiochem) for CaMKKβ or LKB1 activation of AMPK respectively, for 10 min at 37°C. 200ng activated AMPK was added to 30µl SAMS assay mix with 10µl γ-^{32}P -ATP/$MgCl_2$, incubated for 15min at 30°C, and 20µl spotted onto P81 paper. To measure non-specific binding of P81 paper, 200ng activated AMPK was

added to 30µl SAMS Blank mix (1mM AMP, HGE with 1% (v/v) Triton-100 in 1:2 ratio) with 10µl γ-^{32}P -ATP/$MgCl_2$, incubated for 15min at 30°C, and 20µl spotted onto P81 paper. P81 paper was washed and activity counted as for measuring AMPK activity above. Background incorporation into SAMS peptide in the absence of upstream kinase was subtracted from LKB1/CaMKKβ activity for all results.

2.2.7 Primary hepatocyte isolation and culture

Hepatocytes were isolated by collagenase (Collagenase H, Roche) perfusion of the liver *in situ* under terminal anaesthesia (Foretz *et al.* 1998). Perfusion was carried out by Dr Angela Woods. Cells were collected by centrifugation for 3 min at 500g, and washed in perfusion buffer (Carboxygenated sterile HBSS buffer, pH 7.4 at 37°C containing 138mM NaCl, 50mM Hepes, 5.6mM Glucose, 5.4mM KCl, 0.34mM anhydrous Na_2HPO_4, 0.44mM KH_2PO_4, 4.17mM $NaHCO_3$, 0.5mM EGTA, 0.2µM $CaCl_2$). Cell viability was assessed by Trypan Blue prior to plating at 1.5 × 10^6 cells per well in collagen pre-coated 6 well tissue culture plates (Sigma) or 4 x 10^4 cells in collagen (Invitrogen) coated 24 well Seahorse plates (Seahorse Bioscience) in M199 with Earle's salts (Invitrogen) supplemented with 100 units/ml penicillin, 100 µg/ml streptomycin, 0.1% (w/v) bovine serum albumin, 2% (v/v) Ultroser G (Pall BioSepra), 100 nM dexamethasone (Sigma), 100 nM insulin (Invitrogen), 100 nM triiodothyronine (T_3) (Sigma). After 4 hrs at 37°C in a 5% CO_2 incubator, attached hepatocytes were changed into media with reduced insulin (1nM) and cultured overnight prior to treatments.

Hepatocyte treatments used include 0.6M sortibol for 10mins, 500µM AICAR for 30mins, and 2mM metformin for 2 h. Following treatment, hepatocytes were collected into 50mM Hepes pH7.4, 50mM NaF, 5mM NaPP, 1mM EDTA, 10% (v/v) glycerol with 1% (v/v) triton-100, 1mM DTT, 0.1mM PMSF, 1mM benzamidine, 4µg/ml trypsin inhibitor (HBA), lysed by freeze-thaw from -80°C, centrifuged for 15mins at 13000g at 4°C, and supernatant assayed for AMPK activity.

2.2.8 Glucose output measurement

Cultured hepatocytes were changed into Dulbecco's Modified Eagle's Medium (DMEM) without glucose (Sigma), 3.7g/l $NaHCO_3$, 2mM sodium pyruvate (Invitrogen), 20mM lactate (Invitrogen). Media was taken at various times following treatment. Glucose concentration in media was measured by a colorimetric glucose oxidase method using Enzymatic Glucose Reagent (Thermo Scientific) and calibrated using known glucose concentration standards.

2.2.9 Mitochondrial function

Hepatocyte mitochondrial function was assessed using the Seahorse XF24 System (Seahorse Bioscience). 24 well Seahorse plates (Seahorse Bioscience) were coated with 30µl per well of 0.3mg/ml of collagen (Collagen I rat tail, Invitrogen) in 0.02M acetic acid and dried overnight in laminar flow hood prior to plating of hepatocytes. Hepatocytes were cultured overnight following isolation at 37ºC with 5% CO_2. XF sensor cartridges (Seahorse Bioscience) were hydrated in 1ml per well of calibrant (Seahorse Bioscience) and incubated at 37ºC overnight without CO_2. Hepatocytes were washed and changed into Glycolysis Assay Medium pH 7.4 containing DMEM D5030 (Sigma), 143mM NaCl, 5mM glucose, 1nM insulin, and 100nM dexamethasone 1 h prior to assay and cultured at 37ºC without CO_2. Using the Seahorse XF24 system, Oxygen Consumption Rate (OCR) was measured at baseline, as well as following the sequential addition of respiratory chain inhibitors/uncouplers including 2µg/ml oligomycin, 0.5µM p-trifluoromethoxy carbonyl cyanide phenylhydrazone (FCCP), 20mM ascorbate with 5mM N,N,N',N'-tetramethyl-1,4-phenylene diamine (TMPD), and 5µM each of antimycin A and rotenone. OCR readings for each animal were taken from four hepatocyte wells and normalized to protein concentration in each well as measured by Bradford protein assay (Bio-Rad) (Bradford. 1976) following cell lysis.

2.2.10 Bone measurements

Long bones and tail vertebrae from 13-16 week old male mice were dissected and stored at 4°C in 70% (v/v) ethanol. Soft tissue was removed by gentle scraping. Digital X-ray images were recorded at 10-μm resolution using a Qados Faxitron MX20 variable kV point projection x-ray source (Cross Technologies plc.). Bone length was determined using ImageJ 1.41 software (http://rsb.info.nih.gov/ij/) (Bassett *et al.* 2010) and measurements calibrated by imaging a digital micrometer. Femoral cortical thickness was determined by averaging 5 measurements mid shaft.

2.2.11 Faxitron analysis of bone mineral density

Bone mineral density was measured by faxitron analysis (Bassett *et al.* 2010). Digital images were taken as described for bone measurements above, with the addition of a 1 mm thick steel plate, a 1 mm diameter spectrographically pure aluminium wire, and a 1 mm diameter polyester fiber. Images were converted to 8-bit Tiff format using ImageJ. Bone mineral density was measured by setting the grey level of the polyester to 0, and the grey level of steel to 255, then dividing the grey levels between 0 and 255 into 16 levels through converting to a pseudocolour scheme. The number of pixels of a particular colour representing a particular bone mineral density range is then counted using ImageJ 1.41 software.

2.2.12 Bone RNA extraction and reverse transcription

Following isolation of murine femur, soft tissue was immediately stripped off the bone which was then snap frozen in liquid nitrogen and stored at -80ºC. Bone was crushed using a pulverizer (BioSpec 59013N, Fisher Scientific) frozen by dipping in liquid nitrogen and kept cold on a block of dry ice. 1ml Trizol (Invitrogen) was added to each powdered bone prior to 3 min homogenisation on dry ice followed by a further 5 min homogenisation at room

temperature. Supernatant was collected following centrifugation at 12000g for 10 min at 4ºC. 200µl chloroform was added to the supernatant and thoroughly mixed by shaking for 15 sec before incubating at room temperature for 3 min and centrifugation at 12000g for 10 min at 4 ºC. The upper aqueous phase containing RNA was mixed with 0.53 volume of absolute ethanol and transferred onto an RNeasy column (Qiagen). RNA was extracted according to the RNeasy column protocol including on column DNase treatment. Concentration and purity of RNA was measured using the Nanodrop spectrophotometer (Nanodrop ND-1000, Thermo Scientific). A minimum absorbance ratio of 1.8 measured at 260/280 nm and 260/230 nm was set for all samples, any sample falling below this level was repurified.

Synthesis of cDNA was carried out with equal amounts of total bone RNA (1-2µg) using SuperScript II reverse transcriptase (Invitrogen) according to manufacturer's instructions in the presence of 200ng random primers and 500µM mixed dNTP.

2.2.13 Quantitative real-time PCR

Quantitative real-time PCR was carried out using 1 in 10 diluted cDNA added to 5µM each of the appropriate primers as well as 1x SensiMix SYBR (Bioline) containing SYBR Green I dye, 3mM $MgCl_2$ and dNTPs on a real-time thermo-cylcer (DNA Engine Opticon, Bio-Rad). Following polymerase activation at 95ºC for 10 min, 40 PCR cycles were performed with 15 s each of denaturation at 95ºC, annealing at 60ºC and extension at 72ºC. Primers were selected to produce 100-200bp amplicons spanning at least one exon-exon junction in the target mRNA (See Table 2.1). Satisfactory melting curves were obtained for all primers used.

All samples were analyzed in duplicate with Ct values measured in the exponential phase of the PCR reaction (OpticonMonitor Analysis Software Version 3.1, Bio-Rad), and relative expressions calculated using the $2^{-\Delta\Delta Ct}$ method (Schmittgen 2008). Glyceraldehyde 3-phosphate dehydrogenase (GAPDH) was used as the internal control for the quantification of gene expression. Samples treated without reverse transcriptase enzyme were used as negative controls.

2.2.14 Erythrocyte fragility test

Blood was collected in heparinized microvettes (Sarstedt), mixed and tested within 1 hour of collection. 10µl of blood was added to 2.5ml of increasing concentrations of $NaCl_2$ solution and incubated at room temperature for 30 min before centrifugation at 3000g for 5 min. Optical Density (OD) of the supernatant was measured at 540nm, and the percentage haemolysis calculated from OD measurements taking OD of distilled water as equivalent to 100% haemolysis.

2.2.15 Lipopolysaccharide (LPS) induction of sepsis

16-20 week old individually caged male animals were used for the induction of sepsis. *E.coli* LPS 0111:B4 (Sigma) was injected intraperitoneally at a dose of 8mg/kg. Temperature transponders (IPTT-300, BMDS) were inserted subcutaneously in the right flanks of animals 7 days prior to LPS induction to allow temperature reading using a scanner (Small Smart Reader IPTT, BMDS). Core body temperature was recorded both prior to LPS been given and 12 hours post sepsis induction either using the temperature transponder scanner or using the flexible temperature probe from Homeothermic Blanket System (Harvard Apparatus). All animals were monitored every 2-3 hours and assessed for sepsis severity. Following temperature measurement at 12 hours post induction, animals were sacrificed by cervical dislocation and blood was collected through cardiac puncture.

2.2.16 Serum cytokine measurements

Blood was collected in heparinized microvettes (Sarstedt) and centrifuged at 3000g for 30 min at 4°C. Serum was stored at -80°C until all samples collected. The concentration of cytokines including IL1β, IL6, IL10, TNFα and granulocyte macrophage colony stimulating factor (GM-CSF) were prepared in a multiplexed ELISA assay using fluorescent-coded magnetic beads according to kit instructions (Mouse Cytokine/Chemokine Magnetic Bead

Panel, Milliplex MAG Kit, Millipore), and analyzed on the MAGPIX plate reader (Millipore). Satisfactory results were obtained from quality control samples containing known concentrations of all measured cytokines provided as part of the kit.

2.2.17 Nitric oxide measurement

Greiss assay was used to determine nitrite formed by the spontaneous oxidation of NO under physiological conditions (Ignarro *et al.* 1987) in cell culture supernatant. Samples were incubated with 30µg/ml N-(1-naphthyl) ethylenediamine dihydrochloride and 300µg/ml sulfanilic acid in 0.17% (v/v) phosphoric acid for 30 min at room temperature. Absorbance was measured at 548nm on a spectrophotometer (SpectraMax Gemini, Molecular Probes) and nitrite concentration was calculated using sodium nitrite standards.

In serum samples, as NO is usually present in the form of nitrate, equal volume of 8mg/ml vanadium trichloride was added to serum prior to incubating with the components of the Greiss assay for 30 min at 37ºC. Absorbance was measured at 548nm on a spectrophotometer (SpectraMax Gemini, Molecular Probes) and nitrite concentration was calculated using sodium nitrate standards.

2.2.18 cGMP measurement

cGMP concentration in the serum and in the isolated aorta was measured using the cGMP complete Enzyme ImmunoAssay Kit (Enzo Life Sciences) according to kit instructions. The kit utilises a competitive binding assay using alkaline phosphatase conjugated cGMP and a pNpp substrate that is catalyzed by alkaline phosphatase to produce colourimetric readout. The acetylated format was used in the aorta samples to increase sensitivity. cGMP concentration was calculated from the standards supplied.

2.2.19 White cell count by flow cytometry

Cell viability was assessed by Trypan blue staining and cells aliquoted into 1-2 × 10^6 cells in 100µl Fluorescence-activated cell sorting (FACS) buffer (PBS+ 5% fetal calf seum) for antibody staining. Fluorescent antibody was added at a pre-determined, optimised concentration and the mixture incubated with shaking in the dark for 30min at 4ºC. Stained cells were washed twice in FACS buffer, then resuspended in 500µl FACS buffer and analysed on BD LSR II Flow Cytometer (BD Biosciences).

2.2.20 Splenocyte, thymocyte and lymph node cell isolation

Spleen, thymus and lymph nodes (axillary, inguinal and iliac) were isolated under aseptic conditions and stored in DMEM (Invitrogen) at 4ºC until ready to process. The spleen was forced through a 70µm cell strainer (BD Falcon) using a 5ml syringe plunger, washed twice with DMEM and the cells collected by centrifugation at 500g for 5 min. To lyse red blood cells, the packed cell pellet was resuspended in 1ml ACK lysis buffer (150mM NH_4Cl, 10mM $KHCO_3$, 130mM EDTA, pH7.4) and incubated for 5min at room temperature. The cell pellet was washed once more and resuspended in 1ml of DMEM or FACS buffer (PBS + 5% (v/v) fetal bovine serum).

2.2.21 Peritoneal macrophage isolation and culture

Primary macrophages were isolated by peritoneal PBS wash as described in Zhang *et al.* 2008. Following cervical dislocation, 5-8ml cold PBS was carefully injected into the peritoneal cavity then aspirated and cells in the peritoneal exudates were collected by 5min centrifugation at 400g. The isolated cells were stained with Trypan Blue to confirm viability and 2 × 10^5 nucleated cells were plated per well of 96 well tissue culture plates in macrophage culture media containing DMEM/F12 (Invitrogen), 10% (v/v) fetal bovine serum, 100units/ml penicillin, and 100ug/ml streptomycin. After incubation for 2h at 37°C in a 5%

CO_2 incubator, attached macrophages were washed three times with PBS to remove non-adherent cells leaving 1 × 10^5 macrophages per well for culture overnight prior to treatments as stated in the figure legends.

2.2.22 Macrophage activation

Cultured primary macrophages were primed overnight with IFNγ (eBioscience) and activated with *E.coli* LPS 0111:B4 (Sigma) (Mosser and Zhang, 2008). Macrophage activation was confirmed by measurement of NO production into the culture media using Greiss assay. Optimization with a range of IFNγ and LPS concentration show clear activation as measured by NO production was achieved with 200U/ml of IFNγ, and activated by 24 h treatment with 10ng/ml LPS (See Figure 2.1). Cultured macrophages are activated under these conditions unless otherwise stated.

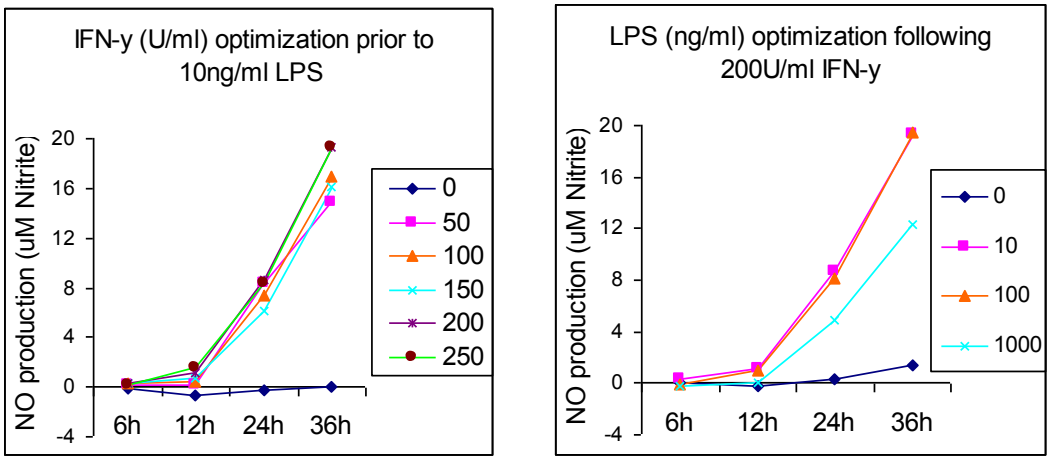

Figure 2.1 Optimization of primary macrophage activation with overnight IFNγ priming and LPS treatment.

2.2.23 Macrophage phagocytosis assay

The Vybrant Phagocytosis Assay Kit (Molecular Probes) was used to measure phagocytosis in activated primary macrophages. Cultured primary macrophages were activated by 24 h treatment with a range of LPS concentrations with or without priming with IFNγ. To measure phagocytosis, the macrophage culture media was aspirated and replaced with 100µg of fluorescent BioParticle suspension in 100µl Hanks' balanced salt solution (HBSS) and incubated for 2 h at 37ºC with 5% CO_2 in the dark. The macrophages are washed with 100µl Trypan Blue solution to remove non-phagocytosed BioParticles prior to measurement using a spectrophotometer at excitation/emission wavelength of 480nm and 520nm respectively. Macrophage samples from each mouse were run in triplicate.

2.2.24 Macrophage migration assay

Primary macrophages were plated on Transwell inserts (Corning) at a density of 1 x 10^5 cells per insert. 5µm pore size translucent polycarbonate 24 well Transwell inserts were used with an equivalent growth area of a 96 well plate well. 10ng/ml recombinant human Vascular Endothelial Growth Factor (VEGF) (PeproTech) was added to 600µl of macrophage culture media in the lower chamber of the Transwell and cells cultured for 6 h at 37ºC with 5% CO_2. Following VEGF stimulated macrophage migration, 3-(4,5-Dimethylthiazol-2-yl)-2,5-diphenyltetrazolium bromide (MTT) assay was used to measure the number of cells remaining on the insert. Macrophage samples from each mouse were run in duplicate.

2.2.25 3-(4,5-Dimethylthiazol-2-yl)-2,5-diphenyltetrazolium bromide (MTT) assay

MTT is converted to insoluble formazan following reduction of the tetrazolium ring by the mitochondria in living cells, dissolving the formazan crystals in DMSO produces a colour change that can be measured between absorbance 500nm and 600nm on a spectrophotometer (Mosmann 1983). 20µl of 5mg/ml MTT reagent (Sigma) was added to

each well of cultured primary macrophages on a 96 well plate, equivalent to each of the upper chambers of 24 well Transwell plate. Following incubation at 37ºC for 1h, the media was carefully removed and 100µl DMSO added. The absorbance of formazan dissolved in DMSO was measured at 590nm (Bio-Rad Model 680 Microplate reader).

2.2.26 Human umbilical vein endothelial cell (HUVEC) culture

HUVEC stock (Invitrogen) was found to be approximately 60% viable by staining with Trypan Blue solution (Sigma) and cultured at 37ºC with 5% CO_2 in Phenol red free Medium 200 (Invitrogen) with Low Serum Growth Supplement (Invitrogen). Final supplemented media contained 2% (v/v) fetal bovine serum, 1µg/ml hydrocortisone, 10ng/ml human epidermal growth factor, 3ng/ml basic fibroblast growth factor and 10µg/ml heparin. Cultured HUVEC was found to have a doubling time of around 24 hours. Cells were detached using 0.25% Trypsin-EDTA (Invitrogen) and split once they reached 70-80% confluency. All experiments were performed using HUVEC from passages 2-3.

2.2.27 HUVEC permeability assay

Transwell inserts (Corning) were coated with 100µl 125µg/ml Matrigel (BD Biosciences) and dried overnight in a laminar flow hood. 5µm pore size translucent polycarbonate 24 well Transwell inserts were used with an equivalent growth area of a 96 well plate well. 5×10^4 HUVEC cells were plated on the Matrigel-coated inserts and cultured for 72 h in HUVEC media to form a monolayer. 100µg of high molecular weight FITC-dextran (Sigma) was added to the HUVEC culture media in the insert and 600µl of HUVEC media was added to the lower chamber. The cells were cultured for 4 h before 50µl of the media in the lower chamber was collected and the fluorescence measured at the absorption/emission wavelength of 492/520nm on a spectrophotometer (SpectraMax Gemini, Molecular Probes).

The presence of the Matrigel layer was found to be essential for the formation of a HUVEC monolayer on the Transwell inserts.

2.2.28 Haematocrit measurement

Whole blood was obtained from incisions into the left ventricle of the heart following sacrifice of the animal and stored in heparinised eppendorfs (Microvette CB300 LH, Sarstedt) until all samples were collected. Micro-haematocrit tubes (Hawksley and Sons) were filled by capillary action and sealed on one end before centrifuged for 10 min at 12000 RPM at room temperature in a micro-haematocrit centrifuge (Microspin, Hawksley and Sons). The length of the red blood cell fraction along the tube as well as the total length of red blood cell, white blood cell and serum fractions was measured using a ruler. The haematocrit was calculated as the ratio between red blood cell fraction length and total length.

2.2.29 LPS sepsis study with STO-609 pretreatment

16-20 week old individually caged male animals were used for the induction of sepsis. Treatment animals were injected intraperitoneally with 10µg/kg of STO-609 (Tocris Bioscience) in 55-65µl 10mM NaOH both 18 h prior to LPS sepsis induction and again just prior to the LPS injection. Control animals were injected twice with 60µl 10mM NaOH only. STO-609 is commonly dissolved in DMSO, however 2 intraperitoneal injections of 100µl DMSO, the volume required for STO-609 treatment at 10µg/kg, was found to effect the severity of LPS sepsis and reduce the temperature drop seen over 12 h. In addition to DMSO and NaOH, STO-609 is also known to be soluble in ethanol.

Following treatment with STO-609, or NaOH only in control animals, *E.coli* LPS 0111:B4 (Sigma) was injected intraperitoneally at a dose of 8mg/kg, and animals were monitored every 2-3 hours and assessed for sepsis severity. Core body temperature was taken both prior to LPS administration and 12 h post sepsis induction using the flexible probe from Homeothermic Blanket System (Harvard Apparatus). Following temperature measurement at 12 h post induction, animals were sacrificed by cervical dislocation and blood was collected through cardiac puncture.

2.2.30 Telemetry transmitter implantation

Implantable mouse BP transmitters (TA11PA-C10, Data Sciences International) were used to measure heart rate, arterial pressure and activity level in 16-18 week old individually caged male animals. The surgical implantation of the telemetry transmitters was kindly carried out by Dr Zhen Wang (Nitric Oxide Signalling Group, MRC Clinical Sciences Centre). Briefly, the mice were anaesthetized with inhaled isofluorane (Abbott); the carotid artery of the mouse was accessed with a ventral midline incision; the left carotid artery was isolated with fine-tipped vessel dilation forceps then punctured with a catheter introducer and the telemetry catheter was inserted into the vessel; 3-4mm of the catheter was advanced into the thoracic aorta and the catheter was secured in place with sutures around the aorta. Through the same incision a subcutaneous tunnel was formed along the right flank and enlarged to form a pocket where the body of the transmitter containing the battery pack was placed. 0.05mg/kg buprenorphine (Alstoe Animal Health) was given by subcutaneous injection just before suture closure of the ventral incision.

2.2.31 Telemetry recording

The animals were left to recover for at least 7 days before telemetry recordings were made using receiver pads (RPC1, Data Sciences International) connected via a data exchange matrix to the Dataquest A.R.T acquisition system and analysis system (Data Sciences International). Heart rate, systolic and diastolic blood pressure, and activity level were recorded from each animal every 10 seconds for 50-60 hours under control conditions and over 8 hours during LPS treatment. For high salt treatment, recordings were made for 2 days prior to and 7 days following the start of the high salt diet, as well as on days 13 and 14 of the high salt diet.

Statistical analysis of telemetry data performed by the Imperial statistics department. Curve fitted by quadratic model, polynomial of degree two, and analysis carried out using SPSS V21.

2.2.32 Aorta lysate preparation

Following isolation of murine thoracic and abdominal aorta down to the celiac trunk, the outer layer of fat and adventitia was immediately stripped off in 4ºC PBS under the dissecting microscope, prior to snap freezing the aorta in liquid nitrogen and storage at -80ºC. Frozen aorta samples were crushed in liquid nitrogen using pestle and mortar before homogenization in HBA. Following centrifugation, the supernatant was collected for activity assays. The pellet was further extracted by dissolving in urea lysis buffer (0.57g/ml urea, 5% (v/v) β-mercaptoethanol, 2% (v/v) Igepal CA-630 (Sigma), 1% (v/v) Pharmalytes buffer pH 3-10 (GE Healthcare), Halt Protease and Phosphatase Inhibitor Cocktail (Pierce)) for 2 min at room temperature. Supernatant was collected following centrifugation at 13000g at 4°C for 15-20min and used for polyacrylamide gel electrophoresis and western blotting.

2.2.33 Polyacrylamide gel electrophoresis

Between 30-75ug of each tissue lysate sample was denatured for 10min at 70ºC with sample buffer (25mM Tris-HCl pH 7.4, 2.5% (v/v) SDS, 1% (v/v) β-mercaptoethanol, 10% (v/v) glycerol, 0.05% (v/v) bromophenol blue), loaded onto Precast Bis-Tris 4-12% polyacrylamide gels (Bio-Rad), and electrophoresed at 200V for 50-60 min in 1x SDS-PAGE running buffer (10x SDS-PAGE Running Buffer, National Diagnostics) in the XCell SureLock Mini-Cell electrophoresis System (Invitrogen). At least one well per gel was loaded with a protein ladder (PageRuler or PageRuler Plus Prestained Protein Ladder, Thermo Scientific).

2.2.34 Western blotting

Proteins separated by polyacrylamide gel electrophoresis were transferred onto PVDF membrane (Millipore Immobilon-FL Transfer Membrane, pore size 0.45μM) by wet transfer using Mini Trans-Blot Cell (Bio-Rad). Both polyacrylamide gel and methanol pre-soaked PVDF were sandwiched between chromatography paper (Whatman) and foam pads inside

the transfer cassette (Bio-Rad). Protein transfer was carried out at 100V for 80 min at 4ºC in transfer buffer (25mM Tris-HCl pH 7.4, 192mM glycine, 20% (v/v) methanol), and protein transfer was confirmed with 0.2% (v/v) ponceau red stain (Sigma).

Following transfer, membranes were blocked with TBS (10mM Tris-HCl pH 7.4, 150mM NaCl, 0.1% Tween 20) with 3% (w/v) BSA for 60 min at room temperature, prior to blotting with primary antibody in TBS with 3% (w/v) BSA overnight at 4ºC. Membranes were washed in TBS and blotted with the appropriate secondary antibody against the primary antibody in HST (10mM Tris-HCl pH 7.4, 500mM NaCl, 0.5% (v/v) Tween 20) with 2% (w/v) milk powder for 60 min at room temperature. Membranes were washed before visualisation using the Odyssey Imaging System (LI-COR Biosciences).

2.2.35 MLCK activity assay

Immunoprecipitation from 30µg tissue incubated with mouse antibody against total MLCK (Clone K36, ascites fluid, Sigma). To measure non-specific antibody binding, immunoprecipitation also carried out with no antibody. Immune complexes were added to 30µl MLCK assay mix (1mM AMP, 1mM $CaCl_2$, 1µM Bovine Brain Calmodulin (Calbiochem), 1mM MLCK smooth muscle substrate peptide [KKRAARATSNVFA] (Sigma), HGE with 1% (v/v) Triton-100), 10µl HGE and 10µl [γ-^{32}P]ATP/$MgCl_2$ (1mM ATP (Perkin Elmer), 25mM $MgCl_2$,), before incubating for 30min at 30°C. Immune complexes then spun down at 13000g and 20µl supernatant spotted onto P81 paper (Whatman). P81 paper washed in 1% (v/v) orthophosphoric acid, blotted dry, then counted for 30 s in Tri-Carb Liquid Scintillation Counter (Perkin Elmer).

2.2.36 Aorta immunohistochemistry

Whole animal perfusion and fixation was carried out in CO_2 sacrificed animals with first phosphate buffered saline (PBS) then 4% (w/v) formaldehyde prior to tissue isolation. Aortas were paraffin mounted, sectioned and stained by C&C Lab Services, High Wycombe, UK.

Images were captured using a Zeiss upright microscope (Axiophot, Zeiss) at the specified magnifications. All measurements were taken using ImageJ 1.41 software.

2.2.37 Urinary epinephrine and electrolyte measurements

Urine samples were collected between 9AM and 10AM from 14-18 week old male mice and spun down to remove cells before storage at -80°C until all samples collected. Urinary epinephrine and creatinine levels as well as sodium and potassium concentrations were determined by the Mouse Biochemistry Laboratories, Cambridge, UK.

2.2.38 High salt study

Mouse BP transmitters (TA11PA-C10, Data Sciences International) were implanted in the thoracic aortas of 16-20 week old individually caged male animals as described previously. The mice were fed control diet (0.32 % NaCl) made by soaking the standard mouse chow pellets (Rat and Mouse No. 3 Breeding Diet, Special Diet Services) in distilled water (150 ml distilled water per 100g of pellets) at 4ºC overnight. Animals were left for at least 7 days before telemetry recordings were made for 48 h to measure baseline heart rates, arterial pressures and activity levels.

A high salt diet (8.32 % NaCl) was made by dissolving 8g of NaCl (VWR International) in the 150ml distilled water prior to soaking 100g of pellets at 4ºC overnight. All animals were given free access to water. Telemetry recordings were made over the course of two weeks to measure baseline heart rates, arterial pressures and activity levels. Animals tolerated both control and the high salt diet as seen by maintenance of bodyweight over the course of two weeks.

2.2.39 Wire myography

14-16 weeks old male mice were used for the assessment of aorta contractility by wire myography kindly carried out by Miss Anna Slaviero (MRC Clinical Sciences Centre). Following sacrifice, murine thoracic aortas were isolated, dissected into 2mm thickness rings and mounted on a wire myography system (Multi-Wire Myography System 610M, DMT). Aorta rings were maintained at 37ºC under 95% O2 and 5% CO2, and washed with physiological salt solution (NaPSS) pH 7.4 containing 118.4mM NaCl, 4.7mM KCl, 1.2mM $MgSO_4$, 1.2mM KH_2PO_4, 24.9mM $NaHCO_3$, 2.5mM $CaCl_2$, 11.1mM glucose and 0.023mM EDTA to allow basal tension recordings. Maximum tensions were also recorded following treatment with potassium salt solution (KPSS) pH 7.4 containing 125mM KCl, 1.2mM $MgSO_4$, 1.2mM KH_2PO_4, 24.9mM $NaHCO_3$, 2.5mM $CaCl_2$ and 11.1mM glucose. Aorta rings were treated with incremental concentrations of phenylephrine (Sigma) and tensions recorded. Incremental sodium nitroprusside (SNP) (Sigma) and acetylcholine (Sigma) treatments were carried out following KPSS treatment and tension recordings made. Basal tension was established in between treatments by washing aorta rings with NaPSS. Measurements were recorded in duplicate samples from each animal.

Data collection and analysis was performed using LabChart 6.0 (ADInstruments).

2.2.40 Cardiac ultrasound

Longitudinal assessment of cardiac function was carried out in male mice over six months. The animals were scanned by ultrasound at 30MHz (Vevo770 system, Visualsonics) under inhaled isofluorane anaesthesia every month between 4 month and 10 month of age to obtain measurements of left ventricle mass, left ventricle wall thickness, left ventricle shortening fraction, and ejection fraction.

2.2.41 Statistical analysis

Bone mineral density data analyzed using Kolmogorov-Smirnov test. Analysis by ANOVA (2-way) and student's t-test were performed using Prism 5 (GraphPad). All data in figures presented as Mean ± Standard Error Mean (SEM) unless otherwise stated. In Chapter 5, statistical analysis of telemetry results was carried out by the Imperial statistics department. The methodology used in the analysis was Mixed Model applied longitudinal data.

Chapter 3. Global phenotyping

In a previous study, global CaMKKβ KO mice were found to have impaired long term memory due to disruptions to the CaMK cascade and no overt physical abnormality (Peters *et al.* 2003). Since, then, conflicting data has been published regarding the food intake and glucose metabolism in separate cohorts of global CaMKKβ KO mice (Means *et al*. 2008; Claret *et al*. 2011). In addition, LKB1 has been shown to preferentially phosphorylate the α2 subunit of AMPK, leading to the suggestion that CaMKKβ may preferentially phosphorylate the α1 subunit of AMPK (Sakamoto *et al.* 2005; Sakamoto *et al*. 2006). This section aims to clarify the role of CaMKKβ in energy metabolism and assess its AMPK isoform preferences in various tissues.

3.1 Global Phenotyping Results

3.1.1 Confirmation of Genotype

The absence of exon 5 in the CaMKKβ KO mice was confirmed by PCR genotyping (Figure 3.1A). Absence of expressed CaMKKβ protein in specific tissues of KO mice was further confirmed by CaMKKβ activity assays of tissue lysates (Figure 3.1B). The addition of Ca^{2+} and calmodulin is required by CaMKKβ immunoprecipitated from tissue lysates for the activation of recombinant AMPK, shown by negligible CaMKKβ acitivity seen without the addition of Ca^{2+} and calmodulin (Figure 3.1B). This is in keeping with published results showing activation of CaMKKβ is required for maximum activity in non bacterially expressed CaMKKβ (Green *et al*. 2011; Tokumitsu *et al*. 2001).

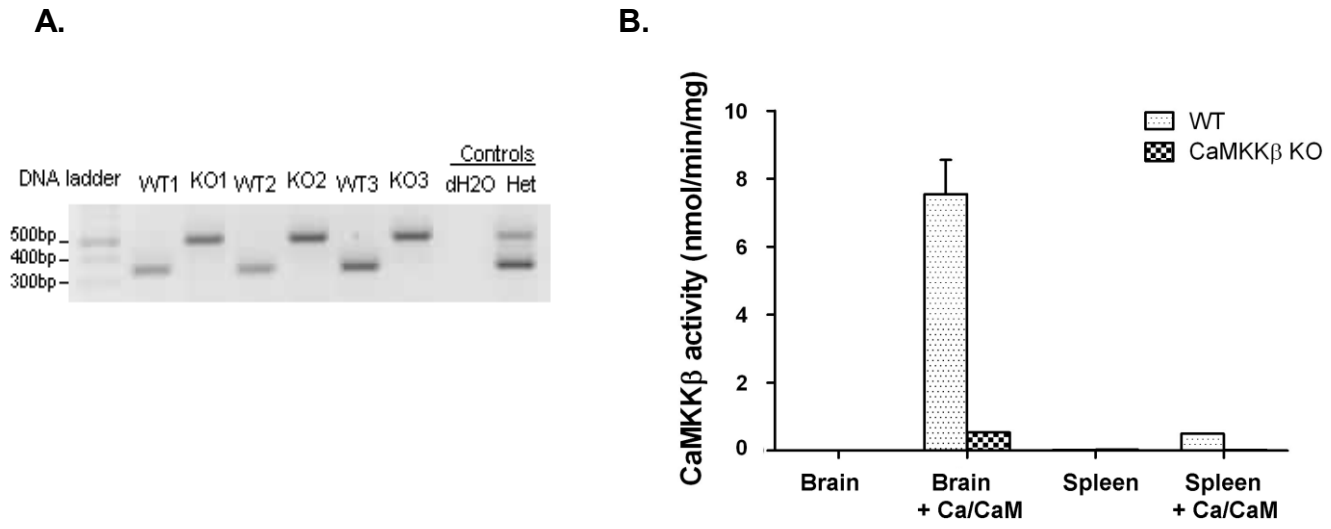

Figure 3.1 Confirmation of CaMKKβ exon deletion and loss of CaMKKβ activity in tissue.

A. Primers designed to differentiate between full length CaMKKβ and alleles with exon 5 deleted were used to amplify DNA from murine ear snip samples by PCR. Products of the expected size, 350bp for the WT allele and 500bp for the KO allele, were detected as shown by the representative agarose gel. **B.** CaMKK β activity in immunoprecipitates from brain and spleen lysates from WT and CaMKKβ KO mice. assayed with (Brain+Ca/CaM and Spleen+Ca/CaM) and without calcium and calmodulin (Brain and Spleen). Activity measured in CaMKKβ immunoprecipitates from tissue lysates by activation of recombinant AMPK α1β1γ1 in the presence or absence of calcium and calmodulin, followed by measurement of recombinant AMPK α1β1γ1 activity by SAMS peptide assay. Results presented as AMPK activity in nmoles [γ^{32}P] incorporation into the peptide per minute per milligram tissue lysate. Assays carried out in triplicate. Results shown are means ± SEM. n=2.

3.1.2 Body weight and composition

During the course of this study, Claret *et al* published results showing CaMKKβ KO mice had similar dietary intake, glucose tolerance, and plasma insulin concentration to WT mice (Claret *et al*. 2011). In our study, no difference was seen in the consumption of food pellets between the WT and CaMKKβ KO mice. At 16 weeks old, there was no difference in body weight between WT, CaMKKβ KO, or CaMKKα KO mice (Figure 3.2A). To assess glucose metabolism, the mice were fasted overnight and blood glucose concentrations were recorded. Consistent with results seen by Claret *et al.* no significant difference was seen in the fasting blood glucose concentrations of CaMKKβ KO mice compared to WT mice (Figure 3.2B). Lipid metabolism was initially assessed by quantifying the accumulation of fat mass. To assess the contribution of fat and muscle mass to body weight, the mice were scanned by Magnetic resonance imaging (MRI) and the percentage body composition of fat and lean muscle was quantified. CaMKKβ KO mice were found to have no significant difference in the percentage of fat and lean muscle compared to WT mice (Figure 3.2C). In addition, no difference was seen when the percentage of fat composition was normalized to either body weight or percentage body composition of lean muscle (Figure 3.2D).

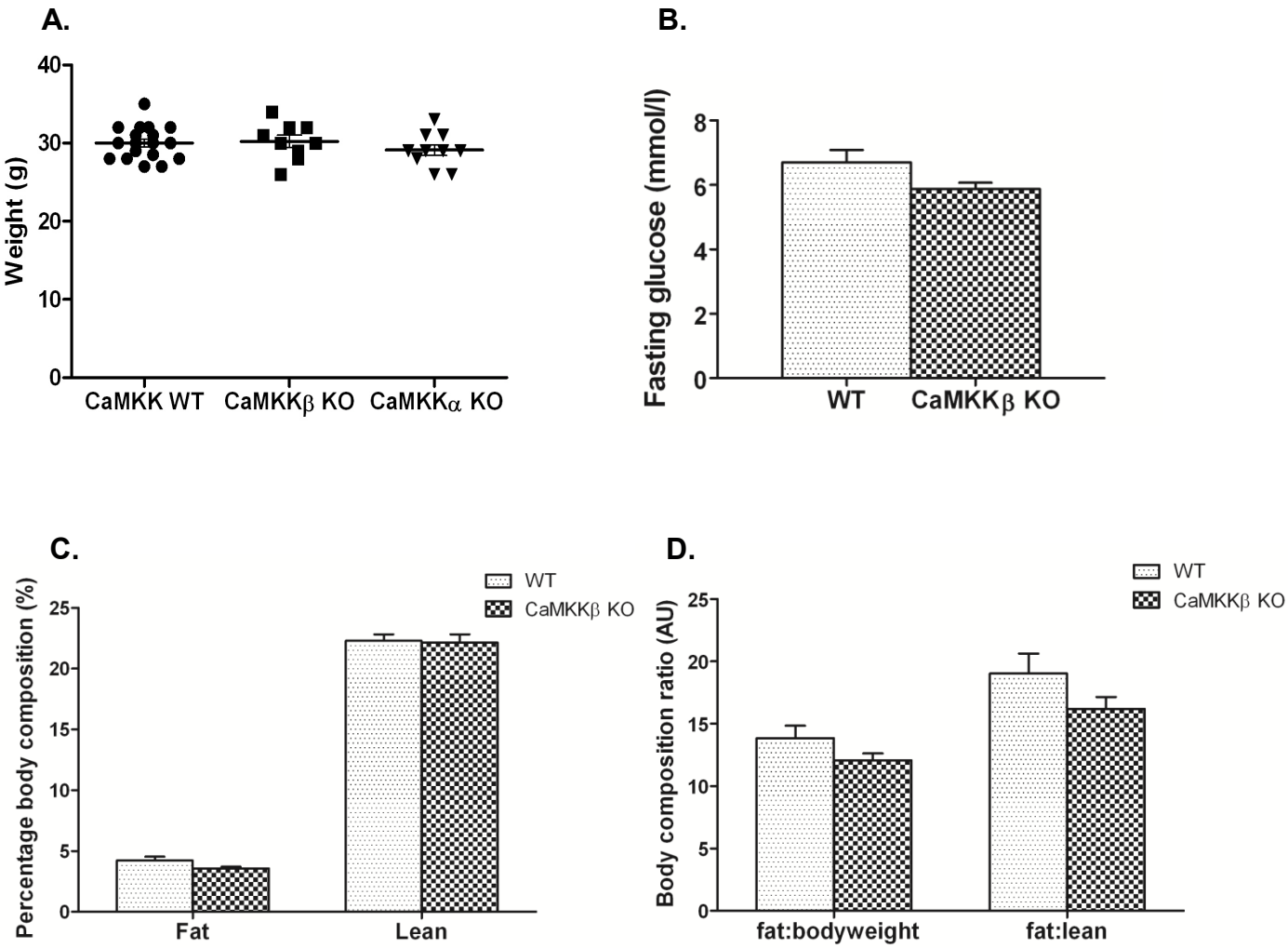

Figure 3.2 Body weight and fat composition of CaMKKβ KO mice.

A. Body weights of 16 week old mice on standard chow diet. WT n=18, CaMKKβ KO n=9, and CaMKKα KO n=10. **B.** Blood glucose concentrations following overnight fast. WT n=5, CaMKKβ KO n=8. **C.** Percentage of fat (Fat) and muscle (Lean) composition in WT and CaMKKβ KO mice as quantified by MRI. WT n=5, CaMKKβ KO n=8. **D.** Ratio comparing percentage body composition of fat against either body weight or muscle. WT n=5, CaMKKβ KO n=8. All results shown in this figure are means ± SEM.

3.1.3 Serum metabolites

Lipid metabolism in the CaMKKβ KO mice was further assessed through measuring cholesterol synthesis and triglyceride breakdown. Serum metabolites from WT, CaMKKβ KO and CaMKKα KO mice were measured. No significant difference in serum total cholesterol, HDL, LDL, triglyceride or free fatty acid concentrations was seen between WT and CaMKKβ KO mice (Figure 3.3).

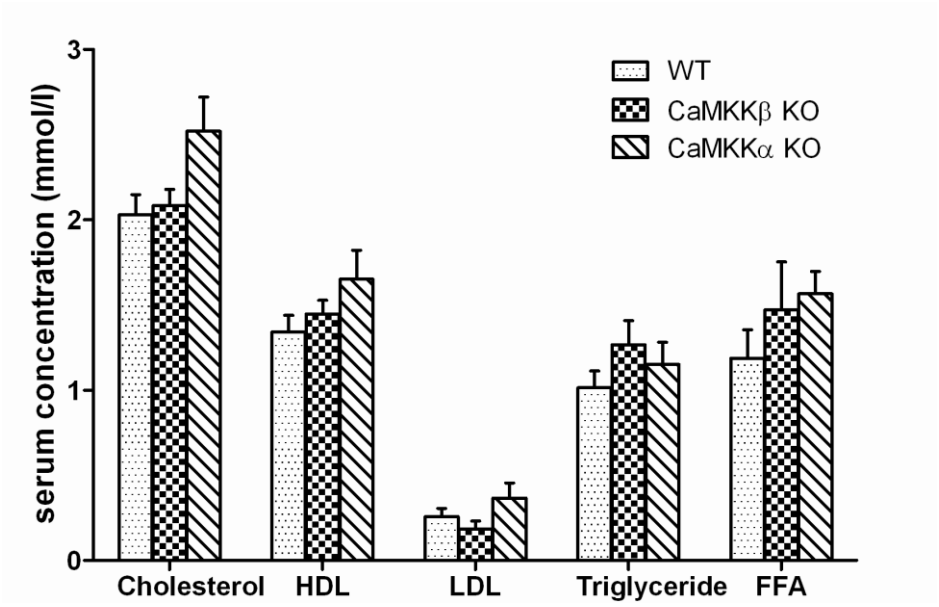

Figure 3.3 Serum metabolite measurements from WT, CaMKKβ KO, and CaMKKα KO mice. Results shown are means ± SEM. n=6.

3.1.4 Primary hepatocyte function

The CaMKKβ KO mice appeared to have normal body weight, fasting glucose, body composition and lipid metabolism. However, during the data collection period for this thesis, a study was published showing reduced hepatocyte glucose production in the liver specific CaMKKβ KO mice (Anderson *et al*. 2012). AMPK is phosphorylated by CaMKKβ and AMPK activity is known to be important for hepatic metabolism, including glucose production and fatty acid synthesis (Andreelli *et al*. 2006; Carling *et al*. 1989; Viollet *et al*. 2009). Therefore, the effect of CaMKKβ deletion on liver glucose production and hepatic AMPK activity was investigated.

3.1.4.1 Hepatic glucose production

To investigate hepatic glucose production, primary hepatocytes were isolated from both WT and global CaMKKβ KO mice by *in situ* perfusion with collagenase. Cells were treated with or without metformin for 2h to look at short term effects and after 24h treatment for longer, possible transcriptional effects. Hepatic glucose production was assessed by measuring the glucose output into the media. Metformin treatment was found to reduce hepatic glucose production (Figure 3.4). No significant difference was seen after 2 or 6 hour in glucose output between WT and CaMKKβ KO hepatocytes in the presence or absence of metformin. (Figure 3.4). This shows that in this model the deletion of CaMKKβ does not affect hepatocyte glucose output.

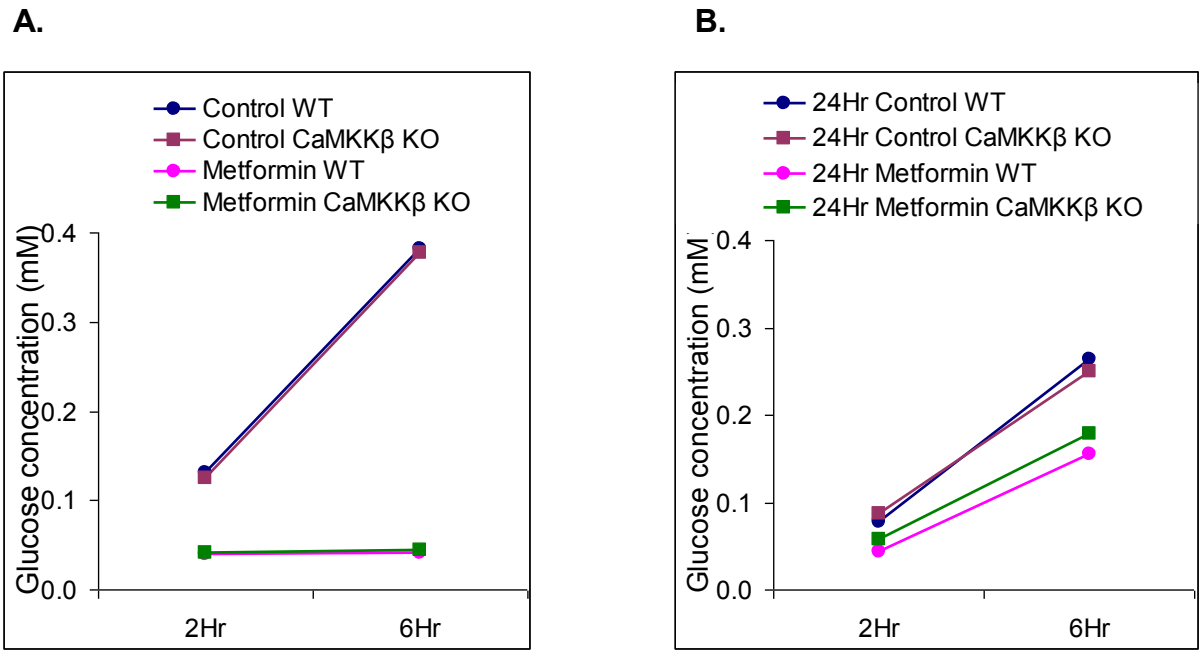

Figure 3.4 Glucose output by WT and CaMKKβ KO cultured primary hepatocytes. Glucose output following 2h or 24h treatment with 500μM Metformin, compared to untreated controls. Assays carried out in duplicate. **A.** 2 hour metformin treatment. **B.** 24 hour metformin treatment. Mean results shown. n=3-4.

3.1.4.2 Hepatic AMPK activity and mitochondrial respiration

The affect of CaMKKβ deletion on both liver and primary hepatocyte AMPK activity was also investigated. Due to the effect of altering nucleotide levels after dissection of liver we also investigated AMPK levels in isolated hepatocytes which were harvested in a way as to avoid causing alterations in ATP:ADP ratios. However, there was no significant difference in AMPK activity in either total liver lysates or isolated primary hepatocyte lysates from WT and CaMKKβ KO mice (Figures 3.5 and 3.8). The cultured primary hepatocytes were treated with various compounds known to alter AMPK activity. AMPK activity was similarly increased in WT and CaMKKβ KO hepatocytes treated by either sorbitol, AICAR, or Metformin (Figure 3.5).

AMPK is also known to activate PGC1α in hepatocytes and skeletal muscle cells (Guigas *et al*. 2007; Jäger *et al.* 2007); therefore the involvement of CaMKKβ in hepatocyte mitochondria biogenesis was investigated. Mitochondrion function was assessed in the WT and CaMKKβ KO primary hepatocytes by measuring oxygen consumption at basal levels, through the inhibition of ATP synthase by oligomycin, as well as through electron transport inhibition by antimycin A and rotenone, using a Seahorse XF24 Analyser to measure oxygen consumption. FCCP was added to stimulate mitonchondrial respiration by uncoupling ATP synthesis from electron transport, and complex IV activation was confirmed by the addition of ascorbate and TMPD. Primary hepatocytes from CaMKKβ KO mice were found to have normal mitochondrial function (Figure 3.6).

These results suggest the deletion of CaMKKβ does not appear to affect hepatic AMPK activity or hepatocyte mitochondrial function.

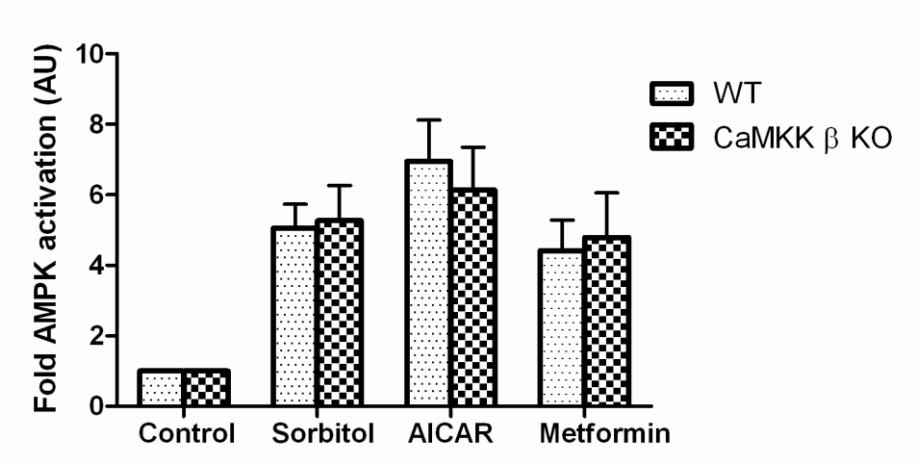

Figure 3.5 AMPK activity in cultured primary hepatocytes from WT and CaMKKβ KO mice following AMPK activation treatment.

Primary hepatocytes isolated from WT and CaMKKβ KO mice by *in situ* perfusion with collagenase. Cultured hepatocytes were treated as follows: Control: untreated, Sorbitol: 0.6M for 10min, AICAR: 500μM for 30min, Metformin: 2mM for 2h. Cells were lysed rapidly into buffer and snap frozen. AMPK activity was measured in immunoprecipitates by the SAMS peptide in a radioisotope incorporation assay. Results are shown as fold AMPK activation normalised to total AMPK activity in untreated cells. Assays carried out in duplicate. Results shown are means ± SEM. n=3-4.

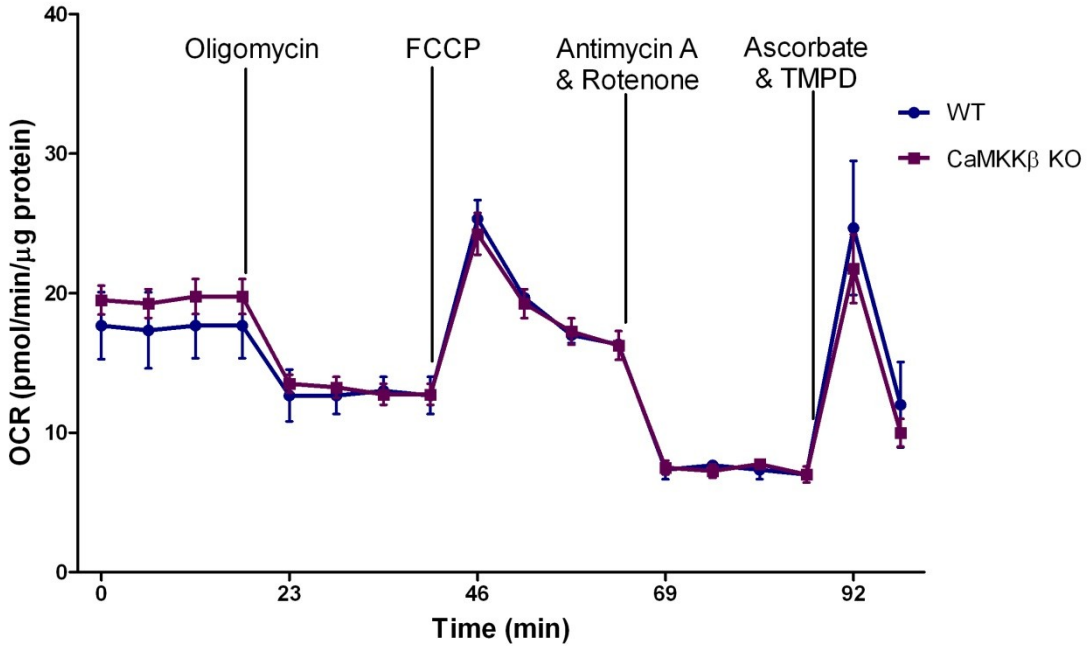

Figure 3.6 Hepatocyte mitochondrial function.

Mitochondrial function of primary hepatocytes isolated from WT and CaMKKβ KO mice was assessed using The Seahorse to measure oxygen consumption rate (OCR) at basal respiration and following treatment with 2μg/ml oligomycin, 0.5μM FCCP, 5μM each of antimycin A and rotenone, and 20mM ascorbate with 5mM TMPD. Assays carried out in triplicate. Results shown are means OCR normalised to protien concentration ± SEM. WT n=3, CaMKKβ KO n=4.

3.1.5 Kinase activity in tissue lysates

In the absence of an obvious global phenotype, the presence of a tissue specific phenotype was investigated. Initially, the activity of CaMKKβ, AMPK and LKB1 was measured in a panel of tissues.

3.1.5.1 Tissue specific CaMKKβ activity

CaMKKβ activity was measured in a panel of WT tissues by immunoprecipitation and activation of recombinant AMPKα1β1γ1 complex. Brain and testes were found to have the highest CaMKKβ activity; with several tissues including spleen, aorta and prostate having moderate CaMKKβ activity. Heart, liver and muscle were found to have negligible CaMKKβ activity (Figure 3.7).

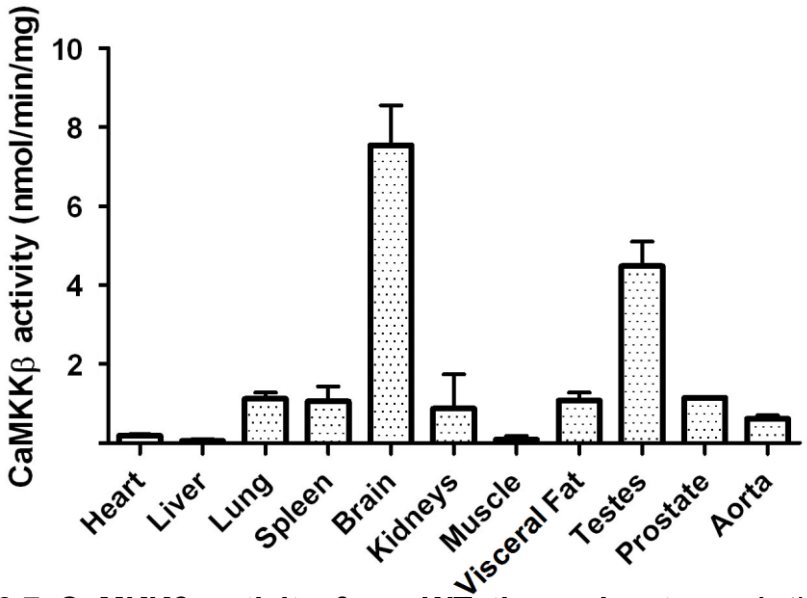

Figure 3.7 CaMKKβ activity from WT tissue lysates. Activity measured in CaMKKβ immunoprecipitates from tissue lysates by activation of recombinant AMPK α1β1γ1 in the presence of calcium and calmodulin, followed by measurement of recombinant AMPK α1β1γ1 activity by incubation with SAMS peptide in a radioisotope incorporation assay. Results presented as nmoles [γ-^{32}P] incorporation into the peptide per minute per milligram tissue lysate. Results shown are means ± SEM. n=4; testes and erythrocytes n=3.

3.1.5.2 Tissue specific AMPKα1 and AMPKα2 activity

AMPK activity was measured in a panel of tissues from WT and CaMKKβ KO mice (Figure 3.8A and 3.8B). To investigate the presence of an AMPKα subunit specific phenotype, complexes containing AMPKα1 and AMPKα2 subunits were isolated by immunoprecipitation before AMPK activity was measured. Consistent with published literature, AMPKα2 activity was found to be highest in the heart, followed by the liver (Figure 3.8B). Lung, spleen and fat tissue had very little AMPKα2 activity; and AMPKα2 activity was negligible in erythrocytes (Figure 3.8B). In contrast, AMPK α1 activity was found to be significantly higher in spleen than all other tissues assayed (Figure 3.8A). Interestingly, the variation in tissue specific AMPKα1 activity appeared to mirror the CaMKKβ activity seen (Figure 3.7 and 3.8A), excluding brain with particularly high CaMKKβ activity and spleen with particularly high AMPKα1 activity. No significant difference was found in liver, skeletal muscle or adipose tissue lysates between CaMKKβ WT and KO. Strikingly, spleen and erythrocyte lysates from CaMKKβ KO mice showed significantly reduced AMPKα1 activity compared to WT mice (Figure 3.8A), though no compensatory change in AMPKα2 activity was seen (Figure 3.8B). No difference in AMPKα2 activity was seen between WT and CaMKKβ KO mice (Figure 3.8A).

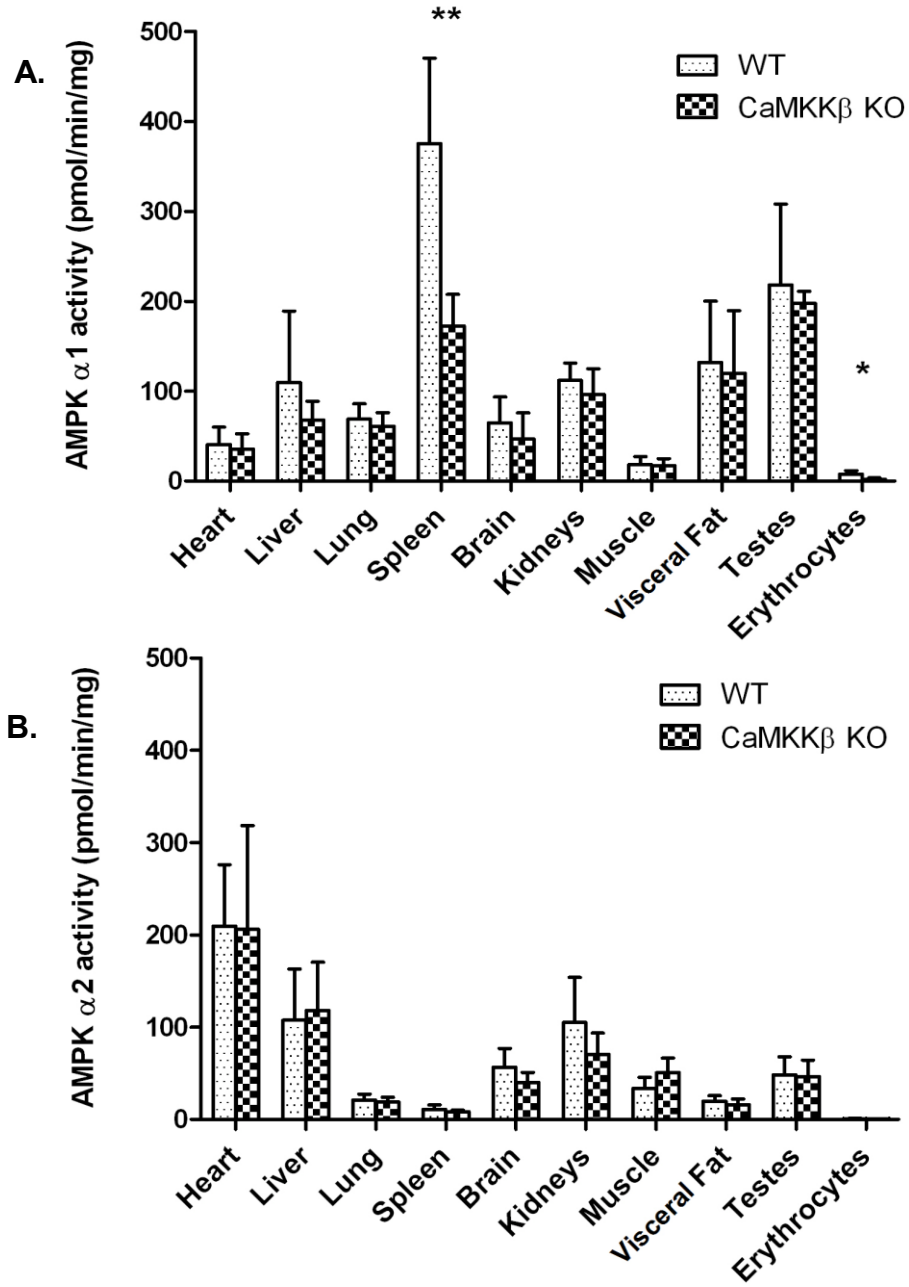

Figure 3.8 Comparing AMPK activity in a panel of tissues from WT and CaMKKβ KO mice. **A.** Activity of AMPKα1 complexes in WT and CaMKKβ KO murine tissue lysates measured by immunoprecipitating AMPKα1 from the respective tissues followed by incubation with SAMS peptide in a radioisotope incorporation assay. ** Comparison between WT and CaMKKβ KO spleen lysate. * Comparison between WT and CaMKKβ KO erythrocyte lysate. **B.** Activity of AMPKα2 complexes in WT and CaMKKβ KO murine tissue lysates measured by immunoprecipitating AMPKα2 from the respective tissues followed by incubation with SAMS peptide in a radioisotope incorporation assay. All assays carried out in duplicate. All results presented as pmoles [γ-^{32}P] incorporation into the peptide per minute per milligram tissue lysate. All results shown in this figure are means ± SEM. n=4; testes and erythrocytes n=3. Student's *t*-test: **P<0.01; *P<0.5.

3.1.5.3 Tissue specific LKB1 activity

To address the possibility of compensation by increased LKB1 activation of AMPK in the absence of CaMKKβ, LKB1 was immunoprecipitated from the panel of WT and CaMKKβ KO tissue lysates and LKB1 activity was measured by activation of recombinant AMPK α1β1γ1. The highest LKB1 activity was seen in the lysates of testes and brain; with moderate activity seen in heart, liver, lung, spleen, kidney, muscle and fat; and low activity seen in erythrocytes. No significant difference was seen in LKB1 activity between CaMKKβ KO and WT tissue lysates (Figure 3.9).

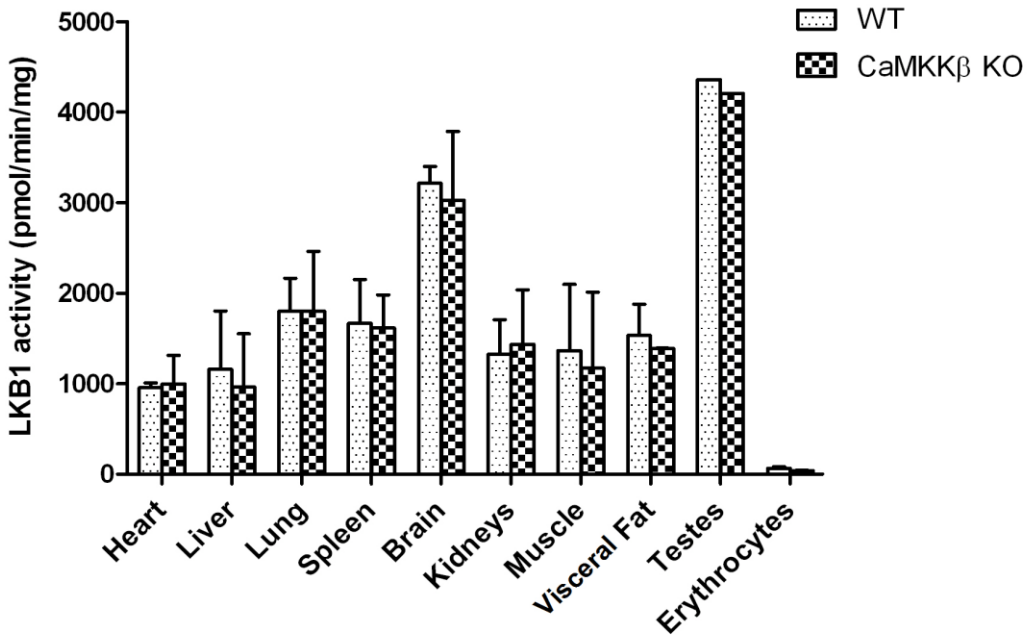

Figure 3.9 LKB1 activity from tissue lysates.

Activity measured in LKB1 immunoprecipitates from tissue lysates by activation of recombinant AMPK α1β1γ1, followed by measurement of recombinant AMPK α1β1γ1 activity by incubation with SAMS peptide in a radioisotope incorporation assay. Assays carried out in triplicate. Results presented as pmoles [γ-^{32}P] incorporation into the peptide per minute per milligram tissue lysate. Results shown are means ± SEM except for testes. Testes n=1, all other tissues n=2.

3.1.6 CaMKK β KO mice have normal bone length and bone density

The suggestion that CaMKKβ may be involved in bone turnover was raised by several studies showing associations between the CaMK cascade with the proliferation and functions of osteoblasts (Pederson *et al*. 2008; Oury *et al*. 2010). In addition, AMPKα1 was also shown to be involved in trabecular bone formation (Shah *et al*. 2010). Both osteoclasts and osteoblasts are known to express only AMPKα1 subunit as part of the AMPK complex (Shah *et al*. 2010). As deletion of CaMKKβ appears to only affect AMPKα1 activity (Figure 3.8), we thought it worthwhile to investigate the presence of a bone phenotype in the CaMKKβ KO mice.

Femurs, tibiae, humeri and radii were isolated from WT and CaMKKβ KO mice, and measured for changes to bone length and bone mineral content. However, no significant difference was detected in long bone length, femur cortical thickness or in the tibial ulnar ratio (Figure 3.10A). There was also no significant difference in bone mineral density content between WT and CaMKKβ KO mice (Figure 3.10C).

To investigate potential compensation by CaMKKα and LKB1, RNA was extracted from crushed murine femurs and gene expression was measured by cDNA synthesis through reverse transcription followed by quantitative real-time PCR. An increase of around two fold was seen in the expression of both CaMKKα and LKB1 in CaMKKβ KO bone compared to WT (Figure 3.10D); however statistical significance was not reached due to large variations within groups.

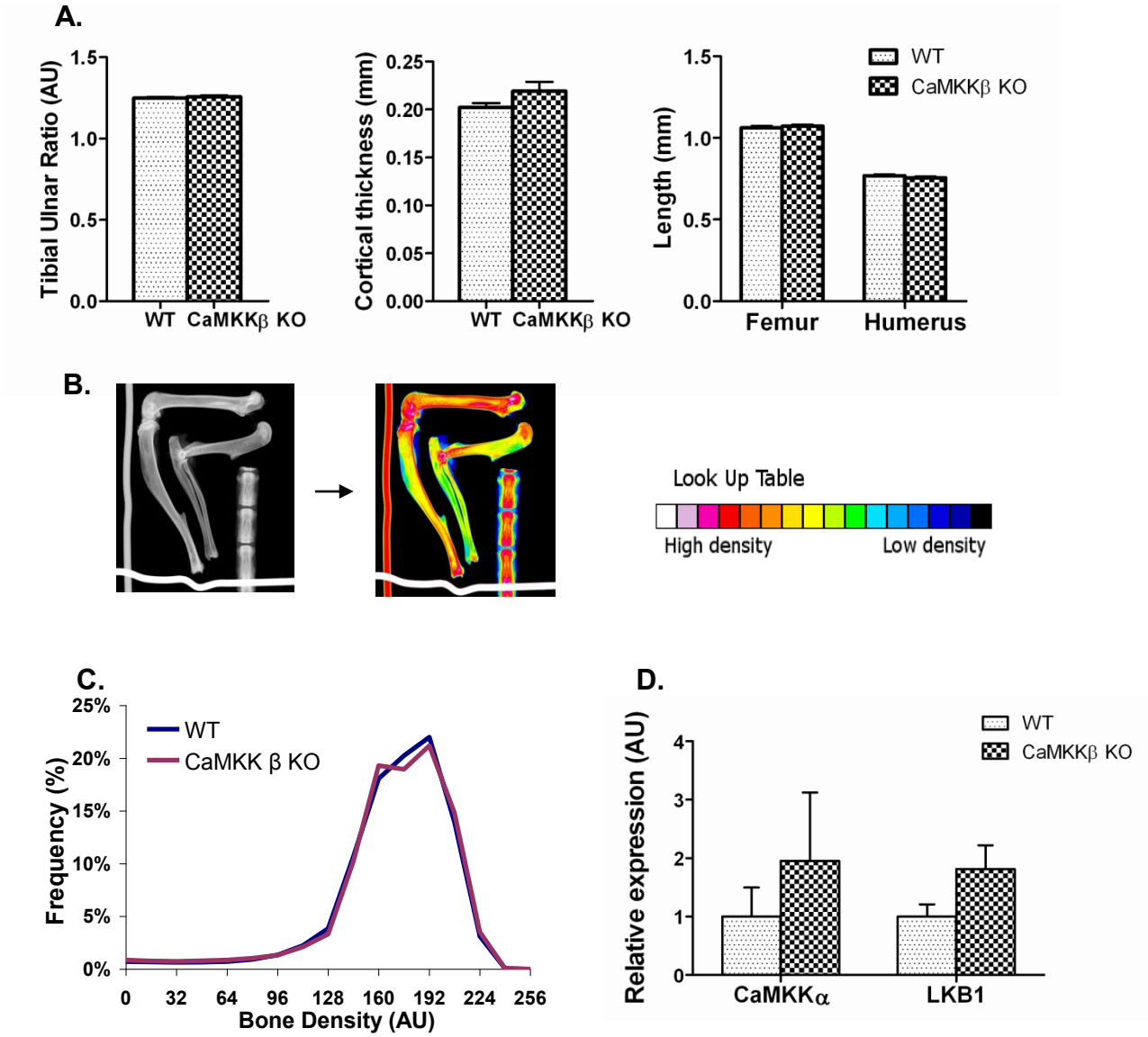

Figure 3.10 Bone mineralization measurements.

A. Measurements of tibial ulnar ratio, femoral and humeral length, and femoral cortical thickness in WT and CaMKKβ KO mice. n=5 and 7 respectively. **B.** Images demonstrate conversion from grey scale X-ray image to colour image using a Look Up Table prior to pixel counting using ImageJ software. This process is used to quantify bone mineralisation density. **C**. Bone mineralization density in WT and CaMKKβ KO mice. Relative frequency and cumulative frequency histograms of mineralization density from femur. n=5 and 7 for WT and CaMKKβ KO respectively. **D.** CaMKKα and LKB1 expression in WT and CaMKKβ KO mice measured by cDNA synthesis from crushed murine femur extracted RNA through reverse transcription followed by quantitative real-time PCR. results shown are gene expression in CaMKKβ KO mice normalised to expression in WT mice. Assays carried out in triplicate. n=4. All results shown in this figure are means ± SEM.

3.1.7 Increased osmotic fragility seen in CaMKKβ KO erythrocytes

It has been shown that AMPKα1 KO mice have reduced erythrocyte fragility, leading to anaemia and splenomegaly through increased erythrocyte lysis (Wang *et al.* 2010). To investigate if the reduced AMPKα1 activity seen in the CaMKKβ KO mice resulted in a similar phenotype, erythrocyte osmotic fragility was measured in erythrocytes isolated from WT, CaMKKβ KO, and CaMKKα KO mice. In contrast to the AMPKα1 KO mice, erythrocytes from both CaMKKβ KO and CaMKKα KO mice showed increased osmotic fragility at 4.5g/l NaCl (Figure 3.11A). At 16 weeks, no splenomegaly is seen in the CaMKKβ KO mice (Figure 3.11B), and they also do not develop anaemia (Chapter 4, figure 4.6).

Whilst trying to confirm the loss of CaMKKβ expression in the KO, it was noted that CaMKKβ activity could not be detected in immunoprecipitations of up to 500ug erythrocyte lysate (Figure 3.11C, representative results from 200ug lysate shown). Erythrocyte lysate from CaMKKβ KO contained a significant reduction in LKB1 activity compared to WT (Figure 3.11D), which could account for the reduction in erythrocyte AMPKα1 activity seen.

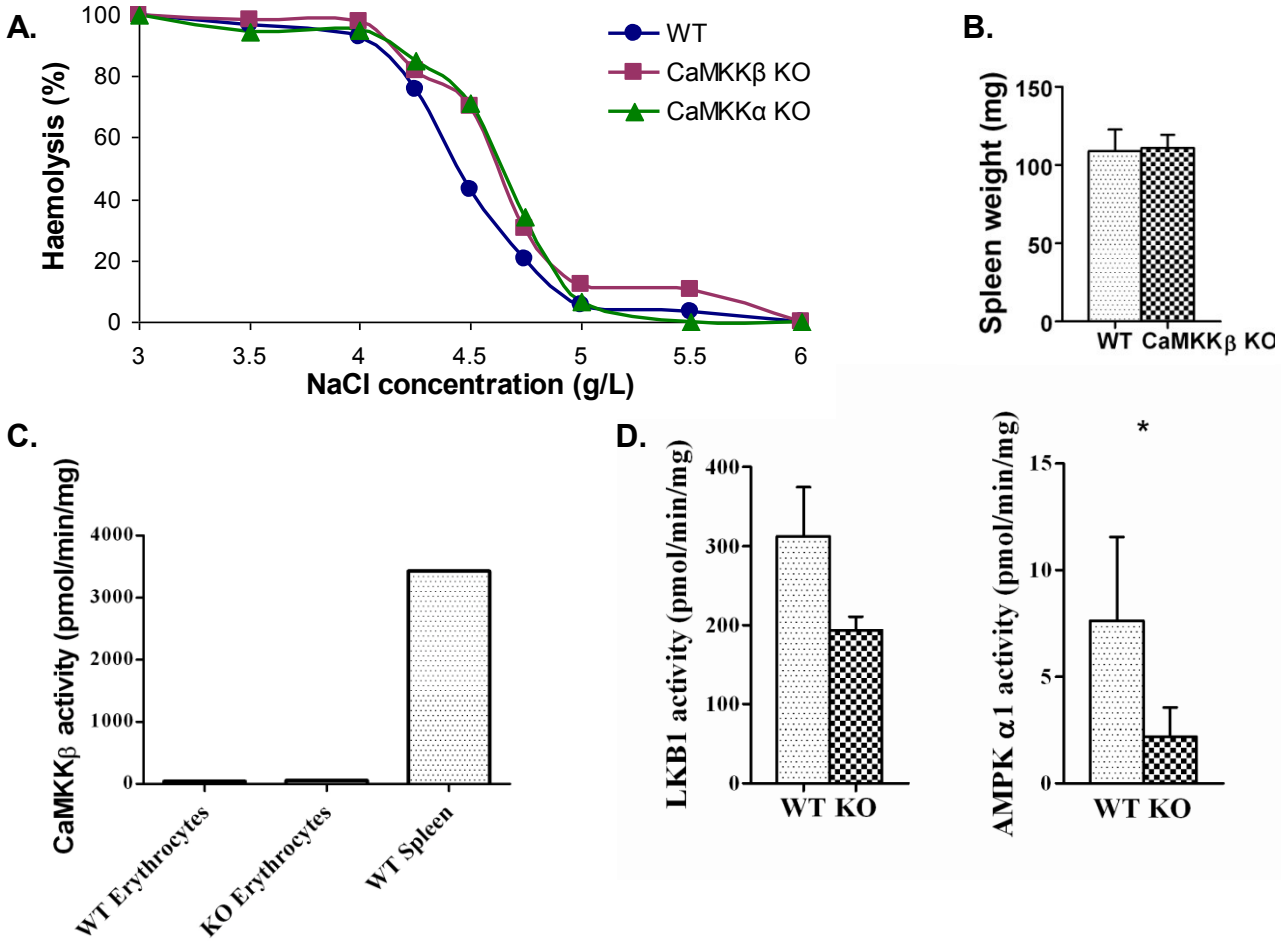

Figure 3.11 Investigating osmotic fragility in erythrocytes from CaMKKβ KO mice.

A. Erythrocyte osmotic fragility assay showing percentage of cell lysis at NaCl concentrations between 3g/L and 6g/L. Results shown are means. WT n=5, CaMKKβ KO n=5, CaMKKα KO n=3. **B.** Murine spleen weights at 16 weeks in WT and CaMKKβ KO mice. n=5-6. **C.** CaMKKβ activity in WT and CaMKKβ KO erythrocyte lysates, compared to WT spleen lysate. Activity measured in CaMKKβ immunoprecipitates from tissue lysates by activation of recombinant AMPK α1β1γ1 in the presence of calcium and calmodulin, followed by measurement of recombinant AMPK α1β1γ1 activity by incubation with SAMS peptide in a radioisotope incorporation assay. Assays carried out in duplicate. **D.** LKB1 activity in WT and CaMKKβ KO erythrocyte lysates (Not statistically significant), n=3, in comparison with AMPKα1 activity in WT and CaMKKβ KO erythrocyte lysates (Enlarged from Figure 3.8A). Activity measured in LKB1 immunoprecipitates from tissue lysates by activation of recombinant AMPK α1β1γ1, followed by measurement of recombinant AMPK α1β1γ1 activity by incubation with SAMS peptide in a radioisotope incorporation assay. Assays carried out in triplicate. Results presented as pmoles [γ-^{32}P] incorporation into the peptide per minute per milligram tissue lysate. All results shown in this figure are means ± SEM. n=2-4. Student's *t*-test: *P<0.5.

3.1.8 Loss of CaMKKβ confers protection against LPS induced sepsis

AMPK activity was found to be significantly reduced in the spleen lysates of CaMKKβ KO mice compared to WT (Figure 3.8A). As splenectomy is known to result in an increased susceptibility to bacterial infections (Styrt 1990), an LPS sepsis murine model was set up to assess the immune response in CaMKKβ KO mice. To investigate the effect of reduced AMPK activity seen in the spleens of CaMKKβ KO mice (Figure 3.8A), LPS endotoxin was used to induce sepsis in individually caged, 16 weeks old male WT, CaMKKβ KO, and CaMKKα KO mice. In mice, LPS sepsis is known to be associated with a drop in body temperature, with a body temperature of below 30ºC associated with non-survival (Saito *et al*. 2003; Nemzek *et al*. 2008). Therefore, body temperature was recorded as a marker of sepsis severity as well as the development of qualitative signs including hunched posture, piloerection, reduced mobility, and reduced response to external stimuli. LPS dosage was optimized on C57BL/6 mice to produce a consistent significant drop in body temperature at 12 hours post induction (data not shown). The temperature drop at 12 hours post LPS injection was significantly reduced in the CaMKKβ KO mice compared to WT (Figure 3.12A and 3.12B), with WT mice dropping their core temperature by 15.42 ± 0.66 °C compared to a 10.63 ± 1.17°C temperature drop in CaMKKβ KO mice. In addition, the WT mice also appeared physically less well during LPS sepsis, becoming more immobile, shivery, and less interested in their environment compared to the CaMKKβ KO mice. This suggests that the absence of CaMKKβ activity confers protection against LPS induced sepsis. Protection was not seen in CaMKKα KO mice, dropping their core temperature by 15.29 ± 0.68 °C 12 hours post sepsis induction (figure 3.12C), suggesting there may be a CaMKKβ specific mechanism for the protection.

To investigate whether the improved body temperature and physiological signs seen in CaMKKβ KO mice could be replicated through pharmacological inhibition of CaMKKβ activity in WT mice (Tokumitsu *et al*. 2002), WT mice were treated twice with 10μg/kg STO-609 by intraperitoneal injections prior to induction of LPS sepsis. At 12 hour post LPS induction, the body temperature in STO-609 treated WT mice was found to be higher than control treated WT mice (Figure 3.12D); indicating STO-609 treatment can also protect against LPS induced sepsis.

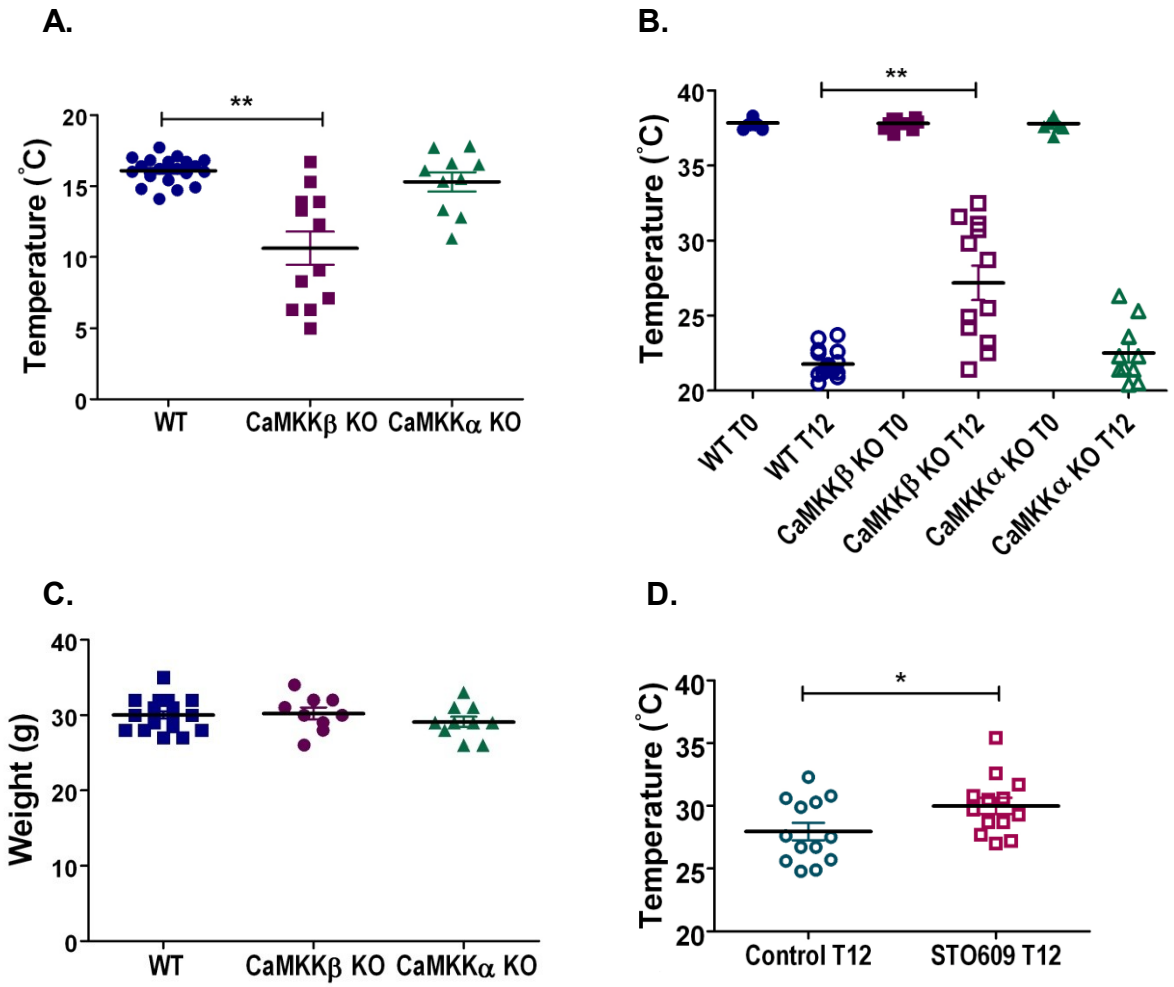

Figure 3.12 The effect of CaMKKβ deletion on LPS induced sepsis.

A. Temperature drop 12 hours following induction of LPS sepsis by intraperitoneal injection of LPS in CaMKKβ KO mice, compared with WT and CaMKKα KO. WT n=21, CaMKKβ KO n=12, CaMKKα KO n=10. **B.** Core temperature measurements prior to induction (T0), and 12 hours after induction of sepsis (T12) in WT and CaMKKβ KO mice. WT n=21, CaMKKβ KO n=12, CaMKKα KO n=10. **C.** Similar body weights seen in WT, CaMKKβ KO and CaMKKα KO mice. WT n=21, CaMKKβ KO n=12, CaMKKα KO n=10. **D.** Body temperature in untreated (Control) or STO-609 treated (STO609) WT mice 12 hours following LPS induction of sepsis. n=13. All results shown in this figure are means ± SEM. Student's *t*-test: **P<0.01; *P<0.05.

3.2 Discussion

3.2.1 Summary of principal chapter findings

Metabolic phenotyping was carried out in global CaMKKβ KO mice to determine the tissue specific functions of CaMKKβ, and in particular, its involvement in AMPKα subunit specificity. Potential compensation by LKB1 upregulation was also assessed. The main results are summarized below:

1). Global deletion of CaMKKβ does not alter food intake or body weight.

2). No significant change in glucose metabolism is found in CaMKKβ KO mice. They have normal fasting glucose levels and normal hepatocyte glucose production.

3). Isolated CaMKKβ KO primary hepatocytes have normal glycolytic respiration as measured by inhibition of ATP synthase (oligomycin) and respiratory chain complexes (rotenone and antimycin A).

4). Global deletion of CaMKKβ does not alter lipid metabolism as measured by serum cholesterol and triglyceride levels.

5). CaMKKβ KO mice have normal bone length and bone density, indicating normal bone turnover with unaltered osteoblast and osteoclast function.

6). In contrast to AMPKα1 KO mice, CaMKKβ KO mice have erythrocytes with increased osmotic fragility, not associated with anaemia or splenomegaly.

7). Global deletion of CaMKKβ provides protection against LPS induced sepsis.

8). LKB1 can phosphorylate and activate both AMPKα1 and α2 subunits *in vivo*.

3.2.2 No overt metabolic phenotype in global CaMKKβ KO mice under basal conditions

CaMKKβ does not appear to be involved in metabolism under basal, unstressed conditions. No difference was found in body weight, serum cholesterol concentration, or serum triglyceride concentration between wild-type and CaMKKβ KO mice. Downstream of CaMKKβ, no difference was seen in AMPKα1 or α2 activity in liver, skeletal muscle or adipose tissue lysates between wild-type or CaMKKβ KO mice. The absence of CaMKKβ also has no effect on either AMPK activity or glucose production in isolated hepatocytes both under basal conditions and when treated with known activators of AMPK. The results from this study support previously published data showing normal food intake, weight gain and glucose tolerance in the CaMKKβ KO mice (Claret *et al.* 2011), in contrast to the reduced food intake, reduced body weight and improved glucose tolerance reported by Anderson *et al* (Anderson *et al.* 2008). In addition to showing reduced body weight and protection against impaired glucose tolerance, the study by Anderson *et al* also showed reduced AMPK activity in the hypothalamus of the CaMKKβ KO mice (Anderson *et al.* 2008). The AMPK activity in whole brain lysate was found to be the same between WT and CaMKKβ KO in this study (Figure 4A and 4B).

Recently, a separate paper was published by Anderson *et al* (Anderson *et al*. 2012) showing increased fatty acid turnover resulting in increased serum cholesterol and triglyceride concentrations, as well as reduced hepatocyte glucose production in their liver specific CaMKKβ KO mice; again, in contrast to the results seen in this study. There is clear discrepancy between the results from this study and the findings from the Means lab (Anderson *et al*. 2008 and 2012) but the cause is unknown. The mice used have been

backcrossed onto the same C57/Black6 background. The kinase domain of CaMKKβ (Figure 6.1) is the site of deletion for both cohorts of mice used, exon 5 deletion in this study (Peters *et al*. 2003) and exon 2-4 deletion in the Means lab.

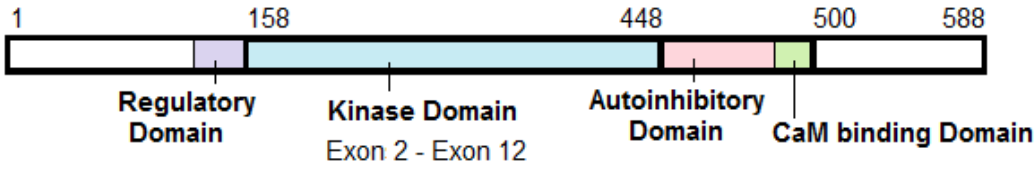

Figure 3.13 Diagram of murine CaMKKβ illustrating the main functional domains. (adapted from Mutsuko *et al*. 2011).

Hepatocyte mitochondrial function including basal respiration, ATP turnover, and respiratory reserve were all assessed and found to be unaltered in CaMKKβ KO mice, providing further evidence that the absence of CaMKKβ does not alter metabolism.

It can be argued that the lack of metabolic phenotype seen in CaMKKβ KO mice could be due to compensation of alternative pathways. However, there is no significant increase in AMPKα2 activity to compensate for the changes in AMPKα1 activity, and LKB1 activity also remains similar between WT and CaMKKβ KO tissue lysates with the exception of erythrocytes where there is a small difference observed. Nevertheless, it remains possible, that the lack of change in AMPK activity seen results from compensation by additional unknown upstream activators of AMPK. In addition, the differences in AMPK activity may be masked by the possible full activation of AMPK due to LKB1 activity following the rapid depletion of ATP during tissue dissection.

As CaMKKβ does not appear to be involved in the metabolic processes controlled by AMPK, it was important to clarify the relationship between LKB1 and AMPK. *AMPKα1* KO mice also show no metabolic phenotype, in contrast to *AMPKα2* KO mice which have previously been shown to exhibit increased body weight, increased adipose tissue mass, impaired

glucose tolerance, as well as impaired insulin secretion and sensitivity (Viollet *et al.* 2003). *In vitro*, both LKB1 and CaMKKβ can activate AMPK complexes with both α1 and α2 subunits, however, it was unclear whether this was also the case *in vivo* and, more importantly, had any physiological function. The AMPK activity data in the CaMKKβ KO mice provides evidence that LKB1 does phosphorylate both subunits. In the absence of CaMKKβ, AMPKα1 activation is similar to that seen in wild-type in most tissues, suggesting CaMKKβ activity is not essential for AMPK activity in most tissues under basal conditions.

3.2.3 CaMKKβ KO mice have normal long bone length and bone mineral density

No difference was seen in the cortical thickness or bone mineral density of 12 week old male global CaMKKβ KO mice. A possible explanation is compensation at the local level and redundancy at the global hormonal level. CaMK I was shown to be involved in the proliferation of osteoblasts *in vitro*, with deletion by siRNA in osteoblasts leading to reduced osteoblast proliferation (Pedersen *et al*. 2008). AMPK also regulates osteoblast proliferation and bone formation: activation of AMPK by AICAR in primary osteoblasts led to increased bone formation; and conversely inhibition of AMPK reduced bone formation (Shah *et al.* 2010). In keeping with this, studies have shown reduced trabecular bone density in global *AMPKα1* KO mice (Jeyabalanet *et al*. 2012). However, no evidence of altered osteoblast proliferation and increased bone formation was seen in the global CaMKKβ KO mice. This may be explained by compensation through increased CaMKKα and LKB1 gene expression as seen in CaMKKβ KO bone. Although statistical significance was not reached, the relative expression of both CaMKKα and LKB1 was almost doubled in CaMKKβ KO bones. Assessment of protein expression was considered and found to be outside the scope of this project as the extraction and isolation of protein from bone is a complex process due to bone mineralization.

The control of bone density is also known to be regulated by hormones. Recently, an *in vivo* murine study where CaMKKβ was deleted in SF1 neurons in the ventromedial nucleus of the hypothalamus showed reduced trabecular density in both vertebrae and long bones at 12 weeks (Oury *et al.* 2010). CaMK IV was suggested as the downstream mediator, as the

same study showed *CaMK IV* deletion in SF1 neurons produced a similar phenotype to *CaMKKβ* deletion. However, the significance of bone density regulation by SF1 neurons is unclear, as the activity of CaMK IV, a downstream target of CaMKKβ, is known to be reduced in CaMKKβ KO hypothalamus (Peters *et al*. 2003) but no change in trabecular density is seen in the global CaMKKβ KO mice. Further activation of the pathway, such as leptin injections, may be required for a bone phenotype to be seen in global CaMKKβ KO mice. Leptin is known to inhibit bone mass accrual through reduced serotonin synthsis and reduced stimulation of SF1 neurons (Yadav *et al*. 2009). AMPK activity in the hypothalamus can also be inhibited by leptin (Minokoshi *et al*. 2002 and 2004), although under unstressed conditions, CaMKKβ does not appear to be required for AMPK activity in the brain, as seen by the unaltered AMPK activity in CaMKKβ KO brain lysates. It is also possible that the changes in AMPK activity in CaMKKβ KO brain may be masked by the activation of LKB1 during the isolation of brain tissue as this process is limited by procedural speed.

3.2.4 CaMKKβ KO erythrocytes have increased osmotic fragility

Erythrocytes have been shown to contain AMPK complexes with α1 subunits only. Anaemia as well as splenomegaly is seen in mice lacking AMPKα1 as a result of reduced erythrocyte life span. (Wang *et al.* 2010). Reduced osmotic fragility was shown and the reduced deformability of these erythrocytes in response to shear stress is proposed as the mechanism for the increased haemolysis seen (Foretz *et al.* 2010). The same phenotype is not present in CaMKKβ KO mice. In contrast to the *AMPKα1* KO, erythrocytes lacking CaMKKβ were shown to have increased osmotic fragility compared to wild-type (Figure 6A). The altered osmotic fragility was seen in both CaMKKβ KO and *CaMKKα* KO cells, suggesting the involvement of the CaMK cascade in either the erythrocyte membrane ion transporters or the maintenance of cell membrane integrity. However, the physiological relevance of the increased osmotic fragility seen is currently unclear, as neither CaMKKβ KO or *CaMKKα* KO mice show anaemia or splenomegaly (data not shown), and the difference was significant at a NaCl concentration outside the physiological range.

As CaMKKβ activity was not detectable in WT erythrocytes, LKB1 appears to be the upstream kinase responsible for AMPK activity in erythrocytes. Deletion of *CaMKKβ* led to

both reduced LKB1 activity (Figure 11C) and AMPKα1 activity in erythrocytes through an unknown mechanism. LKB1 is known to be constitutively active (Lizcano *et al.* 2004), suggesting the reduction in LKB1 activity likely results from reduced LKB1 expression, perhaps in the bone marrow haematopoietic stem cells responsible for erythrocyte production and protein synthesis. The transcription regulator CREB is known to be activated by CaMKK in neurons (Peters *et al.* 2003; Wayman *et al.* 2008), and also activated by CaMK IV in T lymphocytes (Yu *et al.* 2001); although the activation of transcription by the CaMK cascade has not been shown in haematopoietic stem cells, the data presented in this thesis raises the possibility of a novel link between CaMKK activity and LKB1expression that has not previously been studied.

3.2.5 Loss of CaMKKβ activity confers protection against LPS induced sepsis

Sepsis describes a clinical syndrome characterized by systemic inflammation occurring in response to known or suspected infections. Bolus injection of LPS is used in murine models of sepsis as studies in human volunteers have shown injection of LPS can induce signs and symptoms similar to those reported in septic patients (Buras *et al.* 2005). Interestingly, the loss of CaMKKβ appears to protect mice against LPS induced sepsis, as shown by reduced temperature drop in not only the CaMKKβ KO mice and also WT mice treated with the CaMKKβ inhibitor, STO-609.

The inhibition of CaMKKβ by STO-609 is not very specific (Tokumitsu *et al*. 2002). At 2 hour following intraperitoneal injection of 10μg/kg STO-609 in mice, the plasma concentration of STO-609 was previously shown to be between 200 and 400ng/g (Massie et al. 2011), which is equivalent to a plasma concentration of 6 to 12 μg/ml STO-609 assuming an average 30g mouse with 2 ml of plasma. The tissue availability of intraperitoneally injected STO-709 is unclear. In addition to inhibition of CaMKKβ, STO-609 may also inhibit CaMK I, CaMK IV, AMPK, CaMK II and MLCK at the plasma concentration of 6 to 12μg/ml.

Recently both CaMK I and IV, when activated by CaMKKα and β, have been implicated in LPS induced sepsis through macrophage cytokine release. CaMK IV was shown to be required for the release of High-Mobility Group Box 1 (HMG B1), a late stage pro-inflammatory cytokine, in LPS treated murine primary peritoneal macrophages (Zhang *et al.* 2008). CaMK I was found to be involved in the production of Interleukin-10 as well as the release of HMG B1 in both LPS treated murine primary peritoneal macrophages and in mice undergoing a caecal ligation and puncture model of sepsis (Zhang *et al.* 2011). The loss of CaMKKβ could lead to reduced activation of CaMK I and CaMK IV, and result in reduced inflammatory cytokine production through the above mechanisms. However, it does not explain the lack of protection seen in *CaMKKα* KO mice. Protection through the CaMK pathway could occur if it involves tissue with minimal CaMKKα activity; or alternatively, the protective effect could be masked in the *CaMKKα* KO mice by a compensatory mechanism such as increased CaMKKβ activity.

The inflammatory response during sepsis is potentially regulated by CaMKKβ through not only the CaMK cascade but also AMPK. Inhibition of AMPK activity in macrophages has been shown to inhibit the LPS induced production of IL6 and TNFα (Sag *et al*. 2008; Yang *et al*. 2010), both potent pro-inflammatory cytokines and pyrogens (Netea *et al*. 2000). Similar to the reduced AMPK activity seen in erythrocytes, the loss of CaMKKβ could potentially reduce AMPK activity in macrophages leading to reduced LPS induced pro-inflammatory cytokine production and therefore limit sepsis progression.

A second possible mechanism for the protection against LPS induced sepsis seen in CaMKKβ KO mice involves the production of NO, a mediator of septic shock. During sepsis, iNOS can be upregulated by both endotoxins and inflammatory cytokines, leading to the overproduction of NO, resulting in vasodilation, myocardial toxicity, and mortality. In macrophages, iNOS expression and further NO production has been shown to be dependent on the presence of NO produced by eNOS (Connelly *et al.* 2003). As eNOS has been shown to be activated by AMPK (Chen *et al.* 2009), it is possible the loss of CaMKKβ could lead to reduced iNOS expression, NO production, and therefore improved circulation during sepsis.

Improved circulation during sepsis could also occur through vascular resistance to vasodilation and hypotension. AMPK was found to be involved in vessel contractility by phosphorylation and inhibition of the MLC kinase, MLCK (Horman *et al*. 2008); and recently it has also been shown to activate the MLC phosphatase regulatory subunit, MYPT1, leading to vasodilation (Wang *et al*. 2011). CaMKKβ could potentially regulate vessel contractility through AMPK, with increased blood pressure seen in CaMKKβ KO mice compared to WT. Investigations into possible mechanisms will be further discussed in the next two chapters of this thesis.

3.2.6 Comparing LPS and the Caecal ligation puncture model of sepsis

The LPS sepsis model used in this study does not fully represent the conditions present in bacterial sepsis. Unlike bacteria, the LPS used to induce sepsis contains only the components of bacterial cell wall and will not replicate within the host organism. The production of NO is known to be important for the bactericidal properties of macrophages (Vazquez-Torres *et al.* 2008). Reduced production of NO in a global CaMKKβ KO mice could potentially lead to reduced phagocytosis by macrophages on exposure to bacteria, and result in overwhelming sepsis through bacterial replication and destruction of host tissue. Induction of sepsis through caecal ligation puncture (CLP) (Hubbard *et al.* 2005), which releases gut bacteria into the murine peritoneum from the caecum, can provide an alternative model to LPS injection. This model has previously been validated to allow adjustment of the resulting sepsis severity through the size of needle puncture and the number of punctures made (Buras *et al.* 2005). The CLP model may be a more clinically relevant model of peritonitis for the investigation of sepsis, however it is technically more challenging than the LPS sepsis model and is its use is limited by animal numbers and the technical availability.

In summary it appears that under basal conditions CaMKKβ plays an undetectable role in general homeostasis and metabolism. However under conditions of extreme stress, such as found during sepsis, the absence of CaMKKβ activity appears to be advantageous. This will be investigated in detail in the next chapter.

Chapter 4. The function of CaMKKβ in inflammation

In the previous chapter, the function of CaMKKβ in general metabolism was explored. One of the striking findings was the reduced deterioration in physical condition seen in CaMKKβ KO mice during LPS induced sepsis. In this chapter, the effect of global CaMKKβ deletion on the main inflammatory pathways involved in sepsis will be investigated in order to elucidate the possible mechanisms involved, including inflammatory mediator production, white blood cell proliferation, macrophage activation and altered vascular permeability.

4.1 Investigating the function of CaMKKβ in inflammation

4.1.1 Measurement of serum cytokine production following LPS treatment

Cytokines and inflammatory mediators are the main components of sepsis progression. The binding of LPS to TLR receptors on leukocytes results in the release of both pro-inflammatory cytokines including IL1β or TNFα, as well as the anti-inflammatory cytokine IL10 (Poltorak *et al.* 2000; Nduka and Parrilo. 2009). The severity of the inflammatory response directly correlates with the concentration of the pro-inflammatory cytokines and inversely correlates with IL10 (Blackwell and Christman. 1996; Damas *et al*. 1997; Banchereau *et al*. 2012). To compare the inflammatory state between WT and CaMKKβ KO mice during LPS sepsis, serum was collected at 12 hour post LPS injection and cytokine levels were measured using a multiplexed cytokine ELISA kit. Serum cytokine concentrations from control mice were below the level of detection and unable to be measured. 12 hours after the LPS injection, the serum concentration of IL6 was found to be higher in CaMKKβ KO compared to WT mice; no difference was seen in the serum concentration of IL10 or the pro-inflammatory cytokines: IL1β, IL6 or TNFα (Figure 4.1). The serum concentration of granulocyte-macrophage colony stimulating factor (GM-CSF) was also measured as an indicator of macrophage proliferation. The serum concentration of GM-CSF in CaMKKβ KO mice was found to be similar to WT mice following LPS treatment (Figure 4.1).

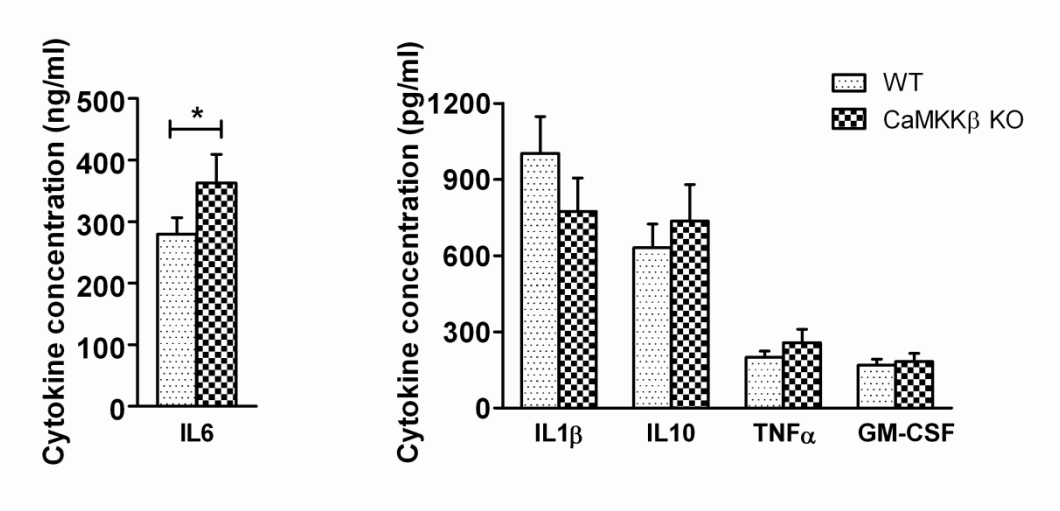

Figure 4.1 Serum cytokine concentrations 12 hour post LPS injection.

Serum was collected from WT and CaMKKβ KO mice 12 hours after intraperitoneal LPS injection, the concentration of a panel of cytokines was measure using a magnetic multiplexed ELISA assay kit. Results shown are means ± SEM. WT n=17, KO n=10. Student's *t*-test: *P<0.5.

4.1.2 Serum NO production following LPS treatment

During sepsis, NO plays an important role in both the activation of leukocytes as well as the control of vascular blood flow. The presence of LPS and increased concentrations of pro-inflammatory cytokines lead to the expression of iNOS in both endothelial cells and macrophages, resulting in increased production of NO. In addition to cytokine measurements, the amount of NO released as measured in serum nitrite concentration provides an alternative indication of inflammation severity (Petros *et al*. 1991; Cauwels. 2007). To investigate whether NO synthesis was involved in the sepsis protection, the nitrite concentration was measured in serum samples collected from untreated and LPS treated mice. The nitrite in serum is often present in the oxidized nitrate form, therefore prior to measurement of nitrite concentration, all serum samples were deproteinated and treated with a reducing agent to convert the nitrate back to nitrite.

LPS treatment caused a significant increase in serum NO production (Figure 4.2A). However, there was no difference seen in either untreated or 12h LPS serum nitrite concentration between the WT and CaMKKβ KO mice (Figure 4.2A), indicating similar NO production following LPS treatment.

Following its production, NO is able to diffuse into vascular smooth muscle cells where it binds to and activates guanylyl cyclase which catalyses the conversion of GTP to cGMP. Therefore, changes in the concentration of NO correlates with changes in cGMP concentration. When the concentration of cGMP was measured in the serum of 12h LPS treated mice, no difference was seen between WT and CaMKKβ KO (Figure 4.2B), supporting the lack of difference seen in serum nitrite concentration.

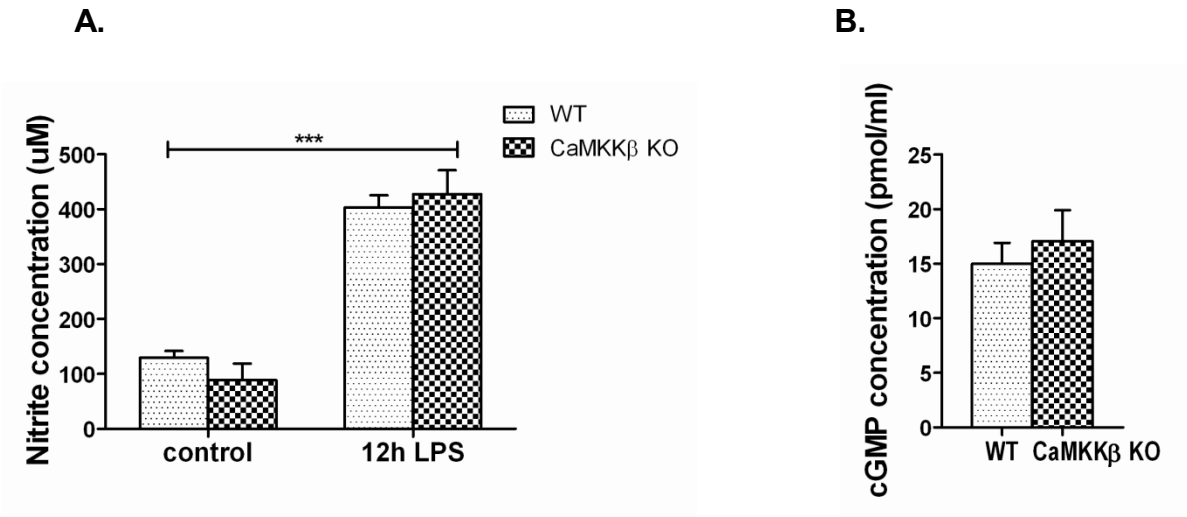

Figure 4.2 Serum NO and cGMP concentration following LPS treatment.

A Serum was collected from WT and CaMKKβ KO mice 12 hours after intraperitoneal injection of saline (control) and LPS (12h LPS), nitrite concentration was measured by Greiss assay. *** Comparison of serum nitrite concentration between control and LPS treated mice. ANOVA: ***P<0.01. Control n=4-5, 12h LPS n=12-13. **B** Serum was collected from WT and CaMKKβ KO mice 12 hours after intraperitoneal LPS injection, serum cGMP concentration was measured using the cGMP complete Enzyme ImmunoAssay Kit. n=6. All results shown in this figure are means ± SEM.

4.1.3 Leukocyte count following 6 hour LPS treatment

As the lack of difference seen in both cytokine concentration and NO production in the WT and CaMKKβ KO mice following LPS treatment could be masked by a difference in the proliferation of neutrophils and macrohpages, the percentage population of these cells were measured by flow cytometry of blood leukocytes isolated from both untreated and 6h LPS treated mice. As would be expected, Neutrophilia is seen following 6h LPS (Figure 4.3). However, no difference is seen in the percentage blood population of either macrophages or neutrophils, in both untreated and LPS treated WT and CaMKKβ KO mice.

4.1.3.1 Leukocyte populations in blood and the lymphoid organs

The CaMK cascade, and in particular CaMKIV, has previously been implicated in the activation of T lymphocytes by promoting gene transcription (Ho *et al.* 1996; Yu et al 2000). Therefore, T lymphocyte and B lymphocyte populations were measured in blood and the lymphoid organs including $CD4^+$ T lymphocytes, $CD8^+$ T lymphocytes, $CD25^+$ regulatory T lymphocytes, as well as $CD44^+$ activated T lymphocytes by flow cytometry. No difference is seen in any of the leukocyte populations measured between WT and CaMKKβ KO mice (Figure 4.5). As would be expected, lymphocytes predominate in the lymphoid organs, and only T lymphocytes are present in the thymus (Figure 4.5).

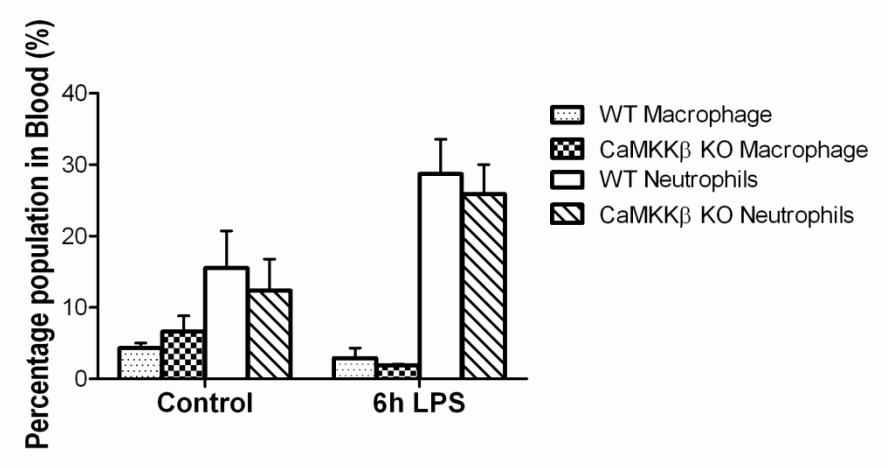

Figure 4.3 Macrophage and neutrophil count in blood. Percentage blood population of macrophages and neutrophils from 6 hours post saline (Control) and LPS treated WT and CaMKKβ KO mice were measured by flow cytometry. Results shown are means ± SEM. n=3-6.

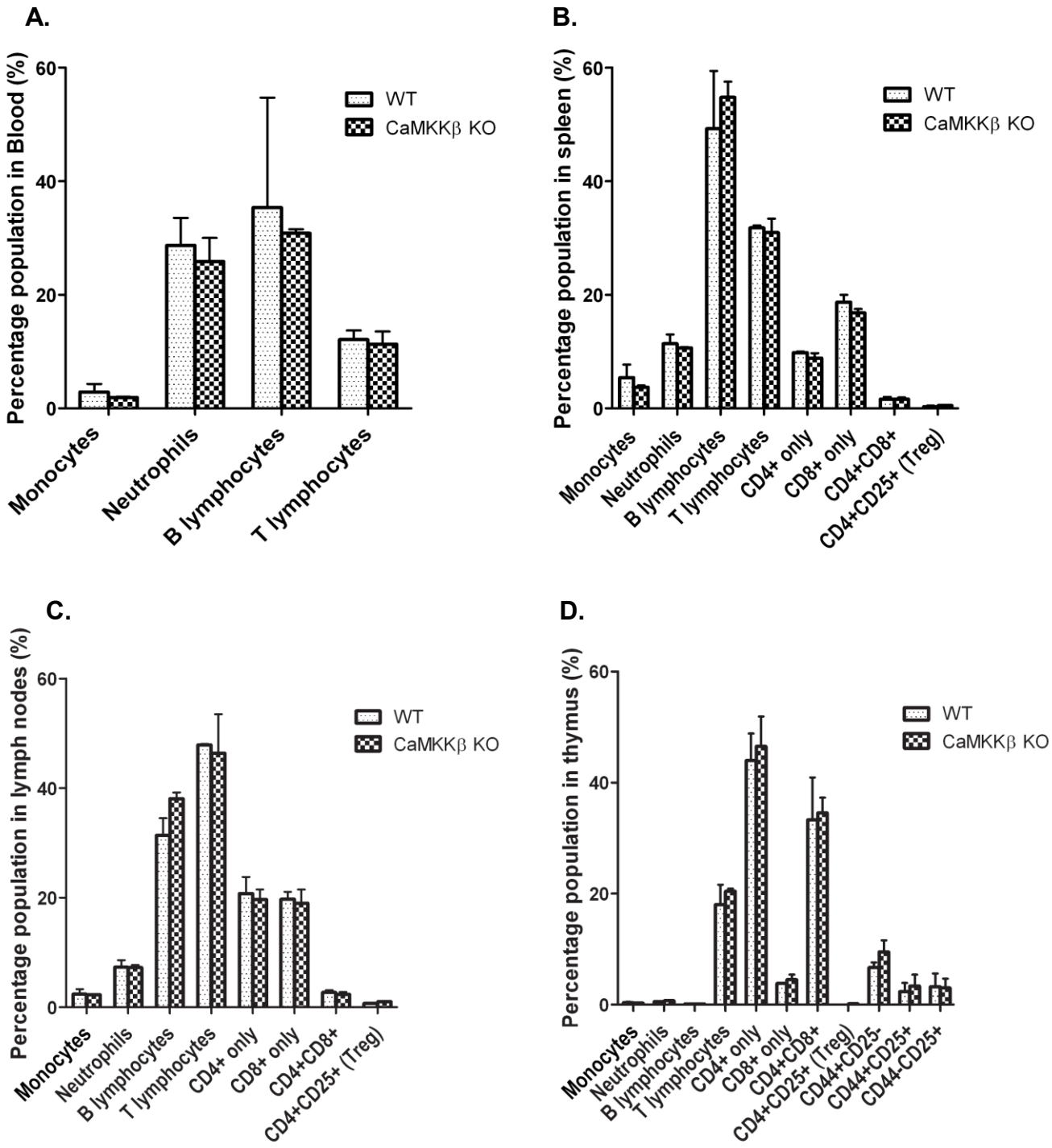

Figure 4.4 Leukocyte count in blood and lymphoid organs.

No significant difference in percentage leukocyte populations in blood and lymphoid tissues in 6 hour LPS treated WT and CaMKKβ KO mice when measured by flow cytometry. T lymphocyte populations include $CD4^+$, $CD8^+$, $CD25^+$, $CD44^+$ and combinations of these seen during development. **A.** Blood. n=3-6. **B.** Spleen. n=2. **C.** Lymph nodes. n=2. **D.** Thymus. n=2. All results shown in this figure are means ± SEM.

4.1.4 CaMKKβ function in macrophage migration

To further determine the role of CaMKKβ in leukocyte activation, peritoneal macrophages were isolated from untreated WT and CaMKKβ KO mice, cultured for 24 hours and characterized. Cultured macrophages maintain F4/80 receptor staining for up to 8 days in culture following isolation as shown by flow cytometry of a representative sample (Figure 4.5A).

4.1.4.1 AMPK activity in LPS treated macrophages

As AMPK activity was found to be reduced in CaMKKβ KO erythrocytes, AMPK activity was measured in cultured macrophages and also found to be significantly reduced in CaMKKβ KO. To assess AMPK activity in LPS activated macrophages, the cultured macrophages were primed with 100ng/ml IFNγ overnight before activation with 10ng/ml LPS treatment. Following 24 hour LPS treatment, AMPK activity was found to be similarly reduced in both WT and CaMKKβ KO mice (Figure 4.5B). Therefore, the loss of CaMKKβ appears to reduce macrophage AMPK activity but does not appear to be involved in LPS induced reduction in AMPK activity.

4.1.4.2 LPS induced macrophage activation

The activation of macrophages was assessed by NO production and macrophage phagocytosis. NO production as measured by media nitrite concentration was increased by 24 hour after 10ng/ml LPS treatment following IFNγ priming; no difference was seen in NO production between WT and CaMKKβ KO macrophages with or without LPS treatment (Figure 4.5C). Correspondingly, macrophage phagocytosis as measured by uptake of fluorescent conjugated *E.coli* bioparticles was increased by increasing concentrations of LPS treatment, but no difference is seen between the WT and CaMKKβ KO macrophages when treated for 24 hours with 100ng/ml LPS (Figure 4.5D). Without priming by overnight

treatment with IFNγ, the uptake of bioparticles by LPS treated macrophages is similar to untreated macrophages, indicating IFNγ priming is essential for LPS induced macrophage activation.

4.1.4.3 CaMKKβ regulates VEGF dependent macrophage migration

Many of the signalling and cytoskeletal proteins involved in the regulation of macrophage phagocytosis are also involved in macrophage migration (Jones. 2000; Swanson and Hoppe. 2004; Beemiller *et al*. 2010). To investigate if CaMKKβ is involved in the regulation of macrophage migration, Transwell assays were set up with and without the chemoattractant VEGF in the lower wells. Following macrophage migration through the Transwell membrane, only a proportion of the macrophages would detach from the underside of the membrane and fall into the lower wells, therefore, the number of macrophages in the lower wells was found to be poorly representative of actual number of migrated macrophages. Instead, the conversion of tetrazolium salt to formazan by macrophage mitochondria as used in MTT assays was found to correlate well with the number of macrophages (Figure 4.5E), and was used to measure the number of remaining non-migrated macrophages from which the percentage of non-migrated macrophages was calculated. VEGF induced migration was found to be significantly reduced in CaMKKβ KO macrophages compared to WT as shown by the greater number of non-migrated CaMKKβ KO macrophage (Figure 4.5F). However the significance of this difference is unclear. No difference was found in the number of macrophages in blood from LPS treated WT and CaMKKβ KO mice. It is possible the number of tissue macrophages may be reduced in CaMKKβ KO mice, if this is the case, the tissue macrophages do not appear to affect LPS sepsis severity as no reduction in cytokine or nitrite concentration is seen in CaMKKβ KO mice following LPS treatment.

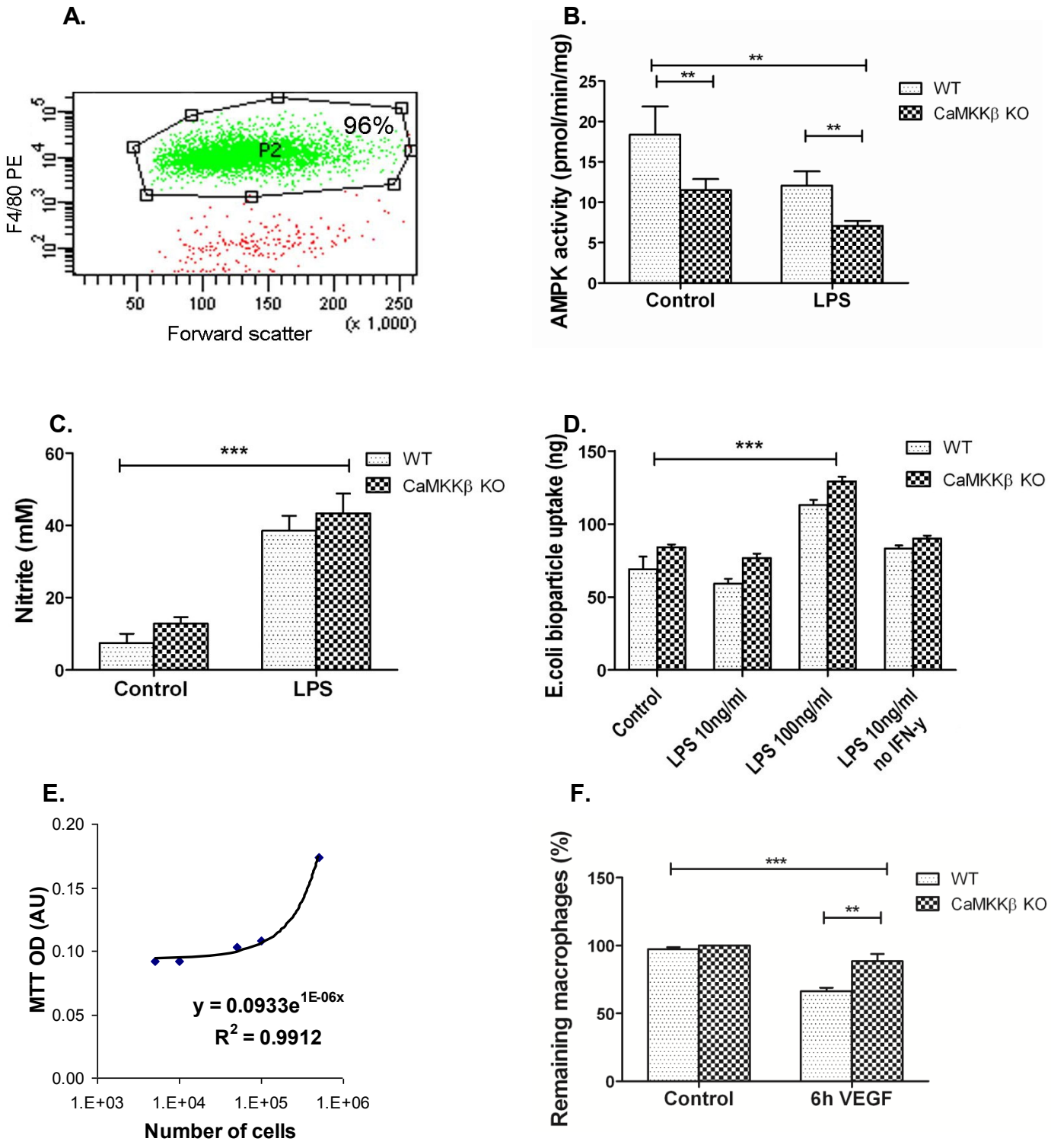

Figure 4.5 Macrophage function.

A. Representative flow cytometry result of cultured peritoneal macrophages 8 days post isolation. F4/80 staining shown in green (P2, 96%). **B.** AMPK activity in 24 hour LPS treated cultured macrophages measured by immunoprecipitation of AMPKβ followed by incubation with SAMS peptide in a radioisotope incorporation assay. Assays performed in

duplicate. Results presented as pmoles [γ-^{32}P] incorporation into the peptide per minute per milligram cell lysate. n=5-7 **C.** NO production from untreated (Control) and 24 hour 10ng/ml LPS treated (LPS) cultured macrophages as measured by Greiss assay. n=5-7. **D.** Phagocytosis of fluorescent conjugated *E.coli* bioparticles by macrophages: untreated (Control), 24 hour 10ng/ml LPS only (LPS control), and 24 hour LPS following IFNγ priming (LPS 10ng/ml and LPS 100ng/ml). n=3. **E.** MTT assay showing relationship between number of cultured macophages and optical density measured. **F.** Macrophage motility measured by transwell assay. Results presented as percentage of remaining non migrated CaMKKβ KO macrophages. Assay performed in triplicate. n=3. All results shown in this figure are means ± SEM. ANOVA: ***P<0.001; **P<0.1; *P<0.5.

4.1.5 Loss of CaMKKβ activity does not affect endothelial permeability

The endothelium is an important barrier for macrophage tissue access as well as for the distribution of invading pathogens. The production of NO through iNOS by endothelial cells drives the inflammatory process during the progression of sepsis. Bradykinin, thrombin and VEGF have all been shown to induce CaMKKβ dependent AMPK activation in endothelial cells (Stahmann *et al*. 2006; Mount *et al*. 2008; Stahmann *et al*. 2010); and activation of AMPK in human aortic endothelial cells has been shown to increase NO synthesis (Morrow *et al*. 2003). Therefore, the affects of CaMKKβ inhibition on AMPK activation and endothelial permeability was investigated.

4.1.5.1 CaMKKβ inhibition does not affect endothelial permeability under basal conditions

Human umbilical vein endothelial cells (HUVEC) were cultured and treated with both activators and inhibitors of CaMKKβ to investigate the effects on AMPK activity as well as HUVEC monolayer permeability, AMPK activity was increased by 3 fold following ionomycin treatment (Figure 4.6A). This increase in AMPK activity was found to be CaMKKβ dependent. Treatment of the cells with ionomycin in the presence of STO609 prevented activation of AMPK (Figure 4.6A). The establishment of human umbilical vein endothelial cell monolayers on matrigel coated Transwell membranes was established through the significant reduction in fluorescein isothiocyanate (FITC) bound dextran permeability across the membranes. The FITC bound dextran permeability was not significantly different between untreated HUVEC monolayer and STO609 treated HUVEC monolayer (Figure 4.6B), suggesting that CaMKKβ inhibition by STO609 does not affect HUVEC monolayer permeability by FITC bound dextran.

4.1.5.2 Loss of CaMKKβ does not affect haematocrit increase during LPS sepsis

In addition to the production of inflammatory mediators, the endothelium also functions to increase macrophage tissue infiltration during sepsis through increased permeability. The

increased permeability contributes to the development of hypotension seen during sepsis as proteins move out of the intravascular compartment followed by water leading to a reduction in the intravascular volume; resulting in haemoconcentration and an increase in haematocrit (van Lambalgen *et al*. 1988). When haematocrit was measured in control and LPS treated WT and CaMKKβ KO mice, no difference was seen in basal haematocrit or 6 hour post LPS haematocrit in both WT and CaMKKβ KO mice (Figure 4.6C); suggesting the loss of CaMKKβ does not affect the change in endothelial permeability following LPS treatment.

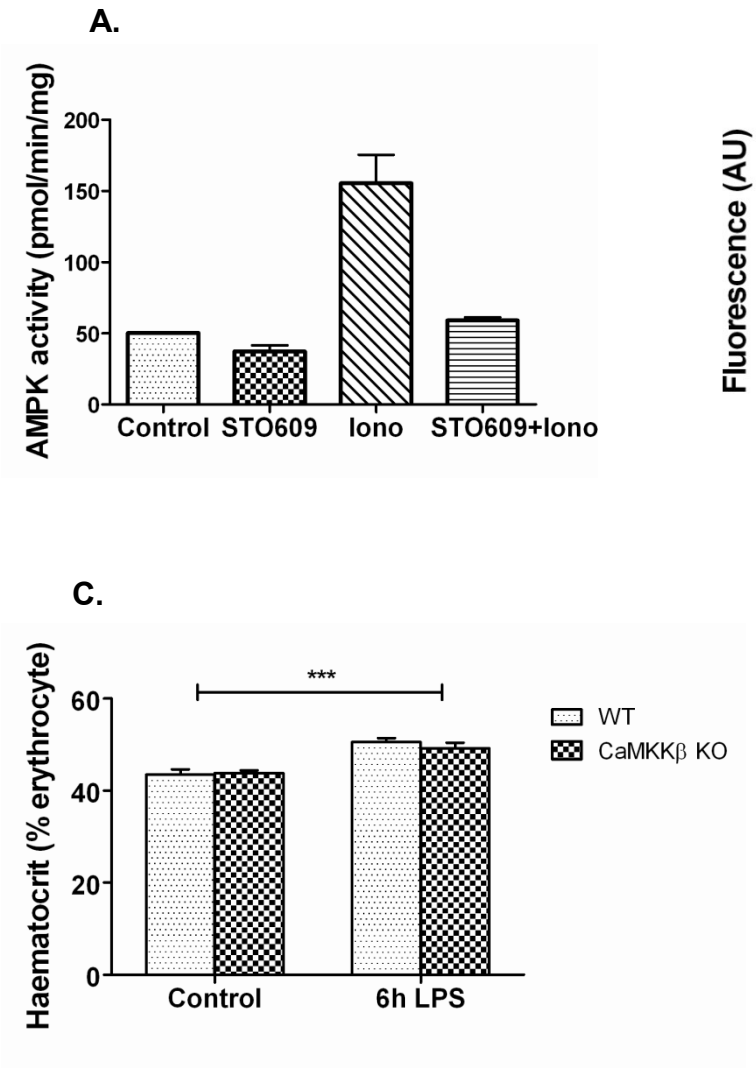

Figure 4.6 Human umbilical vein endothelial cell monolayer permeability and *in vivo* LPS induced haematocrit change.

A. AMPK activity in treated cultured HUVEC measured by immunoprecipitation of AMPKβ followed by incubation with SAMS peptide in a radioisotope incorporation assay. All assays carried out in duplicate. All results presented as pmoles [γ-^{32}P] incorporation into the peptide per minute per milligram cell lysate. Control: untreated, STO609: 10ng/ml STO-609 for 40h, Iono: 1μM Ionomycin for 10min, STO609+Iono, 10ng/ml STO-609 for 40h with 10min 1μM Ionomycin. n=2. **B.** FITC-dextran Fluorescence of Transwell flow through in untreated (Control) and 40 hour 10ng/ml STO-609 treated (STO609) cultured HUVEC monolayers. Fluorescence of flow through shown for matrigel only Transwell without HUVEC monolayer (FITC-dextran) for comparison as positive control. n=3. **C.** Haematocrit measurements in untreated (Control) and 6 hour LPS treated (6h LPS) WT and CaMKKβ KO mice. n=3-7. All results shown in this figure are means ± SEM. ANOVA: ***P<0.001.

4.1.6 Loss of either AMPKα1 or AMPKα2 does not confer protection against LPS induced sepsis

The previous chapter presented data showing the loss of CaMKKβ but not CaMKKα appears to improve LPS sepsis severity; however the loss of CaMKKβ does not appear to reduce either the systemic inflammation or macrophage activation caused by the presence of LPS. To further investigate if the protection against LPS sepsis seen in CaMKKβ KO mice is mediated through AMPK, LPS induced temperature change was recorded from both global AMPKα1 KO and AMPKα2 KO mice. At 10 hours following LPS treatment, no significant difference was seen in the LPS induced temperature drop in either AMPKα1 or AMPKα2 KO mice compared to WT (Figure 4.7B and 4.8B). An added complication of looking at the AMPKα1 mice however is that they are known to have anaemia and splenomegaly (Foretz *et al*. 2010) which may complicate any phenotype, and therefore may not be comparable to the CaMKKβ KO mice. Anaemia is known to be associated with reduced tissue oxygen delivery and has been shown to independently contribute to sepsis mortality (Reade *et al*. 2010).

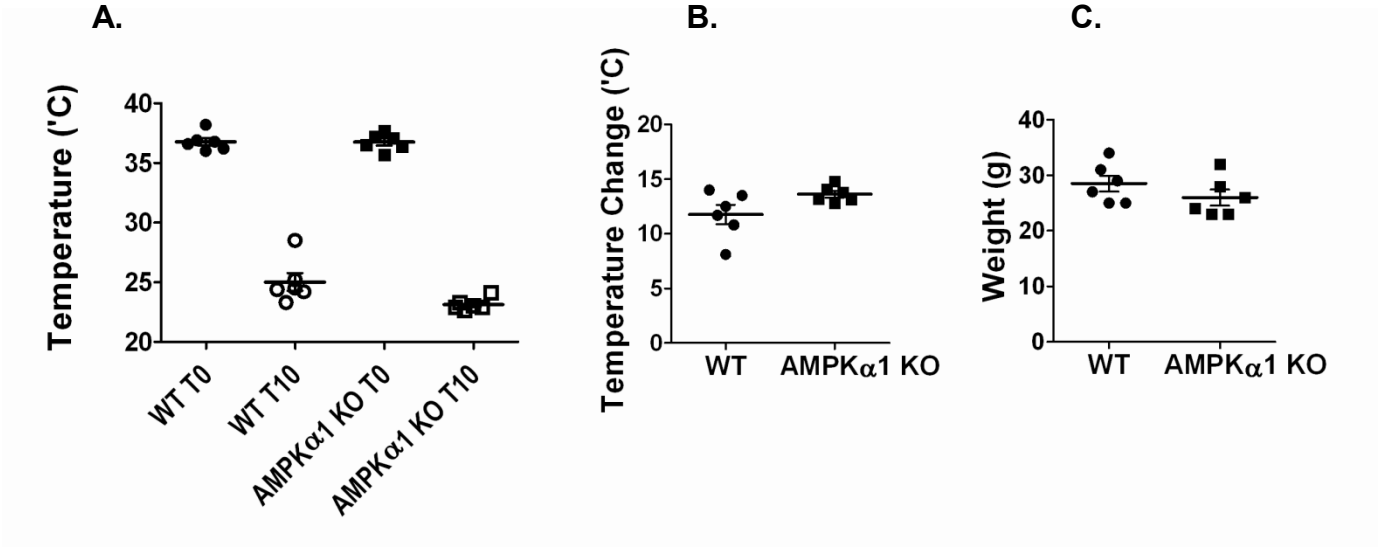

Figure 4.7 LPS sepsis study in global AMPKα1 KO mice.

A. Body temperatures prior to (T0) and 10 hour following LPS induction (T10) in WT and global AMPKα1 KO mice. **B.** 10 hour LPS induced temperature drop. **C.** Body weight measurements. All results shown in this figure are means ± SEM. n=6.

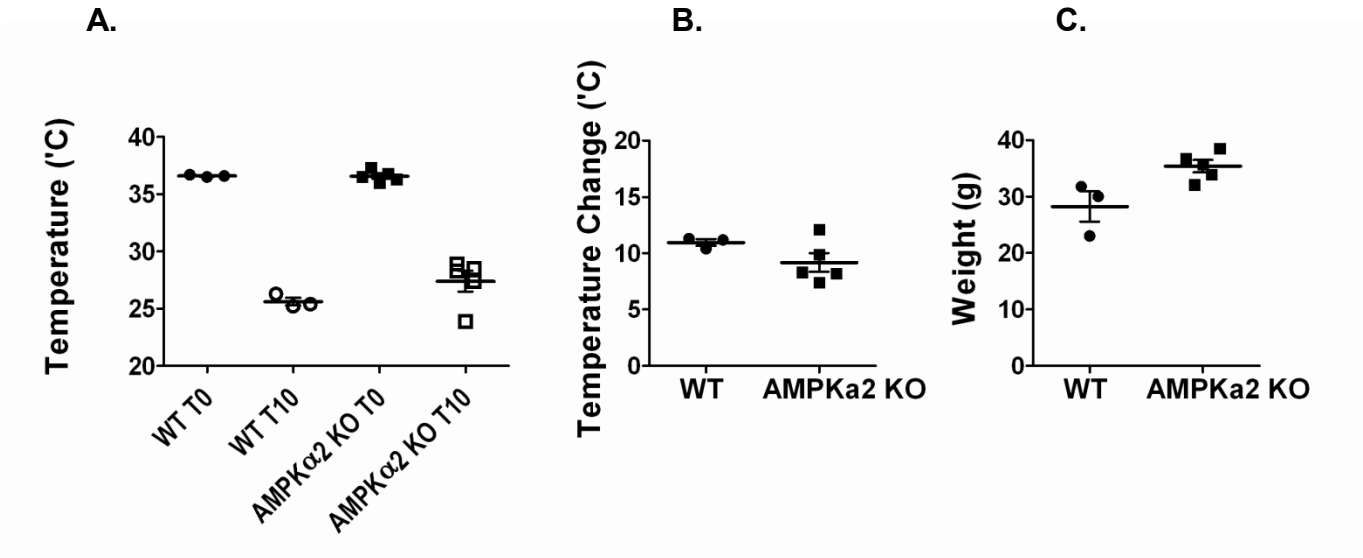

Figure 4.8 LPS sepsis study in global AMPKα2 KO mice.

A. Body temperatures prior to (T0) and 10 hour following LPS induction (T10) in WT and global AMPKα2 KO mice. **B.** 10 hour LPS induced temperature drop. **C.** Body weight measurements. All results shown in this figure are means ± SEM. WT n=3, AMPKα2 KO n=5.

4.2 Discussion

4.2.1 Summary of principal chapter findings

Protection from LPS sepsis in the CaMKKβ KO mice was shown in the previous chapter. Possible mechanisms including NO and cytokine production, white blood cell proliferation, macrophage activation and vascular permeability were investigated. The loss of CaMKKβ does not appear to confer an anti-inflammatory phenotype. Results from investigations into the inflammatory pathways are summarized here:

1). AMPK activity is reduced in CaMKKβ KO primary macrophages compared to WT primary macrophages under basal conditions and and reduced further by LPS treatment to a similar amount compared to WT mice, implying that the reduction in AMPK activity following LPS treatment is not dependent on CaMKKβ activity.

2). Concentration of the cytokine IL6 was found to be higher in the serum of CaMKKβ KO mice 12 hours following LPS sepsis induction compared to WT. No difference was seen in the serum concentration of IL1β, IL10, TNFα, GM-CSF or NO.

3). CaMKKβ is required for VEGF induced macrophage migration.

4). CaMKKβ is not essential for macrophage activation by LPS treatment or the resulting NO production and phagocytosis.

5). CaMKKβ is not essential for neutrophil and macrophage proliferation during LPS induced sepsis.

6). CaMKKβ is not essential for lymphocyte development in the thymus.

7). Global deletion of CaMKKβ does not appear to affect vascular permeability as measured in human umbilical vein endothelial cells with or without STO609 treatment, or *in vivo* by haematocrit count under control conditions or following LPS treatment.

8). Pharmacological treatment with STO609 appears to confer protection from LPS sepsis in mice.

9). Global AMPKα 1 or AMPKα2 KO mice do not appear to be protected from LPS sepsis.

4.2.2 LPS inhibits AMPK activity independently of CaMKKβ

In this chapter, data presented show CaMKKβ independent inhibition of AMPK activity by LPS treatment in primary macrophages. This is evident as AMPK is inhibited following LPS treatment in cell with CaMKKβ from WT mice as well as in CaMKKβ depleted cells from CaMKKβ KO mice (Figure 4.5B). Although basal activity of AMPK is lower in CaMKKβ KO cells there is an equivalent fall in AMPK activity following LPS treatment as there is in WT cells. Sag *et al* previously showed that 100ng/ml LPS treatment reduced AMPK phosphorylation in murine bone marrow derived macrophages by around 70% within 1 hour of treatment (Sag *et al*. 2008). More recently, Yang *et al* found 100ng/ml LPS treatment of RAW264.7 cell line macrophages not only reduced AMPK phosphorylation and activation relative to total AMPK after 2 hours, but also inhibited both LKB1 and AMPKα1 gene expression (Yang *et al*. 2010). The NFκB pathways by which LPS induces gene expression has been well studied (Guha and Mackman, 2001); more recently LPS has also been shown to inhibit insulin gene expression via TLR4 signalling (Amyot *et al* 2012). The inhibition of

AMPKα1 gene expression is particularly relevant as α1 is the predominant AMPK subunit present in macrophages (Sag *et al*. 2008). As AMPK activation is known to promote macrophage proliferation and phagocytosis (Bae *et al*. 2011). The inhibition of AMPK expression and activation by LPS appears to be another bacterial mechanism for combating the host immune system. The LPS induced reduction in AMPK activity appears to be CaMKKβ independent, but could possible be explained if the change in AMPK activity was mediated by reduced gene expression of AMPKα1 and the constitutively active LKB1.

4.2.3 CaMKKβ regulates LPS induced NFκB activation but does not affect PI3K signalling

CaMKKβ has pro-inflammatory functions as shown by the increased serum IL6 concentration in CaMKKβ KO mice following LPS treatment. Transcription of inflammatory cytokines including IL6 is induced by NFκB following its activation and translocation into the nucleus (Cinel *et al*. 2009). The binding of LPS to TLR4 on the cell membranes leads to recruitment of MyD88 which activates IκB kinase (IKK); resulting in the degradation of the NFκB inhibitory protein and release of NFκB into the nucleus (Karin and Delhase. 2000). The reduced AMPK activity in CaMKKβ KO primary macrophages suggest that the regulation of AMPK may be mediated at least partly through CaMKKβ. AMPK has been reported to negatively regulate the LPS induced NFκB pathway activation with increased IL6 and also TNFα expression seen in macrophages transfected with dominant negative AMPK and reduced cytokine expression in a constitutively active AMPK transfected macrophage cell line (Sag *et al*. 2008; Yang *et al*. 2010). The mechanism for the regulation is unclear, though AMPK activation of Sirtuin 1 (SIRT1) has been suggested leading to deacetylation and inhibition of NFκB (Yang *et al*. 2010).

Interestingly, the loss of CaMKKβ does not appear to affect LPS induced production of the anti-inflammatory cytokine IL10, suggesting the production of IL10 is regulated by a CaMKKβ independent pathway. Independent from IL6 production, LPS induced IL10 production in macrophages is known involve p38 activation downstream of PI3K/AKT (Ma *et al*. 2001). In addition, LPS induced TNFα expression is also known to be mainly regulated by the

activation of PI3K/AKT followed by activation of the MAPK/ERK pathway in macrophages (Van der Bruggen *et al*. 1999). The unaltered serum IL10 and TNFα expression seen in CaMKKβ KO mice suggests CaMKKβ is not required for LPS induced activation of the PI3K/AKT and downstream cytokine production. AMPK has been shown to regulate LPS induced IL10 expression in a macrophage cell line (Sag *et al*. 2008), suggesting that LKB1 is the likely upstream regulating kinase involved. Downstream of CaMKKβ, CaMK I has been reported to be involved in LPS induced IL10 production, with increased IL10 release in a macrophage cell line transfected with constitutively active CaMK Iα and reduced IL10 release in RNAi treated macrophages (Zhang *et al*. 2011). Indicating CaMKKα activity is sufficient for the regulation of the CaMK cascade in cytokine production by macrophages.

4.2.4 CaMKKβ regulates VEGF induced macrophage migration

VEGF activation of tyrosine kinase receptors induced migration was found to be reduced in primary macrophages from CaMKKβ KO mice compared to WT, suggesting CaMKKβ is involved in the regulation of macrophage chemotaxis. Chemotaxis in response to bacterial components, cytokines or chemokines is an important function for leukocytes including neutrophils and macrophages. The cell motility involved in chemotaxis is a complex process involving the transmission of the chemotaxis signal to the cytoskeletal proteins. The chemotaxis attractants bind receptors on the plasma membrane and activate a complex signalling network resulting in the activation of the cell motility proteins: Cdc42, Rac and RhoA GTPases. In brief, chemotaxis attractants bind to specific serpentine receptors as well as tyrosine kinase receptors, colony stimulating factor 1 receptors (CSF1R) on macrophages and activates PI3K signalling, resulting in the production of phosphatidylinositol triphosphate (PIP_3) and the activation of guanine nucleotide exchange factors (GEFs) which in turn activates Cdc42, Rac and RhoA (Jones. 2000). Cdc42 and Rac regulates the extension of filopodia and lamellipodia respectively; whereas activation of RhoA induces the formation of stress fibers, actin filaments associated with myosin fibres important for cell contraction (Ridley and Hall.1992; Nobes and Hall.1995). Cdc42, Rac, and RhoA have also been shown to activate each other sequentially in a cascade, with Cdc42 activating Rac, and Rac activating RhoA (Ridley *et al*. 1992). For cell motility to occur, the generation of lamellipodia through actin polymerization is required in the direction of movement, followed by contraction

of the cell body to detach the rear of the cell and complete the movement (Jones. 2000; Ridley. 2001). The activation of cell contraction by RhoA is essential for cell motility, shown by loss of motility in a macrophage cell line treated with a pharmacological inhibitor of Rho (Jones. 2000). The mechanisms by which RhoA regulates cell contractility is not entirely clear. RhoA has been shown to activate Rho kinase (ROCK) leading to the phosphorylation of non muscle myosin light chain regulatory units (NMLC), potentially through the phosphorylation and inhibition of MYPT1 by ROCK (Kimura *et al*. 1996; Totsukawa *et al*. 2004). In addition to inhibition, constitutive activation of RhoA also led to the loss of macrophage motility, indicating RhoA medicated cell contraction and macrophage motility is dependent on the temporal activation of RhoA in response to ligand stimulation (Allen *et al*. 1998).

It is unclear where CaMKKβ may exert its regulatory effects on the complex network of signals involved in the control of macrophage chemotaxis. Recent work by Wang *et al* show that AMPK activates MLCP through reduced phosphorylation of MYPT1 in human smooth muscle cells as well as vascular smooth muscle cells isolated from AMPKα1 and α2 KO mice (Wang *et al*. 2011). They further show the activation of AMPK promotes the binding of RhoA to p190 GTP activation protein (GAP) leading to the inhibition of RhoA activity, reduced ROCK activity, reduced MYPT1 Thr696 phosphorylation, and also decreased activity of smooth muscle myosin light chain regulatory units (Wang *et al*. 2011). Through the regulation of MYPT1, MLCP is able to dephosphorylate MLC (Somlyo and Somlyo. 2003); thus raising the possibility of a negative regulatory mechanism between CaMKKβ activity and MLC contraction through AMPK, RhoA and MYPT1.

To test this hypothesis, extensive western blotting was carried out to assess the phosphorylation of MYPT1. Unfortunately, none of the total and various phospho antibodies for MYPT1 tested were sufficiently sensitive to detect MYPT from primary macrophage lysates, aorta lysates or human embryonic kidney cell lysates. The optimisation of an assay for the quantification of ROCK activity from aorta lysates is currently ongoing.

4.2.5 CaMKKβ is not involved in macrophage phagocytosis

Phagocytosis of pathogens is an important function for macrophages. The activation of TLR4 by LPS has been shown to stimulate macrophage phagocytosis (Anand *et al*. 2007); however the signalling mechanisms are currently not clear. Macrophage phagocytosis is known to be initiated through the recognition of pathogen antigens by membrane Fc receptors and signalled through PI3K (Beemiller *et al*. 2010), with the rearrangement of the cytoskeleton mediated by the Rho GTPases: Cdc42 and Rac, as well as their downstream effectors including p21 activate protein (PAK1) (Swanson and Hoppe. 2004; Beemiller *et al*. 2010). Cdc42 and RAC are required for actin filament rearrangement: with Cdc42 recruited to the leading edge of the phagocytic cup where it is activated to stimulate actin polymerization; and RAC regulating phagosome closure to induce particle uptake (Beemiller *et al*. 2010).

Data presented in this thesis show CaMKKβ does not appear to be involved in either the regulation of macrophage phagocytosis or the stimulation of phagocytosis by LPS. This is in contrast to results from a recent study by Racioppi *et al*. showing reduced phagocytosis in untreated and LPS treated primary macrophages isolated from their cohort of global CaMKKβ KO mice (Racioppi *et al*. 2012). The reason for the discrepancy is unclear. Racioppi *et al*. also showed resistance to LPS induced sepsis by their global CaMKKβ KO mice; however they contribute it to a novel mechanism of increased phospho proline-rich tyrosine kinase 2 (PYK2) degradation, reduced NFβB activation, and resulting reduced serum cytokine concentrations of IFNγ, TNFα, IL6 and IL10 following LPS treatment (Racioppi *et al*. 2012). PYK2 is a member of the focal adhesion kinase (FAK) family, and pharmacological inhibition of PYK2 was previously shown to inhibit TNFα expression through the MAPK/ERK signalling in adherent monocytes but had no affect on nonadherent monocytes (Rosengart *et al*. 2002). Interestingly, a separate study showed reduced LPS induced NFκB activation and IL1β production following PYK2 knockdown by microRNA transfection in an LPS treated macrophage cell line (Xi *et al*. 2010); however comparison with the study by Racioppi *et al* is not possible as no data is presented for either serum IL1β cytokine concentration or macrophage mRNA expression following LPS treatment (Racioppi *et al*. 2012).

In summary, the protection conferred by the depletion of CaMKKβ against LPS induced sepsis does not appear to be mediated through significantly altered inflammatory response to the LPS in the global CaMKKβ KO mice in comparison to WT mice. As the occurrence of septic shock is a significant cause of mortality in sepsis (Sakr *et al*. 2006; Esteban *et al*. 2007), the study investigates the affects of CaMKKβ depletion on blood pressure regulation in the following chapter.

Chapter 5. The regulation of blood pressure by CaMKKβ

Clinically, one of the major causes of mortality following bacterial infection is the development of septic shock, which describes severe sepsis induced hypotension which is resistant to fluid treatment. The activation of eNOS by AMPK resulting in the release of nitric oxide has been shown in human aortic endothelial cells (Morrow *et al*. 2003), suggesting the possible involvement of AMPK in vasodilation and blood pressure regulation. AMPK has also beenshown to phosphorylate MLCK *in vitro* leading to reduced Ca^{2+}/calmodulin binding which is required for its activation (Horman *et al*. 2008). So far, there is no data on the involvement of CaMKKβ on the regulation of blood pressure. This chapter investigates the effect of global CaMKKβ deletion on blood pressure and its contribution to sepsis induced hypotension.

5.1. Investigating the regulation of blood pressure by CaMKKβ

5.1.1 CaMKKβ KO mice have higher baseline systolic and diastolic blood pressure compared to WT mice

Initially, cardiovascular parameters were assessed using telemetry transmitters surgically inserted into the descending thoracic aorta of both WT and CaMKKβ KO mice. Once the mice have recovered from surgery, heart rate, blood pressure and activity levels were recorded using telemetry receivers. The 24 hour baseline telemetry recordings show significantly higher systolic and diastolic blood pressure in CaMKKβ KO mice compared to WT mice, particularly during night time when the mice are more active (Figure 5.1A and 5.1B). No difference in heart rate was found between WT and CaMKKβ KO mice (Figure 5.1C).

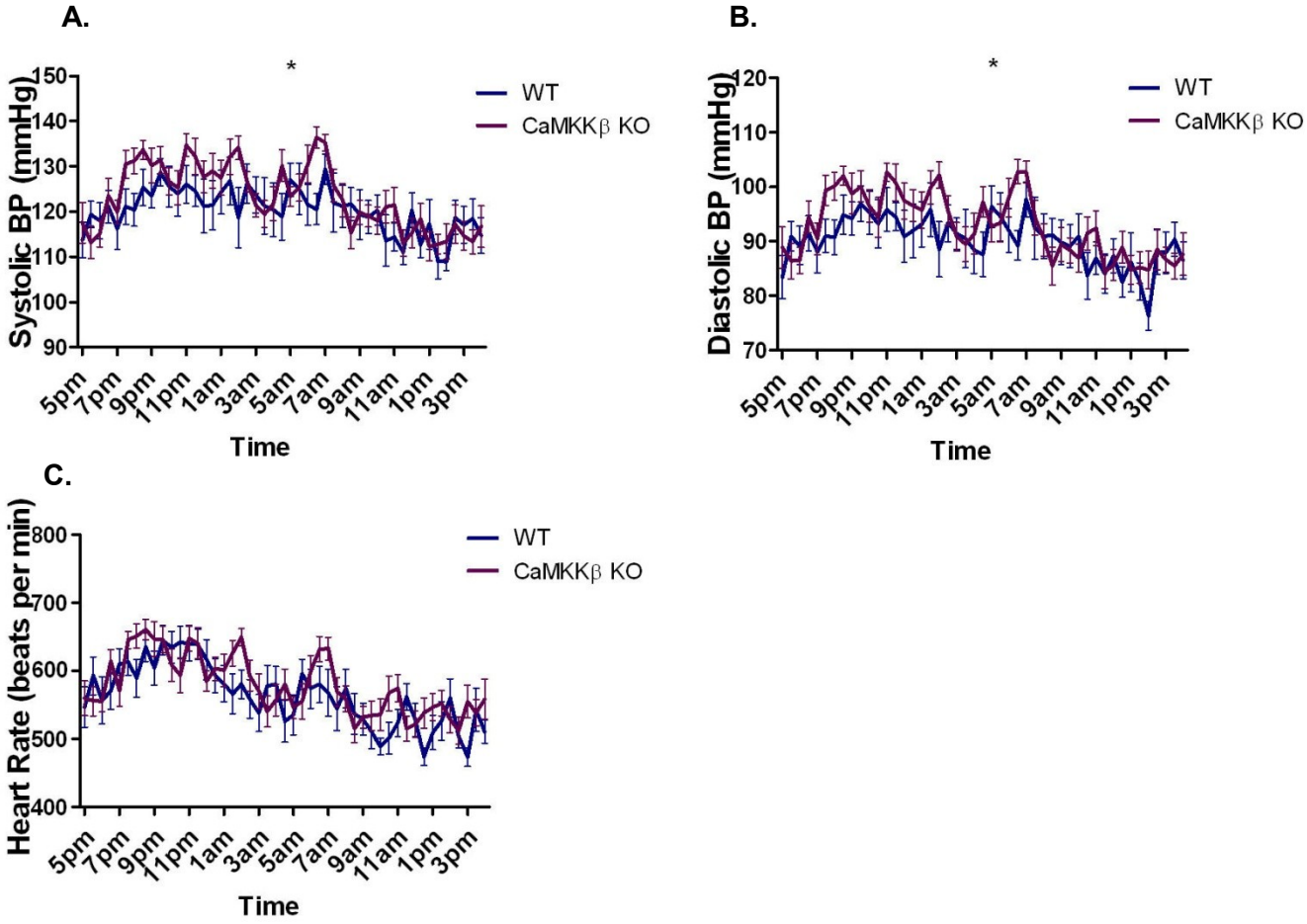

Figure 5.1 Baseline telemetry results.

Surgically inserted telemetry transponders were used to measure various parameters over a 24h period in WT and CaMKKβ KO mice. **A.** shows systolic blood pressure in millimetres of mercury (mmHg). **B.** shows diastolic blood pressure in millimetres of mercury (mmHg). **C.** shows heart rate in beats per minute.

Results are shown as mean±SEM. WT n=9, CaMKKβ n=12. Statistical analysis carried out by Imperial statistics department. The methodology used in the analysis was Mixed Model applied longitudinal data. *P<0.05.

5.1.2 CaMKKβ KO mice are resistant to LPS induced hypotension

To investigate whether blood pressure control is involved in the protection against LPS sepsis seen in CaMKKβ KO mice, heart rate, blood pressure and activity levels were recorded before and during the progression of sepsis. During the 7 hours following LPS injection, the systolic and diastolic blood pressure drops in both WT and CaMKKβ KO mice, this drop in blood pressure can be explained as vasodilation occurs following the release of NO from leukocytes and endothelial cells (Figure 5.2A and 5.2B). The drop in systolic blood pressure is initially similar between WT and CaMKKβ KO mice, until a certain time point following LPS injection (350 minutes, $p<0.05$), then the drop in systolic blood pressure slows down in CaMKKβ KO mice compared to WT mice (Figure 5.2A). The change in diastolic blood pressure follows a similar pattern to systolic blood pressure, where a slower drop in diastolic blood pressure occurs in CaMKKβ KO mice compared to WT mice after a certain time point (330 minutes, $p<0.05$) (Figure 5.2B). Heart rate was also found to slow down during the 7 hours following LPS injection in both WT and CaMKKβ KO mice; and higher heart rate was seen in CaMKKβ KO mice compared to WT mice after LPS injection (after 210 minutes, $p<0.05$) (Figure 5.2C).

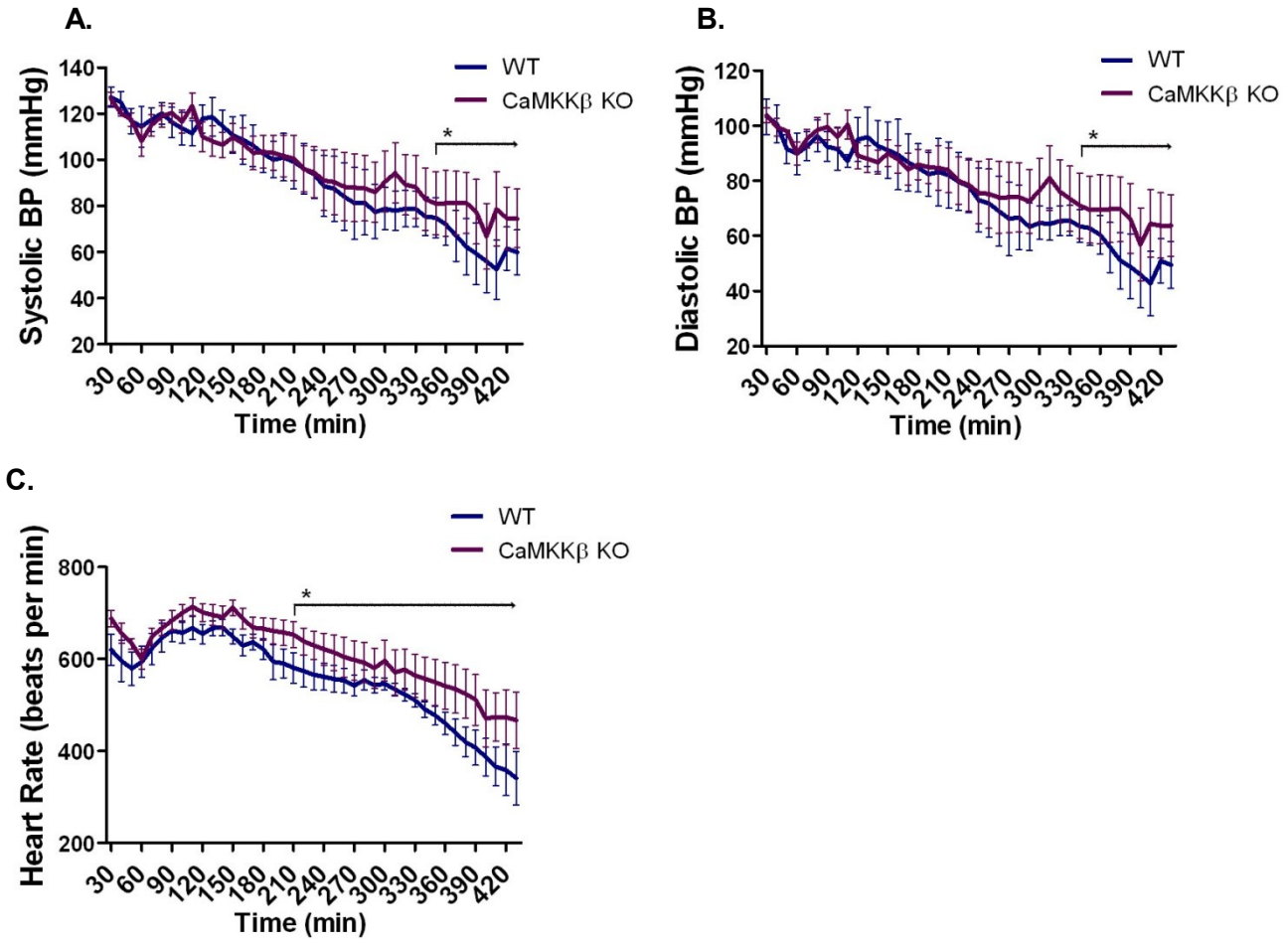

Figure 5.2 LPS telemetry results.

Surgically inserted telemetry transponders were used to measure various parameters over 7 hours following intraperitoneal LPS injection in WT and CaMKKβ KO mice. **A.** shows systolic blood pressure in millimetres of mercury (mmHg). **B.** shows diastolic blood pressure in millimetres of mercury (mmHg). **C.** shows heart rate in beats per minute.

Results are shown as mean±SEM. n=5. Statistical analysis carried out by Imperial statistics department. The methodology used in the analysis was Mixed Model applied longitudinal data. *P<0.05.

5.1.3 Investigating CaMKKβ and downstream affects in vasculature

CaMKKβ expression and kinase activity were assessed in aorta lysates. As shown in figure 5.3, there is measureable CaMKKβ activity and detectable CaMKKβ protein in aorta lysates from WT mice which is almost undetectable in CaMKKβ KO mice. This raises the possibility that CaMKKβ expressed in blood vessels could underlie the mechanism of increased blood pressure seen in CaMKKβ KO mice.

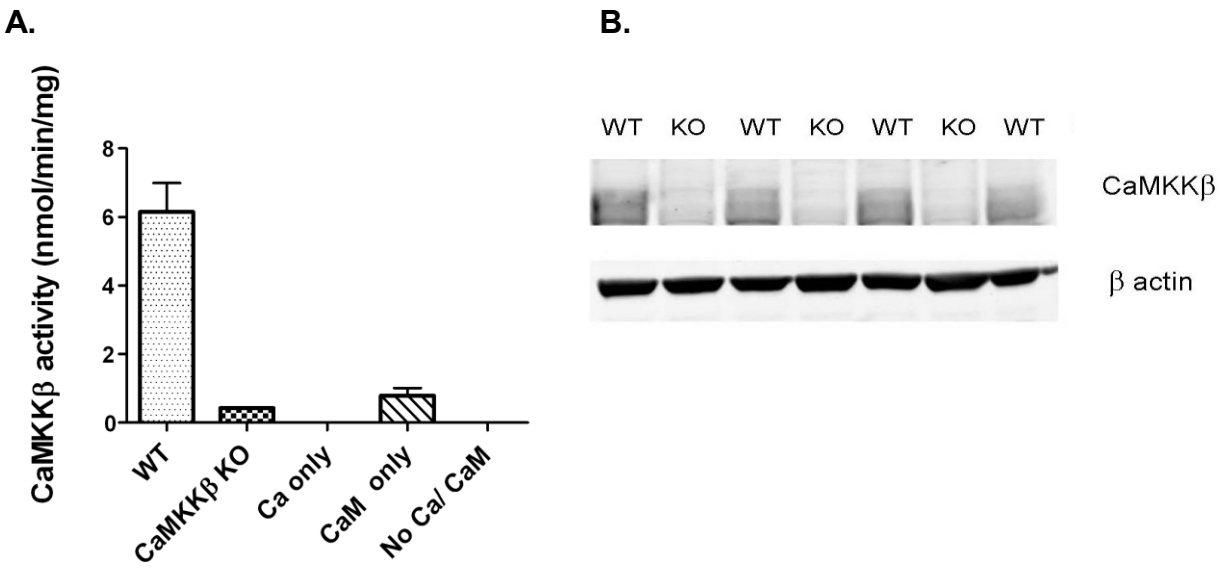

Figure 5.3 CaMKKβ expression and activity in the aorta.

A. CaMKKβ activity in WT and CaMKKβ KO aorta lysates as measured by immunoprecipitation of CaMKKβ from aorta lysates; followed by activation of recombinant AMPK α1β1γ1 in buffer containing calcium and calmodulin (WT and CaMKKβ KO), calcium only (Ca only), Calmodulin only (CaM only), or without calcium or calmodulin (No Ca/CaM); and measurement of recombinant AMPKα1β1γ1 activity. Assays carried out in duplicate. Results presented as nmoles [γ-^{32}P] incorporation into the peptide per minute per milligram tissue lysate. Results are shown as mean±SEM. n=2. **B.** A western blot of aorta lysates from WT and CaMKKβ KO mice probed with antibodies against CaMKKβ and β actin.

5.1.4 Loss of CaMKKβ increases myosin light chain phosphorylation in aorta lysates

To investigate the possible mechanism of blood pressure control by CaMKKβ in the vasculature, blood vessel contraction was assessed by comparing the phosphorylation of MLC in WT and CaMKKβ KO aorta lysates. Aorta myosin light chain Ser19 phosphorylation leads to shortening of the smooth muscle cells, contraction of the blood vessel and results in increased blood pressure. In aorta lysates from untreated mice, the phosphorylation of MLC was found to be significantly increased in CaMKKβ KO aorta lysates compared to WT (Figure 5.4). MLC phosphorylation is similarly decreased following LPS treatment in both WT and CaMKKβ KO aorta lysates (Figure 5.4); this may be explained by an increase in MLC dephosphorylation as a result of LPS induced NO release. In keeping with the increased MLC phosphorylation seen in untreated CaMKKβ KO aorta lysates, MLC phosphorylation was also higher in the CaMKKβ KO aorta lysates following LPS treatment compared to WT aorta lysates (Figure 5.4), suggesting that the increased MLC phosphorylation results from loss of CaMKKβ and this is sustained through LPS sepsis.

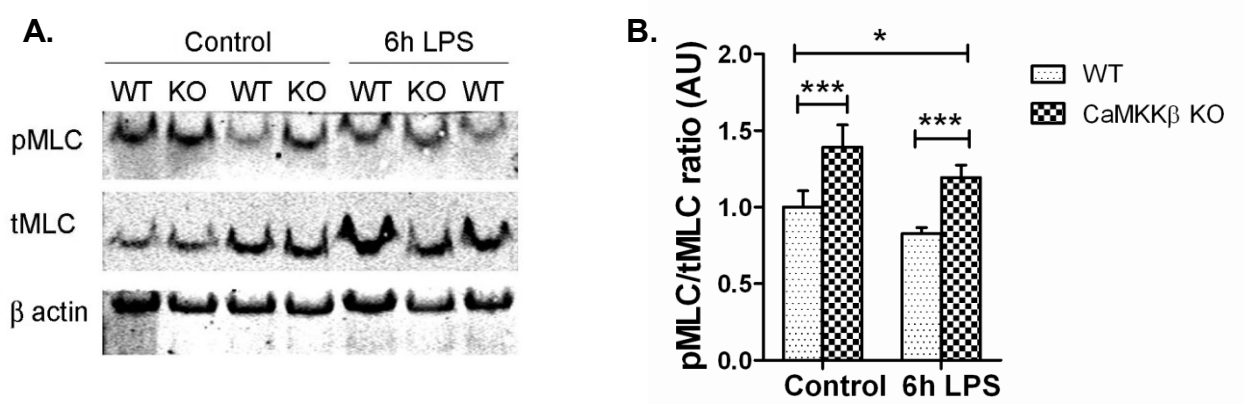

Figure 5.4 MLC phosphorylation in aorta lysates.
MLC phosphorylation in aorta lysates from untreated (Control) and 6 hour LPS treated (6h LPS) WT and CaMKKβ KO mice. **A.** Representative western blot of aorta lysates from untreated (Control) and 6h LPS treated (LPS) WT and CaMKKβ KO mice. Blots were probed with antibodies against pSer19 MLC (pMLC), total MLC (tMLC) and β actin. **B.** Quantification of Ser19 MLC phosphorylation as a ratio of pS19 MLC and total MLC expression (pMLC/tMLC) from western blots. Results are shown as mean±SEM. Control n=6, 6h LPS n=9. ANOVA: ***P<0.001, *P<0.05.

5.1.5 Loss of CaMKKβ increases myosin light chain kinase activity in aorta lysates

The phosphorylation of MLC is determined by the balance between phosphorylation by MLCK and dephosphorylation by MLCP. To investigate whether MLCK is a downstream target of CaMKKβ in the control of MLC phosphorylation, MLCK activity was measured in aorta lysates from WT and CaMKKβ KO mice. LPS treatment significantly increased MLCK activity in both WT and CaMKKβ KO aorta lysates (Figure 5.5A). Following 6 hours LPS treatment, higher MLCK activity was present in the CaMKKβ KO aorta lysates compared to WT; whereas no significant difference was seen between MLCK activity between WT and CaMKKβ KO mice in aorta lysates from untreated mice. Total MLCK protein expression is similar between WT and CaMKKβ KO aorta lysates when compared to β actin expression (Figure 5.5B).

MLCP activity as measured by MYPT1 phosphorylation could not be assessed due to technical difficulties (See section 4.2.4).

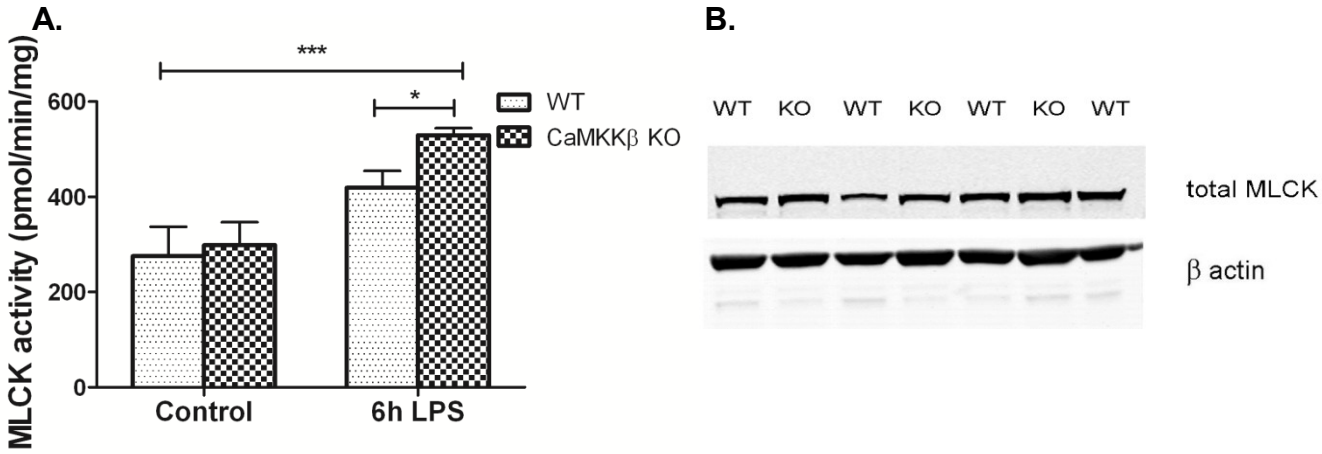

Figure 5.5 Aorta MLCK activity.
A. MLCK activity in aorta lysates from untreated (Control) and 6 hour LPS treated (6h LPS) WT and CaMKKβ KO mice. MLCK was immunoprecipitated from aorta lysates and incubated with recombinant MLC peptide to assess MLCK activity. Assays carried out in duplicate. Results presented as pmoles [γ-^{32}P] incorporation into the peptide per minute per milligram tissue lysate. Results are shown as mean±SEM. Control n=3, 6h LPS n=8. ANOVA: ***P<0.001, *P<0.05. **B.** A western blot of aorta lysates from LPS treated WT and CaMKKβ KO mice probed with antibodies against total MLCK and β actin.

5.1.6 Loss of CaMKKβ has no effect on nitric oxide activity in aorta lysates

The expression of iNOS is induced by LPS binding to TLR4, leading to the production of NO by macrophages and endothelial cells during sepsis. NO diffuses into vascular smooth muscle cells and induces the production of cGMP, leading to the activation of MYPT1 by PKG, resulting in dephosphorylation of MLC and vasodilation. In keeping with the similar reduction in MLC phosphorylation seen in WT and CaMKKβ KO aorta lysates during LPS sepsis (Figure 5.4), no change was seen in the serum NO and cGMP concentrations of CaMKKβ KO mice following LPS treatment compared to WT (Figure 4.2). Both cGMP concentration and PKG expression in aorta lysates were also assessed and found to be comparable between WT and CaMKKβ KO mice (Figure 5.6).

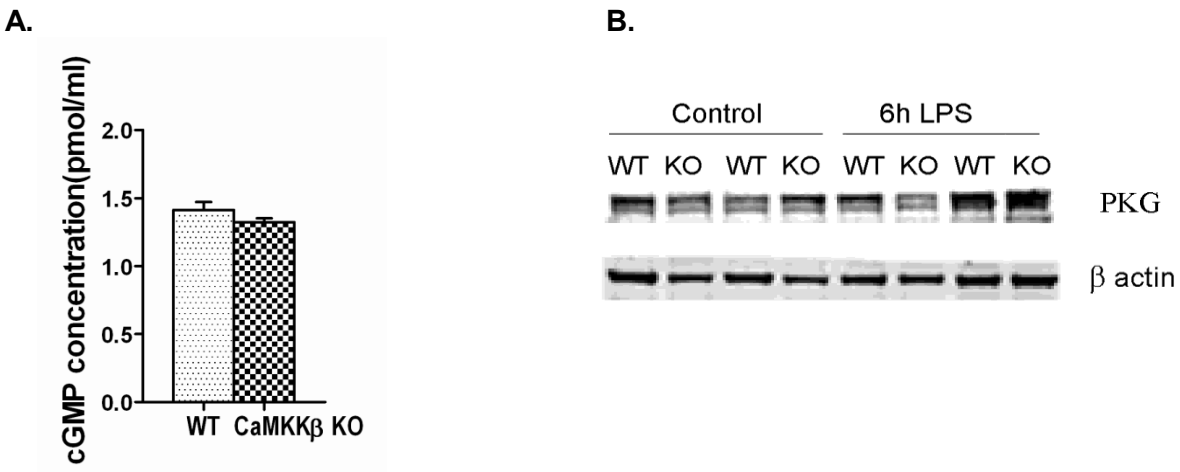

Figure 5.6 cGMP concentration and PKG expression in the aorta.
A. Aorta cGMP concentration as measured using an immunoassay kit in 6h LPS treated WT and CaMKKβ KO aorta lysates. Assays carried out in duplicate. Results are shown as mean±SEM. n=3. **B.** Western blot of untreated (Control) and 6h LPS treated (LPS) WT and CaMKKβ KO aorta lysates probed with antibodies against PKG and β actin.

5.1.7 AMPK activity in aorta lysates

As AMPK has previously been shown to be involved in the regulation of blood pressure (Wang *et al*. 2011) and is known to be phosphorylated by CaMKKβ, AMPK activity was measured in WT and CaMKKβ KO aorta lysates from both untreated and 6 hour LPS treated mice to assess its involvement in the blood pressure phenotype seen in CaMKKβ KO mice. AMPK*α*1 subunit activity was found to be significantly reduced following 6 hour LPS treatment compared to untreated in both WT and CaMKKβ KO mice aorta lysates; AMPK*α*2 subunit activity and total AMPK activity as measured in immunoprecipitates of AMPKβ complexes were reduced in 6 hour LPS treated aorta lysates but did not reach statistical significance (Figure 5.7). These results are in keeping with that seen in LPS treated cultured macrophages where LPS treatment significantly reduced AMPK*α*1 subunit activity (Figure 4.5B). No significant difference was seen in AMPK activity between WT and CaMKKβ KO aorta from either untreated or 6 hour LPS treated mice (Figure 5.7).

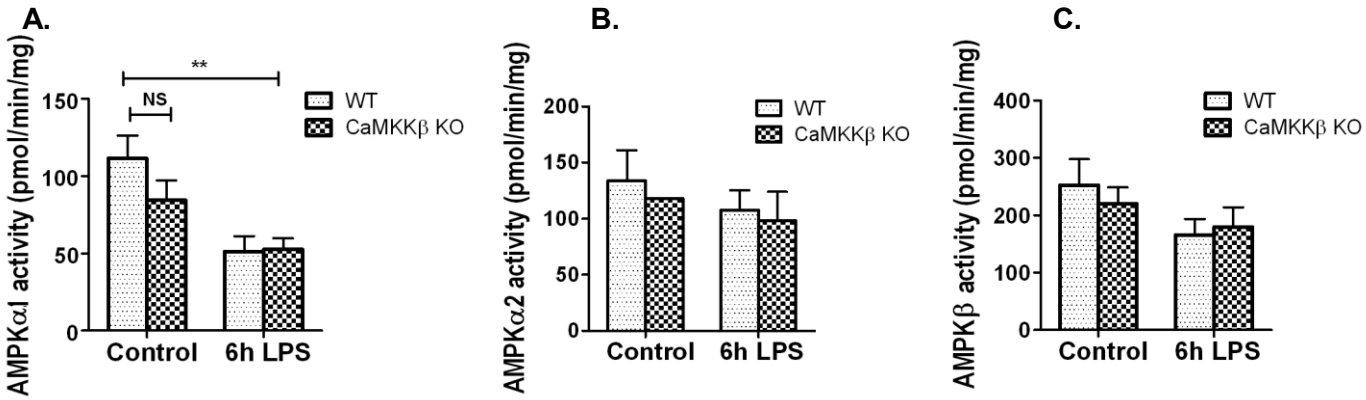

Figure 5.7 AMPK activity in the aorta.

The activity of AMPK*α*1 and AMPK*α*2 subunit complexes as well as total AMPK activity were measured in aorta from untreated (Control) and 6h LPS treated (6h LPS) WT and CaMKKβ KO mice by immunoprecipitation of the respective complex from aorta lysates and incubation with SAMS peptide in a radioisotope incorporation assay. **A.** shows AMPK*α*1 activity. **B.** shows AMPK*α*2 activity. **C.** shows total AMPK activity.

All assays carried out in duplicate. Results presented as pmoles [γ-^{32}P] incorporation into the peptide per minute per milligram tissue lysate. Results are shown as mean±SEM. Control n=3, 6h LPS n=4. ANOVA: **P<0.01.

5.1.8 CaMKKβ KO mice have normal aorta histology

The aorta wall is composed of three concentric layers including tunica intima, tunica media and tunica adventitia. Tunica intima is composed of an innermost endothelial layer in contact with blood flow, as well as a layer of connective tissue between the endothelial layer and tunica media. The tunica media in the aorta is the thickest of the three layers; it is composed of organised smooth muscle cells and appears to be the major contributor to aorta contractility. The structure of the tunica media layer has been shown to be importance for transmitting the force generated by the movement of phosphorylated myosin fibres across actin filaments to aorta wall contraction (Standley *et al*. 2002). The smooth muscle actin filaments are known to form a helical pattern spiralling around the aorta to optimise force generation during vessel contraction (Standley *et al*. 2002); with alterations to actin structure leading to loss of contraction and vessel wall weakness, resulting in aneurysms (Bergeron *et al*. 2011). Smooth muscle cells express elastin and collagen into the extracellular matrix which form circular bands around the aorta, providing stretch and stiffness respectively to maintain the basal vessel tone (Wagenseil and Mecham. 2012). The outer layer, tunica adventitia, is mainly composed of myofibroblasts which also produce collagen.

To investigate the possibility that the loss of CaMKKβ may increase blood pressure through altered aorta structure, perfused aortas were isolated and fixed in formaldehyde prior to paraffin embedding, sectioning and staining. Representative images at 2.5x and 10x magnification of aorta sections stained with haematoxylin and eosin (H&E), elastin van graffin (EVG), smooth muscle actin (SMA), and picosirius red are presented in figure 5.8. No difference was seen in any of the following measurements: aorta wall thickness, tunica media thickness, tunica adventicia thickness, or the number of elastin bands in CaMKKβ KO mice compared to WT mice (Figure 5.9A and 5.9B). Aortas from CaMKKβ KO mice also had normal medial thickness as calculated by the ratio of tunica media thickness to the number of elastin bands (Figure 5.9A).

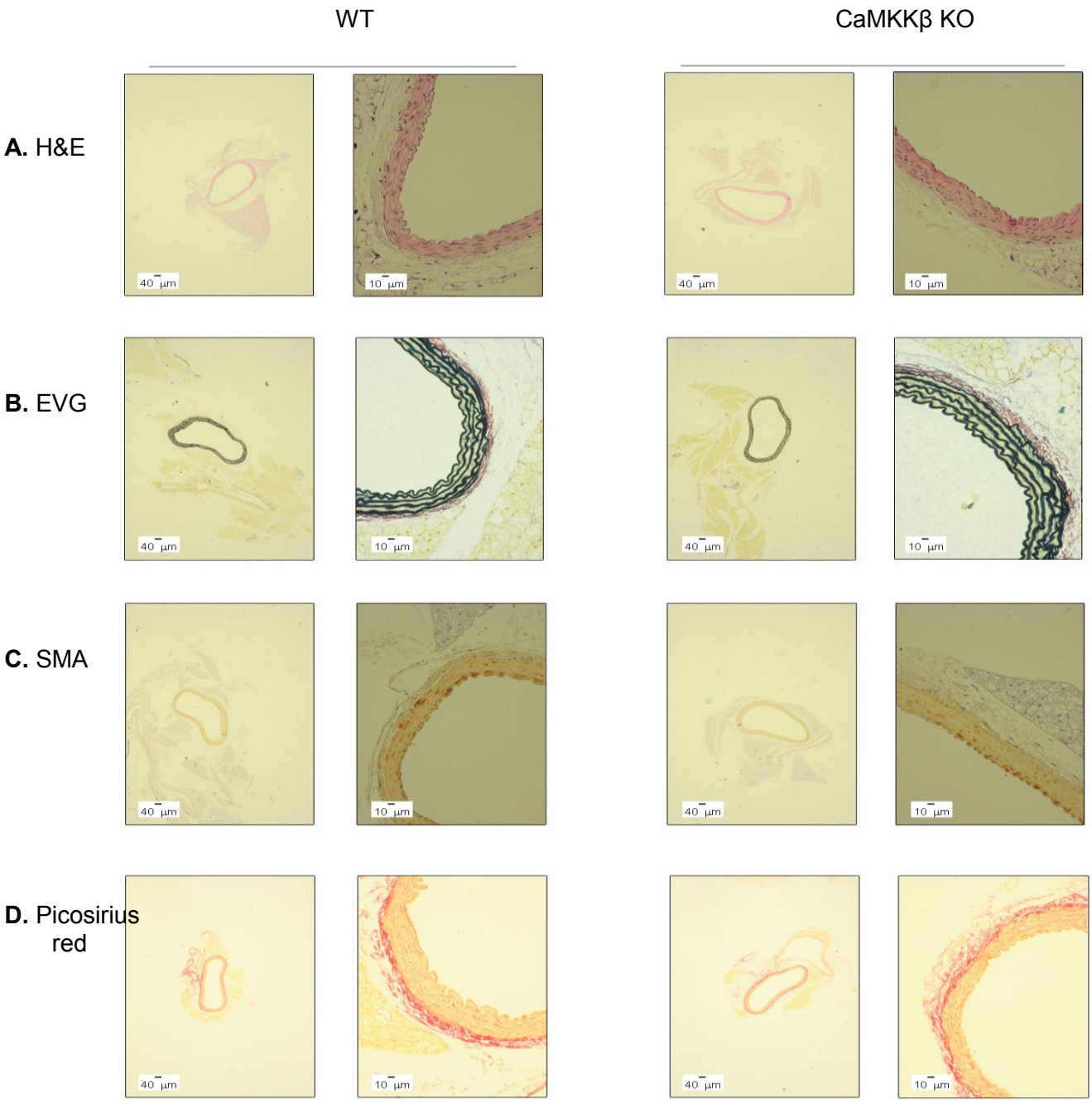

Figure 5.8 Aorta histology.

Representative images of formaldehyde fixed, sectioned and stained aorta from WT and CaMKKβ KO mice at 2.5x and 10x magnification.

A. Haematoxylin and eosin stain (H&E). **B.** Elasin staining with elastin van graffin (EVG). **C.** Staining with smooth muscle actin antibody (SMA). **D.** Collagen staining with picosirius red.

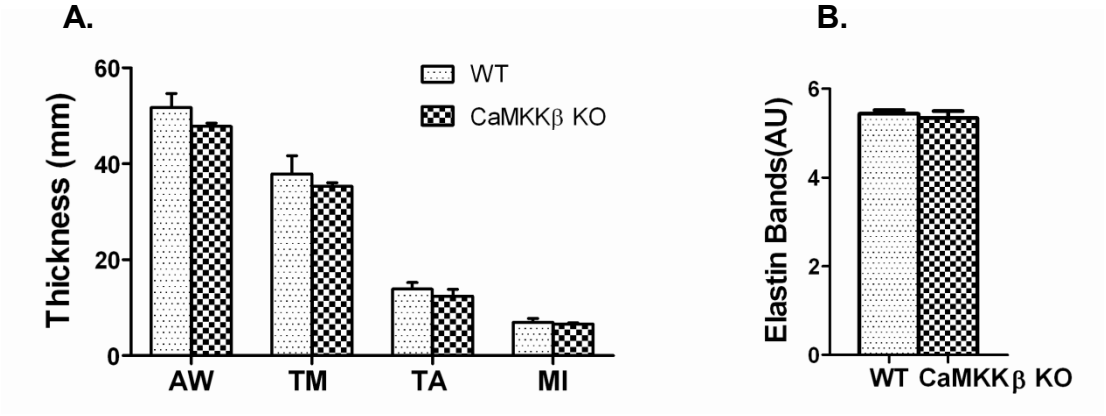

Figure 5.9 Aorta histology measurements.

A. WT and CaMKKβ KO aorta images were taken at 10x magnification and the following measurements quantified using ImageJ software. AW: Aorta wall thickness, TM: tunica media, TA: tunica adventitia, MI: medial interval. **B.** Number of elastin bands present in the WT and CaMKKβ KO aorta wall on histology. All measurements made in quadruplicate from 2 aorta sections from each mouse. Results are shown as mean±SEM. n=4 mice.

5.1.9 CaMKKβ KO mice have normal kidney function

As AMPK is known to phosphorylate the renal tubule sodium potassium channel NKCC2 and alter kidney salt reabsorption (Fraser *et al*. 2005 and 2007), urinary electrolyte concentrations were measured in CaMKKβ KO mice to investigate the contribution of kidney function to the high blood pressure seen. No difference was found in either sodium, potassium or chloride concentrations between urine samples from WT and CaMKKβ KO mice (Figure 5.10A). In addition, phosphorylation of AMPK at Thr172 and the phosphorylation of NKCC2 at Ser126 were found to be similar between WT and CaMKKβ KO kidney lysates as shown by western blotting (Figure 5.10B).

Produced in the adrenal glands in response to stress and activation of the sympathetic nervous system, the hormone adrenaline is a potent vasoconstrictor that is excreted by the kidneys. To investigate the potential involvement of the sympathetic nervous system, urinary adrenaline concentration normalised to creatinine was measured and found to be similar between WT and CaMKKβ KO mice (Figure 5.10C); suggesting the increased blood pressure seen in the CaMKKβ KO mice does not result from increased adrenaline production. However the increased activation of the sympathetic nervous system cannot not be excluded, as the noradrenaline concentration could not be measured due to assay unavailability.

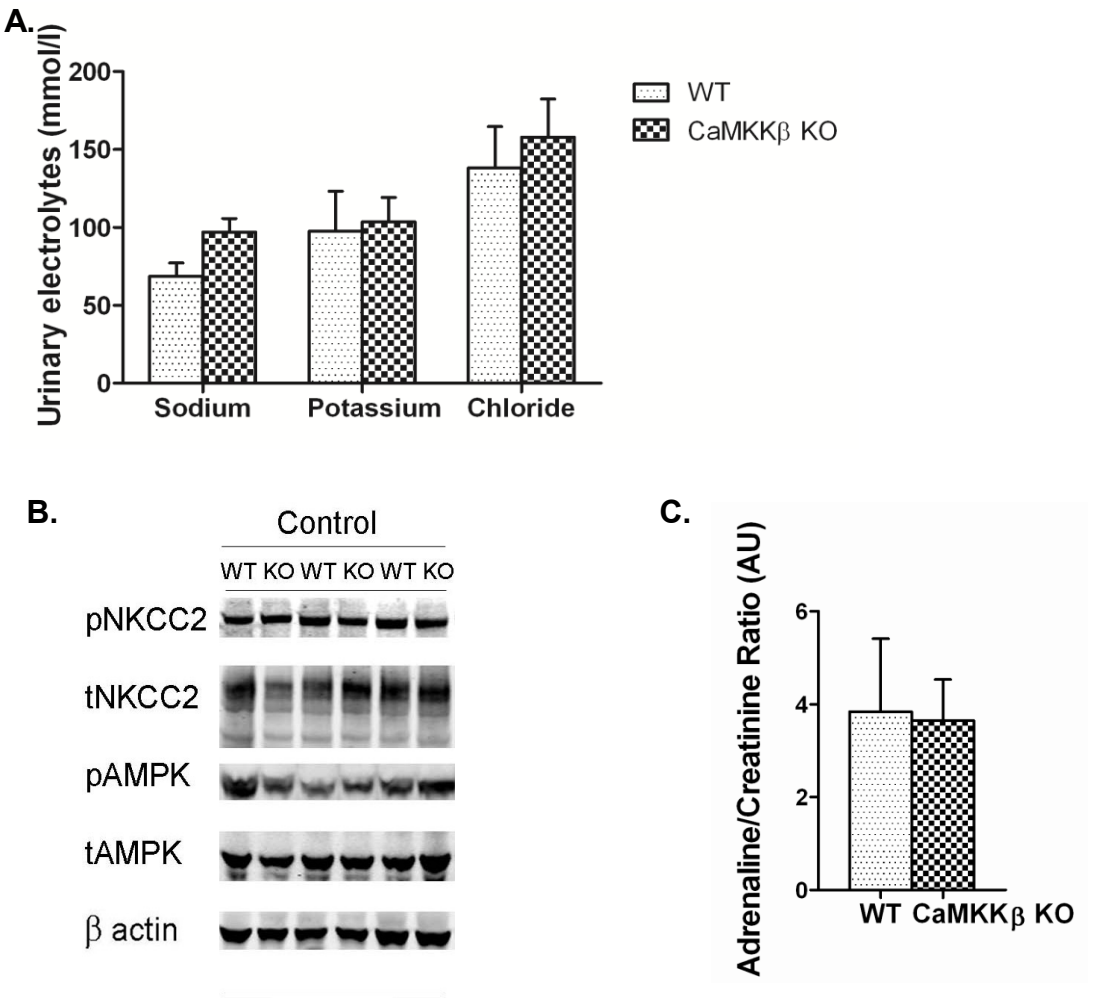

Figure 5.10 Comparing kidney function in WT and CaMKKβ KO mice.

A. Urinary sodium, potassium and chloride concentration in WT and CaMKKβ KO mice on normal diet. Results are shown as mean±SEM. WT n=5, CaMKKβ KO n=4. **B.** Western blots of kidney lysates from WT and CaMKKβ KO mice on a normal diet probed with antibodies against pSer126 NKCC2 (pNKCC2), total NKCC2 (tNKCC2), pThr172 AMPK (pAMPK), total AMPK (tAMPK) expression using an antibody against AMPKβ, as well as β actin. **C.** Urinary adrenaline concentration in WT and CaMKKβ KO mice normalised to urinary creatinine concentration. Results are shown as mean±SEM. WT n=5, CaMKKβ KO n=4.

5.1.10 Aged CaMKKβ KO mice have reduced cardiac function

High blood pressure is a known risk factor for the development of heart failure due to increased development of both left ventricular hypertrophy and coronary heart disease (Haslett *et al*. 2002; Houser *et al*. 2012). To assess the physiological significance of the high blood pressure seen in CaMKKβ KO mice under basal conditions, echocardiogram was carried out at regular intervals over a six month period until the mice were 12 month old to determine the affect of CaMKKβ loss on long term cardiac function. By 10 month, CaMKKβ KO mice were found to have significantly reduced ejection fraction as well as left ventricular shortening compared to WT (Figure 5.11C and 5.11D respectively); indicating reduced left ventricle function and reduced overall cardiac output. Cardiac hypertrophy was not seen in up to 12 month old CaMKKβ KO mice, as shown by similar left ventricle mass and left ventricular wall thickness between WT and CaMKKβ KO mice (Figure 5.11A and Figure 5.11B).

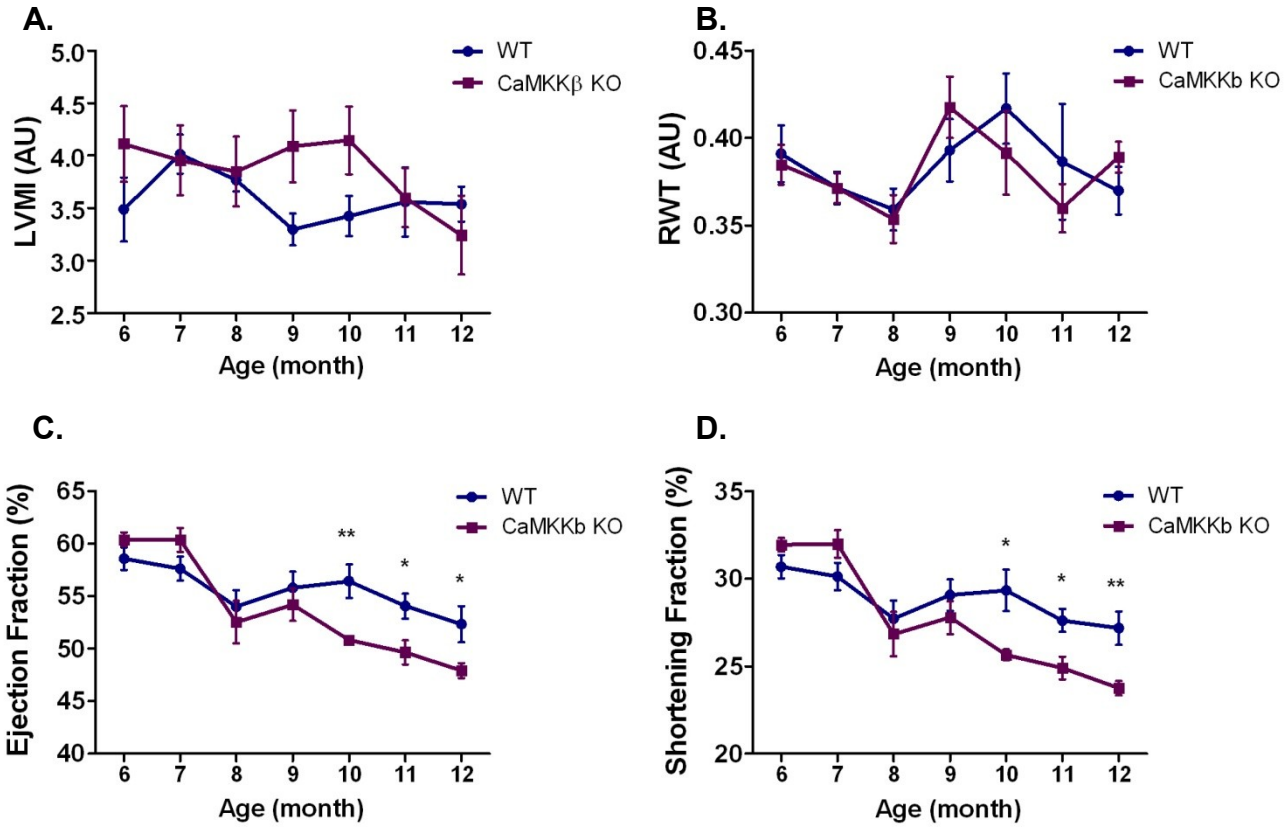

Figure 5.11 Comparing cardiac function in 6 to 12 month old WT and CaMKKβ KO mice.

WT and CaMKKβ KO mice were assessed by cardiac ultrasound under isoflurane anaesthesia monthly until 12 month old. **A.** Left ventricular mass of WT and CaMKKβ KO mice were measured on cardiac ultrasound and normalised to body weight to determine left ventricular mass index (LVMI). **B.** Left ventricle wall thickness was measured on cardiac ultrasound and normalised to left ventricle diameter during diastole to determine the relative wall thickness (RWI). **C.** Percentage ejection fraction was measured on cardiac ultrasound in WT and CaMKKβ KO mice. **D.** Percentage shortening fraction was measured on cardiac ultrasound in WT and CaMKKβ KO mice. All results in this figure are shown as mean±SEM. WT n=5, CaMKKβ n=8. Student's t-test: **P<0.01, *P<0.05.

5.2 Discussion

5.2.1 Summary of principal chapter findings

In the previous two chapters, the loss of CaMKKβ activity was shown to protect against LPS induced sepsis without inhibiting macrophage activation or reducing inflammatory cytokine production. In this chapter, we have tried to investigate the possible mechanism of the protection against LPS seen in CaMKKβ KO mice via a vascular phenotype. CaMKKβ KO mice were found to have higher blood pressure compared to WT mice and increased blood vessel MLC phosphorylation resulting in increased vessel contraction. The main results are summarized below:

1). CaMKKβ KO mice were found to have higher blood pressure compared to WT mice under basal condition. At 12 month, CaMKKβ KO mice were found to have reduced ejection fraction and ventricular shortening compared to WT mice, indicating worse cardiac function.

2). Loss of CaMKKβ confers resistance against LPS induced hypotension.

3). Absence of CaMKKβ results in increased phosphorylation of MLCK and MLC in aorta lysates from CaMKKβ KO mice both under basal conditions and following LPS treatment compared to WT mice.

4). No difference was seen in serum NO concentration or cGMP concentration in aorta lysates indicating that CaMKKβ is not involved in NO production or aorta cGMP expression.

5). AMPK activity was found to be reduced in aorta lysates from LPS treated mice; however similar reduction in AMPK activity was seen in aorta lysates from both WT and CaMKKβ KO mice.

6). No obvious difference was seen on CaMKKβ KO aorta histology compared to WT aorta.

7). Loss of CaMKKβ does not affect kidney function or NKCC2 phosphorylation in kidney lysates. No difference was seen in urinary creatinine or electrolyte concentration between WT and CaMKKβ KO mice.

5.2.2 LPS reduces aorta MLC phosphorylation

The phosphorylation of MLC on Ser19 regulates the formation of myosin cross bridges on actin filaments and controls smooth muscle cell contration (Adelstein andConti 1975; Rembold *et al*. 1992; Somlyo and Somlyo. 1994). Although TLR4 receptors are known to be expressed on vascular smooth muscle cells (Pryshchep *et al*. 2008); little is known regarding the affect of LPS on the contractile function of smooth muscle. One recent study showed a dose dependent contractile dysfunction in human colonic smooth muscle cells following TLR4 activation by LPS which was partially prevented by treatment with pharmacological inhibition of NFκB (Scirocco *et al*. 2010). Data presented in this chapter show reduced aorta MLC phosphorylation despite activation of MLCK activity following LPS treatment. In keeping with the reduction in aorta MLC phosphorylation; telemetry recordings show decreases in both systolic and diastolic blood pressure following LPS treatment. The difference between MLCK activity and MLC phosphorylation can be explained by increased dephosphorylation of MLC due to increased serum concentration of NO in LPS treated mice. Leukocytes and the endothelium are known to produce NO following LPS induced expression of iNOS (Ding *et al*. 1990; Vo *et al*. 2005). Although LPS induced iNOS expression and NO production has been shown in vascular smooth muscle cells (Ohta *et al*. 2011); its physiological significance is unclear as isolated aortic rings with the endothelium removed are resistant to LPS induced vasodilation (Vo *et al*. 2005).

So far, investigation of LPS induced MLCK activity has concentrated on the regulation of tight junctions in both epithelium and endothelium. Through pharmacological inhibition of MLCK, activation of TLR4 by LPS has been shown to cause tight junction dysfunction through activation of MLCK leading to increased permeability of airway epithelium, intestinal endothelium and vascular endothelium (Eutamene *et al*. 2005; Moriez *et al*. 2005; Bogatcheva *et al*. 2011). In keeping with this, data in the previous chapter show increased murine haematocrit following LPS sepsis indicating increased vascular endothelial permeability. Little is known regarding the effect of LPS on aortic smooth muscle function, this chapter presents evidence supporting the activation of MLCK by LPS in the aorta which may antagonise the dephosphorylation of MLC by induced NO which in turn contributes to the regulation of blood pressure during sepsis.

5.2.3 CaMKKβ regulates aorta MLCK activation of MLC during LPS sepsis

During LPS sepsis, CaMKKβ appears to reduce MLC phosphorylation through inhibition of MLCK activty in the aorta. The protection conferred to STO609 treated WT mice against LPS sepsis is consistent with that the loss of CaMKKβ activity rather than its expression is important for the protection seen. Interestingly, although an increase in MLCK activity is seen in aortas from LPS treated CaMKKβ KO mice compared to WT mice, no difference was seen in aorta MLCK activity from untreated WT and CaMKKβ mice. One explanation would be activation of CaMKKβ by LPS, therefore accentuating the difference in MLCK activity between WT and CaMKKβ KO aorta following LPS treatment. An increase in vascular endothelial cell intracellular calcium concentration is seen following LPS induced TLR4 activation (Bogatcheva *et al*. 2011); a similar mechanism could lead to activation of CaMKKβ in vascular smooth muscle cells. In keeping with the increased MLCK activity seen in aorta from LPS treated CaMKKβ KO mice compared to WT, the phosphorylation of MLC was also found to be increased as shown by data presented in this chapter.

The inhibition of MLCK by CaMKKβ provides an important internal brake on the activation of MLCK by increasing calcium concentrations. Increased vessel calcium sensitivity is a known risk factor for coronary artery vasospasms, along with polymorphism in the eNOS gene (Stern and Bayes de Luna. 2009; Morikawa *et al*. 2010). Calcium channel blockers and long acting nitrates are both used in the treatment of coronary artery vasospasms (Stern and Bayes de Luna. 2009); however, the cause of vessel calcium sensitivity leading to vasospasms remains unclear. Data presented in this chapter provides a novel regulatory mechanism for calcium activation of smooth muscle MLCK (Figure 5.12).

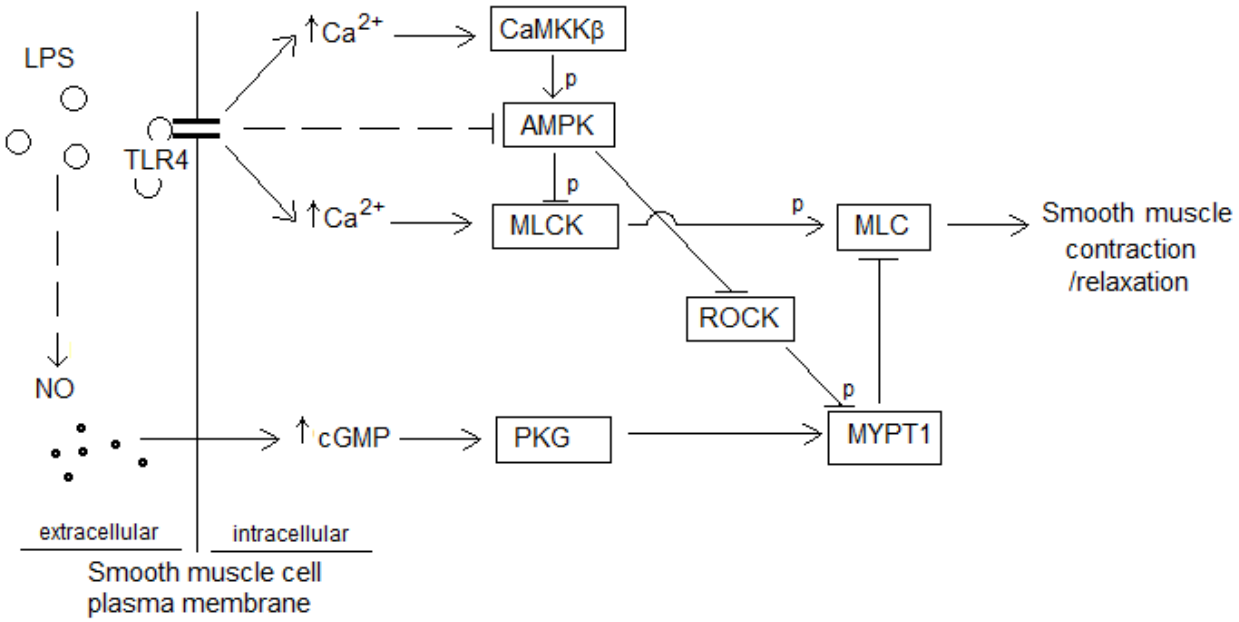

Figure 5.12 Proposed mechanism of MLC regulation by CaMKKβ through MLCK to control blood pressure during LPS sepsis. TLR4 activation in vascular smooth muscle cells potentially increase cytosol calcium concentration resulting in activation of MLCK and CaMKKβ. The activation of MLCK by calcium is limited by CaMKKβ activation, potentially through activation of AMPK by CaMKKβ and phosphorylation of MLCK, resulting in controlled phosphorylation of MLC. The activation of MLC is antagonized by the production of NO during LPS sepsis by immune cells and the endothelium, leading to increased activation of MLCP and dephosphorylation of MLC, resulting in overall smooth muscle relaxation and vasodilation. AMPK has been shown to inhibit MLC phosphorylation through inhibition of ROCK, dephosphorylation of MYPT1 and activation of MLCP (Wang *et al*. 2011). Loss of CaMKKβ leads to increased MLCK activity and MLC phosphorylation during LPS sepsis, resulting in reduced smooth muscle relaxation and reduced hypotension.

5.2.4 CaMKKβ regulates vessel contraction through activation of MLC

CaMKKβ KO mice were found to have increased baseline blood pressure compared with WT mice, suggesting CaMKKβ not only regulates blood pressure during LPS sepsis but also functions to maintain baseline blood vessel tone. Data presented in this chapter show increased MLC phosphorylation in the aorta of untreated CaMKKβ KO mice compared to WT mice. As aorta MLCK activity does not significantly differ between WT and CaMKKβ KO mice at baseline, the difference in MLC phosphorylation seen may be explained by altered MYPT1 dephosphorylation of MLC.

Unfortunately, MLCP activity could not be assessed due to technical difficulties (See section 4.2.4). However, the involvement of CaMKKβ in MLC dephosphorylation by MLCP through the MLCP regulatory subunit MYPT1 is supported by a recent study by Wang *et al*. showing the activation of AMPK in vascular smooth muscle cells leads to inhibition of ROCK, dephosphorylation of MYPT1, activation of MCLP and dephosphorylation of MLC (Wang *et al*. 2011).

5.2.5 Loss of CaMKKβ does not significantly alter aorta structure

Within the blood vessel wall, the layers of smooth muscle are arranged in the form of concentric helices spiralling around the lumen of the vessel (Standley *et al*. 2002). Studies indicate the alignment of vascular smooth muscle cells results from the cyclic nature of vessel stretch resulting from the arterial pressure generated by the left ventricle (Kanda and Matsuda. 1993; Standley *et al*. 2002); although the mechanisms by which this is accomplished remain unclear. *In vivo*, vascular smooth muscle cells are arranged in layers within the aorta wall to achieve maximal vessel contraction or dilation with minimal smooth muscle cell shortening or lengthening, respectively (Fultz *et al*. 2000). Between the layers of smooth muscle cells, bands of extracellular matrix composed of elastin and collagen provide stretch and stiffness respectively to maintain the basal vessel tone (Wagenseil and Mecham. 2012). Therefore, in addition to the contractility of smooth muscle cells, the control of vessel

lumen size and consequently blood pressure is also dependent on the alignment of the vascular smooth muscle cells as well as the structure and composition of the extracellular matrix.

To assess blood vessel structure and investigate the possibility of a mechanical cause for the high blood pressure seen in CaMKKβ KO mice, immunohistochemistry of formaldehyde fixed aorta sections from WT and CaMKKβ KO mice was carried out to stain for smooth muscle cell alignment, smooth muscle actin composition, and the distribution of extracellular matrix proteins. No difference was seen in either muscle layer thickness or the number of elastin bands within the WT and CaMKKβ KO mice. Similar staining was also seen for the distribution pattern of elastin, smooth muscle actin and collagen within the aorta wall; suggesting the loss of CaMKKβ does not significantly alter aorta structure. Smooth muscle cell alignment was difficult to assess due to the helical nature of the smooth muscle layers around the aorta wall which causes variations within the pattern of smooth muscle cells seen on each aorta section. Therefore, the possibility of altered smooth muscle cell alignment within blood vessel walls contributing to the high blood pressure seen in CaMKKβ KO mice cannot be excluded.

5.2.6 Loss of CaMKKβ does not affect kidney function

Abnormal NaCl handling by the kidneys is known to contribute to the development of high blood pressure through sodium and water retention (Haslett *et al*. 2002; Meneton *et al*. 2005). Significantly reduced urinary excretion of sodium has been shown to be present during the development of hypertension in several hypertensive rat strains (Meneton *et al*. 2005). The ascending limb of loops of Henle in the kidneys reabsorbs 25-30% of filtered NaCl from the tubule lumen via the kidney specific NKCC2 cotransporters, and NKCC2 activity have been shown to contribute to sodium retention and the development of high blood pressure (Gliménez 2006; Ares *et al*. 2011). In humans, mutations in the gene coding for NKCC2 result in decreased or absent activity characterized by the severe NaCl loss and decreased blood pressure seen in Bartter syndrome type 1; conversely, increased NKCC2 activity is associated with the development of hypertension (Ares *et al*.2011).

To investigate the role of kidney function and NKCC2 activity in the development of high blood pressure seen in CaMKKβ KO mice, urinary electrolyte were analyzed as an indirect measurement of baseline kidney NaCl handling and NKCC2 activity. CaMKKβ KO mice were found to have similar urinary sodium, potassium and chloride excretion compared to WT mice indicating CaMKKβ KO mice have normal kidney function. Total NKCC2 expression was also unchanged in kidneys from CaMKKβ KO mice compared to WT mice; with similar NKCC2 Ser126 phosphorylation, the site known to be phosphorylated by AMPK (Fraser *et al*. 2007), seen in kidneys from WT and CaMKKβ KO mice.

5.2.7 Loss of CaMKKβ affects long term cardiac function

To assess the physiological significance of the high blood pressure seen in CaMKKβ KO mice under basal conditions, cardiac echo was carried out at regular intervals in up to 12 month old mice to determine the affect of CaMKKβ loss on long term cardiac function. Fractional shortening describes the reduction in left ventricle diameter during systole compared to diastole whereas ejection fraction describes the percentage of blood volume pumped out of the left ventricle during systole; providing quantitative measures of left ventricular contractility and cardiac output respectively (Hoit *et al*. 1997; Rottman *et al*. 2007). By 10 month old, CaMKKβ KO mice were found to have significantly reduced ejection fraction as well as left ventricular shortening compared to WT; suggesting the development of hypertensive heart disease and heart failure.

High blood pressure is a well known risk factor for the development of heart failure (Haslett *et al*. 2002; Houser *et al*. 2012). The classical paradigm of hypertensive heart disease is that persistently elevated blood pressure leads to a degree of compensated ventricular hypertrophy with ventricular wall thickening but normal ejection fraction; which eventually transitions to heart failure with reduced ejection fraction and fractional shortening (Levy *et al*. 1990). Data presented in this chapter show reduced cardiac function in the older CaMKKβ KO mice with no indication of cardiac hypertrophy as shown by normal left ventricular mass

and wall thickness; providing support for the alternative theory suggesting the development of either left ventricular hypertrophy or failure in response to high blood pressure in the absence of transitional cardiac injury in hypertensive heart disease (Drazner 2005).

5.2.8 The benefits and limitations of mouse models

During this study, several different transgenic mouse models of gene deletions were used to investigate the function of CaMKKβ in metabolism, LPS sepsis and the regulation of blood pressure. Rodents are used to model human diseases as they have the same organ and systemic physiology as humans; in addition, they have the benefit of high reproductive rates, ease of handling, and relatively low cost of use. The mouse (*Mus musculus*) in particular, is the most common mammal used for genetic phenotyping (Simmona. 2008). The mouse genome has a similar number of protein producing genes compared to the human genome and eighty percent of genes are present in both genomes (Emes *et al*. 2003).

One of the main disadvantages of using mouse models is the limited technology available for physiological measurements due to the size of the animals. The measurement of arterial stiffness by pulse wave velocity was not possible in the mouse models due to technical limitations. For the measurement of blood pressure in mice, use of radiotelemetry in conscious animals was used in preference to tail cuff sphygmomanometer both for its sensitivity (Bubb *et al*. 2012), as well as allowing the measurement of conscious blood pressure. However, the surgical techniques involved requires a high degree of expertise and is both time and labour intensive which reduced the feasibility of large numbers of animals.

Chapter 6. Summary and future directions

CaMKKβ is known to activate AMPK as well as the CaMK cascade, however, little is known of the physiological functions of CaMKKβ outside the nervous system. To investigate the functions of CaMKKβ and its involvement in the control of metabolism by AMPK, the global CaMKKβ KO mice were characterized both under baseline conditions and also during LPS sepsis to model activation of the immune system as well as sepsis induced hypotension. This thesis provides evidence for the regulation of blood pressure by CaMKKβ both under baseline conditions and during sepsis induced hypotension.

6.1 Conclusions

1). Globally, CaMKKβ does not appear to be required for the metabolic functions of AMPK measured in this study as shown by the lack of metabolic phenotype seen in CaMKKβ KO mice, suggesting that LKB1 is the main upstream regulator for the metabolic pathways controlled by AMPK. AMPK is a key regulator of metabolism and is known to control the energy production and utilisation in an organism on multiple levels including mitochondrial function, tissue glucose and fatty acid metabolism, as well as food intake and energy expenditure (Kahn *et al*. 2005; Carling. 2005; Schneeberger and Claret. 2012). The regulation of metabolism by LKB1 activation of AMPK is in keeping with previous findings in skeletal muscle specific LKB1 KO mice showing impaired contraction stimulated glucose uptake (Sakamoto *et al*. 2005); and indicates LKB1 may be involved in the regulation of mitochondrial function as well as the hormonal control of energy balance.

2). The loss of CaMKKβ in mice protects against the physical deterioration and temperature drop that occurs during LPS sepsis as shown in both CaMKKβ KO mice and STO-609 treated WT mice. This protection is likely to be mediated through the maintenance of systemic blood pressure. Pretreatment of the CaMKKβ KO mice with blood pressure lowering pharmacological agents such as inhibitors of β-adrenergic receptors prior to LPS

treatment could clarify the involvement of blood pressure in the LPS sepsis seen; however interpretation of the results may be complicated by the effect of the pharmacological agent on cardiac function.

3). In the immune system, the involvement of CaMKKβ in macrophage migration as well as LPS induced cytokine production and macrophage activation were investigated. The regulation of MLC by CaMKKβ in macrophages was suggested by reduced VEGF induced migration of primary macrophages isolated from CaMKKβ KO mice compared to WT mice. Loss of CaMKKβ appears to increase LPS induced IL6 but not IL10 production; indicating the regulation of NFκB activation by CaMKKβ. CaMKKβ is not required for LPS induced macrophage activation, nitric oxide production or phagocytosis. In addition, CaMKKβ is not required for the production of nitric oxide both under baseline condictions and following LPS treatment.

4). CaMKKβ regulates blood pressure both under baseline conditions and during sepsis induced hypotension; as shown by increased systemic blood pressure in the CaMKKβ KO mice compared to WT matched littermates persisting through sepsis induced hypotension. Over time, the high blood pressure resulting from loss of CaMKKβ leads to impaired cardiac function as shown by reduced cardiac output and contractility in the CaMKKβ KO mice compared to WT matched littermates. Blood vessel contraction, kidney function, and aorta histology were investigated to look for causes of the high blood pressure seen in CaMKKβ KO mice. CaMKKβ does not appear to be required for either sodium reabsorption or the phosphorylation of NKCC2 by AMPK in the kidneys. Aorta histology was also similar between the WT and CaMKKβ KO mice. Blood vessel contraction was assessed through the quantification of aorta MLC phosphorylation; and was found to be significantly increased in the CaMKKβ KO mice compared to WT both under baseline conditions and during sepsis induced hypotension.

Under baseline conditions, the mechanism for regulating aortic MLC phosphorylation by CaMKKβ is not entirely clear. CaMKKβ activity does not affect MLCK phosphorylation and activation without LPS treatment; although the reduction in MLC phosphorylation can

potentially occur through a chain of phosphorylation events following AMPK activation, including ROCK activity inhibition and MYPT1 activation resulting in MLC dephosphorylation, previously shown in vascular aortic smooth muscle cells (Wang *et al*. 2011). Following LPS treatment, CaMKKβ activation causes the phosphorylation and inhibtion of MLCK in the aorta resulting in reduced MLC phosphorylation. It is unclear if CaMKKβ phosphorylates MLCK directly or through the activation of AMPK. The availability of transgenic AMPK mice for blood pressure measurement following LPS treatment would provide important information regarding the involvement of AMPK in this pathway.

6.2 Future directions

The mechanism through which CaMKβ controls MLC phosphorylation requires clarification. Further evidence is needed to confirm the involvement of AMPK in the regulation of MLC phosphorylation by CaMKKβ. Plans are underway for blood pressure telemetry recordings in global AMPKβ1 KO mice both under basal conditions and during LPS sepsis. In contrast to the AMPKα1 KO mice, the AMPKβ1 KO mice do not display either anaemia or splenomegaly; therefore provides a better haemodynamic model for the investigation of the role of AMPK in blood pressure regulation.

The regulation of blood pressure by CaMKKβ has been shown to persist during reductions in blood pressure as shown by LPS sepsis induced hypotension. An area for future investigation would be the effect of the development of high blood pressure on its regulation by CaMKKβ. High dietary salt intake is a well described risk factor for high blood pressure in salt sensitive individuals (Luft and Weinberger. 1982). A European prospective follow up study showed 44% of their healthy recruited participants were salt sensitive; and the salt sensitive individuals were 75% more likely to develop hypertension over fifteen years compared to salt resistant individuals (Barba *et al*. 2007). The CaMKKβ KO mice have been backcrossed onto the C57BL/6 background; as the C57BL/6 mice are known to be salt

sensitive (Leonard *et al*. 2006), the CaMKKβ KO mice may provide a good model for the investigation of salt sensitive hypertension.

Another area for future investigation is the clinical implications of blood pressure regulation by CaMKKβ, in particular, the pharmacological inhibition of CaMKKβ during sepsis induced hypotension. Currently, treatment of sepsis induced hypotension involves fluid treatment followed by the use of vasopressors to raise blood pressure and improve organ perfusion. Common vasopressors include catecholamines, such as norepinephrine and dopamine, which act on the adrenergic receptors; as well as vasopressin and its analogues acting on the vasopressin receptors. A recent Cochrane review found none of six commonly used vasopressors superior to any other when used alone or in combination in the treatment of septic shock, sepsis induced hypotension resistant to fluid resuscitation (Havel *et al*. 2011). More significantly, despite the multiple vasopressors currently available for the treatment of hypotension, septic shock carries a high mortality rate of 45-50% (Sakr *et al*. 2006; Esteban *et al*. 2007). Data from a large European prospective multicentered observational study found the incidence of septic shock to be 31 cases per 100,000 people per year with 1 in 12 cases of hospital admissions for sepsis developing septic shock after 2-5 days (Esteban *et al*. 2007). It is clear that improved treatments for septic shock are urgently needed, particularly when epidermiological studies show that the incidence of septic shock appears to be rising (Martin *et al*. 2003). Although much more investigation is clearly required to clarify the underlying mechanisms of blood pressure regulation by CaMKKβ, the inhibition of CaMKKβ provides a novel target for the treatment of septic shock.

References

Adelstein, R. S. and M. A. Conti (1975). Phosphorylation of platelet myosin increases actin-activated myosin ATPase activity. Nature 256(5518): 597-8.

Ageta-Ishihara, N., S. Takemoto-Kimura, M. Nonaka, A. Adachi-Morishima, K. Suzuki, S. Kamijo, H. Fujii, T. Mano, F. Blaeser, T. A. Chatila, H. Mizuno, T. Hirano, Y. Tagawa, H. Okuno and H. Bito (2009). Control of cortical axon elongation by a GABA-driven Ca2+/calmodulin-dependent protein kinase cascade. J Neurosci 29(43): 13720-9.

Allen, W. E., D. Zicha, A. J. Ridley and G. E. Jones (1998). A role for Cdc42 in macrophage chemotaxis. J Cell Biol 141(5):1147-57.

Altun, B. and M. Arici (2006). Salt and blood pressure: time to challenge. Cardiology 105(1): 9-16.

Amyot, J., M. Semache, M. Ferdaussi, G. Fontés and V. Poitout. (2012). . Lipopolysaccharides impair insulin gene expression in isolated islets of Langerhans via Toll-Like Receptor-4 and NF-κB signalling. PLoS ONE 7(4):e36200.

An, J. H., J. Y. Yang, B. Y. Ahn, S. W. Cho, J. Y. Jung, H. Y. Cho, Y. M. Cho, S. W. Kim, K. S. Park, S. Y. Kim, H. K. Lee and C. S. Shin (2010). Enhanced mitochondrial biogenesis contributes to Wnt induced osteoblastic differentiation of C3H10T1/2 cells. Bone 47(1): 140-50.

Anand, R. J., J. W. Kohler, J. A. Cavallo, J. Li, T. Dubowski and D. J. Hackam (2007). Toll-like receptor 4 plays a role in macrophage phagocytosis during peritoneal sepsis. J Pediatr Surg 42(6):927-32; discussion 933.

Anderson, K. A., F. Lin, T. J. Ribar, R. D. Stevens, M. J. Muehlbauer, C. B. Newgard and A. R. Means (2012). Deletion of CaMKK2 from the liver lowers blood glucose and improves whole-body glucose tolerance in the mouse. Mol Endocrinol 26(2): 281-91.

Anderson, K. A., R. L. Means, Q. H. Huang, B. E. Kemp, E. G. Goldstein, M. A. Selbert, A. M. Edelman, R. T. Fremeau and A. R. Means (1998). Components of a calmodulin-dependent protein kinase cascade. Molecular cloning, functional characterization and cellular localization of Ca2+/calmodulin-dependent protein kinase kinase beta. J Biol Chem 273(48): 31880-9.

Anderson, K. A., T. J. Ribar, F. Lin, P. K. Noeldner, M. F. Green, M. J. Muehlbauer, L. A. Witters, B. E. Kemp and A. R. Means (2008). Hypothalamic CaMKK2 contributes to the regulation of energy balance. Cell Metab 7(5): 377-88.

Andersson, U., K. Filipsson, C. R. Abbott, A. Woods, K. Smith, S. R. Bloom, D. Carling and C. J. Small (2004). AMP-activated protein kinase plays a role in the control of food intake. J Biol Chem 279(13): 12005-8.

Andreelli, F., M. Foretz, C. Knauf, P. D. Cani, C. Perrin, M. A. Iglesias, B. Pillot, A. Bado, F. Tronche, G. Mithieux, S. Vaulont, R. Burcelin and B. Viollet (2006). Liver adenosine monophosphate-activated kinase-alpha2 catalytic subunit is a key target for the control of hepatic glucose production by adiponectin and leptin but not insulin. Endocrinology 147(5): 2432-41.

Andrews, Z. B., Z. W. Liu, N. Walllingford, D. M. Erion, E. Borok, J. M. Friedman, M. H. Tschop, M. Shanabrough, G. Cline, G. I. Shulman, A. Coppola, X. B. Gao, T. L. Horvath and S. Diano (2008). UCP2 mediates ghrelin's action on NPY/AgRP neurons by lowering free radicals. Nature 454(7206): 846-51.

Ares, G. R., P. S. Caceres and P. A. Ortiz (2011). Molecular regulation of NKCC2 in the thick ascending limb. Am J Physiol Renal Physiol 301(6):F1143-59.

Ares, G. R., M. Z. Haque, E. Delpire and P. A. Ortiz (2012). Hyperphosphorylation of Na-K-2Cl cotransporter in thick ascending limbs of Dahl salt-sensitive rats. Hypertension 60(6):1464-70.

Asai, Y., H. Uchida, H. Yamamoto, Y. Ohyama, T. Jinno, Y. Taiji, K. Ochiai and T. Ogawa (2000). Prevention of endotoxin-induced lethality in mice by calmodulin kinase activator. FEMS Immunol Med Microbiol 27(3): 201-10.

Aughton, K. L., K. Hamilton-Smith, J. Gupta, J. S. Morton, C. P. Wayman and V. M. Jackson (2008). Pharmacological profiling of neuropeptides on rabbit vaginal wall and vaginal artery smooth muscle *in vitro*. Br J Pharmacol 155(2): 236-43.

Bain, J., L. Plater, M. Elliott, N. Shpiro, C. J. Hastie, H. Mclauchlan, I. Klevernic, J. S. C. Arthur, D. R. Alessi and P. Cohen (2007). The selectivity of protein kinase inhibitors: a further update. Biochem J 408(Pt 3): 297-315.

Banchereau, J., V. Pascual and A. O'Garra (2012). From IL-2 to IL-37: the expanding spectrum of anti-inflammatory cytokines. Nat Immunol 13(10): 925-31.

Banko, M. R., J. J. Allen, B. E. Schaffer, E. W. Wilker, P. Tsou, J. L. White, J. Villen, B. Wang, S. R. Kim, K. Sakamoto, S. P. Gygi, L. C. Cantley, M. B. Yaffe, K. M. Shokat and A. Brunet (2011). Chemical genetic screen for AMPKalpha2 substrates uncovers a network of proteins involved in mitosis. Mol Cell 44(6): 878-92.

Barnes, B. R., S. Glund, Y. C. Long, G. Hjalm, L. Andersson and J. R. Zierath (2005). 5'-AMP-activated protein kinase regulates skeletal muscle glycogen content and ergogenics. FASEB J 19(7): 773-9.

Barnes, B. R., S. Marklund, T. L. Steiler, M. Walter, G. Hjalm, V. Amarger, M. Mahlapuu, Y. Leng, C. Johansson, D. Galuska, K. Lindgren, M. Abrink, D. Stapleton, J. R. Zierath and L. Andersson (2004). The 5'-AMP-activated protein kinase gamma3 isoform has a key role in carbohydrate and lipid metabolism in glycolytic skeletal muscle. J Biol Chem 279(37): 38441-7.

Bassett, J. H., A. Boyde, P. G. Howell, R. H. Bassett, T. M. Galliford, M. Archanco, H. Evans, M. A. Lawson, P. Croucher, D. L. St Germain, V. A. Galton and G. R. Williams (2010). Optimal bone strength and mineralization requires the type 2 iodothyronine deiodinase in osteoblasts. Proc Natl Acad Sci U S A 107(16): 7604-9.

Baumgarten, G., P. Knuefermann, G. Schuhmacher, V. Vervolgyi, J. von Rappard, U. Dreiner, K. Fink, C. Djoufack, A. Hoeft, C. Grohe, A. A. Knowlton and R. Meyer (2006). Toll-like receptor 4, nitric oxide, and myocardial depression in endotoxemia. Shock 25(1): 43-9.

Beemiller, P., Y. Zhang, S. Mohan, E. Levinsohn, I. Gaeta, A.D. Hoppe and J. A. Swanson (2010). A Cdc42 activation cycle coordinated by PI 3-kinase during Fc receptor-mediated phagocytosis. Mol Biol Cell 21(3):470-80.

Behr-Roussel, D., A. Oudot, S. Caisey, O. L. Coz, D. Gorny, J. Bernabe, C. Wayman, L. Alexandre and F. A. Giuliano (2008). Daily treatment with sildenafil reverses endothelial dysfunction and oxidative stress in an animal model of insulin resistance. Eur Urol 53(6): 1272-80.

Behr-Roussel, D., A. Oudot, S. Compagnie, D. Gorny, O. Le Coz, J. Bernabe, C. Wayman, L. Alexandre and F. Giuliano (2008). Impact of a long-term sildenafil treatment on pressor

response in conscious rats with insulin resistance and hypertriglyceridemia. Am J Hypertens 21(11): 1258-63.

Beier, I., R. Dusing, H. Vetter and U. Schmitz (2008). Epidermal growth factor stimulates Rac1 and p21-activated kinase in vascular smooth muscle cells. Atherosclerosis 196(1): 92-7.

Bergeron, R., S. F. Previs, G. W. Cline, P. Perret, R. R. Russell, 3rd, L. H. Young and G. I. Shulman (2001). Effect of 5-aminoimidazole-4-carboxamide-1-beta-D-ribofuranoside infusion on *in vivo* glucose and lipid metabolism in lean and obese Zucker rats. Diabetes 50(5): 1076-82.

Bergeron, S. E., E. W. Wedermeyer, R. Lee, K. K. Wen, M. McKane, A. R. Pierick, A. P. Berger, P. A. Rubenstein and H. L. Bartlett (2011). Allele-specific effects of thoracic aortic aneurysm and dissection alpha-smooth muscle actin mutations on actin function. J Biol Chem 286(13):11356-69.

Berquist, R. K., W. E. Berquist, C. O. Esquivel, K. L. Cox, K. I. Wayman and I. F. Litt (2008). Non-adherence to post-transplant care: prevalence, risk factors and outcomes in adolescent liver transplant recipients. Pediatr Transplant 12(2): 194-200.

Birk, J. B. and J. F. Wojtaszewski (2006). Predominant alpha2/beta2/gamma3 AMPK activation during exercise in human skeletal muscle. J Physiol 577(Pt 3): 1021-32.

Biswas, S. K. and E. Lopez-Collazo (2009). Endotoxin tolerance: new mechanisms, molecules and clinical significance. Trends Immunol 30(10): 475-87.

Blackwell, T. S. and J. W. Christman (1996). Sepsis and cytokines: current status. Br J Anaesth 77(1): 110-7.

Blaeser, F., M. J. Sanders, N. Truong, S. Ko, L. J. Wu, D. F. Wozniak, M. S. Fanselow, M. Zhuo and T. A. Chatila (2006). Long-term memory deficits in Pavlovian fear conditioning in Ca2+/calmodulin kinase kinase alpha-deficient mice. Mol Cell Biol 26(23): 9105-15.

Blaustein, M. P., F. H. Leenen, L. Chen, V. A. Golovina, J. M. Hamlyn, T. L. Pallone, J. W. Van Huysse, J. Zhang and W. G. Wier (2012). How NaCl raises blood pressure: a new paradigm for the pathogenesis of salt-dependent hypertension. Am J Physiol Heart Circ Physiol 302(5): H1031-49.

Bogatcheva, N.V., M. A. Zemskova, C. Poirier, T. Mirzapoiazova, I, Kolosova, A. R. Bresnick and A. D. Verin (2011). The suppression of myosin light chain (MLC) phosphorylation during the response to lipopolysaccharide (LPS): beneficial or detrimental to endothelial barrier? J Cell Physiol 226(12):3132-46.

Bone, R. C., R. A. Balk, F. B. Cerra, R. P. Dellinger, A. M. Fein, W. A. Knaus, R. M. Schein and W. J. Sibbald (1992). Definitions for sepsis and organ failure and guidelines for the use of innovative therapies in sepsis. The ACCP/SCCM Consensus Conference Committee. American College of Chest Physicians/Society of Critical Care Medicine. Chest 101(6): 1644-55.

Bovellan, M., M. Fritzsche, C. Stevens and G. Charras (2010). Death-associated protein kinase (DAPK) and signal transduction: blebbing in programmed cell death. FEBS J 277(1): 58-65.

Bradford, M. M. (1976). A rapid and sensitive method for the quantitation of microgram quantities of protein utilizing the principle of protein-dye binding. Anal Biochem 72: 248-54.

Bradley, E. A., E. C. Eringa, C. D. Stehouwer, I. Korstjens, G. P. van Nieuw Amerongen, R. Musters, P. Sipkema, M. G. Clark and S. Rattigan (2010). Activation of AMP-activated protein kinase by 5-aminoimidazole-4-carboxamide-1-beta-D-ribofuranoside in the muscle microcirculation increases nitric oxide synthesis and microvascular perfusion. Arterioscler Thromb Vasc Biol 30(6): 1137-42.

Bright, N. J., C. Thornton and D. Carling (2009). The regulation and function of mammalian AMPK-related kinases. Acta Physiol (Oxf) 196(1): 15-26.

Brown, K. A., S. D. Brain, J. D. Pearson, J. D. Edgeworth, S. M. Lewis and D. F. Treacher (2006). Neutrophils in development of multiple organ failure in sepsis. Lancet 368(9530): 157-69.

Bubb, K. J., R. S. Khambata and A. Ahluwalia (2012). Sexual dimorphism in rodent models of hypertension and atherosclerosis. Br J Pharmacol 167(2):298-312.

Bultot, L., S. Horman, D. Neumann, M. P. Walsh, L. Hue and M. H. Rider (2009). Myosin light chains are not a physiological substrate of AMPK in the control of cell structure changes. FEBS Lett 583(1): 25-8.

Buras, J. A., B. Holzmann and M. Sitkovsky (2005). Animal Models of sepsis: setting the stage. Nat Rev Drug Discov 4(10): 854-865.

Cao, W., M. Sohail, G. Liu, G. A. Koumbadinga, V. G. Lobo and J. Xie (2011). Differential effects of PKA-controlled CaMKK2 variants on neuronal differentiation. RNA Biol 8(6): 1061-72.

Carling, D. (2004). The AMP-activated protein kinase cascade--a unifying system for energy control. Trends Biochem Sci 29(1): 18-24.

Carling, D., P. R. Clarke, V. A. Zammit and D. G. Hardie (1989). Purification and characterization of the AMP-activated protein kinase. Copurification of acetyl-CoA carboxylase kinase and 3-hydroxy-3-methylglutaryl-CoA reductase kinase activities. Eur J Biochem 186(1-2): 129-36.

Carling, D., M. J. Sanders and A. Woods (2008). The regulation of AMP-activated protein kinase by upstream kinases. Int J Obes (Lond) 32 Suppl 4: S55-9.

Carling, D., C. Thornton, A. Woods and M. J. Sanders (2012). AMP-activated protein kinase: new regulation, new roles? Biochem J 445(1): 11-27.

Carling, D., V. A. Zammit and D. G. Hardie (1987). A common bicyclic protein kinase cascade inactivates the regulatory enzymes of fatty acid and cholesterol biosynthesis. FEBS Lett 223(2): 217-22.

Carrillo-Sepulveda, M. A. and M. L. Barreto-Chaves (2010). Phenotypic modulation of cultured vascular smooth muscle cells: a functional analysis focusing on MLC and ERK1/2 phosphorylation. Mol Cell Biochem 341(1-2): 279-89.

Cauwels, A. (2007). Nitric oxide in shock. Kidney Int 72(5): 557-65.

Chen, Z., I. C. Peng, W. Sun, M. I. Su, P. H. Hsu, Y. Fu, Y. Zhu, K. DeFea, S. Pan, M. D. Tsai and J. Y. Shyy (2009). AMP-activated protein kinase functionally phosphorylates endothelial nitric oxide synthase Ser633. Circ Res 104(4): 496-505.

Chen, Z. P., K. I. Mitchelhill, B. J. Michell, D. Stapleton, I. Rodriguez-Crespo, L. A. Witters, D. A. Power, P. R. Ortiz de Montellano and B. E. Kemp (1999). AMP-activated protein kinase phosphorylation of endothelial NO synthase. FEBS Lett 443(3): 285-9.

Cinel, I. and S. M. Opal (2009). Molecular biology of inflammation and sepsis: a primer. Crit Care Med 37(1): 291-304.

Clapham, D. E. (1995). Calcium signaling. Cell 80(2): 259-68.

Claret, M., M. A. Smith, C. Knauf, H. Al-Qassab, A. Woods, A. Heslegrave, K. Piipari, J. J. Emmanuel, A. Colom, P. Valet, P. D. Cani, G. Begum, A. White, P. Mucket, M. Peters, K. Mizuno, R. L. Batterham, K. P. Giese, A. Ashworth, R. Burcelin, M. L. Ashford, D. Carling and D. J. Withers (2011). Deletion of Lkb1 in pro-opiomelanocortin neurons impairs peripheral glucose homeostasis in mice. Diabetes 60(3): 735-45.

Colomer, J. and A. R. Means (2007). Physiological roles of the Ca2+/CaM-dependent protein kinase cascade in health and disease. Subcell Biochem 45: 169-214.

Connelly, L., A. T. Jacobs, M. Palacios-Callender, S. Moncada and A. J. Hobbs (2003). Macrophage endothelial nitric-oxide synthase autoregulates cellular activation and pro-inflammatory protein expression. J Biol Chem 278(29): 26480-7.

Connelly, L., M. Madhani and A. J. Hobbs (2005). Resistance to endotoxic shock in endothelial nitric-oxide synthase (eNOS) knock-out mice: a pro-inflammatory role for eNOS-derived no *in vivo*. J Biol Chem 280(11): 10040-6.

Cori, G. T. and A. A. Green (1943). Crystalline muscle phosphorylase: II. Prosthetic group. J Biol Chem 151: 31-38.

Cunha, F. Q., J. Assreuy, D. W. Moss, D. Rees, L. M. Leal, S. Moncada, M. Carrier, C. A. O'Donnell and F. Y. Liew (1994). Differential induction of nitric oxide synthase in various organs of the mouse during endotoxaemia: role of TNF-alpha and IL-1-beta. Immunology 81(2): 211-5.

Cuschieri, J., D. Gourlay, I. Garcia, S. Jelacic and R. V. Maier (2003). Modulation of endotoxin-induced endothelial function by calcium/calmodulin-dependent protein kinase. Shock 20(2): 176-82.

Dagher, Z., N. Ruderman, K. Tornheim and Y. Ido (1999). The effect of AMP-activated protein kinase and its activator AICAR on the metabolism of human umbilical vein endothelial cells. Biochem Biophys Res Commun 265(1): 112-5.

Damas, P., J. L. Canivet, D. de Groote, Y. Vrindts, A. Albert, P. Franchimont and M. Lamy (1997). Sepsis and serum cytokine concentrations. Crit Care Med 25(3): 405-12.

Dauphinee, S. M. and A. Karsan (2006). Lipopolysaccharide signaling in endothelial cells. Lab Invest 86(1): 9-22.

Daval, M., F. Diot-Dupuy, R. Bazin, I. Hainault, B. Viollet, S. Vaulont, E. Hajduch, P. Ferre and F. Foufelle (2005). Anti-lipolytic action of AMP-activated protein kinase in rodent adipocytes. J Biol Chem 280(26): 25250-7.

Davare, M. A., D. A. Fortin, T. Saneyoshi, S. Nygaard, S. Kaech, G. Banker, T. R. Soderling and G. A. Wayman (2009). Transient receptor potential canonical 5 channels activate Ca2+/calmodulin kinase Igamma to promote axon formation in hippocampal neurons. J Neurosci 29(31): 9794-808.

Davare, M. A., T. Saneyoshi, E. S. Guire, S. C. Nygaard and T. R. Soderling (2004). Inhibition of calcium/calmodulin-dependent protein kinase kinase by protein 14-3-3. J Biol Chem 279(50): 52191-9.

Davis, B. J., Z. Xie, B. Viollet and M. H. Zou (2006). Activation of the AMP-activated kinase by antidiabetes drug metformin stimulates nitric oxide synthesis *in vivo* by promoting the association of heat shock protein 90 and endothelial nitric oxide synthase. Diabetes 55(2): 496-505.

Deji, N., S. Kume, S. Araki, K. Isshiki, H. Araki, M. Chin-Kanasaki, Y. Tanaka, A. Nishiyama, D. Koya, M. Haneda, A. Kashiwagi, H. Maegawa and T. Uzu (2012). Role of angiotensin II-mediated AMPK inactivation on obesity-related salt-sensitive hypertension. Biochem Biophys Res Commun 418(3): 559-64.

Denison, F. C., N. J. Hiscock, D. Carling and A. Woods (2009). Characterization of an alternative splice variant of LKB1. J Biol Chem 284(1): 67-76.

Dey, N. B., J. L. Busch, S. H. Francis, J. D. Corbin and T. M. Lincoln (2009). Cyclic GMP specifically suppresses Type-Ialpha cGMP-dependent protein kinase expression by ubiquitination. Cell Signal 21(6): 859-66.

Ding, A., C. F. Nathan, J. Graycar, R. Derynck. D. J. Stuehr and S. Srimal (1990). Macrophage deactivating factor and transforming growth factors-beta 1 -beta 2 and -beta 3 inhibit induction of macrophage nitrogen oxide synthesis by IFN-gamma. J Immunol 145:940.

Dobransky, T. and R. J. Rylett (2005). A model for dynamic regulation of choline acetyltransferase by phosphorylation. J Neurochem 95(2): 305-13.

Doi, K., A. Leelahavanichkul, P. S. Yuen and R. A. Star (2009). Animal models of sepsis and sepsis-induced kidney injury. J Clin Invest 119(10): 2868-78.

Drazner, M.H. (2005). The transition from hypertrophy to failure: how certain are we? Circulation 112:936–938.

Dyer, A. R., R. Stamler, P. Elliott and J. Stamler (1995). Dietary salt and blood pressure. Nat Med 1(10): 994-6.

Emes, R. D., L. Goodstadt, E. E. Winter and C. P. Ponting (2003). Comparison of the genomes of human and mouse lays the foundation of genome zoology. Hum Mol Genet 12 (7): 701-709.

Esteban, A., F. Frutos-Vivar, N. D. Ferguson, O. Penuelas, J. A. Lorente, F. Gordo, T. Honrubia, A. Algora, A. Bustos, G. Garcia, I. R. Diaz-Reganon and R. R. de Luna (2007). Sepsis incidence and outcome: contrasting the intensive care unit with the hospital ward. Crit Care Med 35(5): 1284-9.

Eutamene, H., V. Theodorou, F. Schmidlin , V. Tondereau, R. Garcia-Villar, C. Salvador-Cartier, M. Chovet, C. Bertrand and L. Bueno (2005). LPS-induced lung inflammation is linked to increased epithelial permeability: role of MLCK. Eur Respir J 25(5):789-96.

Evans, A. M., K. J. Mustard, C. N. Wyatt, C. Peers, M. Dipp, P. Kumar, N. P. Kinnear and D. G. Hardie (2005). Does AMP-activated protein kinase couple inhibition of mitochondrial oxidative phosphorylation by hypoxia to calcium signaling in O2-sensing cells? J Biol Chem 280(50): 41504-11.

Fadok, V. A., D. L. Bratton, A. Konowal, P. W. Freed, J. Y. Westcott and P. M. Henson (1998). Macrophages that have ingested apoptotic cells *in vitro* inhibit proinflammatory cytokine production through autocrine/paracrine mechanisms involving TGF-beta, PGE2, and PAF. J Clin Invest 101(4): 890-8.

Feng, J., M. Ito, K. Ichikawa, N. Isaka, M. Nishikawa, D. J. Hartshorne and T. Nakano (1999). Inhibitory phosphorylation site for Rho-associated kinase on smooth muscle myosin phosphatase. J Biol Chem 274(52): 37385-90.

Fernandes, C. J., Jr., N. Akamine and E. Knobel (2008). Myocardial depression in sepsis. Shock 30 Suppl 1: 14-7.

Ferri, N. (2012). AMP-activated protein kinase and the control of smooth muscle cell hyperproliferation in vascular disease. Vascul Pharmacol 56(1-2): 9-13.

Finlay, D. and D. A. Cantrell (2011). Metabolism, migration and memory in cytotoxic T cells. Nat Rev Immunol 11(2): 109-17.

Fischer, E. H. and E. G. Krebs EG (1955). Conversion of phosphorylase b to phosphorylase a in muscle extracts. J Biol Chem 216 (1): 121–132.

Fisslthaler, B. and I. Fleming (2009). Activation and signaling by the AMP-activated protein kinase in endothelial cells. Circ Res 105(2): 114-27.

Ford, R. J., S. R. Teschke, E. B. Reid, K. K. Durham, J. T. Kroetsch and J. W. Rush (2012). AMP-activated protein kinase activator AICAR acutely lowers blood pressure and relaxes isolated resistance arteries of hypertensive rats. J Hypertens 30(4): 725-33.

Foretz, M., N. Ancellin, F. Andreelli, Y. Saintillan, P. Grondin, A. Kahn, B. Thorens, S. Vaulont and B. Viollet (2005). Short-term overexpression of a constitutively active form of AMP-activated protein kinase in the liver leads to mild hypoglycemia and fatty liver. Diabetes 54(5): 1331-9.

Foretz, M., S. Guihard, J. Leclerc, V. Fauveau, J. P. Couty, F. Andris, M. Gaudry, F. Andreelli, S. Vaulont and B. Viollet (2010). Maintenance of red blood cell integrity by AMP-activated protein kinase alpha1 catalytic subunit. FEBS Lett 584(16): 3667-71.

Foretz, M., S. Hebrard, J. Leclerc, E. Zarrinpashneh, M. Soty, G. Mithieux, K. Sakamoto, F. Andreelli and B. Viollet (2010). Metformin inhibits hepatic gluconeogenesis in mice independently of the LKB1/AMPK pathway via a decrease in hepatic energy state. J Clin Invest 120(7): 2355-69.

Fortin, C. F., P. P. McDonald, T. Fulop and O. Lesur (2010). Sepsis, leukocytes, and nitric oxide (NO): an intricate affair. Shock 33(4): 344-52.

Fraser, S., P. Mount, R. Hill, V. Levidiotis, F. Katsis, D. Stapleton, B. E. Kemp and D. A. Power (2005). Regulation of the energy sensor AMP-activated protein kinase in the kidney by dietary salt intake and osmolality. Am J Physiol Renal Physiol 288(3): F578-86.

Fraser, S. A., I. Gimenez, N. Cook, I. Jennings, M. Katerelos, F. Katsis, V. Levidiotis, B. E. Kemp and D. A. Power (2007). Regulation of the renal-specific Na+-K+-2Cl- co-transporter NKCC2 by AMP-activated protein kinase (AMPK). Biochem J 405(1): 85-93.

Fredriksson, K., U. Flaring, C. Guillet, J. Wernerman and O. Rooyackers (2009). Muscle mitochondrial activity increases rapidly after an endotoxin challenge in human volunteers. Acta Anaesthesiol Scand 53(3): 299-304.

Frigo, D. E., M. K. Howe, B. M. Wittmann, A. M. Brunner, I. Cushman, Q. Wang, M. Brown, A. R. Means and D. P. McDonnell (2011). CaM kinase kinase beta-mediated activation of the growth regulatory kinase AMPK is required for androgen-dependent migration of prostate cancer cells. Cancer Res 71(2): 528-37.

Fryer, L. G., F. Foufelle, K. Barnes, S. A. Baldwin, A. Woods and D. Carling (2002). Characterization of the role of the AMP-activated protein kinase in the stimulation of glucose transport in skeletal muscle cells. Biochem J 363(Pt 1): 167-74.

Fujimoto, T., N. Hatano, N. Nozaki, S. Yurimoto, R. Kobayashi and H. Tokumitsu (2011). Identification of a novel CaMKK substrate. Biochem Biophys Res Commun 410(1): 45-51.

Fukuda, K., Y. Ozaki, K. Satoh, S. Kume, M. Tawata, T. Onaya, K. Sakurada, M. Seto and Y. Sasaki (1997). Phosphorylation of myosin light chain in resting platelets from NIDDM patients is enhanced: correlation with spontaneous aggregation. Diabetes 46(3): 488-93.

Fultz, M.E., C. Li, W. Geng and G. L. Wright (2000). Remodeling of the actin cytoskeleton in the contracting A7r5 smooth muscle cell. J Muscle Res Cell Motil 21:775–787.

Furchgott, R. F. and J. V. Zawadzki (1980). The obligatory role of endothelial cells in the relaxation of arterial smooth muscle by acetylcholine. Nature 288(5789): 373-6.

Galanos, C. and M. A. Freudenberg (1993). Mechanisms of endotoxin shock and endotoxin hypersensitivity. Immunobiology 187(3-5): 346-56.

Gao, L., A. Grant, I. Halder, R. Brower, J. Sevransky, J. P. Maloney, M. Moss, C. Shanholtz, C. R. Yates, G. U. Meduri, M. D. Shriver, R. Ingersoll, A. F. Scott, T. H. Beaty, J. Moitra, S. F.

Ma, S. Q. Ye, K. C. Barnes and J. G. Garcia (2006). Novel polymorphisms in the myosin light chain kinase gene confer risk for acute lung injury. Am J Respir Cell Mol Biol 34(4): 487-95.

Gao, N., J. Huang, W. He, M. Zhu, K. E. Kamm and J. T. Stull (2013). Signaling through Myosin Light Chain Kinase in Smooth Muscles. J Biol Chem 288: 7596-7605.

Garton, A. J., D. G. Campbell, D. Carling, D. G. Hardie, R. J. Colbran and S. J. Yeaman (1989). Phosphorylation of bovine hormone-sensitive lipase by the AMP-activated protein kinase. A possible antilipolytic mechanism. Eur J Biochem 179(1): 249-54.

Gaskin, F. S., K. Kamada, M. Y. Zuidema, A. W. Jones, L. J. Rubin and R. J. Korthuis (2011). Isoform-selective 5'-AMP-activated protein kinase-dependent preconditioning mechanisms to prevent postischemic leukocyte-endothelial cell adhesive interactions. Am J Physiol Heart Circ Physiol 300(4): H1352-60.

Gibot, S., A. Cariou, L. Drouet, M. Rossignol and L. Ripoll (2002). Association between a genomic polymorphism within the CD14 locus and septic shock susceptibility and mortality rate. Crit Care Med 30(5): 969-73.

Goirand, F., M. Solar, Y. Athea, B. Viollet, P. Mateo, D. Fortin, J. Leclerc, J. Hoerter, R. Ventura-Clapier and A. Garnier (2007). Activation of AMP kinase alpha1 subunit induces aortic vasorelaxation in mice. J Physiol 581(Pt 3): 1163-71.

Gonzalez, L. O., M. D. Corte, J. Vazquez, S. Junquera, R. Sanchez, A. C. Alvarez, J. C. Rodriguez, M. L. Lamelas and F. J. Vizoso (2008). Androgen receptor expresion in breast cancer: relationship with clinicopathological characteristics of the tumors, prognosis, and expression of metalloproteases and their inhibitors. BMC Cancer 8: 149.

Gordon, S. and F. O. Martinez (2010). Alternative activation of macrophages: mechanism and functions. Immunity 32(5): 593-604.

Gormand, A., E. Henriksson, K. Strom, T. E. Jensen, K. Sakamoto and O. Goransson (2011). Regulation of AMP-activated protein kinase by LKB1 and CaMKK in adipocytes. J Cell Biochem 112(5): 1364-75.

Granucci, F. and I. Zanoni (2009). The dendritic cell life cycle. Cell Cycle 8(23): 3816-21.

Green, M. F., K. A. Anderson and A. R. Means (2011). Characterization of the CaMKKbeta-AMPK signaling complex. Cell Signal 23(12): 2005-12.

Green, M. F., J. W. Scott, R. Steel, J. S. Oakhill, B. E. Kemp and A. R. Means (2011). Ca2+/Calmodulin-dependent protein kinase kinase beta is regulated by multisite phosphorylation. J Biol Chem 286(32): 28066-79.

Greenberg, A. K., S. Basu, J. Hu, T. Yie, K. M. Tchou-Wong, W. N. Rom and T. C. Lee (2002). Selective p38 activation in human non-small cell lung cancer. Am J Respir Cell Mol Biol 26(5):558-64.

Grobe, J. L., B. A. Buehrer, A. M. Hilzendeger, X. Liu, D. R. Davis, D. Xu and C. D. Sigmund (2011). Angiotensinergic signaling in the brain mediates metabolic effects of deoxycorticosterone (DOCA)-salt in C57 mice. Hypertension 57(3): 600-7.

Guest, C. B., E. L. Deszo, M. E. Hartman, J. M. York, K. W. Kelley and G. G. Freund (2008). Ca2+/calmodulin-dependent kinase kinase alpha is expressed by monocytic cells and regulates the activation profile. PLoS One 3(2): e1606.

Guha, M and N. Mackman (2001). LPS induction of gene expression in human monocytes. Cell Signal 13(2):85-94.

Guigas, B., N. Taleux, M. Foretz, D. Detaille, F. Andreelli, B. Viollet and L. Hue (2007). AMP-activated protein kinase-independent inhibition of hepatic mitochondrial oxidative phosphorylation by AICA riboside. Biochem J 404(3): 499-507.

Gupta, J., R. Russell, C. Wayman, D. Hurley and V. Jackson (2008). Oxytocin-induced contractions within rat and rabbit ejaculatory tissues are mediated by vasopressin V1A receptors and not oxytocin receptors. Br J Pharmacol 155(1): 118-26.

Guyton, A. C., T. G. Coleman, A. V. Cowley, Jr., K. W. Scheel, R. D. Manning, Jr. and R. A. Norman, Jr. (1972). Arterial pressure regulation. Overriding dominance of the kidneys in long-term regulation and in hypertension. Am J Med 52(5): 584-94.

Hardie, D. G. and D. Carling (1997). The AMP-activated protein kinase--fuel gauge of the mammalian cell? Eur J Biochem 246(2): 259-73.

Hartley, C. J., G. E. Taffet, L. H. Michael, T. T. Pham and M. L. Entman (1997). Noninvasive determination of pulse-wave velocity in mice. Am J Physiol 273(1 Pt 2): H494-500.

Hashimoto, Y. and T. R. Soderling (1990). Phosphorylation of smooth muscle myosin light chain kinase by Ca2+/calmodulin-dependent protein kinase II: comparative study of the phosphorylation sites. Arch Biochem Biophys 278(1): 41-5.

Haslett, C., E. R. Chilvers, N. A. Boon, N. Colledge and J. A. Hunter (2002). Davidson's principles and practice of medicine. 19th Edition. Edinburgh, Churchill Livingston.

Havel, C., J. Arrich, H. Losert, G. Gamper, M. Mullner and H. Herkner (2011). Vasopressors for hypotensive shock. Cochrane Database Syst Rev(5): CD003709.

Hawley, S. A., D. A. Pan, K. J. Mustard, L. Ross, J. Bain, A. M. Edelman, B. G. Frenguelli and D. G. Hardie (2005). Calmodulin-dependent protein kinase kinase-beta is an alternative upstream kinase for AMP-activated protein kinase. Cell Metab 2(1):9-19.

He, W. Q., Y. J. Peng, W. C. Zhang, N. Lv, J. Tang, C. Chen, C. H. Zhang, S. Gao, H. Q. Chen, G. Zhi, R. Feil, K. E. Kamm, J. T. Stull, X. Gao and M. S. Zhu (2008). Myosin light chain kinase is central to smooth muscle contraction and required for gastrointestinal motility in mice. Gastroenterology 135(2):610-20.

He, W. Q., Y. N. Qiao, C. H. Zhang, Y. J. Peng, C. Chen, P. Wang, Y. Q. Gao, X. Chen, T. Tao, X. H. Su, C. J. Li, K. E. Kamm, J. T. Stull and M. S. Zhu (2011). Role of myosin light chain kinase in regulation of basal blood pressure and maintenance of salt-induced hypertension. Am J Physiol Heart Circ Physiol 301(2): H584-91.

Hess, C. N., R. Kou, R. P. Johnson, G. K. Li and T. Michel (2009). ADP signaling in vascular endothelial cells: ADP-dependent activation of the endothelial isoform of nitric-oxide synthase requires the expression but not the kinase activity of AMP-activated protein kinase. J Biol Chem 284(47): 32209-24.

Higashihara, M., M. Watanabe, S. Usuda and K. Miyazaki (2008). Smooth muscle type isoform of 20 kDa myosin light chain is expressed in monocyte/macrophage cell lineage. J Smooth Muscle Res 44(1): 29-40.

Ho, N., M. Gullberg and T. Chatilla (1996). Activation protein 1-dependent transcriptional activation of interleukin 2 gene by Ca2+/calmodulin kinase type IV/Gr. J Exp Med 184(1):101-12.

Hofmann, F., A. Ammendola and J. Schlossmann (2000). Rising behind NO: cGMP-dependent protein kinases. J Cell Sci 113 (Pt 10): 1671-6.

Hoit, B. D., Z. U. Khan, C. M. Pawloski-Dahm and R. A. Walsh (1997). *In vivo* determination of left ventricular wall stress-shortening relationship in normal mice. Am J Physiol 272(2 Pt 2):H1047-52.

Hong, F., B. D. Haldeman, D. Jackson, M. Carter, J. E. Baker and C. R. Cremo (2011). Biochemistry of smooth muscle myosin light chain kinase. Arch Biochem Biophys 510(2): 135-46.

Hong, S. P., F. C. Leiper, A. Woods, D. Carling and M. Carlson (2003). Activation of yeast Snf1 and mammalian AMP-activated protein kinase by upstream kinases. Proc Natl Acad Sci U S A 100(15):8839-43.

Hong, T. J., J. E. Ban, K. H. Choi, Y. H. Son, S. M. Kim, S. K. Eo, H. J. Park, B. Y. Rhim and K. Kim (2009). TLR-4 agonistic lipopolysaccharide upregulates interleukin-8 at the transcriptional and post-translational level in vascular smooth muscle cells. Vascul Pharmacol 50(1-2): 34-9.

Hoppe, A. D. and J. A. Swanson (2004). Cdc42, Rac1, and Rac2 display distinct patterns of activation during phagocytosis. Mol Biol Cell 15(8):3509-19.

Horman, S., N. Morel, D. Vertommen, N. Hussain, D. Neumann, C. Beauloye, N. El Najjar, C. Forcet, B. Viollet, M. P. Walsh, L. Hue and M. H. Rider (2008). AMP-activated protein kinase phosphorylates and desensitizes smooth muscle myosin light chain kinase. J Biol Chem 283(27): 18505-12.

Houser, S. R., K. B. Marguilies, A. M. Murphy, F. G. Spinale, G. S. Francis, S. D. Prabhu, H. A. Rockman, D. A. Kass, J. D. Molkentin, M. A. Sussman and W. J. Kock (2012). Animal models of heart failure: a scientific statement from the American Heart Association. Circ Res 111(1):131-50.

Hsu, F. N., M. C. Chen, M. C. Chiang, E. Lin, Y. T. Lee, P. H. Huang, G. S. Lee and H. Lin (2011). Regulation of androgen receptor and prostate cancer growth by cyclin-dependent kinase 5. J Biol Chem 286(38): 33141-9.

Hsu, L. S., G. D. Chen, L. S. Lee, C. W. Chi, J. F. Cheng and J. Y. Chen (2001). Human Ca2+/calmodulin-dependent protein kinase kinase beta gene encodes multiple isoforms that display distinct kinase activity. J Biol Chem 276(33): 31113-23.

Hubbard, W. J., M. Choudhry, M. G. Schwacha, J. D. Kerby, L. W. Rue, 3rd, K. I. Bland and I. H. Chaudry (2005). Cecal ligation and puncture. Shock 24 Suppl 1: 52-7.

Hurley, R. L., K. A. Anderson, J. M. Franzone, B. E. Kemp, A. R. Means and L. A. Witters (2005). The Ca2+/calmodulin-dependent protein kinase kinases are AMP-activated protein kinase kinases. J Biol Chem 280(32): 29060-6.

Hurley, R. L., L. K. Barre, S. D. Wood, K. A. Anderson, B. E. Kemp, A. R. Means and L. A. Witters (2006). Regulation of AMP-activated protein kinase by multisite phosphorylation in response to agents that elevate cellular cAMP. J Biol Chem 281(48): 36662-72.

Huynh, Q. K. and N. Pagratis (2011). Kinetic mechanisms of Ca++/calmodulin dependent protein kinases. Arch Biochem Biophys 506(2): 130-6.

Ichinose, K., Y. T. Juang, J. C. Crispin, K. Kis-Toth and G. C. Tsokos (2011). Suppression of autoimmunity and organ pathology in lupus-prone mice upon inhibition of calcium/calmodulin-dependent protein kinase type IV. Arthritis Rheum 63(2): 523-9.

Ignarro, L. J., G. M. Buga, K. S. Wood, R. E. Byrns and G. Chaudhuri (1987). Endothelium-derived relaxing factor produced and released from artery and vein is nitric oxide. Proc Natl Acad Sci U S A 84(24): 9265-69.

Iles, K. E. and H. J. Forman (2002). Macrophage signaling and respiratory burst. Immunol Res 26(1-3): 95-105.

Ishii, K. A., T. Fumoto, K. Iwai, S. Takeshita, M. Ito, N. Shimohata, H. Aburatani, S. Taketani, C. J. Lelliott, A. Vidal-Puig and K. Ikeda (2009). Coordination of PGC-1beta and iron uptake in mitochondrial biogenesis and osteoclast activation. Nat Med 15(3): 259-66.

Ishikawa,Y and R. Kurotani. (2008). Cardiac myosin light chain kinase. A new player in the regulation of myosin light chain in the heart. Circulation Research 102: 516-518.

Iyoda, K., Y. Sasaki, M. Horimoto, T. Toyama, T. Yakushijin, M. Sakakibara, M. Takehara, J. Fujimoto, M. Hori, J. W. Wand and N. Hayashi (2003). Involvement of the p38 mitogen-activated protein kinase cascade in hepatocellular carcinoma. Cancer 97(12):3017-26.

Jäger, S., C. Handschin, J. St-Pierre and B. M. Spiegelman (2007). AMP-activated protein kinase (AMPK) action in skeletal muscle via direct phosphorylation of PGC-1alpha. Proc Natl Acad Sci U S A 104(29):12017-22.

Jeninga, E. H., K. Schoonjans and J. Auwerx (2010). Reversible acetylation of PGC-1: connecting energy sensors and effectors to guarantee metabolic flexibility. Oncogene 29(33): 4617-24.

Jeyabalan, J., M. Shah, B. Viollet, J. P. Roux, P. Chavassieux, M. Korbonits and C. Chenu (2012). Mice lacking AMP-activated protein kinase alpha1 catalytic subunit have increased bone remodelling and modified skeletal responses to hormonal challenges induced by ovariectomy and intermittent PTH treatment. J Endocrinol 214(3): 349-58.

Jones, G. E. (2000). Cellular signaling in macrophage migration and chemotaxis. J Leukoc Biol 68(5):593-602.

Jorgensen, S. B., J. N. Nielsen, J. B. Birk, G. S. Olsen, B. Viollet, F. Andreelli, P. Schjerling, S. Vaulont, D. G. Hardie, B. F. Hansen, E. A. Richter and J. F. Wojtaszewski (2004). The alpha2-5'AMP-activated protein kinase is a site 2 glycogen synthase kinase in skeletal muscle and is responsive to glucose loading. Diabetes 53(12): 3074-81.

Jorgensen, S. B., E. A. Richter and J. F. Wojtaszewski (2006). Role of AMPK in skeletal muscle metabolic regulation and adaptation in relation to exercise. J Physiol 574(Pt 1): 17-31.

Jorgensen, S. B., B. Viollet, F. Andreelli, C. Frosig, J. B. Birk, P. Schjerling, S. Vaulont, E. A. Richter and J. F. Wojtaszewski (2004). Knockout of the alpha2 but not alpha1 5'-AMP-activated protein kinase isoform abolishes 5-aminoimidazole-4-carboxamide-1-beta-4-ribofuranosidebut not contraction-induced glucose uptake in skeletal muscle. J Biol Chem 279(2): 1070-9.

Jorgensen, S. B., J. F. Wojtaszewski, B. Viollet, F. Andreelli, J. B. Birk, Y. Hellsten, P. Schjerling, S. Vaulont, P. D. Neufer, E. A. Richter and H. Pilegaard (2005). Effects of alpha-AMPK knockout on exercise-induced gene activation in mouse skeletal muscle. FASEB J 19(9): 1146-8.

Junttila, M.R., S. P. Li and J. Westermarck (2008). Phosphatase-mediated crosstalk between MAPK signaling pathways in the regulation of cell survival. FASEB J *22*(4): 954–65.

Kahn, B. B., T. Alquier, D. Carling and D. G. Hardie (2005). AMP-activated protein kinase: ancient energy gauge provides clues to modern understanding of metabolism. Cell Metab 1(1): 15-25.

Kamm, K. E. and J. T. Stull (2001). Dedicated myosin light chain kinases with diverse cellular functions. J Biol Chem 276(7): 4527-30.

Kanazawa, I., T. Yamaguchi, S. Yano, M. Yamauchi and T. Sugimoto (2009). Activation of AMP kinase and inhibition of Rho kinase induce the mineralization of osteoblastic MC3T3-E1 cells through endothelial NOS and BMP-2 expression. Am J Physiol Endocrinol Metab 296(1): E139-46.

Kanda, K and T. Matsuda (1993). Behavior of arterial wall cells cultured on periodically stretched substrates. Cell Transplant 2:475–484.

Kang, C. and L. Avery (2010). Death-associated protein kinase (DAPK) and signal transduction: fine-tuning of autophagy in Caenorhabditis elegans homeostasis. FEBS J 277(1): 66-73.

Karaghiosoff, M., R. Steinborn, P. Kovarik, G. Kriegshäuser, M. Baccarini, B. Donabauer, U. Reichart, T. Kolbe, C. Bogdan, T. Leanderson, D. Levy, T. Decker and M. Müller (2003). Central role for type I interferons and Tyk2 in lipopolysaccharide-induced endotoxin shock. Nat Immunol 4(5):471-7.

Karin, M. and M. Delhase (2000). The I kappa B kinase (IKK) and NF-kappa B: key elements of proinflammatory signalling. Semin Immunnol 12(1):85-98.

Kato, K., T. Otsuka, A. Kondo, R. Matsushima-Nishiwaki, H. Natsume, O. Kozawa and H. Tokuda (2012). AMP-activated protein kinase regulates PDGF-BB-stimulated interleukin-6 synthesis in osteoblasts: involvement of mitogen-activated protein kinases. Life Sci 90(1-2): 71-6.

Kato, N., F. Takeuchi, Y. Tabara, T. N. Kelly, M. J. Go, X. Sim, W. T. Tay, C. H. Chen, Y. Zhang, K. Yamamoto, T. Katsuya, M. Yokota, Y. J. Kim, R. T. Ong, T. Nabika, D. Gu, L. C. Chang, Y. Kokubo, W. Huang, K. Ohnaka, Y. Yamori, E. Nakashima, C. E. Jaquish, J. Y. Lee, M. Seielstad, M. Isono, J. E. Hixson, Y. T. Chen, T. Miki, X. Zhou, T. Sugiyama, J. P. Jeon, J. J. Liu, R. Takayanagi, S. S. Kim, T. Aung, Y. J. Sung, X. Zhang, T. Y. Wong, B. G. Han, S. Kobayashi, T. Ogihara, D. Zhu, N. Iwai, J. Y. Wu, Y. Y. Teo, E. S. Tai, Y. S. Cho and

J. He (2011). Meta-analysis of genome-wide association studies identifies common variants associated with blood pressure variation in east Asians. Nat Genet 43(6): 531-8.

Kawai, T., O. Takeuchi, T. Fujita, J. Inoue, P. F. Muhlradt, S. Sato, K. Hoshino and S. Akira (2001). Lipopolysaccharide stimulates the MyD88-independent pathway and results in activation of IFN-regulatory factor 3 and the expression of a subset of lipopolysaccharide-inducible genes. J Immunol 167(10): 5887-94.

Kazgan, N., T. Williams, L. J. Forsberg and J. E. Brenman (2010). Identification of a nuclear export signal in the catalytic subunit of AMP-activated protein kinase. Mol Biol Cell 21(19): 3433-42.

Khandrika, L., R. Lieberman, S. Koul, B. Kumar, P. Maroni, R. Chandhoke, R. B. Meacham and H. K. Koul (2009). Hypoxia-associated p38 mitogen-activated protein kinase-mediated androgen receptor activation and increased HIF-1alpha levels contribute to emergence of an aggressive phenotype in prostate cancer. Oncogene 28(9):1248-60.

Kiil, F., K. Aukland and H. E. Refsum (1961). Renal sodium transport and oxygen consumption. Am J Physiol 201: 511-6.

Kilbride, S. M., A. M. Farrelly, C. Bonner, M. W. Ward, K. C. Nyhan, C. G. Concannon, C. B. Wollheim, M. M. Byrne and J. H. Prehn (2010). AMP-activated protein kinase mediates apoptosis in response to bioenergetic stress through activation of the pro-apoptotic Bcl-2 homology domain-3-only protein BMF. J Biol Chem 285(46): 36199-206.

Kim, H. J., K. G. Park, E. K. Yoo, Y. H. Kim, Y. N. Kim, H. S. Kim, H. T. Kim, J. Y. Park, K. U. Lee, W. G. Jang, J. G. Kim, B. W. Kim and I. K. Lee (2007). Effects of PGC-1alpha on TNF-alpha-induced MCP-1 and VCAM-1 expression and NF-kappaB activation in human aortic smooth muscle and endothelial cells. Antioxid Redox Signal 9(3): 301-7.

Kim, H. R., S. Appel, S. Vetterkind, S. S. Gangopadhyay and K. G. Morgan (2008). Smooth muscle signalling pathways in health and disease. J Cell Mol Med 12(6A): 2165-80.

Kim, M., M. Shen, S. Ngoy, G. Karamanlidis, R. Liao and R. Tian (2012). AMPK isoform expression in the normal and failing hearts. J Mol Cell Cardiol 52(5): 1066-73.

Kim, M. S. and K. U. Lee (2005). Role of hypothalamic 5'-AMP-activated protein kinase in the regulation of food intake and energy homeostasis. J Mol Med (Berl) 83(7): 514-20.

Kinoshita, E., E. Kinoshita-Kikuta, K. Takiyama and T. Koike (2006). Phosphate-binding tag, a new tool to visualize phosphorylated proteins. Mol Cell Proteomics 5(4): 749-57.

Kimura, K., M. Ito, M. Amano, K. Chihara, Y. Fukata, M. Nakafuku, B. Yamamori, J. Feng, T. Nakano, K. Okawa, A. Iwamatsu and K. Kaibuchi (1996). Regulation of myosin phosphatase by Rho and Rho-associated kinase (Rho-kinase). Science 273:245–248.

Klein, D. K., H. Pilegaard, J. T. Treebak, T. E. Jensen, B. Viollet, P. Schjerling and J. F. Wojtaszewski (2007). Lack of AMPKalpha2 enhances pyruvate dehydrogenase activity during exercise. Am J Physiol Endocrinol Metab 293(5): E1242-9.

Klemke, R. L., S. Cai, A. L. Giannini, P. J. Gallagher, P. de Lanerolle and D. A. Cheresh (1997). Regulation of cell motility by mitogen-activated protein kinase. J Cell Biol 137(2): 481-92.

Kodiha, M and U. Stochaj (2011). Targeting AMPK for Therapeutic Intervention in Type 2 Diabetes, Medical Complications of Type 2 Diabetes, Colleen Croniger (Ed.). InTech. Available from: http://www.intechopen.com/books/medical-complications-of-type-2-diabetes/targeting-ampk-for-therapeutic-intervention-in-type-2-diabetes

Komarova, Y. and A. B. Malik (2010). Regulation of endothelial permeability via paracellular and transcellular transport pathways. Annu Rev Physiol 72: 463-93.

Kou, R. and T. Michel (2007). Epinephrine regulation of the endothelial nitric-oxide synthase: roles of RAC1 and beta3-adrenergic receptors in endothelial NO signaling. J Biol Chem 282(45): 32719-29.

Kramer, H. F., C. A. Witczak, N. Fujii, N. Jessen, E. B. Taylor, D. E. Arnolds, K. Sakamoto, M. F. Hirshman and L. J. Goodyear (2006). Distinct signals regulate AS160 phosphorylation in response to insulin, AICAR, and contraction in mouse skeletal muscle. Diabetes 55(7): 2067-76.

Krebs, E. G. and E. H. Fischer (1995). Phosphorylase Activity of Skeletal Muscle Extracts. J Biol Chem 216: 113–120.

Kristensen, J. M., A. B. Johnsen, J. B. Birk, J. N. Nielsen, B. R. Jensen, Y. Hellsten, E. A. Richter and J. F. Wojtaszewski (2007). Absence of humoral mediated 5'AMP-activated

protein kinase activation in human skeletal muscle and adipose tissue during exercise. J Physiol 585(Pt 3): 897-909.

Kukimoto-Niino, M., S. Yoshikawa, T. Takagi, N. Ohsawa, Y. Tomabechi, T. Terada, M. Shirouzu, A. Suzuki, S. Lee, T. Yamauchi, M. Okada-Iwabu, M. Iwabu, T. Kadowaki, Y. Minokoshi and S. Yokoyama (2011). Crystal structure of the Ca(2)(+)/calmodulin-dependent protein kinase kinase in complex with the inhibitor STO-609. J Biol Chem 286(25): 22570-9.

Lamb, P., T. Sivashanmugam, M. White, M. Irving, J. Wayman and S. Raimes (2008). Gastric cancer surgery--a balance of risk and radicality. Ann R Coll Surg Engl 90(3): 235-42.

Lee, J. C. and A. M. Edelman (1994). A protein activator of Ca(2+)-calmodulin-dependent protein kinase Ia. J Biol Chem 269(3): 2158-64.

Lee, Y., R. H. Naseem, L. Duplomb, B. H. Park, D. J. Garry, J. A. Richardson, J. E. Schaffer and R. H. Unger (2004). Hyperleptinemia prevents lipotoxic cardiomyopathy in acyl CoA synthase transgenic mice. Proc Natl Acad Sci U S A 101(37): 13624-9.

Lee, Y. S., Y. S. Kim, S. Y. Lee, G. H. Kim, B. J. Kim, S. H. Lee, K. U. Lee, G. S. Kim, S. W. Kim and J. M. Koh (2010). AMP kinase acts as a negative regulator of RANKL in the differentiation of osteoclasts. Bone 47(5): 926-37.

Leonard, A. M., L. L. Chafe, J. P. Montani and B. N. Van Vliet (2006). Increased salt-sensitivity in endothelial nitric oxide synthase-knockout mice. Am J Hypertens 19(12): 1264-9.

Levi, M., H. ten Cate and T. van der Poll (2002). Endothelium: interface between coagulation and inflammation. Crit Care Med 30(5 Suppl): S220-4.

Levine, Y. C., G. K. Li and T. Michel (2007). Agonist-modulated regulation of AMP-activated protein kinase (AMPK) in endothelial cells. Evidence for an AMPK -> Rac1 -> Akt -> endothelial nitric-oxide synthase pathway. J Biol Chem 282(28): 20351-64.

Levy, D., R. J. Garrison, D. D. Savage, W. B. Kannel and W. P. Castelli (1990). Prognostic implications of echocardiographically determined left ventricular mass in the Framingham Heart Study. N Engl J Med 322(22):1561-6.

Lin, F., T. J. Ribar and A. R. Means (2011). The Ca2+/calmodulin-dependent protein kinase kinase, CaMKK2, inhibits preadipocyte differentiation. Endocrinology 152(10): 3668-79.

Lin, Y., T. R. Hupp and C. Stevens (2010). Death-associated protein kinase (DAPK) and signal transduction: additional roles beyond cell death. FEBS J 277(1): 48-57.

Lira, V. A., D. L. Brown, A. K. Lira, A. N. Kavazis, Q. A. Soltow, E. H. Zeanah and D. S. Criswell (2010). Nitric oxide and AMPK cooperatively regulate PGC-1 in skeletal muscle cells. J Physiol 588(Pt 18): 3551-66.

Liu, C. and T. E. Hermann (1978). Characterization of ionomycin as a calcium ionophore. J Biol Chem 253(17): 5892-4.

Liu, C., B. Liang, Q. Wang, J. Wu and M. H. Zou (2010). Activation of AMP-activated protein kinase alpha1 alleviates endothelial cell apoptosis by increasing the expression of anti-apoptotic proteins Bcl-2 and survivin. J Biol Chem 285(20): 15346-55.

Luikart, B. W., W. Zhang, G. A. Wayman, C. H. Kwon, G. L. Westbrook and L. F. Parada (2008). Neurotrophin-dependent dendritic filopodial motility: a convergence on PI3K signaling. J Neurosci 28(27): 7006-12.

Ma, W., W. Lim, K. Gee, S. Aucoin, D. Nandan, M. Kozlowski, F. Diaz-Mitoma and A. Kumar (2001). The p38 mitogen-activated kinase pathway regulates the human interleukin-10 promoter via the activation of Sp1 transcription factor in lipopolysaccharide-stimulated human macrophages. J Biol Chem 276(17):13664-74.

Maarbjerg, S. J., S. B. Jorgensen, A. J. Rose, J. Jeppesen, T. E. Jensen, J. T. Treebak, J. B. Birk, P. Schjerling, J. F. Wojtaszewski and E. A. Richter (2009). Genetic impairment of AMPKalpha2 signaling does not reduce muscle glucose uptake during treadmill exercise in mice. Am J Physiol Endocrinol Metab 297(4): E924-34.

MacIver, N. J., J. Blagih, D. C. Saucillo, L. Tonelli, T. Griss, J. C. Rathmell and R. G. Jones (2011). The liver kinase B1 is a central regulator of T cell development, activation, and metabolism. J Immunol 187(8): 4187-98.

Manning, R. D., Jr., L. Hu, D. Y. Tan and S. Meng (2001). Role of abnormal nitric oxide systems in salt-sensitive hypertension. Am J Hypertens 14(6 Pt 2): 68S-73S.

Manning, G., D.B. Whyte, R. Martinez, T. Hunter and S. Sudarsanam (2002). The protein kinase complement of the human genome. Science 298(5600): 1912–1934.

Martin, G. S., D. M. Mannino, S. Eaton and M. Moss (2003). The epidemiology of sepsis in the United States from 1979 through 2000. N Engl J Med 348(16): 1546-54.

Martinelli, R., M. Gegg, R. Longbottom, P. Adamson, P. Turowski and J. Greenwood (2009). ICAM-1-mediated endothelial nitric oxide synthase activation via calcium and AMP-activated protein kinase is required for transendothelial lymphocyte migration. Mol Biol Cell 20(3): 995-1005.

Martinez-Martin, N., A. Blas-Garcia, J. M. Morales, M. Marti-Cabrera, D. Monleon and N. Apostolova (2012). Metabolomics of the effect of AMPK activation by AICAR on human umbilical vein endothelial cells. Int J Mol Med 29(1): 88-94.

Massie, C. E., A. Lynch, A. Ramos-Montoya, J. Boren, R. Stark, L. Fazli, A. Warren, H. Scott, B. Madhu, N. Sharma, H. Bon, V. Zecchini, D. M. Smith, G. M. Denicola, N. Mathews, M. Osborne, J. Hadfield, S. Macarthur, B. Adryan, S. K. Lyons, K. M. Brindle, J. Griffiths, M. E. Gleave, P. S. Rennie, D. E. Neal and I. G. Mills (2011). The androgen receptor fuels prostate cancer by regulating central metabolism and biosynthesis. EMBO J 30(13): 2719-33.

McConell, G. K., G. P. Ng, M. Phillips, Z. Ruan, S. L. Macaulay and G. D. Wadley (2010). Central role of nitric oxide synthase in AICAR and caffeine-induced mitochondrial biogenesis in L6 myocytes. J Appl Physiol 108(3): 589-95.

Means, A. R. (1994). Calcium, calmodulin and cell cycle regulation. FEBS Lett 347(1): 1-4.

Means, A. R., T. J. Ribar, C. D. Kane, S. S. Hook and K. A. Anderson (1997). Regulation and properties of the rat Ca2+/calmodulin-dependent protein kinase IV gene and its protein products. Recent Prog Horm Res 52: 389-406; discussion 406-7.

Medearis, D. N., Jr., B. M. Camitta and E. C. Heath (1968). Cell wall composition and virulence in Escherichia coli. J Exp Med 128(3): 399-414.

Meng, J., H. Yu, J. Ma, J. Wang, S. Banerjee, R. Charboneau, R. A. Barke and S. Roy (2013). Morphine Induces Bacterial Translocation in Mice by Compromising Intestinal Barrier Function in a TLR-Dependent Manner. PLoS One 8(1):e54040.

Merlin, J., B. A. Evans, R. I. Csikasz, T. Bengtsson, R. J. Summers and D. S. Hutchinson (2010). The M3-muscarinic acetylcholine receptor stimulates glucose uptake in L6 skeletal muscle cells by a CaMKK-AMPK-dependent mechanism. Cell Signal 22(7): 1104-13.

Merrill, G. F., E. J. Kurth, D. G. Hardie and W. W. Winder (1997). AICA riboside increases AMP-activated protein kinase, fatty acid oxidation, and glucose uptake in rat muscle. Am J Physiol 273(6 Pt 1): E1107-12.

Michie, A. M., A. M. McCaig, R. Nakagawa and M. Vukovic (2010). Death-associated protein kinase (DAPK) and signal transduction: regulation in cancer. FEBS J 277(1): 74-80.

Minokoshi, Y., T. Alquier, N. Furukawa, Y. B. Kim, A. Lee, B. Xue, J. Mu, F. Foufelle, P. Ferre, M. J. Birnbaum, B. J. Stuck and B. B. Kahn (2004). AMP-kinase regulates food intake by responding to hormonal and nutrient signals in the hypothalamus. Nature 428(6982): 569-74.

Minokoshi, Y., Y. B. Kim, O. D. Peroni, L. G. Fryer, C. Muller, D. Carling and B. B. Kahn (2002). Leptin stimulates fatty-acid oxidation by activating AMP-activated protein kinase. Nature 415(6869): 339-43.

Miranda, L., S. Carpentier, A. Platek, N. Hussain, M. A. Gueuning, D. Vertommen, Y. Ozkan, B. Sid, L. Hue, P. J. Courtoy, M. H. Rider and S. Horman (2010). AMP-activated protein kinase induces actin cytoskeleton reorganization in epithelial cells. Biochem Biophys Res Commun 396(3): 656-61.

Mizuno, K., A. Antunes-Martins, L. Ris, M. Peters, E. Godaux and K. P. Giese (2007). Calcium/calmodulin kinase kinase beta has a male-specific role in memory formation. Neuroscience 145(2): 393-402.

Mizuno, K., L. Ris, A. Sanchez-Capelo, E. Godaux and K. P. Giese (2006). Ca2+/calmodulin kinase kinase alpha is dispensable for brain development but is required for distinct memories in male, though not in female, mice. Mol Cell Biol 26(23): 9094-104.

Mollen, K. P., R. J. Anand, A. Tsung, J. M. Prince, R. M. Levy and T. R. Billiar (2006). Emerging paradigm: toll-like receptor 4-sentinel for the detection of tissue damage. Shock 26(5): 430-7.

Moriez, R., C.Salvador-Cartier, V. Theodorou, J. Fioramonti, H. Eutamene and L. Bueno (2005). Myosin light chain kinase is involved in lipopolysaccharide-induced disruption of colonic epithelial barrier and bacterial translocation in rats. Am J Pathol 167(4):1071-9.

Morikawa, Y., Y. Mizuno and H. Yasue (2010). Letter by Morikawa et al regarding article, "coronary artery spasm: a 2009 update". Circulation 121(3):e16.

Morrow, V. A., F. Foufelle, J. M. Connell, J. R. Petrie, G. W. Gould and I. P. Salt (2003). Direct activation of AMP-activated protein kinase stimulates nitric-oxide synthesis in human aortic endothelial cells. J Biol Chem 278(34): 31629-39.

Mount, P. F., N. Lane, S. Venkatesan, G. R. Steinberg, S. A. Fraser, B. E. Kemp and D. A. Power (2008). Bradykinin stimulates endothelial cell fatty acid oxidation by CaMKK-dependent activation of AMPK. Atherosclerosis 200(1): 28-36.

Muoio, D. M., K. Seefeld, L. A. Witters and R. A. Coleman (1999). AMP-activated kinase reciprocally regulates triacylglycerol synthesis and fatty acid oxidation in liver and muscle: evidence that sn-glycerol-3-phosphate acyltransferase is a novel target. Biochem J 338 (Pt 3): 783-91.

Murray, P. T., M. E. Wylam and J. G. Umans (1998). Endotoxin impairs agonist-induced calcium mobilization in bovine aortic myocytes by a nitric oxide-independent mechanism. J Lab Clin Med 131(4): 336-43.

Nabeshima, Y., Y. Nonomura and Y. Fujii-Kuriyama (1987). Nonmuscle and smooth muscle myosin light chain mRNAs are generated from a single gene by the tissue-specific alternative RNA splicing. J Biol Chem 262(22): 10608-12.

Nagata, D., M. Mogi and K. Walsh (2003). AMP-activated protein kinase (AMPK) signaling in endothelial cells is essential for angiogenesis in response to hypoxic stress. J Biol Chem 278(33): 31000-6.

Nairn. A. C. and M.R. Picciotto (1994). Calcium/calmodulin-dependent protein kinases. Semin. Cancer Biol. **5(4)**:295–303.

Nakamura, K., Y. Koga, H. Sakai, K. Homma and M. Ikebe (2007). cGMP-dependent relaxation of smooth muscle is coupled with the change in the phosphorylation of myosin phosphatase. Circ Res 101(7): 712-22.

Nduka, O. O. and J. E. Parrillo (2009). The pathophysiology of septic shock. Crit Care Clin 25(4): 677-702, vii.

Negishi, H., Y. Fujita, H. Yanai, S. Sakaguchi, X. Ouyang, M. Shinohara, H. Takayanagi, Y. Ohba, T. Taniguchi and K. Honda (2006). Evidence for licensing of IFN-gamma-induced IFN regulatory factor 1 transcription factor by MyD88 in Toll-like receptor-dependent gene induction program. Proc Natl Acad Sci U S A 103(41): 15136-41.

Nemzek, J. A., K. M. Hugunin and M. R. Opp (2008). Modeling sepsis in the laboratory: merging sound science with animal well-being. Comp Med 58(2): 120-8.

Netea, M.G., B. J. Kullberg and J. W. Van der Meer (2000). Circulating cytokines as mediators of fever. Clin Infect Dis 31 Suppl 5:S178-84.

Neumann, D., A. Woods, D. Carling, T. Wallimann and U. Schlattner (2003). Mammalian AMP-activated protein kinase: functional, heterotrimeric complexes by co-expression of subunits in Escherichia coli. Protein Expr Purif 30(2): 230-7.

Nik-Zainal, S., L. B. Alexandrov, D. C. Wedge, P. Van Loo, C. D. Greenman, K. Raine, D. Jones, J. Hinton, J. Marshall, L. A. Stebbings, A. Menzies, S. Martin, K. Leung, L. Chen, C. Leroy, M. Ramakrishna, R. Rance, K. W. Lau, L. J. Mudie, I. Varela, D. J. McBride, G. R. Bignell, S. L. Cooke, A. Shlien, J. Gamble, I. Whitmore, M. Maddison, P. S. Tarpey, H. R. Davies, E. Papaemmanuil, P. J. Stephens, S. McLaren, A. P. Butler, J. W. Teague, G. Jonsson, J. E. Garber, D. Silver, P. Miron, A. Fatima, S. Boyault, A. Langerod, A. Tutt, J. W. Martens, S. A. Aparicio, A. Borg, A. V. Salomon, G. Thomas, A. L. Borresen-Dale, A. L. Richardson, M. S. Neuberger, P. A. Futreal, P. J. Campbell and M. R. Stratton (2012). Mutational processes molding the genomes of 21 breast cancers. Cell 149(5): 979-93.

Nobes, C. D. and A. Hall (1995). Rho, Rac, and Cdc42 GTPases regulate the assembly of multimolecular focal complexes associated with actin stress fibers, lamellipodia, and filopodia. Cell 81:53–62.

Northcott, C. A., M. N. Poy, S. M. Najjar and S. W. Watts (2002). Phosphoinositide 3-kinase mediates enhanced spontaneous and agonist-induced contraction in aorta of deoxycorticosterone acetate-salt hypertensive rats. Circ Res 91(4): 360-9.

Ohta, S., Y. Hattori, N. Nakanishi, H. Sugimoto and K. Kasai K (2011). Differential modulation of immunostimulant-triggered NO production by endoplasmic reticulum stress inducers in vascular smooth muscle cells. J Cardiovasc Pharmacol 57(4):434-8.

Oury, F., V. K. Yadav, Y. Wang, B. Zhou, X. S. Liu, X. E. Guo, L. H. Tecott, G. Schutz, A. R. Means and G. Karsenty (2010). CREB mediates brain serotonin regulation of bone mass through its expression in ventromedial hypothalamic neurons. Genes Dev 24(20): 2330-42.

Park, I. K. and T. R. Soderling (1995). Activation of Ca2+/calmodulin-dependent protein kinase (CaM-kinase) IV by CaM-kinase kinase in Jurkat T lymphocytes. J Biol Chem 270(51): 30464-9.

Pastor-Soler, N. M. and K. R. Hallows (2012). AMP-activated protein kinase regulation of kidney tubular transport. Curr Opin Nephrol Hypertens 21(5): 523-33.

Paterson, H. M., T. J. Murphy, E. J. Purcell, O. Shelley, S. J. Kriynovich, E. Lien, J. A. Mannick and J. A. Lederer (2003). Injury primes the innate immune system for enhanced Toll-like receptor reactivity. J Immunol 171(3): 1473-83.

Peck-Palmer, O. M., J. Unsinger, K. C. Chang, C. G. Davis, J. E. McDunn and R. S. Hotchkiss (2008). Deletion of MyD88 markedly attenuates sepsis-induced T and B lymphocyte apoptosis but worsens survival. J Leukoc Biol 83(4): 1009-18.

Pedersen, M. E., D. Fortunati, M. Nielsen, S. H. Brorson, T. Lekva, L. S. Nissen-Meyer, V. T. Gautvik, A. Shahdadfar, K. M. Gautvik and R. Jemtland (2008). Calmodulin-dependent kinase 1beta is expressed in the epiphyseal growth plate and regulates proliferation of mouse calvarial osteoblasts *in vitro*. Bone 43(4): 700-7.

Peters, M., K. Mizuno, L. Ris, M. Angelo, E. Godaux and K. P. Giese (2003). Loss of Ca2+/calmodulin kinase kinase beta affects the formation of some, but not all, types of hippocampus-dependent long-term memory. J Neurosci 23(30): 9752-60.

Petros, A., D. Bennett and P. Vallance (1991). Effect of nitric oxide synthase inhibitors on hypotension in patients with septic shock. Lancet 338(8782-8783): 1557-8.

Petti, C., C. Vegetti, A. Molla, I. Bersani, L. Cleris, K. J. Mustard, F. Formelli, G. D. Hardie, M. Sensi and A. Anichini (2012). AMPK activators inhibit the proliferation of human melanomas bearing the activated MAPK pathway. Melanoma Res 22(5): 341-50.

Picciotto, M. R., M. Zoli, G. Bertuzzi and A. C. Nairn (1995). Immunochemical localization of calcium/calmodulin-dependent protein kinase I. Synapse 20(1): 75-84.

Poli-de-Figueiredo, L. F., A. G. Garrido, N. Nakagawa and P. Sannomiya (2008). Experimental models of sepsis and their clinical relevance. Shock 30 Suppl 1: 53-9.

Poltorak, A., P. Ricciardi-Castagnoli, A. Citterio and B. Beutler (2000). Physical contact between LPS and Tlr4 revealed by genetic complementation. Proc Natl Acad Sci USA 97:2163–2167.

Preti, S. C., V. da Cunha, D. V. Vassallo and I. Stefanon (2005). The superoxide dismutase mimetic, tempol, reduces the bioavailability of nitric oxide and does not alter L-NAME-induced hypertension in rats. Basic Clin Pharmacol Toxicol 97(1): 29-34.

Pryshchep, O., W. Ma-Krupa, B. R. Younge, J. J. Goronzy and C. M. Weyand (2008). Vessel-specific Toll-like receptor profiles in human medium and large arteries. Circulation 118(12):1276-84.

Racioppi, L. and A. R. Means (2008). Calcium/calmodulin-dependent kinase IV in immune and inflammatory responses: novel routes for an ancient traveller. Trends Immunol 29(12): 600-7.

Racioppi, L. and A. R. Means (2012). Calcium/calmodulin-dependent protein kinase kinase 2: roles in signaling and pathophysiology. J Biol Chem 287(38): 31658-65.

Racioppi, L., P. K. Noeldner, F. Lin, S. Arvai and A. R. Means (2012). Calcium/calmodulin-dependent protein kinase kinase 2 regulates macrophage-mediated inflammatory responses. J Biol Chem 287(14): 11579-91.

Rafikov, R., F. V. Fonseca, S. Kumar, D. Pardo, C. Darragh, S. Elms, D. Fulton and S. M. Black (2011). eNOS activation and NO function: structural motifs responsible for the posttranslational control of endothelial nitric oxide synthase activity. J Endocrinol 210(3): 271-84.

Raina, H., J. Zacharia, M. Li and W. G. Wier (2009). Activation by Ca2+/calmodulin of an exogenous myosin light chain kinase in mouse arteries. J Physiol 587(Pt 11): 2599-612.

Rainen, L., U. Oelmueller, S. Jurgensen, R. Wyrich, C. Ballas, J. Schram, C. Herdman, D. Bankaitis-Davis, N. Nicholls, D. Trollinger and V. Tryon (2002). Stabilization of mRNA expression in whole blood samples. Clin Chem 48(11): 1883-90.

Raman, V., F. Blaeser, N. Ho, D. L. Engle, C. B. Williams and T. A. Chatila (2001). Requirement for Ca2+/calmodulin-dependent kinase type IV/Gr in setting the thymocyte selection threshold. J Immunol 167(11): 6270-8.

Raman, M., W. Chen and M. H. Cobb (2007). Differential regulation and properties of MAPKs. Oncogene *26(22):* 3100–12.

Ramaswamy, S., P. Tamayo, R. Rifkin, S. Mukherjee, C. H. Yeang, M. Angelo, C. Ladd, M. Reich, E. Latulippe, J. P. Mesirov, T. Poggio, W. Gerald, M. Loda, E. S. Lander and T. R. Golub (2001). Multiclass cancer diagnosis using tumor gene expression signatures. Proc Natl Acad Sci U S A 98(26): 15149-54.

Raney, M. A. and L. P. Turcotte (2006). Regulation of contraction-induced FA uptake and oxidation by AMPK and ERK1/2 is intensity dependent in rodent muscle. Am J Physiol Endocrinol Metab 291(6): E1220-7.

Reade, M. C., L. Weissfeld, D. C. Angus, J. A. Kellum and E. B. Mibrandt (2010). The prevalence of anemia and its association with 90-day mortality in hospitalized community-acquired pneumonia. BMC Pulm Med 10:15.

Reece, K. M., M. D. Mazalouskas and B. E. Wadzinski (2009). The Balpha and Bdelta regulatory subunits of PP2A are necessary for assembly of the CaMKIV.PP2A signaling complex. Biochem Biophys Res Commun 386(4): 582-7.

Rembold, C. M. (1992). Regulation of contraction and relaxation in arterial smooth muscle. Hypertension 20(2): 129-37.

Remick, D. G. (2007). Pathophysiology of sepsis. Am J Pathol 170(5): 1435-44.

Remick, D. G., G. R. Bolgos, J. Siddiqui, J. Shin and J. A. Nemzek (2002). Six at six: interleukin-6 measured 6 h after the initiation of sepsis predicts mortality over 3 days. Shock 17(6): 463-7.

Ridley, A. J. (2001). Rho GTPases and cell migration. J. Cell Sci 114:2713–2722.

Ridley, A. J. and A. Hall (1992). The small GTP-binding protein rho regulates the assembly of focal adhesions and actin stress fibers in response to growth factors. Cell 70:389–399.

Ridley, A. J., H. F. Paterson, C. L. Johnston, D. Diekmann and A. Hall (1992). The small GTP-binding protein Rac regulates growth factorinduced membrane ruffling. Cell 70:401–410.

Rietschel, E. T., T. Kirikae, F. U. Schade, U. Mamat, G. Schmidt, H. Loppnow, A. J. Ulmer, U. Zahringer, U. Seydel, F. Di Padova and et al. (1994). Bacterial endotoxin: molecular relationships of structure to activity and function. FASEB J 8(2): 217-25.

Rosengart, M. R., S. Arbabi, G. J. Bauer, J. Garcia, S. Jelacic and R. V. Maier (2002). The actin cytoskeleton: an essential component for enhanced TNFalpha production by adherent monocytes. Shock 17(2):109-13.

Rubin, L. J., L. Magliola, X. Feng, A. W. Jones and C. C. Hale (2005). Metabolic activation of AMP kinase in vascular smooth muscle. J Appl Physiol 98(1): 296-306.

Russell, R. R., 3rd, J. Li, D. L. Coven, M. Pypaert, C. Zechner, M. Palmeri, F. J. Giordano, J. Mu, M. J. Birnbaum and L. H. Young (2004). AMP-activated protein kinase mediates ischemic glucose uptake and prevents postischemic cardiac dysfunction, apoptosis, and injury. J Clin Invest 114(4): 495-503.

Sag, D., D. Carling, R. D. Stout and J. Suttles (2008). Adenosine 5'-monophosphate-activated protein kinase promotes macrophage polarization to an anti-inflammatory functional phenotype. J Immunol 181(12): 8633-41.

Saha, A. K., X. J. Xu, E. Lawson, R. Deoliveira, A. E. Brandon, E. W. Kraegen and N. B. Ruderman (2010). Downregulation of AMPK accompanies leucine- and glucose-induced increases in protein synthesis and insulin resistance in rat skeletal muscle. Diabetes 59(10): 2426-34.

Saito, H., E. R. Sherwood, T. K. Varma and B. M. Evers (2003). Effects of aging on mortality, hypothermia, and cytokine induction in mice with endotoxemia or sepsis. Mech Ageing Dev 124(10-12): 1047-58.

Sakaguchi, S. and S. Furusawa (2006). Oxidative stress and septic shock: metabolic aspects of oxygen-derived free radicals generated in the liver during endotoxemia. FEMS Immunol Med Microbiol 47(2): 167-77.

Sakamoto, K., A. McCarthy, D. Smith, K. A. Green, D. Grahame Hardie, A. Ashworth and D. R. Alessi (2005). Deficiency of LKB1 in skeletal muscle prevents AMPK activation and glucose uptake during contraction. EMBO J 24(10): 1810-20.

Sakamoto, K., E. Zarrinpashneh, G. R. Budas, A. C. Pouleur, A. Dutta, A. R. Prescott, J. L. Vanoverschelde, A. Ashworth, A. Jovanovic, D. R. Alessi and L. Bertrand (2006). Deficiency of LKB1 in heart prevents ischemia-mediated activation of AMPKalpha2 but not AMPKalpha1. Am J Physiol Endocrinol Metab 290(5): E780-8.

Sakr, Y., K. Reinhart, J. L. Vincent, C. L. Sprung, R. Moreno, V. M. Ranieri, D. De Backer and D. Payen (2006). Does dopamine administration in shock influence outcome? Results of the Sepsis Occurrence in Acutely Ill Patients (SOAP) Study. Crit Care Med 34(3): 589-97.

Salgado, A., J. L. Boveda, J. Monasterio, R. M. Segura, M. Mourelle, J. Gomez-Jimenez and R. Peracaula (1994). Inflammatory mediators and their influence on haemostasis. Haemostasis 24(2): 132-8.

Sandmann, T., L. J. Jensen, J. S. Jakobsen, M. M. Karzynski, M. P. Eichenlaub, P. Bork and E. E. Furlong (2006). A temporal map of transcription factor activity: mef2 directly regulates target genes at all stages of muscle development. Dev Cell 10(6): 797-807.

Saneyoshi, T., G. Wayman, D. Fortin, M. Davare, N. Hoshi, N. Nozaki, T. Natsume and T. R. Soderling (2008). Activity-dependent synaptogenesis: regulation by a CaM-kinase kinase/CaM-kinase I/betaPIX signaling complex. Neuron 57(1): 94-107.

Sanli, T., Y. Storozhuk, K. Linher-Melville, R. G. Bristow, K. Laderout, B. Viollet, J. Wright, G. Singh and T. Tsakiridis (2012). Ionizing radiation regulates the expression of AMP-activated protein kinase (AMPK) in epithelial cancer cells: modulation of cellular signals regulating cell cycle and survival. Radiother Oncol 102(3): 459-65.

Santidrian, A. F., D. M. Gonzalez-Girones, D. Iglesias-Serret, L. Coll-Mulet, A. M. Cosialls, M. de Frias, C. Campas, E. Gonzalez-Barca, E. Alonso, V. Labi, B. Viollet, A. Benito, G. Pons, A. Villunger and J. Gil (2010). AICAR induces apoptosis independently of AMPK and p53 through up-regulation of the BH3-only proteins BIM and NOXA in chronic lymphocytic leukemia cells. Blood 116(16): 3023-32.

Sato, K., A. Suematsu, T. Nakashima, S. Takemoto-Kimura, K. Aoki, Y. Morishita, H. Asahara, K. Ohya, A. Yamaguchi, T. Takai, T. Kodama, T. A. Chatila, H. Bito and H.

Takayanagi (2006). Regulation of osteoclast differentiation and function by the CaMK-CREB pathway. Nat Med 12(12): 1410-6.

Schneeberger, M. and M. Claret (2012). Recent Insights into the Role of Hypothalamic AMPK Signaling Cascade upon Metabolic Control. Front Neurosci 6: 185.

Schraw, T., Z. V. Wang, N. Halberg, M. Hawkins and P. E. Scherer (2008). Plasma adiponectin complexes have distinct biochemical characteristics. Endocrinology 149(5): 2270-82.

Scirocco, A., P. Matarrese, C. Petitta, A. Cicenia, B. Ascione, C. Mannironi, F. Ammoscato, M. Cardi, G. Fanello, M. P. Guarino, W. Malorni and C. Severi (2010). Exposure of Toll-like receptors 4 to bacterial lipopolysaccharide (LPS) impairs human colonic smooth muscle cell function. J Cell Physiol 223(2):442-50.

Selbert, M. A., K. A. Anderson, Q. H. Huang, E. G. Goldstein, A. R. Means and A. M. Edelman (1995). Phosphorylation and activation of Ca(2+)-calmodulin-dependent protein kinase IV by Ca(2+)-calmodulin-dependent protein kinase Ia kinase. Phosphorylation of threonine 196 is essential for activation. J Biol Chem 270(29): 17616-21.

Shah, M., B. Kola, A. Bataveljic, T. R. Arnett, B. Viollet, L. Saxon, M. Korbonits and C. Chenu (2010). AMP-activated protein kinase (AMPK) activation regulates *in vitro* bone formation and bone mass. Bone 47(2): 309-19.

Shaw, R. J., K. A. Lamia, D. Vasquez, S. H. Koo, N. Bardeesy, R. A. Depinho, M. Montminy and L. C. Cantley (2005). The kinase LKB1 mediates glucose homeostasis in liver and therapeutic effects of metformin. Science 310(5754): 1642-6.

Shaw, R. J., K. A. Lamia, D. Vasquez, S.-H. Koo, N. Bardeesy, R. A. DePinho, M. Montminy and L. C. Cantley (2005). The Kinase LKB1 Mediates Glucose Homeostasis in Liver and Therapeutic Effects of Metformin. Science 310(5754): 1642-1646.

Shen, Q., R. R. Rigor, C. D. Pivetti, M. H. Wu and S. Y. Yuan (2010). Myosin light chain kinase in microvascular endothelial barrier function. Cardiovasc Res 87(2): 272-80.

Shima, T., A. Mizokami, T. Miyagi, K. Kawai, K. Izumi, M. Kumaki, M. Ofude, J. Zhang, E. T. Keller and M. Namiki (2012). Down-regulation of calcium/calmodulin-dependent protein

kinase kinase 2 by androgen deprivation induces castration-resistant prostate cancer. Prostate 72(16): 1789-801.

Siarakas, S., E. Damas and W. G. Murrell (1997). The effect of enteric bacterial toxins on the catecholamine levels of the rabbit. Pathology 29(3): 278-85.

Sid, B., L. Miranda, D. Vertommen, B. Viollet and M. H. Rider (2010). Stimulation of human and mouse erythrocyte Na(+)-K(+)-2Cl(-) cotransport by osmotic shrinkage does not involve AMP-activated protein kinase, but is associated with STE20/SPS1-related proline/alanine-rich kinase activation. J Physiol 588(Pt 13): 2315-28.

Sidhu, J. S., Y. S. Rajawat, T. G. Rami, M. H. Gollob, Z. Wang, R. Yuan, A. J. Marian, F. J. DeMayo, D. Weilbacher, G. E. Taffet, J. K. Davies, D. Carling, D. S. Khoury and R. Roberts (2005). Transgenic mouse model of ventricular preexcitation and atrioventricular reentrant tachycardia induced by an AMP-activated protein kinase loss-of-function mutation responsible for Wolff-Parkinson-White syndrome. Circulation 111(1): 21-9.

Simmons, D. (2008) The use of animal models in studying genetic disease: transgenesis and induced mutation. Nature Education 1(1).

Soderling, T. R. (1996). Structure and regulation of calcium/ calmodulin-dependent protein kinases II and IV. Biochim. Biphys. Acta 1297:131–138.

Soff, G. A., T. L. Cornwell, D. L. Cundiff, S. Gately and T. M. Lincoln (1997). Smooth muscle cell expression of type I cyclic GMP-dependent protein kinase is suppressed by continuous exposure to nitrovasodilators, theophylline, cyclic GMP, and cyclic AMP. J Clin Invest 100(10): 2580-7.

Somlyo, A. P. and A. V. Somlyo (1994). Signal transduction and regulation in smooth muscle. Nature 372(6503): 231-6.

Somlyo, A. P. and A. V. Somlyo (2000). Signal transduction by G-proteins, rho-kinase and protein phosphatase to smooth muscle and non-muscle myosin II. J Physiol 522 Pt 2: 177-85.

Somlyo, A. P. and A. V. Somlyo (2003). Ca2+ sensitivity of smooth muscle and nonmuscle myosin II: modulated by G proteins, kinases, and myosin phosphatase. Physiol Rev 83(4):1325-58.

Spyer, K. M. (1982). Central nervous integration of cardiovascular control. J Exp Biol 100: 109-28.

Stahmann, N., A. Woods, D. Carling and R. Heller (2006). Thrombin activates AMP-activated protein kinase in endothelial cells via a pathway involving Ca2+/calmodulin-dependent protein kinase kinase beta. Mol Cell Biol 26(16): 5933-45.

Stahmann, N., A. Woods, K. Spengler, A. Heslegrave, R. Bauer, S. Krause, B. Viollet, D. Carling and R. Heller (2010). Activation of AMP-activated protein kinase by vascular endothelial growth factor mediates endothelial angiogenesis independently of nitric-oxide synthase. J Biol Chem 285(14): 10638-52.

Stein, S. C., A. Woods, N. A. Jones, M. D. Davison and D. Carling (2000). The regulation of AMP-activated protein kinase by phosphorylation. Biochem J 345 Pt 3: 437-43.

Steinberg, G. R., J. W. Rush and D. J. Dyck (2003). AMPK expression and phosphorylation are increased in rodent muscle after chronic leptin treatment. Am J Physiol Endocrinol Metab 284(3): E648-54.

Stern, S. and A. Bayes de Luna (2009). Coronary artery spasm: a 2009 update. Circulation 119(18): 2531-4.

Stockton, R., J. Reutershan, D. Scott, J. Sanders, K. Ley and M. A. Schwartz (2007). Induction of vascular permeability: beta PIX and GIT1 scaffold the activation of extracellular signal-regulated kinase by PAK. Mol Biol Cell 18(6): 2346-55.

Styrt, B. (1990). Infection associated with asplenia: risks, mechanisms, and prevention. Am J Med 88(5N): 33N-42N.

Stern, S. and A. Bayes de Luna (2009). Coronary artery spasm: a 2009 update. Circulation 119(18):2531-4.

Su, A. I., J. B. Welsh, L. M. Sapinoso, S. G. Kern, P. Dimitrov, H. Lapp, P. G. Schultz, S. M. Powell, C. A. Moskaluk, H. F. Frierson, Jr. and G. M. Hampton (2001). Molecular classification of human carcinomas by use of gene expression signatures. Cancer Res 61(20): 7388-93.

Sugden, M. C., P. W. Caton and M. J. Holness (2010). PPAR control: it's SIRTainly as easy as PGC. J Endocrinol 204(2): 93-104.

Suizu, F., Y. Fukuta, K. Ueda, T. Iwasaki, H. Tokumitsu and H. Hosoya (2002). Characterization of Ca2+/calmodulin-dependent protein kinase I as a myosin II regulatory light chain kinase *in vitro* and *in vivo*. Biochem J 367(Pt 2): 335-45.

Sullivan, J. E., K. J. Brocklehurst, A. E. Marley, F. Carey, D. Carling and R. K. Beri (1994). Inhibition of lipolysis and lipogenesis in isolated rat adipocytes with AICAR, a cell-permeable activator of AMP-activated protein kinase. FEBS Lett 353(1): 33-6.

Sung, J. Y. and H. C. Choi (2012). Nifedipine inhibits vascular smooth muscle cell proliferation and reactive oxygen species production through AMP-activated protein kinase signaling pathway. Vascul Pharmacol 56(1-2): 1-8.

Sutherland, C. and M. P. Walsh (2012). Myosin regulatory light chain diphosphorylation slows relaxation of arterial smooth muscle. J Biol Chem 287(29): 24064-76.

Swan, R., C. S. Chung, J. Albina, W. Cioffi, M. Perl and A. Ayala (2007). Polymicrobial sepsis enhances clearance of apoptotic immune cells by splenic macrophages. Surgery 142(2): 253-61.

Tadaishi, M., S. Miura, Y. Kai, E. Kawasaki, K. Koshinaka, K. Kawanaka, J. Nagata, Y. Oishi and O. Ezaki (2011). Effect of exercise intensity and AICAR on isoform-specific expressions of murine skeletal muscle PGC-1alpha mRNA: a role of beta(2)-adrenergic receptor activation. Am J Physiol Endocrinol Metab 300(2): E341-9.

Takata, T., J. Kimura, Y. Tsuchiya, Y. Naito and Y. Watanabe (2011). Calcium/calmodulin-dependent protein kinases as potential targets of nitric oxide. Nitric Oxide 25(2): 145-52.

Takeda, N., E. L. O'Dea, A. Doedens, J. W. Kim, A. Weidemann, C. Stockmann, M. Asagiri, M. C. Simon, A. Hoffmann and R. S. Johnson (2010). Differential activation and antagonistic function of HIF-{alpha} isoforms in macrophages are essential for NO homeostasis. Genes Dev 24(5): 491-501.

Takeuchi, O., K. Hoshino, T. Kawai, H. Sanjo, H. Takada, T. Ogawa, K. Takeda and S. Akira (1999). Differential roles of TLR2 and TLR4 in recognition of gram-negative and gram-positive bacterial cell wall components. Immunity 11(4): 443-51.

Tamas, P., S. A. Hawley, R. G. Clarke, K. J. Mustard, K. Green, D. G. Hardie and D. A. Cantrell (2006). Regulation of the energy sensor AMP-activated protein kinase by antigen receptor and Ca2+ in T lymphocytes. J Exp Med 203(7): 1665-70.

Teng, E. C., L. Racioppi and A. R. Means (2011). A cell-intrinsic role for CaMKK2 in granulocyte lineage commitment and differentiation. J Leukoc Biol 90(5): 897-909.

Thaiparambil, J. T., C. M. Eggers and A. I. Marcus (2012). AMPK regulates mitotic spindle orientation through phosphorylation of myosin regulatory light chain. Mol Cell Biol 32(16): 3203-17.

Thomson, D. M., B. B. Porter, J. H. Tall, H. J. Kim, J. R. Barrow and W. W. Winder (2007). Skeletal muscle and heart LKB1 deficiency causes decreased voluntary running and reduced muscle mitochondrial marker enzyme expression in mice. Am J Physiol Endocrinol Metab 292(1): E196-202.

Thors, B., H. Halldorsson and G. Thorgeirsson (2011). eNOS activation mediated by AMPK after stimulation of endothelial cells with histamine or thrombin is dependent on LKB1. Biochim Biophys Acta 1813(2): 322-31.

Totsukawa, G., Y. Wu, Y. Sasaki, D. J. Hartshorne, Y, Yamakita, S. Yamashiro and F. Matsumura (2004). Distinct roles of MLCK and ROCK in the regulation of membrane protrusions and focal adhesion dynamics during cell migration of fibroblasts. J Cell Biol 164(3):427-39.

Tokumitsu, H., N. Hatano, T. Fujimoto, S. Yurimoto and R. Kobayashi (2011). Generation of autonomous activity of Ca(2+)/calmodulin-dependent protein kinase kinase beta by autophosphorylation. Biochemistry 50(38): 8193-201.

Tokumitsu, H., N. Hatano, H. Inuzuka, S. Yokokura, N. Nozaki and R. Kobayashi (2004). Mechanism of the generation of autonomous activity of Ca2+/calmodulin-dependent protein kinase IV. J Biol Chem 279(39): 40296-302.

Tokumitsu, H., H. Inuzuka, Y. Ishikawa, M. Ikeda, I. Saji and R. Kobayashi (2002). STO-609, a specific inhibitor of the Ca(2+)/calmodulin-dependent protein kinase kinase. J Biol Chem 277(18): 15813-8.

Tokumitsu, H., M. Iwabu, Y. Ishikawa and R. Kobayashi (2001). Differential regulatory mechanism of Ca2+/calmodulin-dependent protein kinase kinase isoforms. Biochemistry 40(46): 13925-32.

Treebak, J. T., S. Glund, A. Deshmukh, D. K. Klein, Y. C. Long, T. E. Jensen, S. B. Jorgensen, B. Viollet, L. Andersson, D. Neumann, T. Wallimann, E. A. Richter, A. V. Chibalin, J. R. Zierath and J. F. Wojtaszewski (2006). AMPK-mediated AS160 phosphorylation in skeletal muscle is dependent on AMPK catalytic and regulatory subunits. Diabetes 55(7): 2051-8.

Treebak, J. T. and J. F. Wojtaszewski (2008). Role of 5'AMP-activated protein kinase in skeletal muscle. Int J Obes (Lond) 32 Suppl 4: S13-7.

Triantafilou, M. and K. Triantafilou (2005). The dynamics of LPS recognition: complex orchestration of multiple receptors. J Endotoxin Res 11(1): 5-11.

Turjanski, A.G., J. P. Vaqué and J.S. Gutkind (2007). MAP kinases and the control of nuclear events. Oncogene *26(*22), 3240–53.

Uehata, M., T. Ishizaki, H. Satoh, T. Ono, T. Kawahara, T. Morishita, H. Tamakawa, K. Yamagami, J. Inui, M. Maekawa and S. Narumiya (1997). Calcium sensitization of smooth muscle mediated by a Rho-associated protein kinase in hypertension. Nature 389(6654): 990-4.

Uematsu, S. and S. Akira (2006). Toll-like receptors and innate immunity. J Mol Med (Berl) 84(9): 712-25.

Uemura, A., Y. Naito, T. Matsubara, N. Hotta and H. Hidaka (1998). Demonstration of a Ca2+/calmodulin dependent protein kinase cascade in the hog heart. Biochem Biophys Res Commun 249(2): 355-60.

Ulevitch, R. J. and P. S. Tobias (1995). Receptor-dependent mechanisms of cell stimulation by bacterial endotoxin. Annu Rev Immunol 13: 437-57.

Van der Bruggen, T., S. Nijenhuis, E. van Raaij, J. Verhoef and B. S. van Asbeck (1999). Lipopolysaccharide-induced tumor necrosis factor alpha production by human monocytes involves the raf-1/MEK1-MEK2/ERK1-ERK2 pathway. Infect Immun 67(8):3824-9.

Van Lambalgen, A. A., M. T. Rasker, G. C. van den Bos and L. G. Thijs (1988). Effects of endotoxemia on systemic plasma loss and hematocrit in rats. Microvasc Res 36(3):291-304.

Vazquez-Torres, A., T. Stevanin, J. Jones-Carson, M. Castor, R. C. Read and F. C. Fang (2008). Analysis of nitric oxide-dependent antimicrobial actions in macrophages and mice. Methods Enzymol 437: 521-38.

Versari, D., E. Daghini, A. Virdis, L. Ghiadoni and S. Taddei (2009). Endothelium-dependent contractions and endothelial dysfunction in human hypertension. Br J Pharmacol 157(4): 527-36.

Vicente-Manzanares, M., X. Ma, R. S. Adelstein and A. R. Horwitz (2009). Non-muscle myosin II takes centre stage in cell adhesion and migration. Nat Rev Mol Cell Biol 10(11): 778-90.

Villena, J. A., B. Viollet, F. Andreelli, A. Kahn, S. Vaulont and H. S. Sul (2004). Induced adiposity and adipocyte hypertrophy in mice lacking the AMP-activated protein kinase-alpha2 subunit. Diabetes 53(9): 2242-9.

Vinet, J., S. Carra, J. M. Blom, M. Harvey, N. Brunello, N. Barden and F. Tascedda (2003). Cloning of mouse Ca2+/calmodulin-dependent protein kinase kinase beta (CaMKKbeta) and characterization of CaMKKbeta and CaMKKalpha distribution in the adult mouse brain. Brain Res Mol Brain Res 111(1-2): 216-21.

Viollet, B., F. Andreelli, S. B. Jorgensen, C. Perrin, A. Geloen, D. Flamez, J. Mu, C. Lenzner, O. Baud, M. Bennoun, E. Gomas, G. Nicolas, J. F. Wojtaszewski, A. Kahn, D. Carling, F. C. Schuit, M. J. Birnbaum, E. A. Richter, R. Burcelin and S. Vaulont (2003). The AMP-activated protein kinase alpha2 catalytic subunit controls whole-body insulin sensitivity. J Clin Invest 111(1): 91-8.

Viollet, B., F. Andreelli, S. B. Jorgensen, C. Perrin, A. Geloen, D. Flamez, J. Mu, C. Lenzner, O. Baud, M. Bennoun, E. Gomas, G. Nicolas, J. F. P. Wojtaszewski, A. Kahn, D. Carling, F. C. Schuit, M. J. Birnbaum, E. A. Richter, R. Burcelin and S. Vaulont (2003). The AMP-activated protein kinase alpha 2 catalytic subunit controls whole-body insulin sensitivity. Journal of Clinical Investigation 111(1): 91-98.

Viollet, B., L. Lantier, J. Devin-Leclerc, S. Hebrard, C. Amouyal, R. Mounier, M. Foretz and F. Andreelli (2009). Targeting the AMPK pathway for the treatment of Type 2 diabetes. Front Biosci 14: 3380-400.

Wagenseil, J. E. and R. P. Mecham (2012). Elastin in large artery stiffness and hypertension. J Cardiovasc Transl Res 5(3):264-73.

Wain, L. V., G. C. Verwoert, P. F. O'Reilly, G. Shi, T. Johnson, A. D. Johnson, M. Bochud, K. M. Rice, P. Henneman, A. V. Smith, G. B. Ehret, N. Amin, M. G. Larson, V. Mooser, D. Hadley, M. Dorr, J. C. Bis, T. Aspelund, T. Esko, A. C. Janssens, J. H. Zhao, S. Heath, M. Laan, J. Fu, G. Pistis, J. Luan, P. Arora, G. Lucas, N. Pirastu, I. Pichler, A. U. Jackson, R. J. Webster, F. Zhang, J. F. Peden, H. Schmidt, T. Tanaka, H. Campbell, W. Igl, Y. Milaneschi, J. J. Hottenga, V. Vitart, D. I. Chasman, S. Trompet, J. L. Bragg-Gresham, B. Z. Alizadeh, J. C. Chambers, X. Guo, T. Lehtimaki, B. Kuhnel, L. M. Lopez, O. Polasek, M. Boban, C. P. Nelson, A. C. Morrison, V. Pihur, S. K. Ganesh, A. Hofman, S. Kundu, F. U. Mattace-Raso, F. Rivadeneira, E. J. Sijbrands, A. G. Uitterlinden, S. J. Hwang, R. S. Vasan, T. J. Wang, S. Bergmann, P. Vollenweider, G. Waeber, J. Laitinen, A. Pouta, P. Zitting, W. L. McArdle, H. K. Kroemer, U. Volker, H. Volzke, N. L. Glazer, K. D. Taylor, T. B. Harris, H. Alavere, T. Haller, A. Keis, M. L. Tammesoo, Y. Aulchenko, I. Barroso, K. T. Khaw, P. Galan, S. Hercberg, M. Lathrop, S. Eyheramendy, E. Org, S. Sober, X. Lu, I. M. Nolte, B. W. Penninx, T. Corre, C. Masciullo, C. Sala, L. Groop, B. F. Voight, O. Melander, C. J. O'Donnell, V. Salomaa, A. P. d'Adamo, A. Fabretto, F. Faletra, S. Ulivi, F. Del Greco, M. Facheris, F. S. Collins, R. N. Bergman, J. P. Beilby, J. Hung, A. W. Musk, M. Mangino, S. Y. Shin, N. Soranzo, H. Watkins, A. Goel, A. Hamsten, P. Gider, M. Loitfelder, M. Zeginigg, D. Hernandez, S. S. Najjar, P. Navarro, S. H. Wild, A. M. Corsi, A. Singleton, E. J. de Geus, G. Willemsen, A. N. Parker, L. M. Rose, B. Buckley, D. Stott, M. Orru, M. Uda, M. M. van der Klauw, W. Zhang, X. Li, J. Scott, Y. D. Chen, G. L. Burke, M. Kahonen, J. Viikari, A. Doring, T. Meitinger, G. Davies, J. M. Starr, V. Emilsson, A. Plump, J. H. Lindeman, P. A. Hoen, I. R. Konig, J. F. Felix, R. Clarke, J. C. Hopewell, H. Ongen, M. Breteler, S. Debette, A. L. Destefano, M. Fornage, G. F. Mitchell, N. L. Smith, H. Holm, K. Stefansson, G. Thorleifsson, U. Thorsteinsdottir, N. J. Samani, M. Preuss, I. Rudan, C. Hayward, I. J. Deary, H. E. Wichmann, O. T. Raitakari, W. Palmas, J. S. Kooner, R. P. Stolk, J. W. Jukema, A. F. Wright, D. I. Boomsma, S. Bandinelli, U. B. Gyllensten, J. F. Wilson, L. Ferrucci, R. Schmidt, M. Farrall, T. D. Spector, L. J. Palmer, J. Tuomilehto, A. Pfeufer, P. Gasparini, D. Siscovick, D. Altshuler, R. J. Loos, D. Toniolo, H. Snieder, C. Gieger, P. Meneton, N. J. Wareham, B. A. Oostra, A. Metspalu, L. Launer, R.

Rettig, D. P. Strachan, J. S. Beckmann, J. C. Witteman, J. Erdmann, K. W. van Dijk, E. Boerwinkle, M. Boehnke, P. M. Ridker, M. R. Jarvelin, A. Chakravarti, G. R. Abecasis, V. Gudnason, C. Newton-Cheh, D. Levy, P. B. Munroe, B. M. Psaty, M. J. Caulfield, D. C. Rao, M. D. Tobin, P. Elliott and C. M. van Duijn (2011). Genome-wide association study identifies six new loci influencing pulse pressure and mean arterial pressure. Nat Genet 43(10): 1005-11.

Wang, H., O. Bloom, M. Zhang, J. M. Vishnubhakat, M. Ombrellino, J. Che, A. Frazier, H. Yang, S. Ivanova, L. Borovikova, K. R. Manogue, E. Faist, E. Abraham, J. Andersson, U. Andersson, P. E. Molina, N. N. Abumrad, A. Sama and K. J. Tracey (1999). HMG-1 as a late mediator of endotoxin lethality in mice. Science 285(5425): 248-51.

Wang le, F., M. Patel, H. M. Razavi, S. Weicker, M. G. Joseph, D. G. McCormack and S. Mehta (2002). Role of inducible nitric oxide synthase in pulmonary microvascular protein leak in murine sepsis. Am J Respir Crit Care Med 165(12): 1634-9.

Wang, S., G. L. Dale, P. Song, B. Viollet and M. H. Zou (2010). AMPKalpha1 deletion shortens erythrocyte life span in mice: role of oxidative stress. J Biol Chem 285(26): 19976-85.

Wang, S., B. Liang, B. Viollet and M. H. Zou (2011). Inhibition of the AMP-activated protein kinase-alpha2 accentuates agonist-induced vascular smooth muscle contraction and high blood pressure in mice. Hypertension 57(5): 1010-7.

Wayman, G. A., S. Impey, D. Marks, T. Saneyoshi, W. F. Grant, V. Derkach and T. R. Soderling (2006). Activity-dependent dendritic arborization mediated by CaM-kinase I activation and enhanced CREB-dependent transcription of Wnt-2. Neuron 50(6): 897-909.

Wayman, G. A., Y. S. Lee, H. Tokumitsu, A. J. Silva and T. R. Soderling (2008). Calmodulin-kinases: modulators of neuronal development and plasticity. Neuron 59(6): 914-31.

Wayman, G. A., H. Tokumitsu and T. R. Soderling (1997). Inhibitory cross-talk by cAMP kinase on the calmodulin-dependent protein kinase cascade. J Biol Chem 272(26): 16073-6.

Weixelbaumer, K. M., P. Raeven, H. Redl, M. van Griensven, S. Bahrami and M. F. Osuchowski (2010). Repetitive low-volume blood sampling method as a feasible monitoring tool in a mouse model of sepsis. Shock 34(4): 420-6.

Westphal, R. S., K. A. Anderson, A. R. Means and B. E. Wadzinski (1998). A signaling complex of Ca2+-calmodulin-dependent protein kinase IV and protein phosphatase 2A. Science 280(5367): 1258-61.

Witczak, C. A., N. Fujii, M. F. Hirshman and L. J. Goodyear (2007). Ca2+/calmodulin-dependent protein kinase kinase-alpha regulates skeletal muscle glucose uptake independent of AMP-activated protein kinase and Akt activation. Diabetes 56(5): 1403-9.

Woods, A., P. C. Cheung, F. C. Smith, M. D. Davison, J. Scott, R. K. Beri and D. Carling (1996). Characterization of AMP-activated protein kinase beta and gamma subunits. Assembly of the heterotrimeric complex *in vitro*. J Biol Chem 271(17): 10282-90.

Woods, A., K. Dickerson, R. Heath, S. P. Hong, M. Momcilovic, S. R. Johnstone, M. Carlson and D. Carling (2005). Ca2+/calmodulin-dependent protein kinase kinase-beta acts upstream of AMP-activated protein kinase in mammalian cells. Cell Metab 2(1): 21-33.

Woods, A., S. R. Johnstone, K. Dickerson, F. C. Leiper, L. G. Fryer, D. Neumann, U. Schlattner, T. Wallimann, M. Carlson and D. Carling (2003). LKB1 is the upstream kinase in the AMP-activated protein kinase cascade. Curr Biol 13(22): 2004-8.

Woods, A., I. Salt, J. Scott, D. G. Hardie and D. Carling (1996). The alpha1 and alpha2 isoforms of the AMP-activated protein kinase have similar activities in rat liver but exhibit differences in substrate specificity *in vitro*. FEBS Lett 397(2-3): 347-51.

Woollard, K. J. and F. Geissmann (2010). Monocytes in atherosclerosis: subsets and functions. Nat Rev Cardiol 7(2): 77-86.

Xi, C. X., F. Xiong, Z. Zhou, L, Mei and W. C. Xiong (2010). PYK2 interacts with MyD88 and regulates MyD88-mediated NF-kappaB activation in macrophages. J Leukoc Biol 87(3):415-23.

Xiao, B., M. J. Sanders, E. Underwood, R. Heath, F. V. Mayer, D. Carmena, C. Jing, P. A. Walker, J. F. Eccleston, L. F. Haire, P. Saiu, S. A. Howell, R. Aasland, S. R. Martin, D. Carling and S. J. Gamblin (2011). Structure of mammalian AMPK and its regulation by ADP. Nature 472(7342): 230-3.

Yadav, V. K., F. Oury, N. Suda, Z. W. Liu, X. B. Gao, C. Confavreux, K. C. Klemenhagen, K. F. Tanaka, J. A. Gingrich, X. E. Guo, L. H. Tecott, J. J. Mann, R. Hen, T. L. Horvath and G.

Karsenty (2009). A serotonin-dependent mechanism explains the leptin regulation of bone mass, appetite, and energy expenditure. Cell 138(5): 976-89.

Yang, Y., D. Atasoy, H. H. Su and S. M. Sternson (2011). Hunger states switch a flip-flop memory circuit via a synaptic AMPK-dependent positive feedback loop. Cell 146(6): 992-1003.

Yin, G., Q. Zheng, C. Yan and B. C. Berk (2005). GIT1 is a scaffold for ERK1/2 activation in focal adhesions. J Biol Chem 280(30): 27705-12.

Yu, C. T., H. M. Shih and M. Z. Lai (2001). Multiple signals required for cyclic AMP-responsive element binding protein (CREB) binding protein interaction induced by CD3/CD28 costimulation. J Immunol 166(1):284-92.

Zanoni, I. and F. Granucci (2010). Differences in lipopolysaccharide-induced signaling between conventional dendritic cells and macrophages. Immunobiology 215(9-10): 709-12.

Zarrinpashneh, E., K. Carjaval, C. Beauloye, A. Ginion, P. Mateo, A. C. Pouleur, S. Horman, S. Vaulont, J. Hoerter, B. Viollet, L. Hue, J. L. Vanoverschelde and L. Bertrand (2006). Role of the alpha2-isoform of AMP-activated protein kinase in the metabolic response of the heart to no-flow ischemia. Am J Physiol Heart Circ Physiol 291(6): H2875-83.

Zhang, H., D. W. Niesel, J. W. Peterson and G. R. Klimpel (1998). Lipoprotein release by bacteria: potential factor in bacterial pathogenesis. Infect Immun 66(11): 5196-201.

Zhang, T. and Q. Feng (2010). Nitric oxide and calcium signaling regulate myocardial tumor necrosis factor-alpha expression and cardiac function in sepsis. Can J Physiol Pharmacol 88(2): 92-104.

Zhang, X., L. Guo, R. D. Collage, J. L. Stripay, A. Tsung, J. S. Lee and M. R. Rosengart (2011). Calcium/calmodulin-dependent protein kinase (CaMK) Ialpha mediates the macrophage inflammatory response to sepsis. J Leukoc Biol 90(2): 249-61.

Zhang, X., D. Wheeler, Y. Tang, L. Guo, R. A. Shapiro, T. J. Ribar, A. R. Means, T. R. Billiar, D. C. Angus and M. R. Rosengart (2008). Calcium/calmodulin-dependent protein kinase (CaMK) IV mediates nucleocytoplasmic shuttling and release of HMGB1 during lipopolysaccharide stimulation of macrophages. J Immunol 181(7): 5015-23.

Zhao, X., J. W. Zmijewski, E. Lorne, G. Liu, Y. J. Park, Y. Tsuruta and E. Abraham (2008). Activation of AMPK attenuates neutrophil proinflammatory activity and decreases the severity of acute lung injury. Am J Physiol Lung Cell Mol Physiol 295(3): L497-504.

Zhao, Z. S. and E. Manser (2005). PAK and other Rho-associated kinases--effectors with surprisingly diverse mechanisms of regulation. Biochem J 386(Pt 2): 201-14.

Appendix 1. Substrates of AMPK containing the α1 or α2 subunit (Kodiha and Stochaj 2011).

Substrates for AMPKα1	**Function**	**Effect of phosphorylation**	**Primary intracellular localization**
Acc1; Subunit of acetyl-CoA carboxylase, ACC	Carboxylates acetyl-CoA, thereby generating malonyl-CoA; this step is rate-limiting for FA biosynthesis.	inhibition	cytoplasm
Acc2; Subunit of acetyl-CoA carboxylase, ACC	Carboxylates acetyl-CoA, thereby generating malonyl-CoA; this step is rate-limiting for FA biosynthesis.	inhibition	mitochondria (outer mitochondrial membrane)
AMPKβ1	Catalytic subunit of AMPK	potential autoregulation	cytoplasm, nucleus
AMPKγ1	Regulatory subunit of AMPK	enzymatic activity, localization	cytoplasm, nucleus
CFTR chloride channel	Cystic fibrosis transmembrane conductance regulator,	inhibits PKA dependent stimulation of CFTR	plasma membrane, ER, cytoplasmic vesicle; early endosome
ChREBP	Transcription factor; repressor	inactivation of DNA binding	nucleus, cytoplasm
CK1-ε (CK1 epsilon)	Ser/thr kinase; member of the casein kinase 1 (CK1) family; phosphorylates mPer2	increase of CK1-ε activity; control of circadian clock	cytoplasm, nucleus, cell junction, centrosome
CRY1 (cryptochrome)	DNA photolyase, regulates circadian rhythm	phosphorylation leads to destabilization	nucleus, mitochondria, cytoplasm
CRTC-1	CREB-regulated transcriptional coactivator	phosphorylation causes cytoplasmic retention	nucleus, cytoplasm

eEF2K (eEF2 kinase)	Protein kinase; eEF2K modifies and thereby inactivates eEF2	activation of kinase activity	cytoplasm
eNOS	Endothelial nitric oxide synthase (constitutive), EC 1.14.13.39; regulation of cytoskeletal reorganization	activation, promotes deacetylation by SIRT1	plasma membrane, Golgi
GABAB-R1	GABAB receptor subunit; G-protein coupled receptor	increase in receptor function, promotes functional coupling to K+ channels	plasma membrane, ER, dendrite, axon, postsynaptic membrane
GABAB-R2	GABAB receptor subunit; G-protein coupled receptor	increase in receptor function, promotes functional coupling to K+ channels	plasma membrane, ER, dendrite, axon, postsynaptic membrane
GBF1; Golgispecific brefeldin A resistance factor	Guanine nucleotide exchanger for ARF5; mediates ARF5 activation; Golgi to ER trafficking	triggers disassembly of Golgi apparatus	Golgi membrane
GFAT	glutamine-fructose-6-phosphate transaminase 1; EC 2.6.1.16; regulates glucoseflux to hexosamine pathway	1.4 fold increase in enzymatic activity	cytoplasm
GYS1	Glycogen synthase; EC 2.4.1.11	inhibits enzymatic activity	cytoplasm
H2B	Histone H2B	activates stress-induced transcription	nucleus
HDAC5	Histone deacetylase 5; EC3.5.1.98; transcriptional regulator, cell cycle progression, development	reduced binding to GLUT4 promoter → enhanced GLUT4 expression	nucleus (cytoplasm)

HNF4 alpha	Hepatocyte nuclear factor 4 alpha; transcription factor, control of gene expression in hepatocytes	reduced DNAbinding	nucleus
HSL	Hormone sensitive lipase; EC 3.1.1.79; involved in triglyceride lipolysis	inhibition; change in the association with lipid droplets	cytoplasm, lipid droplets
IRS1; adaptor protein	Insulin receptor substrate 1, adaptor protein	modulation of PI3 kinase signaling	cytoplasm
KCNMA1 iso4; α subunit of BKCa channel	Potassium channel, activated in response to membrane depolarization, oxygen sensing in carotid body	inhibition of potassium currents	integral membrane protein, plasma membrane, axon
Kir6.2 (KCNJ11)	Potassium channel, voltage dependent, inward rectifying	might play a role in insulin secretion	plasma membrane
KNS2	Kinesin 2; kinesin light chain 1, motor protein	biological role of modification not known	cytoplasm, microtubules
KPNA2, importin-α1	Adaptor for classical nuclear import	interferes with nuclear import of HuR	cytoplasm, nucleus, nuclear envelope
mTOR	Ser/thr kinase; EC 2.7.11.1; catalytic subunit of mTORC1 and mTORC2	links nutrient supply to translation	cytoplasm
NKCC2 (SLC12A1)	Electroneutral transporter; reabsorption of Na+ and Cl^-; controls cell volume	regulation of transporter activity	plasma membrane
p27Kip1 (CDKN4)	Cyclin-dependent kinase inhibitor 1B, controls cell cycle progression at G1	stabilization of p27; linked to autophagy	nucleus
p300	Protein (histone) acetyltransferase; EC2.3.1.48; transcriptional co-activator	inhibits interaction with nuclear receptors, such as PPARγ	nucleus

p53	Tumor suppressor, transcription factor, cell cycle arrest, DNA repair, apoptosis	stabilization of p300-p53 interaction; controls cell cycle progression	nucleus
PFKFB2	6-Phosphofructo-2-kinase/ fructose-2,6-bisphosphatase 2; EC 2.7.1.105 or EC 3.1.3.46; glycolysis	activation; stimulation of glycolysis	cytoplasm
PFKFB3;	iPFK2 similar to PFKFB2; inducible in monocytes	activation	cytoplasm
PPP1R3C (R5/PTG)	Regulatory subunit of protein phosphatase PP1; controls PP1 activity; targets PP1 to glycogen; stimulation of glycogen synthase	promotes ubiquitination and thereby degradation	glycogen granules
PPP2R5C (B56 γ)	Regulatory subunit of protein phosphatase PP2A; possible role in the regulation and targeting of PP2A	increases PP2A activity	nucleus, chromosomes
Raf1	Ser/thr kinase; EC 2.7.11.1; component of Ras→Raf→MEK1/2→ERK 1/2 signaling pathway		cytoplasm, plasma membrane
Raptor	Regulation of mTORC1 (mammalian target of rapamycin complex 1); functions as scaffold	inhibition of mTORC1; cell cycle arrest	cytoplasm
Rb	Retinoblastoma protein; regulates cell cycle progression at G1; functions as transcriptional co-regulator; tumor suppressor	control of brain development	nucleus
smMLCK	Smooth muscle myosin light chain kinase; ser/thr protein kinase; EC2.7.11.18	reduces activity of smMLCK	cytoplasm

TBC1D1	GTPase activating protein Rab family members; regulates glucose transport	induces binding to 14-3-3 proteins	ER
TIF-IA	Transcription initiation factor for RNA-pol I	reduced rDNA transcription	nucleolus
TORC2 (CRTC2)	Transducer of regulated CREB protein 2; transcriptional regulator	phosphorylation causes cytoplasmic retention	nucleus, cytoplasm
TSC2 (tuberin)	Generates heterodimer with hamartin (TSC1); TSC1/TSC2 functions as GTPase activator of Rheb	enhances TSC2 activity → inhibition of mTOR	cytoplasm
ULK1	Ser/thr kinase; EC 2.7.11.1; binds to mTORC1 via raptor, binding controlled by nutrient supply	control of autophagy	cytoplasm
VASP	Vasodilator-stimulated phosphoprotein; actin regulator	impairs endothelial actin assembly	cytoplasm, cytoskeleton
ZNF692 (AREBP)	Transcriptional regulator, contains zinc finger	reduction in DNA binding	nucleus

Substrates for AMPKα2	**Function**	**Effect of phosphorylation**	**Primary intracellular localization**
ACC1	See above description of AMPKα1 targets		cytoplasm
AS160 (TBC1D4; Akt substrate of 160k)	GTPase activating protein for Rab; implicated in GLUT4 exocytosis in skeletal muscle	not fully understood; may regulate glucose uptake	cytoplasm
HAS2	Hyaluronic acid synthase 2; EC 2.4.1.212; integral membrane protein	inhibition of enzymatic activity	plasma membrane
HDAC5	See above description of AMPKα1 targets		nucleus

p53	See above description of AMPKα1 targets		nucleus
PGC1α	PPAR γ coactivator-1; transcriptional co-activator; association with PPARγ; binds to CREB and nuclear respiratory factors; controls mitochondrial biogenesis	phosphorylation alters activity as transcriptional regulator	nucleus
PLD1	Phospholipase D1 phophatidylcholine specific; EC 3.1.4.4; linked to Ras signaling; involved in membrane trafficking	activation of enzymatic activity	Golgi, ER